Hawaii Ocean Time-series
Data Report 6: 1994

October 1995

Luis Tupas
Fernando Santiago-Mandujano
Dale Hebel
Eric Firing
Roger Lukas
David Karl

University of Hawaii
School of Ocean and Earth Science and Technology
1000 Pope Road
Honolulu, Hawaii 96822
U. S.A.

SOEST TECHNICAL REPORT 95-6

Preface

Scientists working on the Hawaii Ocean Time-series (HOT) program have been making repeated observations of the hydrography, chemistry and biology at a station north of Oahu, Hawaii since October 1988. The objective of this research is to provide a comprehensive description of the ocean at a site representative of the North Pacific subtropical gyre. Cruises are made approximately once a month to the HOT deep-water station (22º 45'N, 158ºW) located about 100 km north of Oahu, Hawaii. Measurements of the thermohaline structure, water column chemistry, currents, primary production and particle sedimentation rates are made on each cruise.

This document reports the data collected in 1994. However, we have included some data from 1988 - 1993 to place the 1994 measurements within the context of our time-series observations. The data reported here are a screened subset of the complete data set. Summary plots are given for CTD, biogeochemical, optical, meteorological and ADCP observations.

In order to provide easy computer access to our data, CTD data at National Oceanographic Data Center (NODC) standard pressures for temperature, potential temperature, salinity, oxygen and potential density are provided in ASCII files on the enclosed diskette. Chemical measurements are also summarized in a set of Lotus-123™ files on the enclosed diskette. The complete data set resides on a Sun workstation at the University of Hawaii. These data are in ASCII format, and can easily be accessed using anonymous file transfer protocol (ftp) or the world-wide-web (WWW) via Internet. Instructions for using the Lotus files and for obtaining the data from the network are presented in Section 8. The entire data set is available at NODC.

Acknowledgments

Many people participated in the 1994 cruises sponsored by the HOT program. They are listed in Table 1.4. We gratefully acknowledge their contributions and support. Thanks are due to Lance Fujieki, David Pence, Daniel Sadler, Terrence Houlihan, Rich Muller, Karen Selph and Jefrey Snyder for participating in most of the 1994 cruises and for the tremendous amount of time and effort they have put into the program. Special thanks are due to Lisa Lum and Caroline Kohan for their excellent administrative support of the program. In addition, we would like to acknowledge the contributions made by Sharon DeCarlo and Lance Fujieki for programming and data management and June Firing and Xiaomei Zhou for ADCP processing. Sut Ian Carolyn Leong, Craig Nosse, Venugopal Sanaka and Nava Zvaig provided additional computer support. Ursula Magaard performed many of the routine chemical analyses. Ted Walsh, John Dore and Georgia Tien performed the nutrient analyses, Sophia Asghar, Reka Domokos, Jim Potemra and Jinchun Yuan the salinity measurements and Jason Killam provided additional technical support. We also would like to thank the captain and crew members of the R/V Moana Wave and the UH Marine Center staff for their efforts. Brenda Lee-Ha assisted in the production of this document. Without the assistance of these people, the data presented in this report could not have been collected, processed, analyzed and reported.

This data set was acquired with funding from the National Science Foundation (NSF) and State of Hawaii general funds. The specific grants which have supported this work are NSF grants OCE-9303094 (WOCE), and OCE-9301368 (JGOFS). We also acknowledge the contributions of Yuan Hui Li (OCE-9315392), Michael Landry (OCE-9218152) and Robert Bidigare (OCE-9315311) and their staff to the scientific efforts of HOT.

Weather buoy data used in this report were obtained by the NOAA National Data Buoy Center (NDBC) and were provided to us by the National Oceanographic Data Center (NODC). We thank Pat Caldwell for his assistance.

1. Introduction

In 1987, the National Science Foundation established a special-focus research initiative termed "The Global Geosciences Program." This program was intended to support studies of the earth as a system of interrelated physical, chemical and biological processes that act together to regulate the habitability of our planet. The stated goals of this program were two-fold. The first goal was to understand the earth-ocean-atmosphere system and how it functions. The second goal was to describe, and eventually predict, major cause-and-effect relationships. Two components of the Global Geosciences Program are the World Ocean Circulation Experiment (WOCE) and the Joint Global Ocean Flux Study (JGOFS). The former is focused on physical oceanographic processes and the latter on biogeochemical processes.

The Hawaii Ocean Time-series (HOT) project was initially funded in 1988 under the sponsorship of both the WOCE and JGOFS programs to make repeated observations of the physics, chemistry and biology of the water column for five years at a station north of Hawaii. Funding from NSF was received in 1993 to continue these observations until 1998. The objectives of HOT are to describe and understand the physical oceanography, and to identify and quantify the processes controlling biogeochemical cycling in the ocean at a site representative of the oligotrophic North Pacific Ocean. The core projects are listed in Table 1.1. In addition to core investigations, HOT cruises have continued to provide logistical support to several ancillary projects (Table 1.2).

Time-series cruises are made on approximately monthly intervals with three stations routinely occupied each month. The HOT deep-water station, also known as Station ALOHA (A Long-term Oligotrophic Habitat Assessment), is approximately 100 km north of Kahuku Point, Oahu, Hawaii (Figure 1.1; Table 1.3). Along the transit route to Station ALOHA, two other stations are occupied. Station Kahe (also referred to as Station 1) is located at 21º 20.6' N, 158º 16.4' W, off Kahe Point, Oahu. Station Kahe is used primarily to test the CTD and other equipment, but it also provides additional time-series data at a near-shore site. Station Kahe is located in approximately 1500 m of water about 16 km from shore (Figure 1.1). Station Kaena (also referred to as Station 6) is the site of an inverted echo sounder (IES) and is located at 21º 50.8' N, 158º 21.8' W.

Station ALOHA (also referred to as Station 2) is defined as a circle with a 6 nautical mile radius centered at 22º 45'N, 158ºW. All sampling at Station ALOHA is conducted within this circle (Figure 1.1). The maximum depth at Station ALOHA is about 4800 m. On several cruises in 1994, another station (Station 3) was occupied along longitude 158º W at a latitude of 23º 25' N. Station 3 was originally part of a series of stations along 158º W established in 1993 to analyze regional variability in hydrography and currents. When time permits, a CTD cast is conducted at Station 3.

The JGOFS and WOCE components of the program measure a variety of parameters during the regular monthly sampling work at Station ALOHA (Table 1.4). Sampling includes a 36-hour burst of CTD casts at roughly 3-hour intervals to obtain temperature, salinity and oxygen profiles from 0 to 1000 dbars. Sampling also includes a deep CTD cast as close to the bottom as possible. In addition, primary production, particle flux and a variety of chemical determinations at discrete depths with continuous profiles of optical parameters are conducted. Current measurements are made using shipboard acoustic doppler current profiler (ADCP).

This report presents selected core data collected during the sixth year of the HOT Program (January-December 1994; Table 1.5). During this period, 9 cruises were conducted using the University of Hawaii research vessel R/V Moana Wave and a total field scientific crew of 57 (Table 1.6).

Table 1.1: HOT Core Projects

Principal Investigator	Institution	Title
Robert Bidigare	University of Hawaii	Core Pigment Measurements
David Karl	University of Hawaii	Joint Gobal Ocean Flux Study Component
Michael Landry	University of Hawaii	Zooplankton Variability and Particulate Fluxes
Yuan-Hui (Telu) Li	University of Hawaii	Inorganic Carbon System Measurements
Roger Lukas	University of Hawaii	World Ocean Circulation Component

Table 1.2: Ancillary Projects Supported by HOT

Principal Investigator	Institution	Agency	Duration	Project title
Marlin Atkinson	Univ. of Hawaii	NSF	12/88-12/95	Calibration Stability of Two New Oxygen Sensors for CTDs
Lisa Campbell	Univ. of Hawaii	NSF	3/91-2/94	Phytoplankton Population Dynamics at the Hawaii ocean Time-series Station
Lisa Campbell	Univ. of Hawaii	NSF	11/94-10/97	Effects of light and nitrogen source on Prochloroccus growth
James Cowen	Univ. of Hawaii	NSF	8/92-12/94	Studies on the Dynamics of Marine Snow and Particle Aggregation in the North Pacific Central Gyre
Steve Emerson	Univ. of Washington	NSF	10/93-9/96	Ocean Oxygen Fluxes
Charles Keeling	UCSD, Scripps	NSF	12/88-12/95	A Study of the Abundance and C13/C12 Ratio of Atmosphere Carbon Dioxide and Oceanic Carbon in Relation to the Global Carbon Cycle
George Luther	Univ. of Delaware	NSF	2/93- 1/96	Iodine Speciation as a Primary Productivity Indicator
Christopher Measures	Univ. of Hawaii	ONR	4/93-12/95	Temporal Variation of Dissolved Trace Element Concentrations in Response to Asian Dust Inputs
Brian Popp	Univ. of Hawaii	NSF	6/91-5/94	Isotopic Analyses of DOC and Cell Concentrates
Paul Quay	Univ. of Washington	NOAA	6/93- 6/96	13C/12C of Dissolved Inorganic Carbon in the Ocean
Hans Thierstein	Geo. Inst. Switzerland	Swiss FIT	1/93-12/95	Calcareous Phytoplankton Dynamics

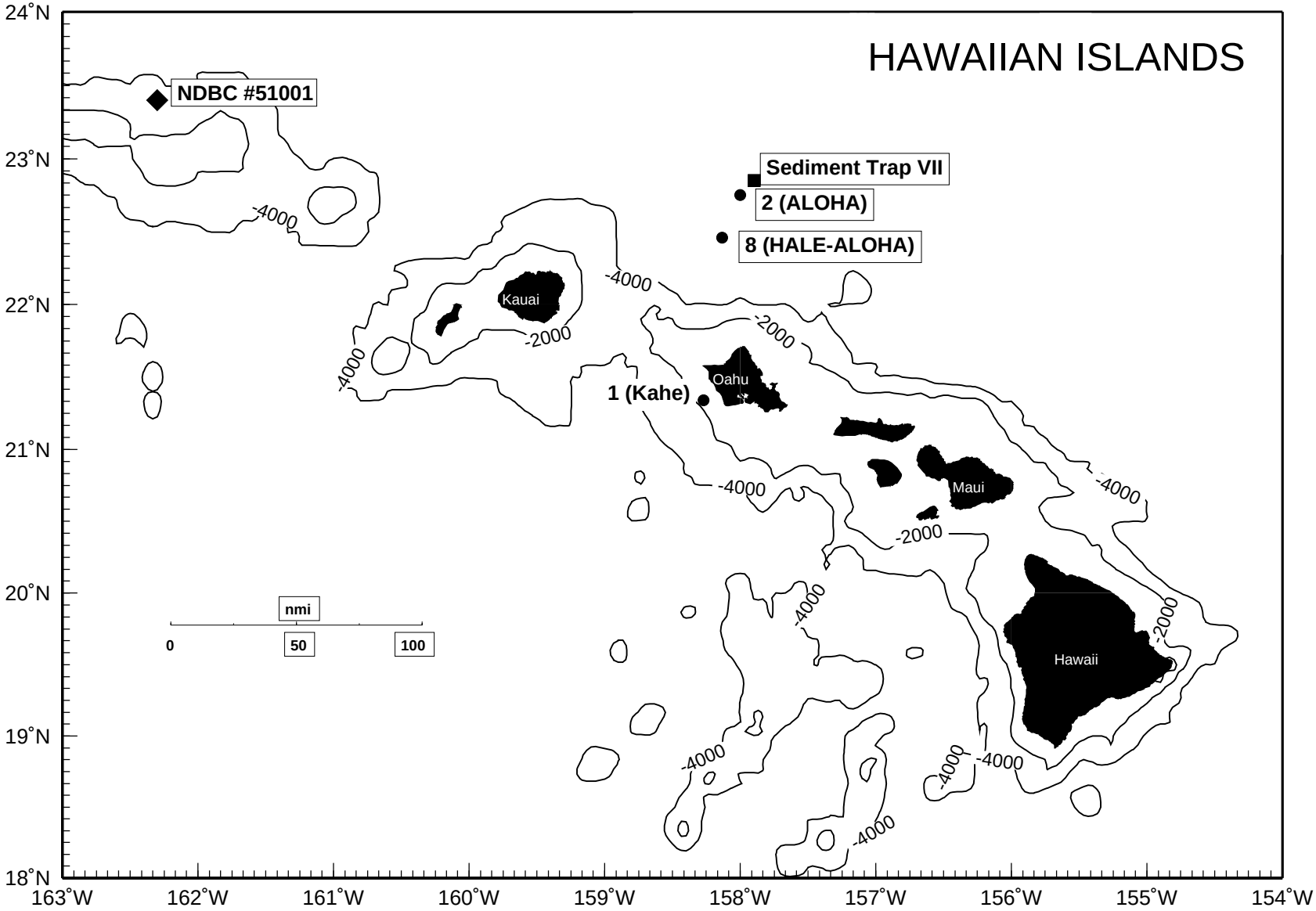

Figure 1.1: Map of the Hawaiian Islands showing the locations of Stations ALOHA, Kahe, Kaena, and the NDBC weather buoys. Lower panel: Expanded view of Station ALOHA (a 6 nautical mile radius circle centered at 22º 45'N, 158º W) and the location of the inverted echo sounders and the bottom-moored sediment

Table 1.3. Locations of the HOT Water Column and Bottom Stations

Station	Coordinates	Approximate depth	Comments
1 (Kahe)	21° 20.6'N 158° 16.4'W	1,500 meters	HOT Program coastal time-series station
2 (ALOHA)	22° 45'N 158° 00'W	4,800 meters	HOT Program open ocean time-series station
3	23° 25'N 158° 00'W	4,800 meters	One of three onshore to offshore transect sites, established in 1993
4	21° 57.8'N 158° 00'W	4,000 meters	One of three onshore to offshore transect sites, established in 1993
5	21° 46.6'N 158° 00'W	450 meters	One of three onshore to offshore transect sites, established in 1993
IES Network			
6 (Kaena)	21° 50.8'N 158° 21.8'W	2,500 meters	May 1993-June 1994, June 1994-October 1995
N	23° 00.7'N 157° 59.9'W	4,800 meters	Feb 1991-Feb 1992, June 1992-May 1993
C	22° 44.9'N 157° 59.9'W	4,800 meters	Feb 1991-Feb 1992, Jun 1992-May 1993 May 1993-June 1994, June 1994-October 1995
SW	22° 37.0'N 158° 14.7'W	4,800 meters	Feb 1991-Feb 1992, Jun 1992- May 1993
SE	22° 30.0'N 157° 45.2'W	4,800 meters	Feb 1991-Feb 1992, June 1992- May 1993
E	22° 44.8'N 157° 54.0'W	4,800 meters	Feb 1991- Feb 1992
Sediment Traps			
ALOHA-I	22° 57.3'N 158° 06.2'W	4,800 meters	1st deployment of bottom-moored sequencing sediment trap, June 1992- Oct 1993
ALOHA-II	23° 6.7'N 157° 55.8'W	4,800 meters	2nd deployment of bottom-moored sequencing sediment trap, Oct 1993 - Oct 1994
Weather Buoys			
Buoy #51026	21° 22'N 156° 57'W		NOAA-NDBC meteorological buoy
Buoy #51001	23° 24'N 162° 18'W		NOAA-NDBC meteorological buoy

Table 1.4: Time-Series Parameters Measured at Station ALOHA

Parameter	Depth Range (m)	Analytical Procedure
I. CTD Measurements		
Depth (pressure)	0-4800	Pressure transducer on SeaBird CTD-rosette package
Temperature	0-4800	Thermistor on Sea-Bird CTD package with frequent calibration
Salinity	0-4800	Conductivity sensor on Sea-Bird CTD package, standardization with Guildline AutoSal #8400 against Wormley standard seawater
Oxygen	0-4800	Polarographic sensor on Sea-Bird CTD package with Winkler standardization
Fluorescence	0-1000	Sea-Tech flash flurometer on Sea-Bird CTD package
Beam Transmission	0-1000	Sea-Tech 25 cm path length beam transmissometer on Sea-Bird CTD package
II. Optical Measurements		
Incident Irradiance (PAR)	Surface	Licor cosine collector and Biospherical 4 π collector
Underwater Irradiance (PAR)	0-150	Biospherical profiling natural fluorometer 4 π Collector
Solar Stimulated Fluorescence (683nm)	0-150	Biospherical profiling natural fluorometer
III. Water Column Chemical Measurements		
Oxygen	0-4750	Winkler titration
Dissolved Inorganic Carbon	0-4750	Coulometry
Titration Alkalinity	0-4750	Automated titration
pH	0-4750	Spectrophotometric
Nitrate Plus Nitrite	0-4750	Autoanalyzer
Soluble Reactive Phosphate	0-4750	Autoanalyzer
Silicate	0-4750	Autoanalyzer
Low Level Nitrate Plus Nitrite	0-200	Chemiluminescence
Low Level Phosphorus	0-200	Magnesium-induced coprecipitation
Dissolved Organic Carbon	0-1000	High temperature catalytic oxidation
Total Dissolved Nitrogen	0-1000	U.V. oxidation
Total Dissolved Phosphorus	0-1000	U.V. oxidation
Particulate Carbon	0-1000	High temperature combustion
Particulate Nitrogen	0-1000	High temperature combustion
Particulate Phosphorus	0-1000	High temperature combustion

Table 1.4: continued

Parameter	Depth Range (m)	Analytical Procedure
IV. Water Column Biomass Measurements		
Chlorophyll *a* and Phaeopigments	0-200	Fluorometric analysis
Plant Pigments	0-200	High performance liquid chromatography
Adenosine 5'-Triphosphate	0-1000	Firefly bioluminescence
Bacteria and Cyanobacteria	0-1000	Flow cytometry
V. Carbon Assimilation and Particle Flux		
Primary Production	0-175	"Clean" ^{14}C incubations
Carbon, Nitrogen, Phosphorus and Mass Flux	150, 300, 500	Free-floating particle interceptor traps
VI. Currents		
Acoustic Doppler Current Profiler	0-300	Hull mounted, RDI #VM-150
Acoustic Doppler Current Profiler	0-4750	Lowered
VII. Moored Instruments		
Inverted Echo Sounder Network (Dynamic height)	100-1000	Acoustic telemetry, CTD calibration
Sequencing Sediment Traps (Particle Flux)	800, 1500, 3000, 4000	McLane Parflux MK7-21

Table 1.5: Summary of 1994 HOT Cruises

HOT	Ship	Depart	Return
51	R/V Moana Wave	18 January 1994	23 January 1994
52	R/V Moana Wave	15 February 1994	20 February 1994
53	R/V Moana Wave	7 March 1994	12 March 1994
54	R/V Moana Wave	17 June 1994	22 June 1994
55	R/V Moana Wave	23 July 1994	28 July 1994
56	R/V Moana Wave	28 August 1994	2 September 1994
57	R/V Moana Wave	21 September 1994	26 September 1994
58A	R/V Moana Wave	13 October 1994	18 October 1994
58B	R/V Moana Wave	19 October 1994	22 October 1994
59	R/V Moana Wave	17 November 1994	22 November 1994

Table 1.6: 1994 Cruise Personnel (shaded area=cruise participant)

Cruise Participants	51	52	53	54	55	56	57	58a	58b	59
Principal Investigators										
Fred Bingham				■						
Eric Firing						■				
Dale Hebel	■	■	■	■	■	■	■	■	■	
David Karl									■	
Michael Landry					■					
Roger Lukas			■							
Luis Tupas		■	■	■	■	■	■			■
University of Hawaii Scientists										
Peter Hacker									■	
Mikel Latasa, Postdoctoral	■					■		■		■
Christoper Measures			■							■
Brian Popp					■					
Renate Scharek, Postdoctoral				■	■	■				
Christopher Winn		■			■			■		
Suzanna.Vink, Postdoctoral							■	■		
Visiting Scientists and Technicians										
Anatoly Arjannikov			■							
Lenore Bennett	■									
Michael Mulroney				■						
Mattheiu Roy-Barman							■			
Jonathan Sharp	■									
Alexander Soloviev			■							
Charles Stump								■		
Bill Weber					■					
University of Hawaii Research Associates										
John Constantinou		■					■			
Lance Fujieki		■			■	■	■	■	■	■
Terrence Houlihan			■	■	■	■	■	■	■	
Julie Kirshtein	■									
Ursula Magaard	■	■			■					■
Rich Muller	■	■	■	■						
Craig Nosse							■	■		■
David Pence	■	■	■	■		■	■	■	■	
Fernando Santiago-Mandujano	■		■		■	■	■	■		
Jefrey Snyder	■	■	■	■	■	■	■	■		■
Georgia Tien										■
Jin Chun Yuan	■	■						■		■
	51	**52**	**53**	**54**	**55**	**56**	**57**	**58a**	**58b**	**59**

Table 1.6: continued

Cruise Participants	51	52	53	54	55	56	57	58a	58b	59
University of Hawaii Graduate Students										
Amy Baylor		■								
Wilfred Braje						■				
James Christian				■	■					■
John Dore	■	■		■			■			
Anthony Fereira, Undergraduate							■			
Jacqueline Johnson										■
Kalpana Kallianpur									■	
Jason Killam, Undergraduate				■						
Hong Bin Liu		■								
Harold Lutz	■			■						
James Potemra		■								
Stewart Reid		■								
Rebecca Reitmeyer										■
Daniel Sadler			■	■		■	■			■
Deborah Schulman					■					■
Karen Selph	■	■	■	■	■	■				■
Paul Troy				■						
Visiting Students										
Heather Anderson								■		
Karin Bjorkmann			■					■		■
Karen Casciotti, REU				■	■					
Helmut Duerrast								■		
Payal Parekh, REU					■					
Louise Schluter		■								
	51	**52**	**53**	**54**	**55**	**56**	**57**	**58a**	**5b**	**59**

2. Sampling Procedures and Analytical Methods

2.1. CTD Profiling

Continuous measurements of temperature, salinity, oxygen, fluorescence and beam transmission are made with a Sea-Bird SBE-09 CTD package described in Tupas et al. (1993). The CTD was upgraded to an SBE-911 plus with dual temperature, salinity and oxygen sensors before cruise HOT-54. A separate duct and pump circulates seawater through the secondary sensors. These sensors provide redundant information useful in the case of a sensor failure, and to detect sensor problems by analyzing the differences between each sensor pair measurements.

A CTD cast to 1000 dbar is made at Station Kahe on each cruise. At Station ALOHA a burst of consecutive CTD casts to 1000 dbar is made over 36 hours to span the local inertial period and three semi-diurnal tidal cycles. One CTD cast close to the bottom is made on each cruise to satisfy WOCE requirements. A Datasonics PSA-900 sonar altimeter was added to the CTD package starting on cruise HOT-49 to measure the distance between the package and the bottom. This, together with the Benthos acoustic pinger has allowed us to obtain profiles within 10 meters of the sea floor (approximately 4750 meters). When time permitted, a second deep cast was obtained at Station ALOHA to observe short time changes in the deep and bottom water. Also, Stations 3 (north of ALOHA), and 6 (Station Kaena) were regularly occupied on most of the cruises.

2.1.1. Data Acquisition and Processing

CTD data were acquired at a rate of 24 samples sec^{-1}. Digital data were stored on an IBM-compatible PC and the analog signal recorded on VHS video tapes. Backups of CTD data were made onto Bernoulli disks and later onto DAT tapes. The raw CTD data were quality controlled and screened for spikes as described in Winn et al. (1993). Data alignment, averaging, correction and reporting were done as described in Tupas et al. (1993). Eddy shed wakes, caused when the rosette entrains water, introduce salinity spikes in the CTD profiles data. These contaminated data were handled using an algorithm which eliminated data collected when the CTD's speed was severely affected by the ship's roll or its acceleration was greater than 0.5 meter s^{-2}. The data were subsequently averaged into 2 dbar pressure bins. Cruise HOT-59 was conducted under rough sea conditions, with heavy ship rolling during all casts causing large vertical velocity fluctuations of the CTD package. The acceleration cutoff value had to be increased between 0.6 and 0.8 m s^{-2} to obtain enough data points to average each bin. Data from cruises with dual CTD sensors (HOT-54 through 59) were additionally screened by obtaining the differences between primary and secondary sensors data. These differences allowed us to identify problems in the sensors. Only the data from one of the TC sensors pair and one of the oxygen sensors are reported here.

Temperature is reported in the ITS-90 scale. Salinity and all derived units were calculated using the UNESCO (1981) routines, salinity is reported in the practical salinity scale (PSS-78). Oxygen is reported in $\mu mol\ kg^{-1}$.

2.1.2. Sensor Corrections and Calibrations

2.1.2.1. pressure

Pressure sensor calibration strategies and procedures are described in Winn et al. (1993) and Tupas et al. (1993). Briefly, this strategy used a high quality quartz pressure transducer as the laboratory transfer standard and a Russka precision dead-weight pressure tester as a primary standard. The primary standard met National Institute of Standards and Technology specifications and was operated under controlled conditions. The transfer standard was a Paroscientific Model 760 pressure gauge equipped with a 10,000 psi transducer. The transfer standard was calibrated by the Oceanographic Data Facility at Scripps Institution of Oceanography against their primary standard in May of 1991, and more recently at the Northwest Regional Calibration Center in September of 1994.

Pressure transducer #26448 was used on all the cruises in 1994. Calibrations against the transfer standard in 1994 are given in Table 2.1. These values have been corrected for the shift in the standard. The 3 January and 8 August offsets were used for the cruises in 1994 (This offset was only used for real-time data acquisitions, as a more accurate offset was determined at the time that the CTD first entered the water on each cast). We did not apply any type of correction due to hysteresis or slope offset, given that these effects were negligible. However, a correction due to slope offset may be necessary in future cruises, as the magnitude of this effect seems to be increasing as seen in the December 1994 calibration results (Table 2.1).

Table 2.1: CTD Pressure Calibrations (decibars)
Sea-Bird SBE-09 #91361 / Pressure Transducer #26448

Calibration date	Offset @ 0 dbar	slope offset @ 4500 dbar	hysteresis
3 January 1994	-5.59	0.16	0.04
8 August 1994	-5.78	0.15	0.20
16 December 1994	-5.82	0.85	0.07

2.1.2.2. temperature

Five Sea-Bird SBE-3-02/F temperature transducers were used in 1994 and were calibrated at Sea-Bird, where a calibration bath has been in service since May 1993 (see Tupas et al., 1993). Sensors had been calibrated regularly every six months until June 1994, when Sea-Bird offered to calibrate the sensors as frequently as possible to ensure temperature accuracies at the 1 x 10^{-3} °C level. Since June 1994, the sensors have been calibrated after every cruise. As a result, the post-cruise sensor intercomparisons that were previously conducted for short term drift evaluations (Tupas et al., 1993) are no longer necessary. Intercomparisons were done only from January to June 1994, although the number of usable intercomparisons was not sufficient to determine the sensors' drift.

Given the availability of dual-sensors since cruise HOT-54, we now calculate temperature differences between the two sensors per cast as a regular procedure to evaluate the quality of the data, and to identify possible problems with the sensors. Mean and standard deviation of the differences are obtained throughout the water column per cast, and in 2 dbar bins from the ensemble of all casts at Station ALOHA. All sensor pairs performed correctly during cruises HOT-54 through 59, showing temperature differences within expected values. The range of variability throughout the whole water column in the mean temperature difference was typically less than $\pm 1 \times 10^{-3}$ °C, with a standard deviation of less than $\pm 0.5 \times 10^{-3}$ °C below 500 dbar. The largest variability was observed in the thermocline, with standard deviation values of up to $\pm 5 \times 10^{-3}$ °C.

The history of the sensors, as well as the procedures followed to obtain the sensor drift from the Sea-Bird calibrations are well-documented in Tupas et al. (1993, 1994a). Sensor #1416 is a new sensor acquired in early 1994. Sensors #1591 and #1601 belong to a new generation of sensors loaned to us by Sea-Bird in July 1994 to be used in the HOT program. Calibration coefficients used in the drift estimates are in Table 2.2. These coefficients were used in the following formulat that gave the temperature (in °C) as a function of the frequency signal (f):

$$\text{temperature} = 1/\{a+b[\ln(f_0/f)]+c[\ln^2(f_0/f)]+d[\ln^3(f_0/f)]\}-273.15$$

Table 2.3 shows the individual cruise temperature corrections obtained from those drifts.

Sensor #886

This sensor was used in cruises HOT-51, 52 and in one cast of HOT-53. It was also used as part of the dual-sensor configuration in cruises HOT-54, 58 and 59. The sensor's electronics were serviced twice during 1994. On 13 June a defective reed switch assembly was removed, and on 4 November the turret joint was resoldered as a prophylactic procedure recommended by Sea-Bird to prevent sensor drift due to micro-cracks in the solder. These procedures produced a small change in the sensor drift rate.

The calibrations between 29 January 1992 and 22 March 1994 were used to determine the drift during cruises HOT-51 through 53. A linear fit to the 0-30°C average offset from each calibration relative to that on 29 January 1992 gave an intercept of 3×10^{-4} °C with a slope of 6.5×10^{-6} °C day^{-1}. The RMS deviation of the offsets from this fit was 7.7×10^{-4} °C.

The 16 December 1993 calibration was used as a baseline to calculate cruises HOT-51 through 53 temperatures. When corrected for linear drift to 1 March 1994 (the midpoint of the cruise dates), this calibration gave the smallest deviation in the 0-5°C temperature range from the set of all calibrations used to determine the drift (also corrected for linear drift to 1 March 1994). The mean deviation of this calibration was -1.4×10^{-4} °C with a range of variation of $\pm 1.5 \times 10^{-4}$ °C. The deviation from this and the other calibrations in the same temperature range was $\pm 4.8 \times 10^{-4}$ °C.

Calibrations after the 13 June and before the 4 November 1994 repairs were used to determine the sensor drift on cruises HOT-54 and 58. The 14 June and 6 July 1994 calibrated data were not used in this determination, as they indicated that the sensor drift was still

stabilizing after the first repair. The 27 October 1994 calibration data were not used either, because it showed an anomalous 0-30°C trace relative to the other calibrations. A linear drift rate of 8.5×10^{-6} °C day^{-1} was obtained with an intercept of -1.8×10^{-5} °C and 1.6×10^{-5} °C RMS from the residuals of the fit. The 12 August 1994 calibration data were used as the baseline for cruises HOT-54 and 58. The mean deviation of this calibration from the others in the 0-5 °C range, corrected for the drift on 15 October 1994, was 5.4×10^{-6} °C, with a $\pm 1.6 \times 10^{-5}$ °C range of variation. The deviation from this and the other calibrations was $\pm 3.9 \times 10^{-5}$ °C.

Calibrations after 4 November 1984 were used to calculate the drift on cruise HOT-59. An intercept of 2.1×10^{-4} °C and a slope of 1.07×10^{-5} °C day^{-1} were obtained, with a RMS of 2.9×10^{-4} °C from the residuals of the fit. The 26 January 1995 was used as baseline calibration, showing a 0-5°C drift-corrected to 20 November 1994 mean deviation of -7.5×10^{-5} °C, with a variation range of $\pm 2.6 \times 10^{-5}$ °C. The deviation from this and the other calibrations was $\pm 3.1 \times 10^{-4}$ °C.

Sensor #1601

This sensor was used in a dual-sensor configuration during cruises HOT-55 through 57. The sensor malfunctioned during a test prior to cruise HOT-58, and it was not used thereafter.

Calibrations of this sensor yielded a drift rate of 3.31×10^{-5} °C day^{-1} with a 2.2×10^{-5} °C intercept and a 6.8×10^{-5} °C RMS from the fit residuals. The calibration showing the smallest 0-5°C mean deviation among the set of all calibrations was that on 12 August 1994, and was used as the baseline calibration. These calibrations were drift-corrected to the midpoint of the cruise dates on 25 August 1994. The deviation was 4.8×10^{-5} °C with a variation range of $\pm 1.0 \times 10^{-5}$ °C. The deviation from all the calibrations in the 0-5°C range on the same date was $\pm 9.9 \times 10^{-5}$ °C.

Sensor #1591

This sensor was used in a dual-sensor CTD configuration during cruises HOT-55 and 59. On 4 November 1994, the turret joint of this sensor was resoldered as a prophylactic procedure to prevent sensor drift. This caused a change in the sensor drift rate.

Calibrations prior to 4 November 1994 were used to determine a sensor drift of 9.21×10^{-6} °C day^{-1} with a -4.7×10^{-5} °C intercept and 8.3×10^{-5} °C RMS from the residuals fit. The 12 August 1994 calibration was used as baseline for cruises HOT-55 through 58. This calibration yielded the smallest 0-5°C mean deviation from the others, all drift-corrected to 5 September 1994 (midpoint date between cruises HOT-55 and 58). The deviation was -9.5×10^{-5} °C with a $\pm 1.0 \times 10^{-5}$ °C range of variation. The deviation from this and all the other calibrations was $\pm 1.2 \times 10^{-4}$ °C.

The calibrations after the sensor's repair were used to determine the drift for cruise HOT-59. The first two of these calibrations (8 November and 11 November) were not included as they were done right after the repair, when the sensor was still stabilizing. The 21 January 1995 showed an anomalous 0-30°C trace relative to the others and was not included in the analysis. The rest of the calibrations yielded a drift rate of -7.8×10^{-6} °C day^{-1} with a 1.8×10^{-4} °C

intercept and 9.4 x 10^{-5} °C RMS for the residuals of the fit. The 8 December 1994 calibration was selected as baseline for cruise HOT-59 based on the same criteria as before. This calibration gave a 0-5°C mean deviation of -2.2 x 10^{-5} °C from all the calibrations with a variation range of ±5.0 x 10^{-6} °C. The deviation from all the calibrations was ±1.0 x 10^{-4} °C.

Sensor #1416

This sensor was used in a dual-sensor configuration during cruise HOT-54. The sensor was opened at Sea-Bird on 13 June 1994 to perform some bench tests with other sensors, and again on 4 November 1994 to resolder the turret joint as in the case of sensor #1591. These two interventions produced changes in the sensor drift rate.

The calibrations after 13 June and before 4 November 1994 were used to determine the drift on cruise 54. The 14 June calibration was not used as the sensor was still stabilizing after the repair. The rest of the calibrations yielded an intercept of 7.7 x 10^{-5} °C and a slope of 1.4 x 10^{-6} °C day^{-1}, with 2.1 x 10^{-4} °C RMS from the residuals of the fit. The 6 July 1994 calibration was used as the baseline for cruise HOT-54. The 0-5°C deviation of this calibration with respect to all of them was -5.1 x 10^{-5} °C with ±1.0 x 10^{-4} °C range of variation. This and all the other calibrations had a deviation of ±3.2 x 10^{-4} °C.

Sensor #741

This sensor was used in all but one cast of cruise HOT-53. The sensor had followed a constant drift from June 1992 until June 1994, when the sensor was repaired after being found faulty during an April-May cruise in the western Pacific. The sensor was giving incorrect temperatures of the order of 10 m°C during that cruise due to an increase in the temperature sensitivity of the sensor. Up and down temperatures traces from various casts were closely examined for anomalies that would indicate that the sensor was already at fault during this cruise. No apparent anomalies were found in the casts, indicating that the sensor's problem developed after cruise HOT-53, probably during shipping.

The calibrations shown in Table 2.2 were used to obtain a sensor drift of -1.06 x 10^{-6} °C day^{-1} with a -2.1 x 10^{-4} °C intercept and 3.5 x 10^{-4} °C RMS from fit residuals. The 16 December 1993 was used as baseline calibration. The 0-5°C deviation of this calibration from all calibrations drift-corrected to the mid-point cruise date was -2.3 x 10^{-4} °C, with a ±1.0 x 10^{-4} °C variation range. The deviation from this and all the other calibrations was ±5.9 x 10^{-4} °C.

2.1.2.3. conductivity

Conductivity sensor #679 was used during all the 1994 cruises. This sensor was repaired after failing during cruise HOT-49. The sensor's cell was replaced and calibrated on 14 October 1993 after being found cracked during a Sea-Bird inspection. Sensor #1336 was used during cruises HOT-54 through 58 in a dual-sensor CTD configuration. Comparisons against sensor #679 revealed a constant offset of about 0.005 in salinity in the upper 300 dbar of all CTD casts. A Sea-Bird evaluation revealed that the offset was caused by sensor #1336, whose cell had been shortened by water penetrating its epoxy jacket. This problem affected the measurements obtained with this sensor in cruises HOT-54 through 58.

Sensor #527 was used during cruise HOT-59 together with sensor #679. This sensor was calibrated on 8 October 1993 and performed correctly compared with sensor #679. Conductivity differences between both sensors were obtained following the same procedure as in the case of the temperature sensors (Section 2.1.2.2). The range of variability throughout the water column was about $\pm$ 1 x 10^{-4} Siemens m^{-1}, with a standard deviation of less than 0.5 x 10^{-4} Siemens m^{-1} below 500 dbar, from the ensemble of all the cruise casts. The largest variability was in the halocline, with standard deviations reaching up to 5 x 10^{-4} Siemens m^{-1} between 50 and 300 dbar. Only the measurements obtained from sensor #679 in all 1994 cruises are reported here.

Conductivity calibration procedures carried out at the North West Regional Calibration Center are described in Winn et al. (1991). The nominal calibrations were used for data acquisition and final calibration was determined empirically by comparing salinity determinations of discrete water samples acquired during each cast. Prior to empirical calibration, conductivity was corrected for thermal inertia (α) of the glass conductivity cell as described in Chiswell et al. (1990). Table 2.3 lists the value of the α parameter used for each cruise.

Preliminary screening of bottle samples and empirical calibration of the conductivity cell are described in Tupas et al. (1993, 1994a). For cruises HOT-51 through 59, the standard deviation cutoff values for screening of bottle samples were 0.0038 (0-150 dbar), 0.0053 (151-500 dbar), 0.0026 (501-1050 dbar), and 0.0012 (1051-5000 dbar).

The conductivity calibration coefficients (b_0, b_1, b_2) resulting from the least squares fit ($\Delta C = b_0 + b_1 C + b_2 C^{2)}$ to the CTD minus bottle conductivities (ΔC) as a function of conductivity (C) are given in Table 2.4. The quality of the CTD calibration is illustrated in Figure 2.1, which shows the differences between the corrected CTD salinities and the bottle salinities as a function of pressure for each cruise. The calibrations were best below 500 dbar because the weaker vertical salinity gradients at depth lead to less error if the bottle and CTD pressures are slightly mismatched.

Table 2.2: Calibration Coefficients for Sea-Bird Temperature Transducers. RMS Residuals from Calibration Give an Indication of Quality of the Calibration

SN	YYMMDD	f_0	a	b	c	d	RMS (m^oC)
886	950216	5901.92	3.68169317e-03	5.96016095e-04	1.46353691e-05	2.17393559e-06	0.02
886	950215	5914.95	3.68037668e-03	5.95951267e-04	1.46231512e-05	2.17428246e-06	0.01
886	950126	5915.30	3.68034334e-03	5.95944051e-04	1.46112949e-05	2.16373996e-06	0.02
886	950121	6259.38	3.64668605e-03	5.94310864e-04	1.42555484e-05	2.17622748e-06	0.03
886	941203	5901.78	3.68171081e-03	5.96014591e-04	1.46250332e-05	2.16516285e-06	0.02
886	941108	5914.56	3.68042917e-03	5.95951172e-04	1.45965127e-05	2.14440552e-06	0.03
886	941104	5914.43	3.68044553e-03	5.95955519e-04	1.46070261e-05	2.15636004e-06	0.02
886	940929	5915.15	3.68044662e-03	5.95951493e-04	1.48046202e-05	2.32074444e-06	0.02
886	940913	5917.67	3.68019623e-03	5.95945359e-04	1.48109830e-05	2.33201503e-06	0.02
886	940812	5917.39	3.68022598e-03	5.95933057e-04	1.47790660e-05	2.30870602e-06	0.02
886	940811	5917.45	3.68021926e-03	5.95925456e-04	1.47580626e-05	2.29396666e-06	0.01
886	940609	5905.37	3.68099287e-03	5.96016210e-04	1.47876013e-05	2.29795203e-06	0.07
886	940322	5905.05	3.68105112e-03	5.96020120e-04	1.48178500e-05	2.32289585e-06	0.06
886	931216	5904.70	3.68108073e-03	5.96027290e-04	1.48092022e-05	2.31314120e-06	0.05
886	930605	5905.69	3.68098370e-03	5.96013394e-04	1.47882243e-05	2.29755837e-06	0.06
886	921218	5967.82	3.67476787e-03	5.95715773e-04	1.48206068e-05	2.52835250e-06	0.39
886	920820	5935.78	3.67798061e-03	5.95648169e-04	1.41980725e-05	1.94572339e-06	0.60
886	920129	5969.00	3.67467842e-03	5.95638784e-04	1.45242521e-05	2.12848528e-06	0.20
1601	940929	5936.47	3.68044486e-03	5.98339794e-04	1.46274191e-05	2.09045375e-06	0.17
1601	940913	5938.99	3.68019443e-03	5.98321456e-04	1.46073617e-05	2.07124133e-06	0.17
1601	940812	5938.83	3.68022455e-03	5.98321759e-04	1.46157504e-05	2.08791250e-06	0.15
1601	940811	5938.89	3.68021765e-03	5.98310926e-04	1.45900357e-05	2.06710894e-06	0.17
1591	950216	6255.41	3.68169061e-03	6.03693580e-04	1.48590071e-05	1.79916622e-06	0.28
1591	950126	6269.39	3.68034080e-03	6.03620439e-04	1.48232127e-05	1.77660433e-06	0.27
1591	941222	6268.80	3.68039400e-03	6.03628837e-04	1.48377872e-05	1.78808699e-06	0.26
1591	941215	6268.74	3.68039983e-03	6.03628141e-04	1.48209310e-05	1.76974758e-06	0.27
1591	941208	6268.75	3.68039928e-03	6.03626833e-04	1.48160894e-05	1.76753661e-06	0.28
1591	941203	6255.20	3.68170815e-03	6.03695159e-04	1.48350099e-05	1.77562177e-06	0.29
1591	941027	6254.95	3.68171099e-03	6.03701324e-04	1.48296741e-05	1.75226976e-06	0.31
1591	940929	6268.02	3.68044356e-03	6.03668575e-04	1.50756970e-05	1.96985150e-06	0.28
1591	940913	6270.69	3.68019334e-03	6.03672458e-04	1.51200886e-05	2.01344369e-06	0.26
1591	940812	6270.41	3.68022293e-03	6.03663667e-04	1.50733597e-05	1.97130107e-06	0.29
1591	940811	6270.44	3.68021614e-03	6.03653016e-04	1.50773730e-05	1.98591308e-06	0.29
1416	941027	6230.67	3.68171490e-03	6.01825889e-04	1.50406397e-05	2.13922692e-06	0.05
1416	940929	6243.65	3.68044491e-03	6.01718285e-04	1.50785544e-05	2.19817967e-06	0.13
1416	940913	6246.31	3.68019471e-03	6.01714914e-04	1.50987095e-05	2.22218235e-06	0.13
1416	940812	6245.93	3.68022440e-03	6.01694729e-04	1.50204697e-05	2.15503456e-06	0.13
1416	940811	6245.98	3.68021737e-03	6.01683500e-04	1.50066078e-05	2.15119355e-06	0.16
1416	940706	6238.27	3.68096718e-03	6.01705924e-04	1.49060291e-05	2.03031704e-06	0.13
741	940526	6169.56	3.68107686e-03	6.02122777e-04	1.52707307e-05	2.38648078e-06	0.24
741	931216	6169.60	3.68108398e-03	6.02142067e-04	1.53434585e-05	2.47225482e-06	0.26
741	930513	6170.47	3.68098624e-03	6.02116588e-04	1.52577583e-05	2.38750692e-06	0.26
741	921218	6234.70	3.67477118e-03	6.01755208e-04	1.48365899e-05	2.06062301e-06	0.38
741	920626	6246.37	3.67361468e-03	6.01608285e-04	1.48891820e-05	2.32038514e-06	0.61

Table 2.3: Temperature and Conductivity Sensor Corrections Including the Thermal Inertia (α) Parameter (see text). Dual TC sensors were used on HOT 54-59.

HOT	Temp Sensor #	T Correction °C	Cond Sensor #	α
51	886	0.0003	679	0.037
52	886	0.0004	679	0.037
53	741	-0.0001	679	0.037
53	886	0.0005	679	0.037
54	886	-0.0004	679	0.028
54	1416	-0.0000	1336	0.020
55	1591	-0.0002	679	0.020
55	1601	-0.0006	1336	0.020
56	1591	0.0002	679	0.028
56	1601	0.0006	1336	0.028
57	1591	0.0004	679	0.028
57	1601	0.0014	1336	0.028
58	1591	0.0006	679	0.020
58	886	0.0005	1336	0.020
59	1591	0.0001	679	0.020
59	886	-0.0007	527	0.020

The final step of conductivity calibration was a cast-dependent bias correction as described in Tupas et al. (1993) to allow for drift during each cruise or for sudden offsets due to fouling (Table 2.5). Note that a change of 1 X 10^{-4} Siemens m^{-1} in conductivity was approximately equivalent to 0.001 in salinity. Table 2.6 gives the mean and standard deviations for the final calibrated CTD minus water sample values.

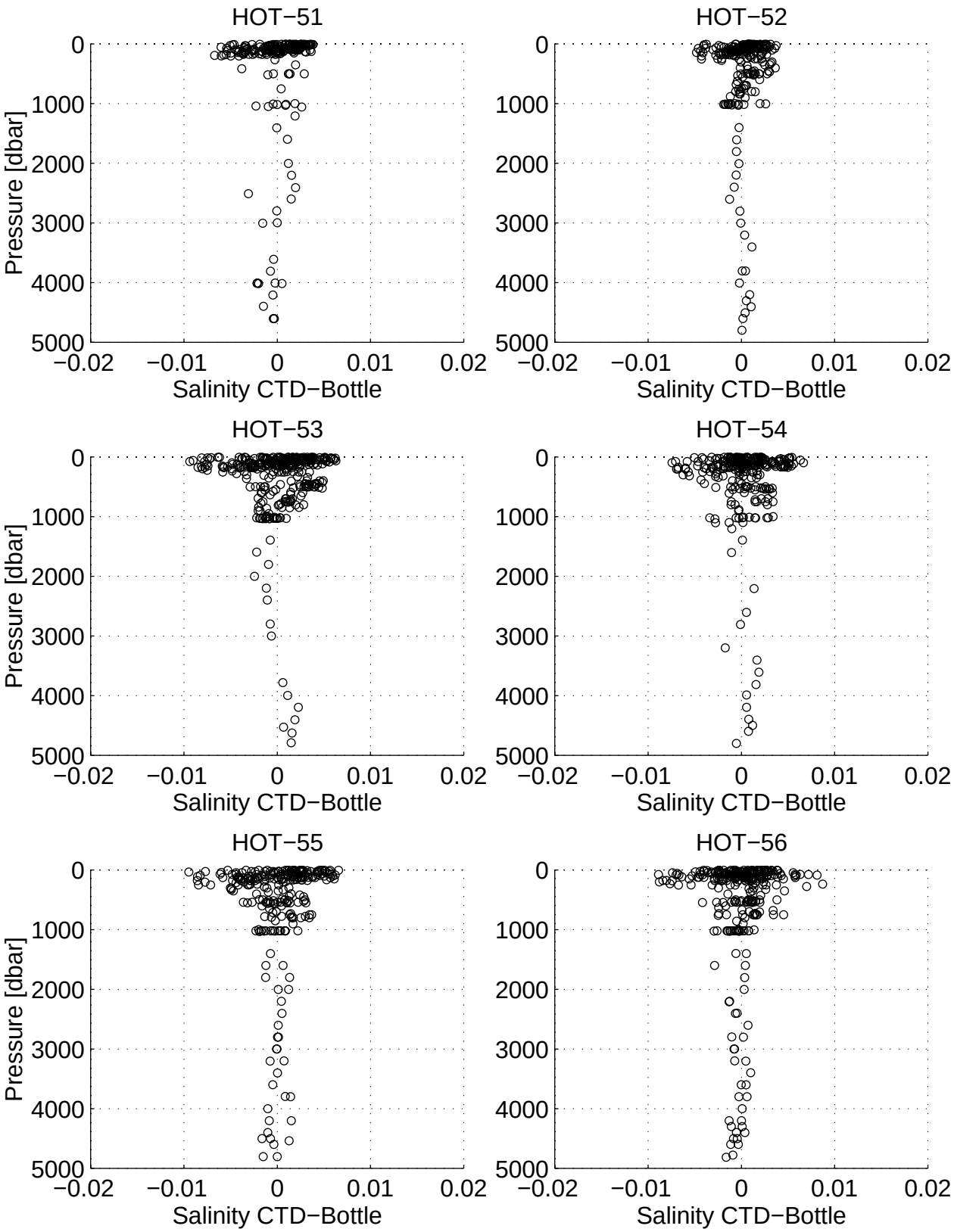

Figure 2.1: Differences between calibrated CTD salinities and bottle salinities for Station ALOHA

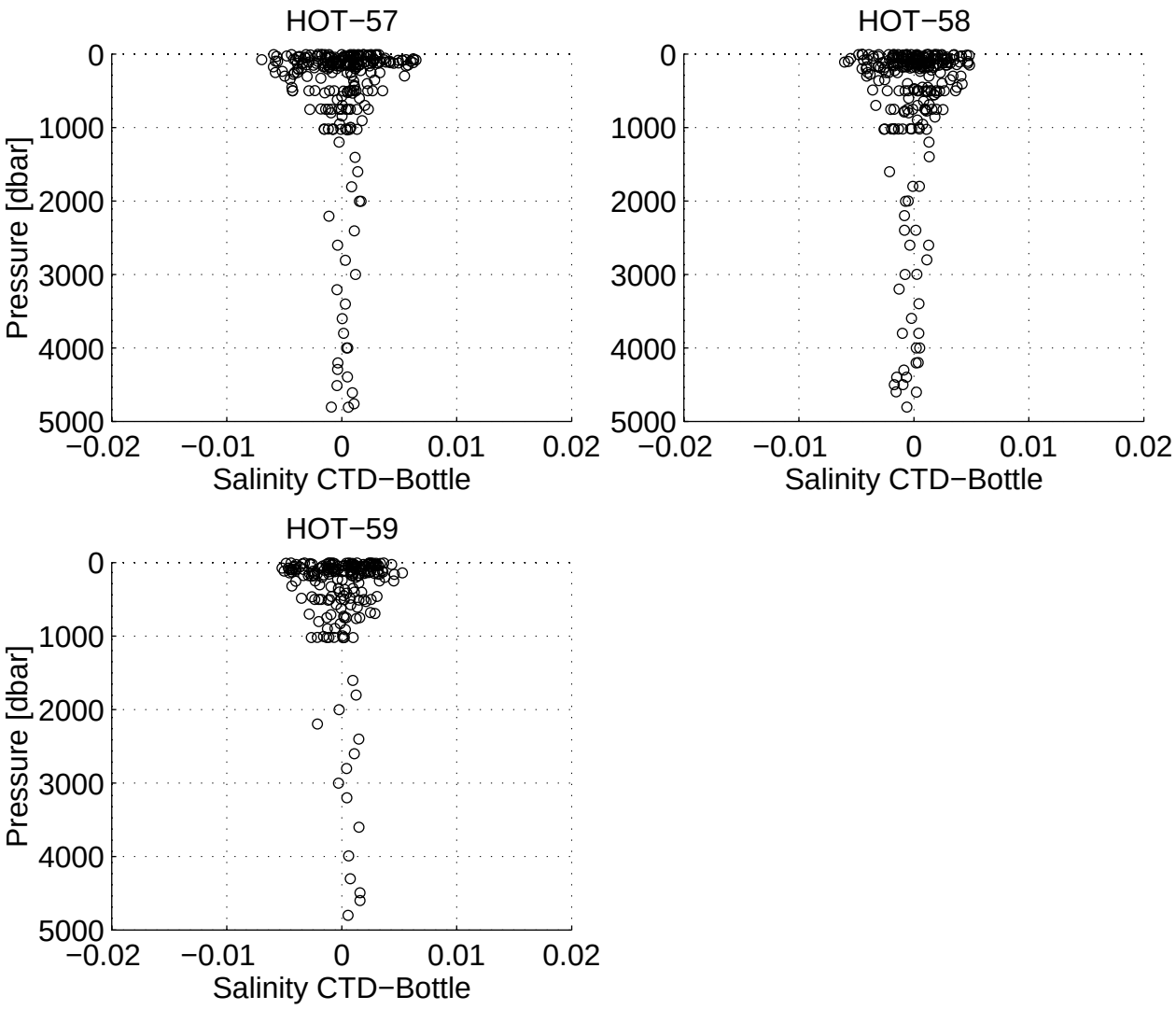

Figure 2.1: continued

Table 2.4:Conductivity Calibration Coefficients

Cruise	Sensor #	b0	b1	b2
51	679	0.000015	-0.000285	
52	679	0.008901	-0.004627	0.000477
53	679	0.013422	-0.006691	0.000697
54	679	0.000809	-0.000679	
	1336	0.000227	-0.000201	
55	679	0.001572	-0.000806	
	1336	0.000510	-0.000275	
56	1336	0.002435	-0.001309	0.000128
	679	0.005245	-0.002677	0.000230
57	1336	0.002188	-0.001166	0.000109
	679	0.004235	-0.002135	0.000171
58	1336	0.000506	-0.000288	
	679	0.004189	-0.002046	0.000168
59	679	0.005144	-0.002503	0.000204
	527	0.005258	-0.002736	0.000234

Table 2.5: Individual Cast Conductivity Offsets (units are Siemens m^{-1}).

Cruise	Station	Cast	C correction
51	2	1	0.00011672
51	2	4	-0.00008016
51	2	5	-0.00021619
51	2	6	-0.00001731
52	2	2	-0.00008146
53	2	2	-0.00023940
53	2	6	-0.00010286
53	2	17	-0.00001033
53	6	1	-0.00051222
54	1	1	-0.00019088
54	2	16	0.00005381
55	2	1	-0.00019795
55	2	21	0.00029719
55	3	1	0.00000000
55	6	1	0.00029719

Table 2.6: CTD-Bottle Salinity Comparison for Each Cruise

		0 to 4700 db		500 to 4700 db	
Cruise	**Sensor**	**Mean**	**St. Dev.**	**Mean**	**St. Dev.**
51	679	0.0000	0.0023	0.0000	0.0015
52	679	0.0001	0.0018	0.0001	0.0010
53	679	0.0003	0.0031	0.0001	0.0016
54	679	0.0001	0.0028	0.0007	0.0017
54	1336	0.0001	0.0025	0.0005	0.0012
55	679	-0.0002	0.0032	0.0001	0.0015
55	1336	-0.0001	0.0024	0.0002	0.0014
56	679	0.0000	0.0027	-0.0001	0.0014
56	1336	0.0000	0.0024	0.0000	0.0014
57	679	0.0000	0.0026	0.0003	0.0011
57	1336	0.0001	0.0025	0.0003	0.0012
58	679	0.0000	0.0021	0.0000	0.0013
58	1336	0.0000	0.0020	0.0001	0.0013
59	679	0.0000	0.0022	0.0000	0.0013
59	527	0.0000	0.0021	0.0000	0.0014

2.1.2.4. oxygen

Two YSI Inc. probes, #13341 and #13251, were used during 1994. Sensor #13251 was used in all the cruises, sensor #13341 was used also in a dual-sensor configuration during cruises HOT-54 through 59. Water bottle oxygen data were screened and the sensors were empirically calibrated following procedures described previously (Winn et al., 1991; Tupas et al., 1993). Analysis of water bottle samples are described in section 2.2.2. The calibration procedure follows Owens and Millard (1985), and consists in fitting on non-linear equation to the CTD oxygen current and oxygen temperature. The bottle values of dissolved oxygen and the downcast CTD observations at the potential density of each bottle trip were grouped together for each cruise to find the best set of parameters with a non-linear least squares algorithm. Two sets of parameters were usually obtained per cruise, corresponding to the casts at Station 1 and 2. In some of the 1994 cruises there was an obvious drift in the CTD oxygen values throughout Station 2 casts, apparently due to sensor electrolyte depletion. These cruises required more than one set of calibration parameters at Station 2.

Comparisons between sensor pairs revealed that sensor #13341 was measuring large voltages in the upper 100 dbar compared to #13251. A close inspection revealed that these values were sometimes reaching the upper bound of the sensor range (5 V), these oxygen values are invalid. The sensor was refurbished with a new head prior to cruise 59, but the problem seems to have been present during cruises HOT-54 through 58.

Sensor #13251 performed correctly during cruises HOT-51 through 53. The oxygen traces from cruise 54 showed a mismatch with the bottle data after calibration, indicating that the sensor malfunctioned. During cruise HOT-55 the sensor failed and gave bad spikes in all the casts. A post-cruise evaluation at Sea-Bird revealed bad contacts between the sensor's head and

the electronics. In light of this problem, sensor #13341 data are reported instead for cruise HOT-55, after the upper 100 dbar from all casts were flagged due to the sensor's problems described above. It was also noticed that the oxygen values from this sensor were drifting during the cruise, requiring three different sets of calibration coefficients for casts at the beginning, the middle and the end of the cruise. In addition, many of the casts exhibited large spikes at various levels, which were flagged as bad. Sensor #13251 data are reported for cruise HOT-54. Although this sensor showed a better calibration than sensor #13341, these data should be used with caution due to the mismatch with the bottle data mentioned before.

The head of sensor #13251 was repaired on 10 August 1994, before cruise HOT-56, but the data obtained during cruises HOT-56, 57 and 58 were not reliable after calibration, indicating further problems with the sensor. In cruise HOT-59, the oxygen trace was noisy, and after the cruise the sensor's membrane was found torn and it was replaced. The data from sensor #13341 are reported here for cruises HOT-56, 57 and 58, after the upper 100 dbar of data were flagged suspect in all casts. In addition, the sensor seemed to have drifted during station 2 casts. These casts required two sets of calibration coefficients (Table 2.7).

Table 2.7 gives the means and standard deviations for the final calibrated CTD oxygen values minus the water sample values. Only results from the sensor's data reported here are included.

Table 2.7: CTD minus Bottle O_2 (µmol kg^{-1}) Comparison for Each Cruise

	Station 1, Kahe Point		Station 2, ALOHA			
	0 to 1500 dbar		0 to 4700 dbar		500 to 4700 dbar	
Cruise	Mean	St. Dev.	Mean	St. Dev.	Mean	St. Dev.
51	0.08	1.51	0.12	2.30	0.34	2.14
52	0.02	1.67	0.04	1.75	0.05	1.85
53	0.03	2.23	0.06	2.21	0.12	2.32
54	0.05	3.10	0.04	2.18	0.07	2.25
55	-0.01	3.45	0.09	0.96	0.10	0.95
			0.09	1.83	0.14	1.44
			0.00	0.13	0.00	0.14
56	0.00	1.61	0.07	1.42	0.09	1.25
			0.00	0.29	0.00	0.33
57	0.00	1.42	0.00	1.26	0.06	0.61
			0.00	1.76	0.31	1.34
58	0.00	2.04	0.00	0.24	0.00	0.25
			0.00	1.52	0.08	1.49
59	0.07	2.55	0.03	1.38	0.07	1.53

2.1.2.5. flash fluorescence

Flash fluorescence was measured with a Sea Tech Model ST0250 flash fluorometer and the data collected with the Sea Bird CTD system. Flash fluorescence traces were collected on as many casts as possible. Because an absolute radiometric standard is not available for flash fluorometers, instrument drift was corrected by checking the relative response of the instrument between cruises using fluorescent plastic sheeting as described in Tupas et al. (1993). A linear relationship of the form Vn = b Vo + a was used to convert all fluorescence data to a common voltage scale, where Vn is the normalized voltage, Vo is the output voltage and a and b are constants derived from the two deep water intervals. The constants during 1994 are given in Table 2.8.

2.1.2.6. beam transmission

Beam transmission was measured with a Sea Tech 25 cm path length transmissometer. Transmission data were collected using the Sea Bird CTD system in a fashion analogous to that described for flash fluorescence. The transmissometer was calibrated as described by the manufacturer before each cruise to correct for instrument drift. To calculate percent transmission the following relationship was used: %T = 20 [(V-offset) (a/b)] where V is the measured voltage, and a and b are the empirically derived calibration factors. The calibration parameters used during 1994 are given in Table 2.8.

Table 2.8: Fluorescence and Transmission Calibration Factors

	Fluorescence		Transmission		
Cruise #	**a**	**b**	**a**	**b**	**offset**
51	2.9318	0.3112	2.282	4.68	0.00
52	2.9318	0.3112	2.282	4.64	-0.001
53	2.9318	0.3112	2.282	4.64	-0.001
54	1.6669	0.6503	19.906	0.000	0.25
55	1.6669	0.6503	19.944	0.000	0.25
56	1.6669	0.6503	19.944	0.000	0.25
57	1.6669	0.6503	no data	no data	no data
58	1.6669	0.6503	20.318	0.0203	0.25
59	1.6669	0.6503	20.318	0.0203	0.25

2.2. Discrete Water Column Measurements

Water samples for chemical analyses were collected at Station Kahe and ALOHA as well as other stations. Sampling strategies and procedures are well documented in the previous data reports (Tupas et al. 1993, Winn et al. 1993) and in the HOT-JGOFS protocol manual (Karl et al. 1990; available over Internet, see Section 8). This data report contains only a subset of the total data base which can be extracted from the accompanying diskette or via anonymous ftp over Internet. To assist in the interpretation of these data and to save users the time to estimate the precision of individual chemical analysis, we have summarized precision estimates from replicate determinations for each constituent on each HOT cruise in 1994.

2.2.1. Salinity

Salinity samples were collected, stored and analyzed as described in Tupas et al. (1993). The results of laboratory standard analyses run for each cruise are presented in Table 2.9. The typical precision estimate for salinity measurements made in 1994 is better than 0.001. The large standard deviation value obtained for cruise HOT-51 is the result of a temperature control problem experienced with the Autosal during the measurement runs for that cruise. The salinities affected by this problem were flagged after comparing them against the calibrated CTD salinities as explained in section 2.1.2.3. A total of 64 bottles from this cruise were flagged bad or suspect, about three times the amount of bottles flagged in any other regular cruise.

Substandard batches were prepared on the following dates: batch #7 was made on 23 March 1993, batch #8 was made on 17 May 1994 and batch #9 was made on 28 Nov 1994. Batch #7a was made on an emergency basis as the amount of substandard water available had become low. Water remaining after batch #7, which was stored in a carboy, was prepared for use as batch #7a. The carboy was not sealed with white oil, thus it was subject to evaporation and had a salinity greater than batch #7. The Autosal was tested with the small amount of batch #7 remaining to make sure it was still performing properly before cruise HOT-52 salinity measurement were made with batch #7a.

Table 2.9: Precision of Salinity Measurements Using Lab Standards

HOT	Mean Salinity ± SD	# Samples*	Substandard Batch #	IAPSO Batch #
51	34.45993 ± 0.032846*	6	7	p118
52	34.54006 ± 0.001052	13	7a	p121
53	34.47379 ± 0.000294	14	8	p121
54	34.47273 ± 0.000699	18	8	p118, p121
55	34.47430 ± 0.001475	25	8	p121
56	34.47373 ± 0.000287	18	8	p121
57	34.47171 ± 0.000475	25	8	p121
58	34.47212 ± 0.000593	26	8	p123
59	34.49174 ± 0.000256	14	9	p123

*Number of samples of substandard salinity measurement taken during each run.
**See text for explanation of high standard deviation.

2.2.2. Oxygen

Oxygen samples were collected and analyzed using a computer controlled potentiometric end-point titration procedure as described in Tupas et al. (1993). As in previous years we measured, using a calibrated digital thermistor, the temperature of the seawater sample within the individual Niskin bottles at the time the iodine flask was filled. This was done to evaluate the magnitude of oxygen sample temperature error which affects the calculation of oxygen concentrations in units of μmol kg^{-1}.

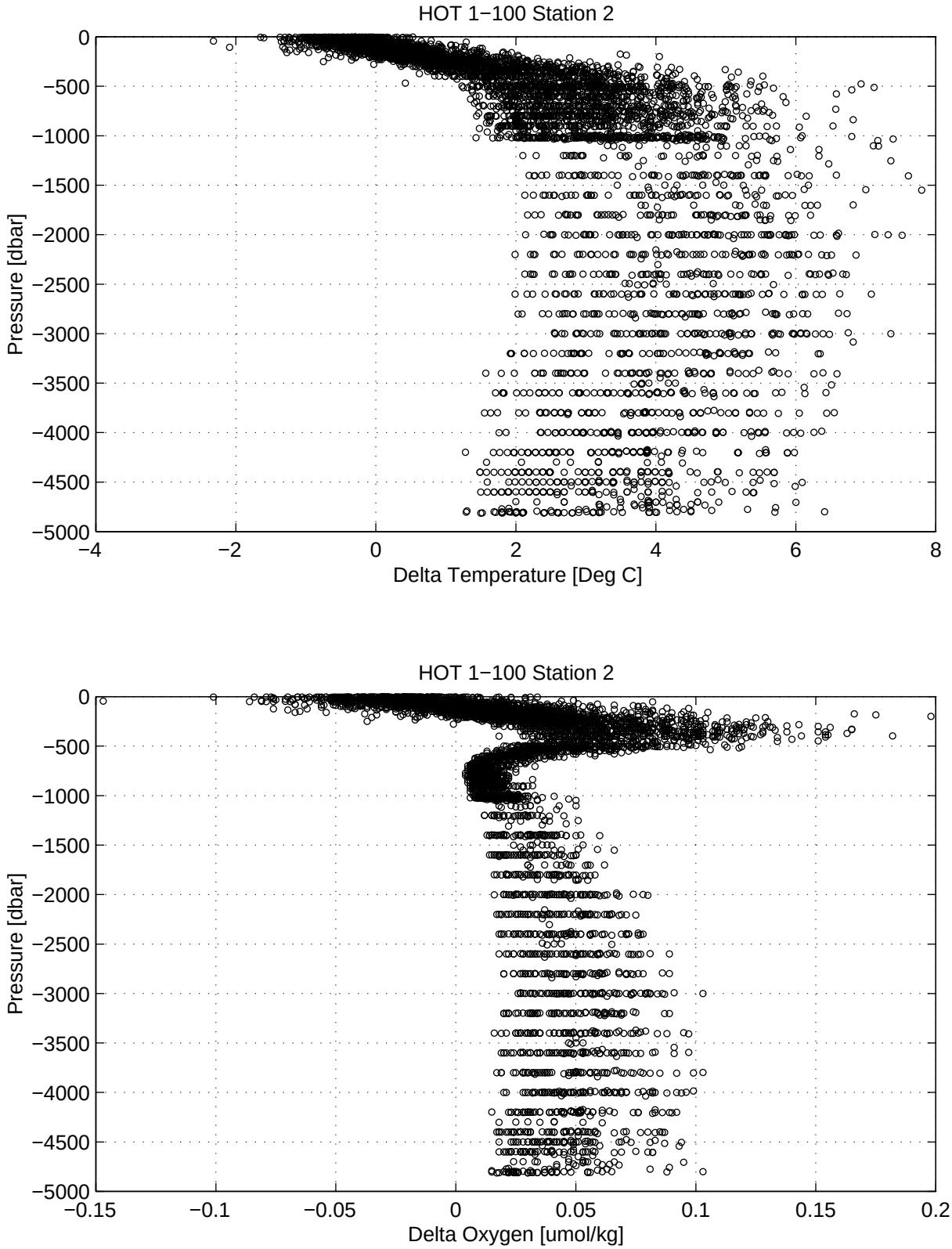

Figure 2.2:Upper Panel: Difference between sample temperature at the time of sample collection and potential temperature calculated from *in situ* temperature at the time of bottle trip. Lower Pannel: Difference in oxygen concentration in units of µmol kg^{-1} using temperatures measured at the time of sample collection and potential temperature computed from *in situ* temperature.

Figure 2.2 (upper panel) shows a plot of the difference between on-deck sample temperature and potential temperature, computed from the in situ
temperature measured at the time of bottle trip, versus pressure. The lower panel of the same figure shows a plot of the difference between oxygen concentration using on-deck and potential temperatures versus pressure. The depth dependent variability in Δ oxygen is a result of the absolute magnitude of the oxygen concentration and the standard procedures we employ for sampling the water column. For work of the highest accuracy, this error should be considered.

The precision of our oxygen analyses was assessed from both an analytical and field perspective and is presented in Table 2.10. The mean analytical and field precision of our oxygen analyses in 1994 was 0.12% and 0.10% with a mean standard deviation of 0.21 and 0.18 µmol l^{-1}, respectively. Oxygen concentrations measured over the 6 years of the program are plotted at three constant potential density horizons in the deep ocean along with their mean and 95% confidence intervals (Figure 2.3). The deviations ranged (maximum - minium values) from a low of 2.5 µmol kg^{-1} at σ_θ = 22.758 to 2.7 µmol kg^{-1} at σ_θ = 27.675. These results indicate that analytical consistency has been maintained over the first 6 yrs of the HOT program.

Table 2.10: Precision of Winkler Titration

HOT	Analytical CV %	Analytical SD µmol l^{-1}	n	Field CV %	Field SD µmol l^{-1}	n
51	0.14	0.26	8	0.11	0.17	21
52	0.12	0.19	8	0.10	0.19	13
53	0.07	0.10	8	0.07	0.12	13
54	0.07	0.09	6	0.11	0.23	10
55	0.15	0.26	6	0.08	0.15	12
56	0.18	0.22	5	0.08	0.15	15
57	0.07	0.13	4	0.15	0.24	16
58	0.22	0.46	5	0.12	0.19	13
59	0.07	0.15	6	0.15	0.29	11

2.2.3. Dissolved Inorganic Carbon and Titration Alkalinity

Samples for dissolved inorganic carbon (DIC) were measured using a Single Operator Multi-parameter Metabolic Analyzer (SOMMA) which was manufactured at the University of Rhode Island and standardized at the Brookhaven National Laboratory. Analyses of primary DIC standards (Tupas et al. 1993) indicated that the precision of replicate samples is approximately 1 µmol kg^{-1}. Titration alkalinity was determined using the Gran titration method as described in Tupas et al. (1993). The precision of the titration procedure was approximately 5 µequiv kg^{-1}. Accuracy was established with certified reference standards obtained from Dr. Andrew Dickson at Scripps Institution of Oceanography.

Figure 2.3: Oxygen versus time at three density horizons at Station ALOHA. Upper panel: Oxygen concentration at potential densities of 27.782, 27.758 and 27.675 during 1994. Lower panel: Oxygen at these same three density horizons including all 6 years of program.

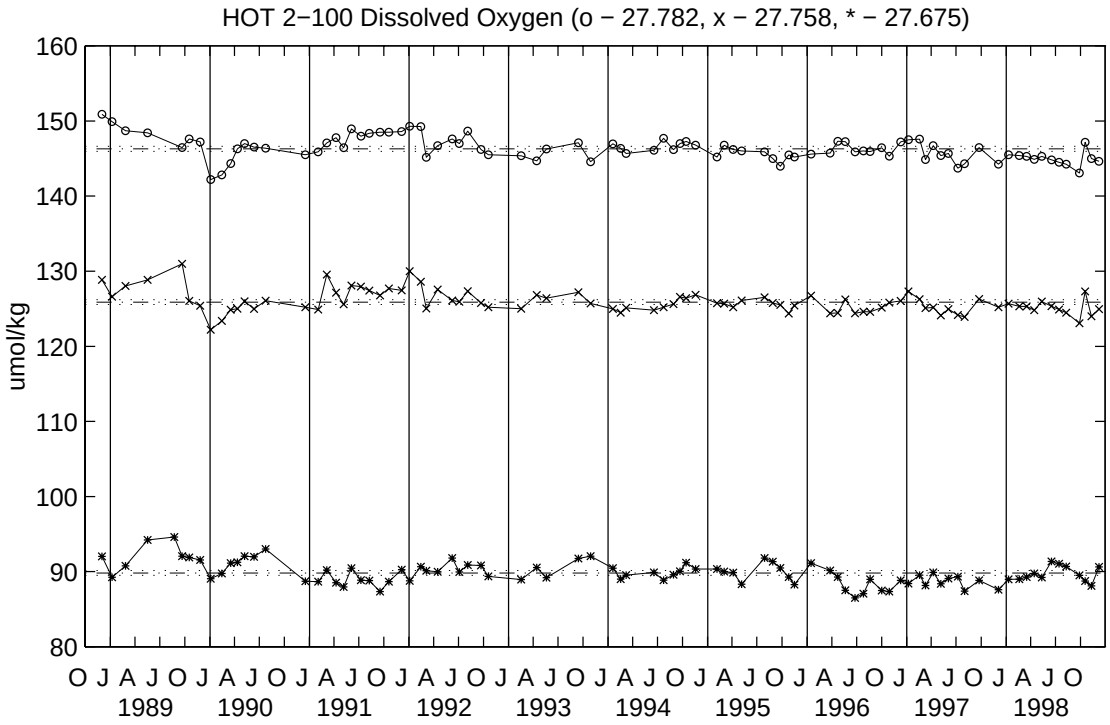

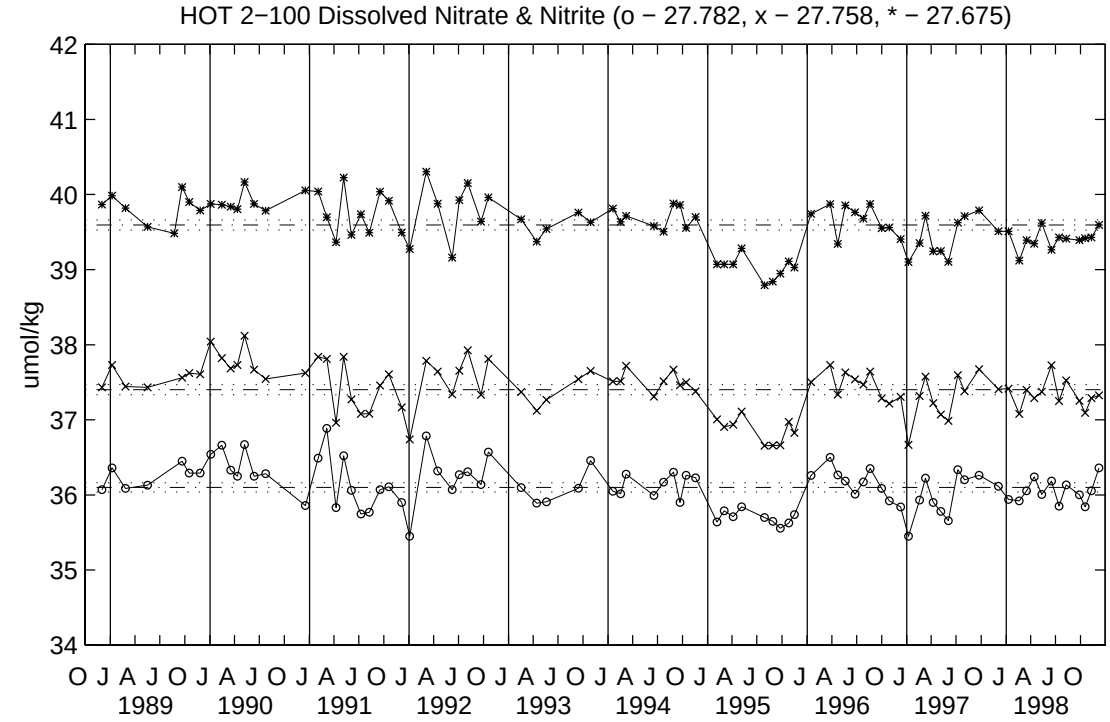

Figure 2.4: As in Figure 2.3, except for concentrations of dissolved nitrate plus nitrite.

2.2.4. pH

In 1994, pH was determined spectrophotometrically using the indicator m-cresol purple following the methods described in Tupas et al. (1993). The absorbance of the mixture was measured at 578 and 434 nm on a Perkin Elmer Model 3 dual-beam spectrophotometer and converted to pH on the seawater scale according to Clayton and Byrne (1993).

2.2.5. Dissolved Inorganic Nutrients

Samples for the determination of dissolved inorganic nutrients (soluble reactive phosphorus, [nitrate+nitrite], and silicate concentrations) were collected as described in Tupas et al. (1993). Analyses were conducted at room temperature on a four-channel Technicon Autoanalyzer II continuous flow system (Winn et al. 1991). A summary of the precision of analyses for 1994 is shown in Table 2.11. Figures 2.4-2.6 show the mean and 95% confidence limits of nutrient concentrations measured at three potential density horizons for the 6 years of the program. In addition to standard automated nutrient analyses, specialized chemical methods (section 2.2.7) were used to determine concentration of nutrients that are normally below the detection limits of autoanalyzer methods.

Table 2.11: Precision of Dissolved Nutrient Analyses

	Soluble Reactive Phosphorus				Nitrate + Nitrite				Silicate			
	Analytical		Field		Analytical		Field		Analytical		Field	
HOT	mean CV (%)	mean SD (µM)	mean CV (%)	mean SD (µM)	mean CV (%)	mean SD (µM)	mean CV (%)	mean SD (µM)	mean CV (%)	mean SD (µM)	mean CV (%)	mean SD (µM)
51	0.8	0.010	0.4	0.006	0.2	0.067	0.5	0.064	0.4	0.13	0.2	0.11
52	0.6	0.010	0.3	0.007	0.2	0.079	0.2	0.031	0.6	0.15	0.4	0.31
53	0.4	0.013	0.3	0.006	0.2	0.091	0.1	0.040	0.1	0.13	0.3	0.29
54	0.4	0.009	0.4	0.007	0.2	0.071	0.3	0.057	0.3	0.18	1.4	0.41
55	0.7	0.015	0.5	0.008	0.4	0.15	0.2	0.050	0.5	0.48	5.1	0.42
56	0.8	0.019	0.4	0.007	0.3	0.058	0.2	0.037	0.2	0.18	2.0	0.58
57	0.9	0.006	0.7	0.010	0.3	0.079	0.2	0.040	0.8	0.23	0.4	0.46
58	0.4	0.008	0.4	0.006	0.2	0.056	0.3	0.067	0.4	0.10	0.5	0.23
59	0.7	0.014	0.7	0.012	0.2	0.058	0.3	0.058	1.2	0.16	0.7	0.68

Figure 2.5: As in Figure 2.3, except for concentrations of soluble reactive phosphate.

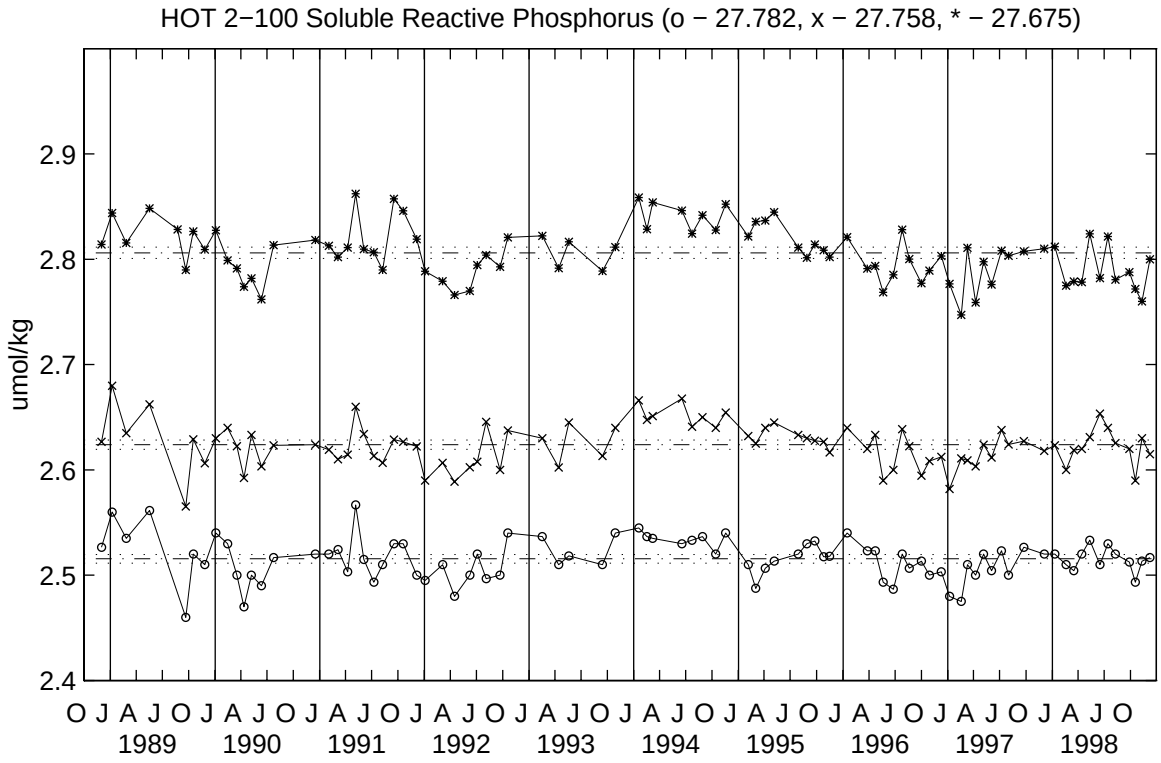

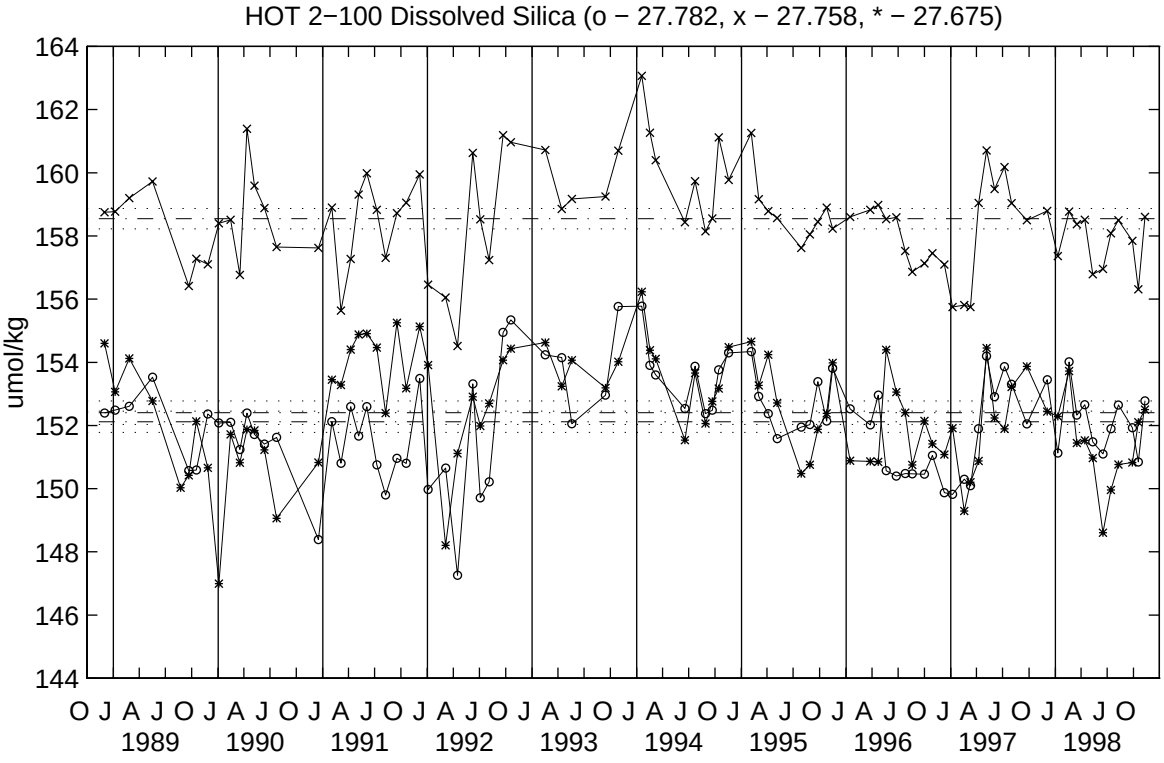

Figure 2.6: As in Figure 2.3, except for concentrations of silicate.

2.2.6. Dissolved Organic Nutrients

Dissolved organic carbon (DOC) was determined by the high temperature catalytic oxidation method described in Tupas et al. (1994). Water samples were collected in acid-washed polyethylene tubes and were stored frozen until analyzed. The oxidation method used a pure platinum catalyst with infrared detection on a LICOR 6252 carbon dioxide analyzer. Dissolved organic nitrogen (DON) was calculated as the difference between total dissolved nitrogen (TDN) and nitrate plus nitrite concentrations determined by the autoanalyzer (Section 2.2.5.). TDN and nitrate plus nitrite were determined as described in Tupas et al. (1993). Dissolved organic phosphorus (DOP) was calculated as the difference between total dissolved phosphorus (TDP) and SRP concentrations. TDP and SRP were determined as described in Tupas et al. (1993). A summary of the precision of these analyses is given in Table 2.12. As of the publication of this report, DOC measurements were incomplete, thus no precision values are available. The data will be on the network before the end of 1995. DON and DOP concentrations over the 6 years of the program at the 500 and 1000 dbar horizon are plotted with their mean and 95% confidence intervals (Figures 2.7 and 2.8).

Table 2.12: Precision of Dissolved Organic Nutrient Analyses

	DON		DOP	
Cruise	**mean cv (%)**	**mean sd (µmol kg^{-1})**	**mean cv (%)**	**mean sd (µmol kg^{-1})**
51	8.1	0.21	5.2	0.011
52	4.2	0.20	3.2	0.005
53	8.1	0.27	8.0	0.016
54	13.0	0.22	4.3	0.011
55	7.1	0.28	1.5	0.002
56	11.1	0.47	14.5	0.026
57	14.2	0.33	6.4	0.007
58	9.8	0.29	4.9	0.007
59	25.0	0.52	14.6	0.019

2.2.7. Low-Level Nutrients

The chemiluminescent method of Cox (1980) as modified for seawater by Garside (1982) was used to determine the nitrate plus nitrite content of surface to 100 meter water samples (Tupas et al. 1993). The limit of detection for nitrate plus nitrite was approximately 2 nM with a precision and accuracy of ±1 nM.

Low level SRP concentrations in the euphotic zone were determined according to the magnesium induced coprecipitation (MAGIC) method of Karl and Tien (1992). Typical precision estimates for triplicate determinations of SRP are from 1-3% with a limit of detection of 10 nmol l^{-1}.

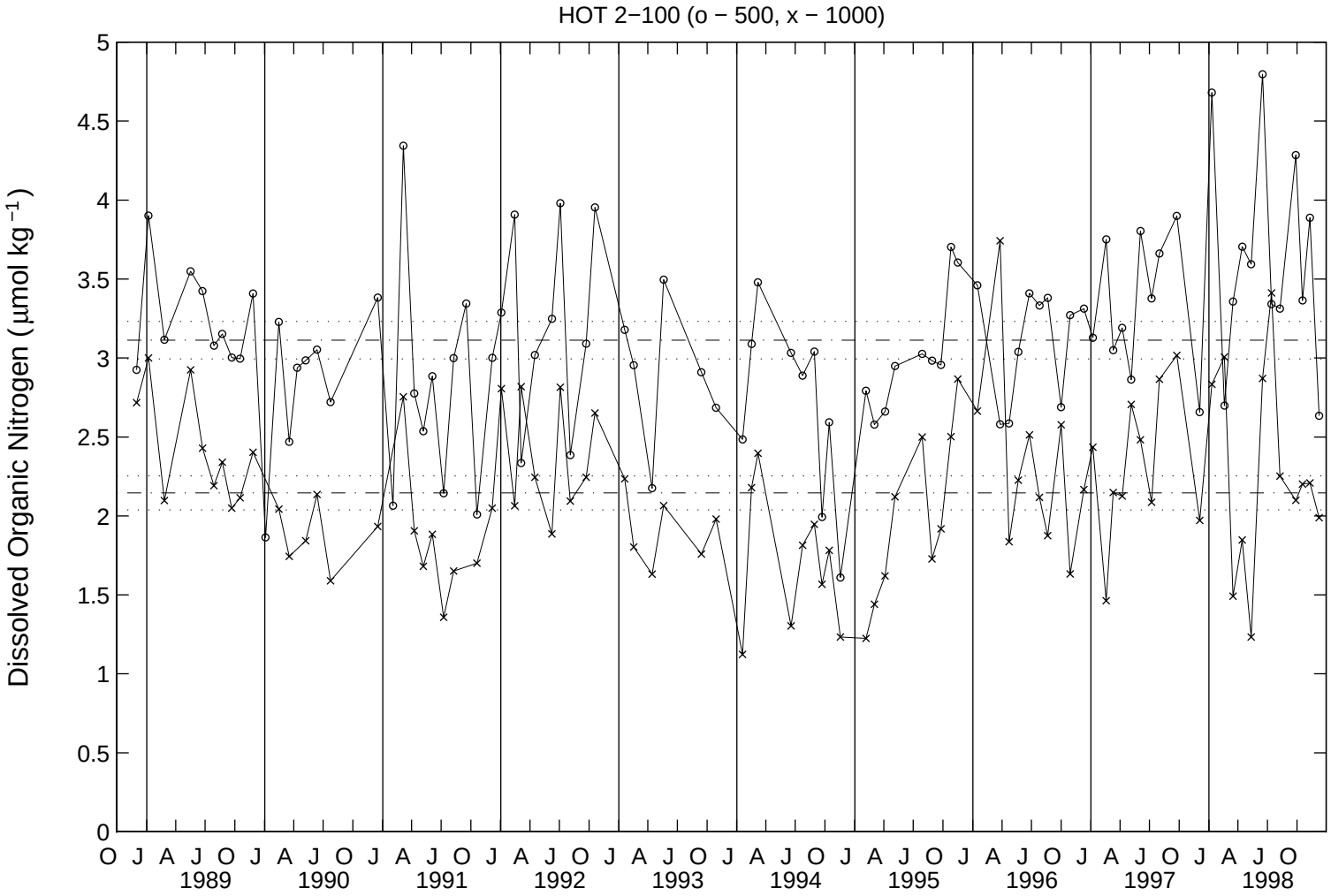

Figure 2.7: DON versus time at 500 and 1000 dbar horizons at Station ALOHA. Upper panel: DON concentrations during 1994. Lower panel: DON concentrations from 1988-1994.

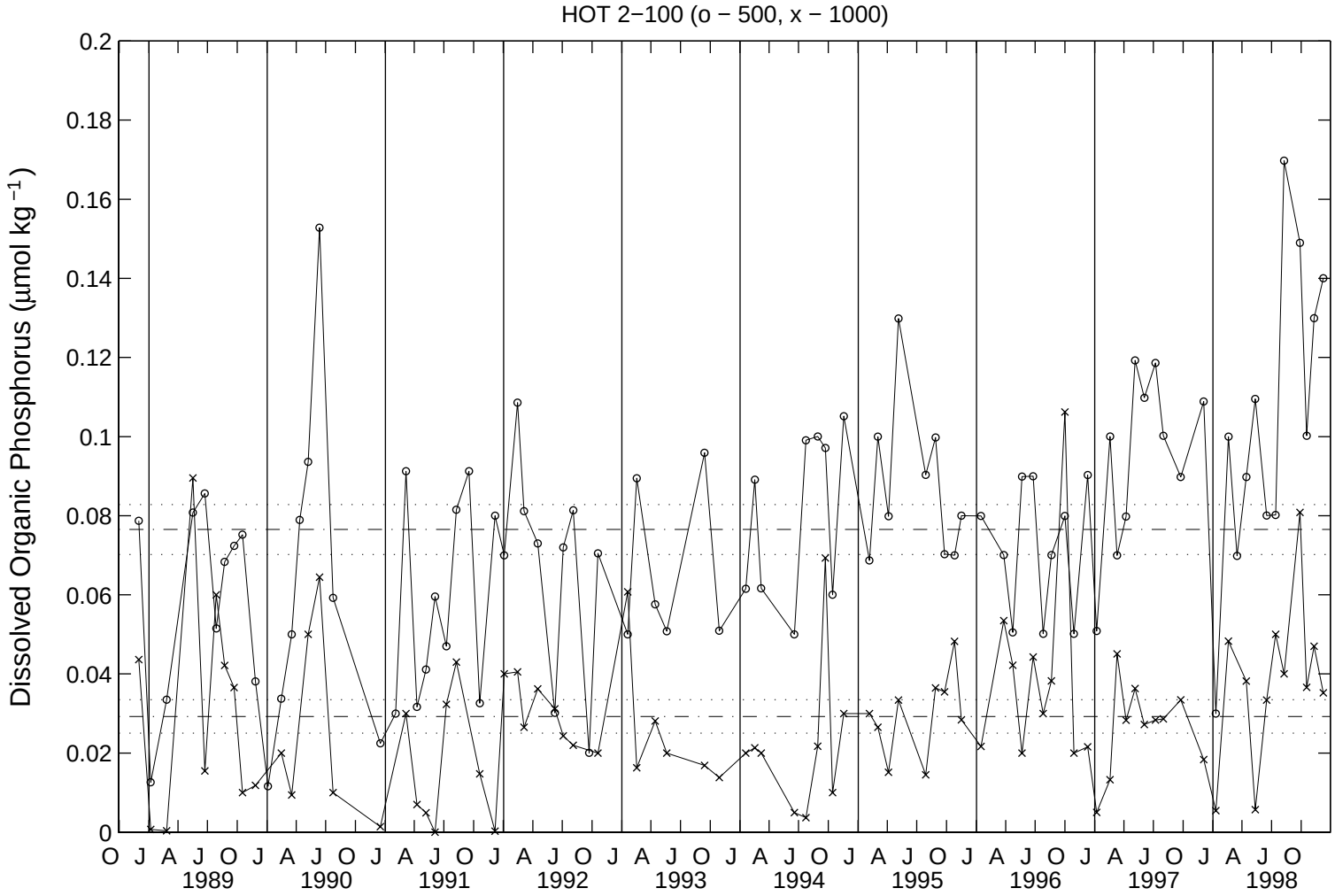

Figure 2.8: Same as Figure 2.7 but for dissolved organic phosphorus.

2.2.8. Particulate Matter

Samples for analysis of particulate matter were prefiltered through 202- µm Nitex mesh to remove large zooplankton and collected onto combusted GF/F glass fiber filters. Particulate carbon (PC) and nitrogen (PN) on the filters were analyzed using a Perkin-Elmer 2400 CHN analyzer for cruises HOT-51 to 53 and with a Europa automated nitrogen and carbon analyzer from cruises HOT-54 to 59. Particulate phosphorus (PP) was analyzed by converting the material to orthophosphate by high temperature ashing followed by acid hydrolysis and determining the orthophosphate content by spectrophotometry.

2.2.9. Pigments

Chlorophyll a (chl *a*) and phaeopigments were measured fluorometrically using 100% acetone as the extractant and standard techniques (Strickland and Parsons, 1972). Analytical precision for this analysis is presented in Table 2.13. Integrated values for pigment concentrations were calculated using the trapezoid rule.

We also measured chl *a* and accessory photosynthetic pigments (Table 2.14) by high performance liquid chromatography (HPLC) according to Bidigare et al. (1990). A new HPLC method following SCOR recommendation was adopted in 1994. This method is a modification of the method developed by Wright et al. (1991). The new method allows for a better separation of lutein and zeaxanthin as well as monovinyl and divinyl chlorophyll *a*. A comparison of the two methods was done on cruise HOT-52. The results are presented in Figure 2.9. The new method does not show any significant difference from the old one but has the advantages mentioned above.

2.2.10. Adenosine 5'-Triphosphate

Water column adenosine 5'-triphosphate (ATP) concentrations were determined using the firefly bioluminesence technique as described by Karl and Holm-Hansen (1978). The precision of ATP determinations in 1993 are given in Table 2.15.

Table 2.13: Precision of Flurometric Chlorophyll *a* and Phaeopigment Analyses

Cruise	Chl *a* CV(%)	SD (µg l^{-1})	Phaeo CV(%)	SD (µg l^{-1})
51	3.4	0.005	5.6	0.012
52	2.5	0.004	5.8	0.011
53	4.6	0.009	5.8	0.014
54	3.2	0.006	5.4	0.009
55	3.4	0.008	4.1	0.012
56	9.0	0.005	4.5	0.006
57	4.2	0.007	7.9	0.024
58	3.3	0.006	7.8	0.022
59	3.6	0.006	3.9	0.009

Table 2.14: HPLC Pigment Analysis

Pigment	RF[a]	RT[b]
Chlorophyll c & Mg 2,4D[c]	0.000236	
Peridinin	0.000498	0.519
19'-Butanoyloxyfucoxanthin	0.000375	0.541
Fucoxanthin	0.000372	0.578
19'-Hexanoyloxyfucoxanthin	0.000364	0.601
Prasinoxanthin	0.000364	0.666
Diadinoxanthin	0.000251	0.758
Alloxanthin	0.000268	0.816
Lutein	0.000344	0.873
Zeaxanthin	0.000273	0.888
Chlorophyll *b* (monovinyl+divinyl)	0.000932	0.953
Chlorophyll *a* (monovinyl)	0.000436	1.000
Chlorophyll *a* (divinyl)	0.000697	1.000
α-carotene	0.000276	1.131
β-carotene	0.000285	1.137

[a]RF - Response Factor (mg pigment per unit absorbance peak area at 436 nm).
[b]RT - Retention Time (relative to chlorophyll *a*)
[c]Chlorophyll c = (c_1+c_2+c_3),
Mg 2,4,D = Mg 2,4, divinyl pheoporphyrin a_5 monomethyl ester

Table 2.15: Precision of ATP Analyses

Cruise	CV (%)	SD (µg m^{-3})
51	11.8	2.0
52	7.2	1.4
53	8.4	2.1
54	9.8	5.3
55	6.4	1.5
56	10.7	2.2
57	11.7	4.0
58	10.8	2.5
59	9.6	3.1

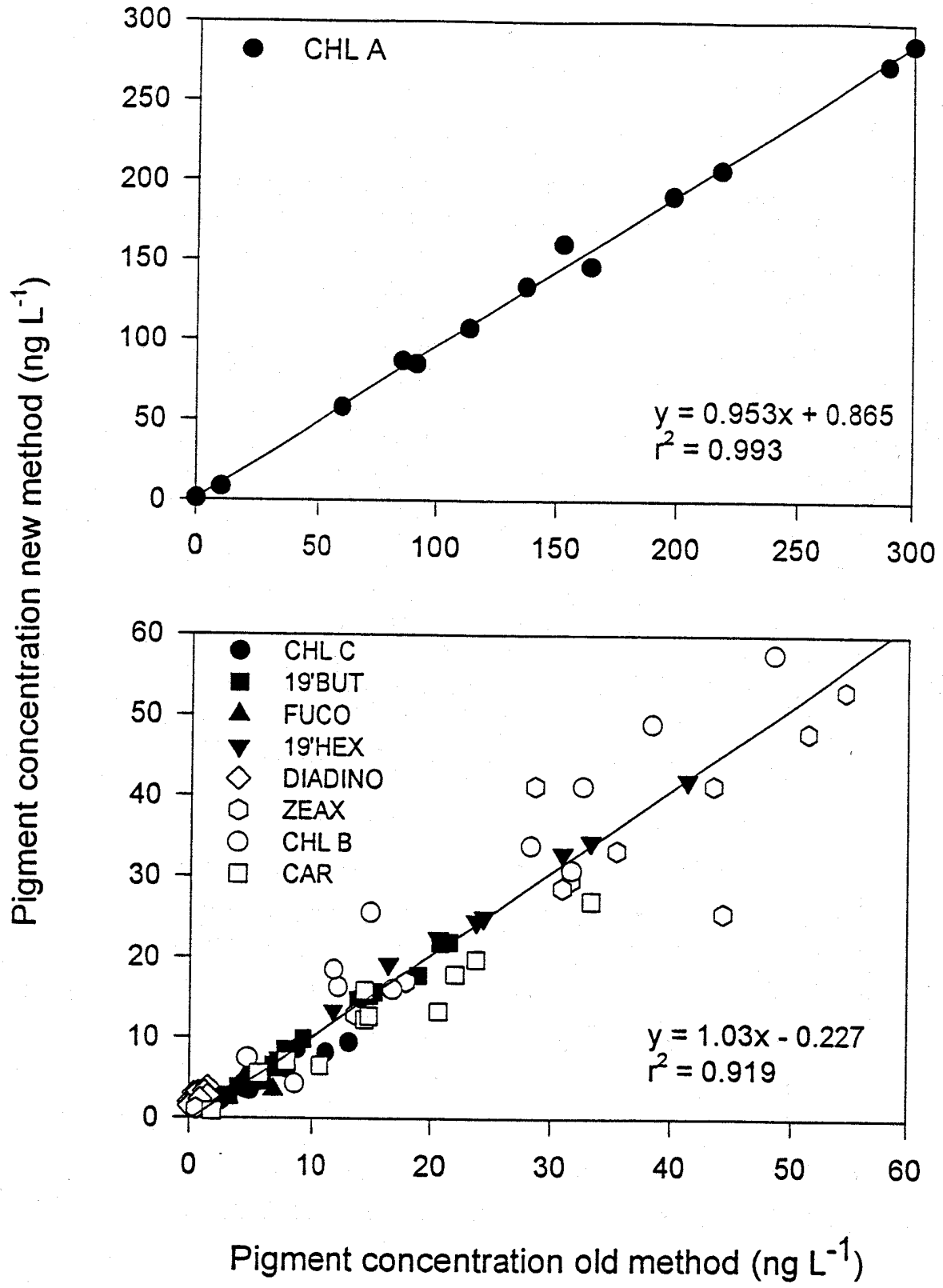

Figure 2.9: Comparison of HPLC methods used to quantify plant pigments

2.3. Biogeochemical Rate Measurements

2.3.1. Primary Productivity

Photosynthetic production of organic matter was measured by a trace-metal clean, C^{14} method. Incubations were conducted in-situ at eight depths for at least 12 hours using a free-drifting array as described by Winn et al. (1991). Integrated carbon assimilation rates were calculated using the trapezoid rule with the shallowest values extended to 0 meters and the deepest extrapolated to a value of zero at 200 meters. The experiment was not conducted during HOT-59 because of gale force conditions during the cruise.

2.3.2. Particle Flux

Particle flux was measured at reference depths of 150, 300 and 500 meters using sediment traps deployed on a free-floating array for approximately 72 hours during each cruise. Sediment trap design and collection methods are described in Winn et al. (1991). Samples were analyzed as described in section 2.2.8. The drifts of the sediment trap arrays are shown in Figure 6.1.1. to 5. The array was not deployed during HOT-59 because of gale force conditions during the cruise.

2.4. ADCP Measurements

Shipboard ADCP data were obtained on all nine HOT cruises using an RDI model VM-150 mounted on the R/V Moana Wave. Major ADCP recording gaps occurred on the following cruises: HOT-51 during the northbound transit and at the start of the on-station period; HOT-54 at the at the start of the cruise and 1.5 days during the on-station period; HOT-59 at the end of the northbound transit. GPS gaps, besides the times mentioned above, occurred on: HOT-55 near the end of the on-station period, HOT-56 near the middle and at the end of the northbound transit. GPS heading was recorded on all cruises except HOT-51 (the Sun workstation was not on-board), with sizable gaps and/or numerous dropouts on HOT-54, HOT-55, HOT-56 and HOT-57.

2.5. Optical Measurements

Incident irradiance at the sea surface was measured on each HOT cruise with a LICOR LI-200 data logger and cosine collector. Vertical profiles of Photosynthetically Available Radiation (PAR) were also obtained using a Biospherical Instrument model PNF-300 optical profiler. The entire data set is available via Internet, as described in Section 8.

2.6. Meteorology

Wind speed and direction, atmospheric pressure, wet- and dry-bulb air temperature, sea surface temperature (SST), cloud cover and sea state were collected at four-hour intervals while on Station ALOHA. Additionally, hourly wind speed and direction were obtained from NDBC buoys 51001 (23.4 N, 162.3W) and 51026 (21.4 N, 156.96 W). The time series of shipboard observations were plotted and obvious outliers were identified and flagged. The SST-dry air temperature and wet-dry air temperature plots helped to identify further outliers. The buoy wind data were plotted during the cruise time period together with the shipboard data which also

helped to identify outliers. Data from buoy #51001 were available during cruises HOT 51 and 52 and HOT 55 to 59; and data from buoy #51026 for cruises HOT-53 and 54.

2.7. Inverted Echo Sounder Network

Two inverted echo sounders (IESs) recorded data during 1994. The IES located at the center of Station ALOHA station (C) was deployed on 19 May 1993 and recovered on 21 June 1994. The data from this IES were unreadable and only a short section of the time series was recovered. Another IES was deployed at Station Kaena on 23 May 1993, and recovered on 18 June 1994. The history of the IESs in the HOT site is well documented in Tupas et al. (1994a). New IESs were deployed at each site at the same time as the recovery dates in 1994. These two IESs were placed in their respective locations in order to span the Hawaiian Ridge Current.

2.8. Bottom Moored Sediment Traps

Two sets of bottom moored sediment traps have been succeffuly deployed and retrieved at a location borth of Station ALOHA (Fig. 1.1). The first set (ALOHA-I) was deployed on June 1992 and retrieved on June 1993. The second set (ALOHA-II) was deployed on September 1993 and retrieved on September 1994. Each set of traps consisted of four McLane MK7-21 sequencing sediment collectors located at 800, 1500, 28000 and 4000 meters. Fresh sampling cups are rotated into the collector position on a 17 day cycle. Samples from each cup are initially split into four 60-ml volumes (also referred to as splits). Each split is further divided into the volumes required for the various analyses (Table 2.16).

Table 2.16: Distribution of Sample Materials From Bottom Moored Sediment Traps

Investigators	Analyses
Karl, Tupas, Hebel. Magaard, Houlihan University of Hawaii	Total mass, dissolved N, P, Si, total and biogenic particulate C, N, P, Si, fluorometric chlorophyll a, phaeopgiments, stable C,N isotopes, bacterial abundance
Bidigare, Latasa, Ondrusek, Scharek University of Hawaii	Plant pigments by HPLC, diatom abundance and composition
Bird University of Quebec at Montreal	Virus abundance
Honjo, Manganini Woods Holie Oceanographic Institute	Lithogenic analysis
Sautter, Dulaney College of Charleston	Foraminiferan abundance

3. Cruise Summaries

3.1. HOT-51: Dale Hebel, Chief Scientist

Ship departed Snug Harbor at 0930, 18 January 1994 with 14 scientists on-board. Weather was generally poor with strong winds and high seas. Stations Kahe, Kaena, ALOHA and 3 were occupied during this cruise. Despite the weather all CTD operations were successfully conducted and all water samples for core and ancillary measurements were taken. Primary production and sediment trap experiments were successfully conducted. During the first deployment of the zooplankton net, the kevlar line parted and the net and associated equipment were lost. The back-up net was used for the remainder of the cruise. A towed surface-water sampler was deployed during transit between stations. A water-transfer system was deployed with the sediment trap array. A continuous water sampler was tested during the cruise. No other problems were encountered during the cruise. The ship docked at Snug Harbor at 0800 on 23 January 1994.

3.2. HOT-52: Dale Hebel, Luis Tupas, Co-Chief Scientists

Ship departed Snug Harbor at 0900, 15 February 1994 with 17 scientists on-board. Weather was generally good with moderate winds and seas. Stations Kahe, Kaena, ALOHA and 3 were occupied during this cruise. All CTD operations were successfully conducted and all water samples for core and ancillary measurements were taken. Primary production and sediment trap experiments were successfully conducted. A new zooplankton net was successfully deployed from the stern using the capstan. The continuous water sampler, water transfer system and surface water sampler were tested during this cruise. No major equipment problems were encountered. The ship docked at Snug Harbor at 0800 on 20 February 1994.

3.3. HOT-53: Roger Lukas, Chief Scientist

Ship departed Snug Harbor at 0900, 5 March 1994 with 14 scientists on-board. Weather was generally good with moderate winds and seas. Stations Kahe, Kaena, ALOHA and 3 were occupied during this cruise. A bow frame was constructed and fitted on the ship to hold an array of sensors. All systems were functioning well during the cruise. A surface water sampler was towed in between stations. All CTD operations were successfully conducted and all water samples for core and ancillary measurements were taken. Primary production and sediment trap experiments were successfully conducted. The zooplankton net was successfully deployed from the stern using the capstan. A free-rising profiler was deployed and retrieved as time permitted. Problems were encountered during the CTD cast at Station Kahe. The cast was aborted and the ship proceeded to Station Kaena as the CTD was repaired. The CTD was repaired and functioning properly at Station Kaena. Work at Station Kahe was completed on the return leg to Snug Harbor. The ship docked at Snug Harbor at 0630 on 12 March 1994.

3.4. HOT-54: Luis Tupas, Chief Scientist

Ship departed Snug Harbor at 0900 on 17 June 1994 with 17 scientist on-board. Weather was generally good with moderate winds and seas. Stations Kahe, Kaena and ALOHA were occupied during this cruise. The inverted echo sounders (IES) at Stations Kaena and ALOHA were successfully recovered despite some difficulties. New IES were deployed at these sites. All CTD operations were successfully conducted with a new CTD pylon and an upgraded CTD SBE-911 plus with dual temperature, conductivity and oxygen sensors. All water samples for core and ancillary measurements were taken. Primary production and sediment trap experiments were successfully conducted. The continuous water sampler and the water transfer system were deployed and recovered without incident. All plankton net tows were successfully done using the capstan. There were no major equipment failures. The ship docked at Snug Harbor at 0800 at 22 June 1994.

3.5. HOT-55: Dale Hebel, Chief Scientist

Ship departed Snug Harbor at 0900 on 23 July 1994 with 17 scientists on-board. Weather was generally good with moderate winds and seas. Stations Kahe, Kaena and ALOHA were occupied during this cruise. During the WOCE deep cast, a medical emergency involving one of the crew members necessitated an immediate medical evacuation. The ship was prepared to transit to Kahuku Point after the cast. A Coast Guard helicopter was sent to meet the ship and evacuate the crew member. Medevac procedures were accomplished and the ship returned to regular science operations. All CTD operations were successfully conducted and all water samples for core and ancillary measurements were taken. Primary production and sediment trap experiments were successfully conducted. During the preparation for a net tow, the capstan was powered up with the gears engaged. The tension on the line lifted the 1-ton lead weight used as a junction point for the line. The weight slid onto the capstan and damaged it. Net tows were aborted after the incident. Aside from that, no major equipment failures or accidents occurred. The ship docked at Snug Harbor at 0700 on 28 July 1994.

3.6. HOT-56: Luis Tupas, Chief Scientist

Ship departed Snug Harbor at 0900 on 28 August 1994 with 13 scientists on-board. Weather was generally good with moderate winds and seas. Stations Kahe, Kaena and ALOHA and 3 were occupied during this cruise. All CTD operations were successfully conducted and all water samples for core and ancillary measurements were taken. Primary production and sediment trap experiments were successfully conducted. Zooplankton net tows were accomplished with a back-up capstan. There were no major equipment failures. The ship docked at Snug Harbor at 0730 on 2 September 1994.

3.7. HOT-57: Luis Tupas, Chief Scientist

Ship departed at 1400 on 20 September 1994 with 17 scientist on-board. The delay was caused by the late arrival of temperature sensors from calibration. Weather was generally good with moderate winds and seas. Stations Kahe, Kaena and ALOHA and 3 were occupied during this cruise. All CTD operations were successfully conducted and all water samples for core and ancillary measurements were taken. Primary production and sediment trap experiments were successfully conducted. Zooplankton net tows were accomplished using a capstan. There were no major equipment failures. The ship docked at Snug Harbor at 0730 on 26 September 1994.

3.8.1 HOT-58A: Dale Hebel, Chief Scientist

The regular HOT program science operations were conducted on this cruise. The ship departed Snug Harbor at 0900 on 13 October 1994 with 16 scientists on-board. Weather was generally good with moderate winds and seas. Stations Kahe, Kaena and ALOHA and 3 were occupied during this cruise. All CTD operations were successfully conducted and all water samples for core and ancillary measurements were taken. Primary production and sediment trap experiments were successfully conducted. Zooplankton net tows were accomplished using a capstan. A minor CTD problem was encountered during the cast at Station 3 but was promptly fixed and a second CTD cast was taken. The ship docked at Snug Harbor at 0700 on 18 October 1994.

3.8.2 HOT-58B: David Karl, Chief Scientist

An instrument test was conducted on 18 October 1994. After all HOT personnel disembarked from 58A, the ship departed at 0900 with JGOFS scientists and technical personnel from Chelsea Instruments. A towed device called the Aquashuttle was tested on this cruise off Waikiki. After the test, the ship returned to Snug Harbor and docked at 1600. All science personnel disembarked.

The ship departed Snug Harbor at 1000 on October 19 with 7 scientists on-board to retrieve and deploy the bottom-moored sediment trap and to conduct tests with the lowered ADCP and the continuous water sampler. Weather was deteriorating and was generally poor with strong winds and rough seas. Although initial interrogation with the mooring was established, efforts to locate the mooring after the release code was transmitted were not successful. After several hours of searching were spent, other science operations such as the testing of the lowered ADCP and the continuous water sampler were conducted. Weather conditions were continuing to deteriorate and plans were made to return to Snug Harbor. Shortly after departure, the radio beacon from the mooring array was received and the strobe lights were visible. Recovery operations were initiated immediately and successfully completed, however, the array was not redeployed. The ship docked at Snug Harbor at 1420 on 22 October 1994.

3.9 HOT-59: Luis Tupas, Chief Scientist

The ship departed Snug Harbor at 0900 on 16 November 1994 with 16 scientists on-board. Weather was bad with strong winds and high seas. Stations Kahe, Kaena and ALOHA were occupied during this cruise. Work at Stations Kahe and Kaena were accomplished without incident. Upon arrival at Station ALOHA, sea conditions prohibited any safe work. The sediment trap experiment was immediately canceled and all other science operations postponed until

weather conditions improved. The weather had improved slightly by November 19 and the first CTD cast was conducted after a safe procedure was established. The primary productivity experiment was canceled due to unsafe conditions. An attempt to conduct a net tow was aborted when waves overcame the personnel on-deck. There were some slight injuries to personnel. CTD casts continued for the required 36-hour period. After the last cast was conducted, the ship immediately departed for Honolulu. The ship docked at Snug Harbor at 1600 on 21 November 1994.

4. Results

4.1. Hydrography

4.1.1. 1994 CTD Profiling Data

Profiles of temperature, salinity, oxygen and potential density (sigma theta) were collected at both Station Kahe and Station ALOHA. The profiles from Station ALOHA during 1994 are presented in Figure 6.2.1. The results of bottle determinations of oxygen, salinity and inorganic nutrients are also shown. In addition, stack plots of CTD temperature and salinity profiles for all 1000 m casts conducted at Station ALOHA are presented (Fig. 6.2.2). The data collected for Station Kahe during 1994 are presented in Figures 6.2.3. The temperature, salinity and oxygen profiles obtained from the deep casts at Station ALOHA during 1994 are presented in Figures 6.2.4 to 6.2.6.

4.1.2. Time-series Hydrography, 1988-1994

The hydrographic data collected during the first 6 years of HOT are presented in a series of contour plots (Figures 6.3.1 to 6.3.14). These figures show the data collected in 1994 within the context of the longer time-series database. The CTD data used in these plots are obtained by averaging the data collected during the 36-hour period of burst sampling. Therefore, much of the variability which would otherwise be introduced by internal tides in the upper ocean has been removed. Figures 6.3.1 and 6.3.2 show the contoured time-series record for potential temperature and density in the upper 1000 dbar for all HOT cruises through 1994. Seasonal variation in temperature for the upper ocean is apparent in the maximum of near-surface temperature of about 26 ^{o}C and the minimum of approximately 23 ^{o}C. Oscillations in the depth of the 5 ^{o}C isotherm below 500 dbar appear to be relatively large with displacements up to 75 dbar. The main pycnocline is observed between 100 and 600 dbar, with a seasonal pycnocline developing between June and December in the 50-100 dbar range (Figure 6.3.2). The cruise-to-cruise changes between February and July 1989 in the upper pycnocline illustrate that variability in density is not always resolved by our quasi-monthly sampling.

Figures 6.3.3 to 6.3.6 show the contoured time-series record for salinity in the upper 1000 dbar for all HOT cruises through 1994. The plots show both the CTD and bottle results plotted against pressure and potential density. Most of the differences between the contoured sections of bottle salinity and CTD salinity are due to the coarse distribution of bottle data in the vertical as compared to the CTD observations. Some of the bottles in Figure 6.3.6 are plotted at density values lower than the indicated sea surface density. This is due to surface density changing from cast to cast within each cruise, and even between the downcast and upcast during a single cast.

Surface salinity is variable from cruise-to-cruise, with no obvious seasonal cycle and some substantial interannual variability. The surface salinity is low in late 1989, increases to a maximum in late 1990, decreases again during 1991 and 1992, rises to an extreme high in late 1993 and decreases again in 1994. The salinity maximum is generally found between 50 and 150 dbar, and within the potential density range 1.024-1.025 kg m^{-3}. A salinity maximum region extends to the sea surface in the later part of 1990 and 1993, as indicated by the 35.2 contour reaching the surface. This contour nearly reaches the surface late in 1988 and 1989. The maximum value of salinity in this feature is subject to short-term variations of about 0.1 which is

probably due to the proximity of Station ALOHA to the region where this water is formed at the sea surface (Tsuchiya, 1968). The variability of this feature is itself variable. Throughout 1989 there were extreme variations of a couple of months duration with 0.2 amplitude. The variability was much smaller and slower, thereafter, except for a few months of rapid variation in earlier 1992. The salinity minimum is found between 400 and 600 dbar (potential density ~1.02635-1.02685 kg m^{-3}). There is no obvious seasonal variation of this feature, but there are distinct periods of higher than normal minimum salinity in early 1989, in the fall of 1990 and early 1992. These variations are related to the episodic appearance at Station ALOHA of energetic fine structure and submesoscale water mass anomalies (Lukas and Chiswell, 1991; Kennan and Lukas, 1995).

Figures 6.3.7 and 6.3.8 show contoured time-series data for oxygen in the upper 1000 dbar at Station ALOHA. The oxygen data show a strong oxycline between 400 and 625 dbar (potential density ~1.02625-1.0270 kg m^{-3}), and an oxygen minimum centered near 800 dbar (1.0272 kg m^{-3}). During 1989, there was a persistent oxygen maximum near 300 dbar (potential density ~1.02575 kg m^{-3}), which weakened afterward. The oxygen minimum exhibited some interannual variability as well, with values less than 30 µmol kg^{-1} appearing in the last half of 1989 and the first half of 1990, reappearing, less intensely, in 1991 and 1992 and again strongly in 1993 and 1994. The surface layer shows a seasonality in oxygen concentrations, with highest values in the winter. This roughly corresponds to the minimum in surface layer temperature (Figure 6.3.1). An oxygen maximum at about 100 m appears in the latter half of 1991 and persists through 1992, reappears again in 1993 and persists through 1994.

Figures 6.3.9. to 6.3.14 show nitrate plus nitrite, soluble reactive phosphate and silicate at Station ALOHA plotted against both pressure and potential density. The nitricline is located between about 200 and 600 dbar (potential density ~1.02575-1.027 kg m^{-3}; Figures 6.3.9 and 6.3.10). Most of the variations seen in these data are associated with vertical displacements of the density structure, and when [nitrate+nitrite] is plotted versus potential density, most of the contours are level. The upper reaches of the water column show considerable variability in density space. The record is dominated by a few short events where nutrients appear to be brought up into the surface layers. These events occurred in March-April, 1990, January, 1992, February 1993 and possible smaller events in September, 1989 and March, 1991 and February 1994. These events are probably important in the upper ocean nutrient balance, but are of such short duration that it is difficult to capture then with quasi-monthly sampling. The SRP and silica records are similar to nitrate plus nitrite.

4.2. Flash Fluorescence and Beam Transmission

Stack plots of the flash fluorescence and beam transmission results from each HOT cruise in 1994 are presented in Figures 6.4.1 to 6.4.9. In situ flash fluorescence profiles show the fluorescence maximum at the base of the euphotic zone, characteristic of the central North Pacific Ocean. Percent transmission profiles consistently show increased attenuation due to increased particle load at depths shallower than 100 dbar. Both fluorescence and beam transmission profiles show the influence of internal waves when plotted against pressure, but remain relatively constant within a cruise when plotted in density space. However, both data sets show substantial cruise-to-cruise variability in these properties.

Representative fluorescence profiles for a period of six years are shown in Figures 6.4.10 and 6.4.11. In order to facilitate comparison, only night-time profiles are presented after normalization to the average density profile obtained from the CTD burst sampling for each cruise. Month-to-month variability in the average depth of the fluorescence maximum is apparent. This is particularly evident in year 3 where the depth of the fluorescence maximum appears to increase in mid to late summer and in year 4 from summer to winter (Figure 6.4.10). The depth of the fluorescence maximum decreased significantly from spring to fall in 1993. Beam transmission profiles for cruises in 1994 are shown in Figure 6.4.12 and 6.4.13. These profiles were collected at approximately midnight and were normalized to the average density profile obtained for each cruise. Beam transmission profiles also show considerable variability on monthly time scales (Figure 6.4.12 and 6.4.13).

4.3. Biogeochemistry

Biogeochemical data collected during 1994 are summarized in Figures 6.5.1-6.5.9. In some cases the results from the first 5 years of the program have been combined to produce these figures.

4.3.1. Dissolved Inorganic Carbon and Titration Alkalinity

Dissolved inorganic carbon (DIC) and titration alkalinity measured in the upper 1000 dbar of the water column over the 6 years of the time-series program are presented in Figures 6.5.1 and 6.5.2. Time-series of titration alkalinity and DIC in the mixed layer are presented in Figure 6.5.3. Titration alkalinity normalized to 35 ppt salinity averages approximately 2305 µmol kg^{-1} and, within the precision of the analysis, appears to remain relatively constant at Station ALOHA. This observation is consistent with the results of Weiss et al. (1982) who conclude that titration alkalinity normalized to salinity remains constant in both the North and South Pacific subtropical gyres. In contrast to titration alkalinity, the concentration of DIC varies annually. DIC in the mixed layer is highest in winter and lowest in summer. This oscillation is consistent with an exchange of carbon dioxide across the air-sea interface driven by temperature dependent changes in mixed layer pCO_2.

Titration alkalinity shows considerable time dependent variability around the shallow salinity maximum, centered at about 125 dbar, and the salinity minimum, centered at about 400 dbar. These variations are largely associated with variability in salinity at these depths and disappear when alkalinity is normalized to 35 ppt. Titration alkalinity normalized to 35 ppt salinity is elevated in surface waters in spring of 1990 and winter of 1994. This corresponds to the appearance of mesoscale eddies at Station ALOHA at this time (Winn et al., 1991).

4.3.2. Low Level Nutrient Profiles

Euphotic zone nutrient concentrations at Station ALOHA are at or well below the detection limits of the autoanalyzer methods. Other analytical techniques and instrumentation are used to measure the nanomolar levels of [nitrate+nitrite] and SRP (section 2.2.7) in these waters. Figures 6.5.4 and 6.5.5 show the profiles obtained from our low level nutrient analyses in 1994. At depths shallower than 100 dbar, SRP is typically less than 150 nmol kg^{-1} and on occasion, as

low as 15 nmol kg^{-1}. SRP concentrations appear to vary by at least 3-fold in this region (Figure 6.5.4). Concentrations of [nitrate+nitrite] at depths less than 100 meters are always less than 10 nmol kg^{-1} and are often less the 5 nmol kg^{-1} (Figure 6.5.5).

4.3.3. Pigments

A contour plot of chl a concentrations measured using standard fluorometric techniques from 0 to 200 dbar over the first 6 years of the program is shown in Figure 6.5.6. As expected a chlorophyll maximum with concentrations up to 300 µg m^{-3} is observed at approximately 100 dbar. The chl a concentrations at depths shallower than 50 meters display a clear annual cycle increasing in the fall and winter and decreasing through spring and summer which is approximately 4-6 months out of phase with the annual oscillation at the base of the euphotic zone (Winn et al., 1995).

4.3.4. Particulate Carbon, Nitrogen and Phosphorus

Particulate carbon (PC), nitrogen (PN) and phosphorus (PP) in the surface ocean over the first six years of the program are shown in Figures 6.5.7 to 6.5.9. PC varies between 1.3-3.0 µmol kg^{-1}, PN between 0.08 -0.65 µmol kg^{-1} and PP between 8 - 35 nmol kg^{-1} in the upper 100 meters of the water column. PC and PN show a clear annual cycle with the greatest particulate concentrations in summer/fall and lowest in winter. A significantly larger PN concentration was observed in the late fall of 1993 with only a slight increase in PC and a decrease in PP. The temporal distribution and magnitude of PC, PN, and PP in 1994 were similar to previous years.

4.4. Primary Production and Particle Flux

4.4.1. Primary Productivity

The results of the ^{14}C incubations and pigment determinations for samples collected from Go-Flo casts in 1994 are presented in Tables 4.4.1 and 4.4.2. Table 4.4.1 presents the primary production and fluorometric pigment measurements made at individual depths on all 1994 cruises. Table 4.4.2 presents integrated values for irradiance, pigment concentration and primary production rates. The pigment concentrations and ^{14}C incorporation rates reported are the average of triplicate determinations. Integrated primary production rates measured over all 6 years of the program are shown in Figure 6.6.1 in order to place the 1994 results within the context of the time-series data set.

Table 4.4.1: Primary Production and Pigment Summary

Cruise	Depth (m)	Mean Chl *a* (mg m^{-3})	Std. Dev. Chl *a* (mg m^{-3})	Mean Phaeo (mg m^{-3})	Std. Dev. Phaeo (mg m^{-3})	Light (mg C m^{-3}) Rep #1	Light (mg C m^{-3}) Rep #2	Light (mg C m^{-3}) Rep #3	Dark (mg C m^{-3}) Rep #1	Dark (mg C m^{-3}) Rep #2	Dark (mg C m^{-3}) Rep #3
51	5	0.135	0.003	0.130	0.000	5.13	4.98	4.63	0.20	0.09	0.08
51	25	0.125	0.017	0.106	0.008	5.47	4.46	4.82	0.13	0.12	0.12
51	45	0.133	0.006	0.104	0.019	0.56	4.08	3.84	0.09	0.09	0.04
51	75	0.141	0.000	0.124	0.018	1.59	1.43	1.55	0.11	0.09	0.08
51	100	0.166	0.018	0.328	0.049	1.03	0.97	0.92	0.06	0.05	0.04
51	125	0.151	0.018	0.127	0.003	0.14	0.15	0.15	0.09	0.11	0.11
51	150	0.129	0.001	0.125	0.007	0.13	0.10	0.10	0.13	0.10	0.10
51	175	0.138	0.013	0.126	0.011	0.09	0.09	0.10	0.09	0.09	0.10
52	5	0.172	0.004	0.111	0.004	8.59	8.14	8.55	0.13	0.09	0.09
52	25	0.181	0.001	0.114	0.02	2.83	5.37	2.50	0.27	0.10	0.14
52	45	0.178	0.003	0.122	0.003	3.05	3.18	2.85	0.08	0.08	0.03
52	75	0.207	0.005	0.149	0.004	0.79	0.85	0.91	0.06	0.06	0.05
52	100	0.204	0.007	0.248	0.011	0.40	0.41	0.34	0.05	0.05	0.06
52	125	0.197	0.007	0.189	0.009	0.14	0.15	0.16	0.05	0.05	0.05
52	150	0.092	0.001	0.202	0.003	0.07	0.08	0.08	0.05	0.05	0.09
52	175	0.029	0.001	0.085	0.004	0.03	0.03	0.03	0.03	0.02	0.06
53	5	0.074	0.005	0.045	0.008	7.74	7.65	6.26	0.14	0.09	0.10
53	25	0.071	0.006	0.054	0.013	6.08	6.37	6.74	0.14	0.12	0.14
53	45	0.079	0.001	0.071	0.000	4.31	3.19	4.68	0.15	0.13	0.03
53	75	0.116	0.019	0.099	0.011	3.10	2.57	2.68	0.13	0.13	0.13
53	100	0.170	0.010	0.162	0.001	1.39	1.27	1.34	0.10	0.10	0.11
53	125	0.252	0.025	0.287	0.016	0.65	0.61	0.50	0.11	0.06	0.05
53	150	0.169	0.000	0.340	0.023	0.32	0.29	0.32	0.07	0.07	0.07
53	175	0.057	0.014	0.125	0.069	0.07	0.08	0.07	0.07	0.07	0.08
54	5	0.059	0.002	0.027	0.003	6.65	8.22	8.06	0.07	0.09	0.09
54	25	0.066	0.010	0.031	0.001	5.77	4.99	3.76	0.14	0.10	0.11
54	45	0.083	0.000	0.063	0.001	3.76	2.79	5.13	0.09	0.08	0.06
54	75	0.116	0.002	0.092	0.002	2.05	2.27	3.29	0.11	0.12	0.09
54	100	0.156	0.007	0.207	0.047	2.23	2.51	2.24	0.09	0.08	0.07
54	125	0.189	0.002	0.301	0.022	0.87	0.92	0.77	0.07	0.07	0.07
54	150	0.169	0.011	0.383	0.023	0.49	0.42	0.43	0.05	0.08	0.07
54	175	0.076	0.000	0.234	0.006	0.11	0.11	0.11	0.04	0.04	0.04

Table 4.4.1: (continued)

Cruise	Depth (m)	Mean Chl *a* (mg m^{-3})	Std. Dev. Chl *a* (mg m^{-3})	Mean Phaeo (mg m^{-3})	Std. Dev. Phaeo (mg m^{-3})	Light (mg C m^{-3}) Rep #1	Light (mg C m^{-3}) Rep #2	Light (mg C m^{-3}) Rep #3	Dark (mg C m^{-3}) Rep #1	Dark (mg C m^{-3}) Rep #2	Dark (mg C m^{-3}) Rep #3
55	5	0.090	0.008	0.084	0.015	8.23	8.74	9.01			
55	25	0.099	0.028	0.073	0.016	6.89	7.68	6.88	0.19	0.15	0.15
55	45	0.205	0.024	0.192	0.061	5.46	8.89	8.61	0.12	0.13	0.12
55	75	0.258	0.037	0.296	0.033	3.45	2.78	3.05	0.06	0.06	0.05
55	100	0.196	0.014	0.419	0.008	1.13	1.11	1.00	0.10	0.06	0.07
55	125	0.076	0.007	0.243	0.017	0.24	0.25	0.25	0.11	0.06	0.05
55	150	0.031	0.000	0.080	0.009	0.05	0.05	0.05	0.05	0.05	0.05
55	175	0.012	0.003	0.042	0.021	0.03	0.03	0.03	0.04	0.03	0.03
56	5	0.075	0.001	0.044	0.004	7.35	8.41	7.71	0.29	0.25	0.27
56	25	0.086	0.002	0.046	0.002	6.45	5.90	6.15	0.19	0.17	0.17
56	45	0.083	0.001	0.048	0.003	6.09	6.32	6.17	0.18	0.19	0.24
56	75	0.141	0.005	0.117	0.007	3.53	3.16	3.17	0.15	0.15	0.15
56	100	0.205	0.014	0.264	0.014	1.47	1.57	1.47	0.07	0.07	0.07
56	125	0.136	0.003	0.354	0.013	0.49	0.48	0.51	0.09	0.05	0.07
56	150	0.047	0.001	0.133	0.003	0.07	0.08	0.08	0.06	0.04	0.05
56	175	0.038	0.004	0.129	0.026	0.10	0.04	0.04	0.04	0.07	0.04
57	5	0.069	0.002	0.049	0.003	5.16	5.44	5.56	0.35	0.31	0.28
57	25	0.070	0.004	0.049	0.001	5.32	6.06	5.52	0.24	0.23	0.20
57	45	0.065	0.003	0.056	0.003	4.47	3.81	4.72	0.18	0.26	0.31
57	75	0.147	0.006	0.127	0.004	2.76	2.58	2.74	0.24	0.24	0.23
57	100	0.217	0.007	0.515	0.024	1.60	1.74	1.65	0.09	0.09	0.13
57	125	0.114	0.004	0.258	0.008	0.35	0.34	0.33	0.08	0.09	0.08
57	150	0.023	0.004	0.072	0.016	0.04	0.05	0.05	0.05	0.06	0.06
57	175	0.021	0.001	0.052	0.003	0.04	0.04	0.03	0.06	0.08	0.06
58	5	0.083	0.003	0.063	0.011	4.89	5.16	5.26	0.20	0.20	0.14
58	25	0.078	0.003	0.068	0.007	4.86	4.24	3.99	0.10	0.10	0.11
58	45	0.087	0.001	0.062	0.013	4.25	4.74	4.43	0.10	0.10	0.10
58	75	0.146	0.003	0.124	0.006	1.40	1.31	1.47	0.09	0.09	0.11
58	100	0.206	0.003	0.268	0.011	0.74	0.86	0.82	0.07	0.07	0.07
58	125	0.217	0.011	0.491	0.011	0.37	0.36	0.32	0.04	0.04	0.04
58	150	0.053	0.000	0.178	0.026	0.07	0.07	0.07	0.04	0.04	0.04
58	175	0.038	0.005	0.083	0.007	0.03	0.03	0.03	0.05	0.05	0.06

Variability in rates of primary production, integrated over the euphotic zone during the first six years of the time-series program, appear to be stochastic with no obvious evidence of a seasonal cycle (but see Winn et al., 1995). Measured rates ranged from less than 200 to greater than 1000 mg C m^{-2} day^{-1} with the highest rate being observed in August 1989. This high rate of primary production coincided with a cyanobacterial bloom observed in surface waters near Station ALOHA on HOT cruise #9 (Karl et al. 1992). This variability, with a range of a factor of 5, is surprisingly large. However, the majority of the primary production estimates were between 250 and 600 mg C m^{-2} d^{-1}, and the average rate of primary production was approximately 450 mg C m^{-2} d^{-1}. Although this value is higher than historical measurements for the central ocean basins (Ryther, 1969), it is consistent with more recent measurements using modern methodology (Martin et al. 1987; Laws et al. 1989; Knauer et al. 1990).

Table 4.4.2: In Situ Primary Production and Pigment Summary (0-200 meters)

	Incident Irradiance (E m^{-2} d^{-1})		Pigments (mg m^{-2})			Assimilation Rates (mgC m^{-2} d^{-1})	
Cruise	cosine	hemi	Chl a	Phaeo	Incubation (hrs)	light	dark
51	28.1		29.8	30.9	12.0	318	18
52	24.8	28.4	33.7	32.0	12.1	313	13
53	41.7	80.7	25.8	30.4	12.0	474	18
54	51.5	92.0	22.2	33.3	13.7	472	15
55	47.5	78.2	23.4	35.3	13.0	584	16
56	49.5	NA	19.5	28.0	14.3	539	23
57	46.5	80.4	17.5	29.0	13.0	428	30
58	30.5	87.6	21.9	32.8	12.7	345	15

4.4.2. Particle Flux

Particulate carbon (PC), nitrogen (PN), phosphorus (PP) and mass fluxes (150, 300 and 500 m) are presented in Table 4.4.3 and Figures 6.6.2 to 6.6.9 for the first 6 years of the program. Carbon flux displays a clear annual cycle with peaks in both the early spring and in the late summer months. The magnitude of particle flux varies by a factor of approximately 3. With the exception of anomalous PP fluxes measured on the first two HOT cruises, temporal variability in PN, PP and mass flux show similar temporal trends, and also vary between cruises by about a factor of 3. Elemental ratios of carbon-to-nitrogen (atom:atom) at 150 m are typically between 6-10 and show no obvious temporal pattern. These particle flux measurements and elemental ratios are consistent with those measured in the central North Pacific Ocean by the VERTEX program (Martin et al. 1987, Kanuer et al. 1990). Nitrogen flux at 150 m, as a percent of photosynthetic nitrogen assimilation (calculated from ^{14}C primary production values assuming a C:N ratio [atom:atom] of 6.6) ranges between 2-10%. The average value (approximately 6.5%) is consistent with the estimate of new production for the oligotrophic central gyres made by Eppley

and Peterson (1979) and with field data from the VERTEX program (Knauer *et al.*, 1990). Average fluxes of PC, PN, PP and mass at 150 m from the first 6 years of the time-series observations are shown in Figures 6.6.2 to 6.6.5. Contour plots of concentration are shown in Figures 6.6.6 to 6.6.9. For carbon, nitrogen, phosphorus and total mass, the flux declines rapidly with depth, presumably due to the rapid dissolution and remineralization of organic particles sinking through the water column. The flux of carbon at 500 m is less than 50% of the flux at 150 m.

4.5. ADCP Measurements

An overview of the shipboard ADCP data is given by the plots of velocity as a function of time and depth while on station (Figures 6.7.1) and the velocity as a function of latitutde and depth during transit to and from Station ALOHA and Station 3 combined (Figures 6.7.2). As in the previous years, currents were highly variable from cruise to cruise and within each cruise.

4.6. Meteorology

The meteorological data collected by HOT program scientists include atmospheric pressure, sea-surface temperature and wet and dry bulb air temperature. These data are presented in Figures 6.8.1 to 6.8.3. As described by Winn et al. (1991), parameters show evidence of annual cycles, although the daily and weekly ranges are nearly as high as the annual range for some variables. Wind speed and direction are also collected on HOT cruises. These data are presented in Figures 6.8.4 to 6.8.12.

4.7. Light Measurements

Integrated irradiance measurements made with the on-deck cosine collector on days that primary production experiments were conducted are presented in Table 4.4.2.

4.8. Buoy and Shipboard Observations

A National Data Buoy Center (NDBC) meteorological buoy is located about 400 km west of Station ALOHA at 23.4°N, 162.3°W. This buoy collects hourly observations of air temperature, sea surface temperature, atmospheric pressure, wind speed and direction and significant wave height. The coherence of these data with the data collected on HOT cruises was examined and reported in Tupas et al. (1993). We concluded from these analyses, that the buoy data can be used to get useful estimates of air temperature, sea-surface temperature and atmospheric pressure at Station ALOHA.

The buoy #51001 described above did not work properly during the time period that included cruises 53 and 54, thus data from another similar buoy located north of Molokai (buoy 51026, 21.4°N, 156.96°W) were used to compare with the wind data obtained during those cruises.

Table 4.4.3: Station ALOHA Sediment Trap Flux Data

		Carbon			Nitrogen			Phosphorus			Mass Flux		
	Depth	Mg m^{-2} d^{-1}			mg m^{-2} d^{-1}			mg m^{-2} d^{-1}			mg m^{-2} d^{-1}		
Cruise	(m)	mean	SD	n	mean	SD		mean	SD	n	mean	SD	n
51	150	27.3	2.6	4	6.4	0.7	4	0.43	0.09	3	65.8	7.1	3
51	300	16.9	2.2	6	4.1	0.2	6	0.086	0.053	3	38.4	5.8	3
51	500	15.8	1.6	4	1.8	1.6	4	0.106	0.037	2	40.2	14.1	3
52	150	21.8	1.2	6	3.85	0.41	6	0.24	0.03	3	75.3	21.4	3
52	300	12.3	2.9	6	1.69	0.39	6	0.08	0.05	3	40.6	10.6	3
52	500	8.9	3.6	6	1.23	0.46	6	0.01	0.00	3	21.2	4.2	3
53	150	22.5	4.2	4	2.45	0.49	4	0.59	0.10	3	49.2	2.3	3
53	300	13.7	0.7	4	0.72	0.13	4	0.11	0.04	3	39.5	13.7	3
53	500	10.5	0.6	2	0.27	0.09	2	0.07	0.04	3	15.0	5.2	3
54	150	23.5	6.9	4	2.10	0.57	4	0.56	0.25	3	71.5	12.9	3
54	200	46.3	4.4	4	3.96	0.38	4	0.47	0.07	3	77.5	14.8	3
54	300	17.3	3.5	4	1.07	0.21	4	0.07	0.02	3	46.9	9.1	3
54	500	13.7	0.8	4	0.80	0.08	4	0.03	0.01	3	32.4	1.5	3
55	150	19.1		1	2.0		1	0.29	0.14	3	69.8	11.2	3
55	200							0.15	0.05	3	49.2	20.1	3
55	300							0.09	0.02	3	26.3	11.4	3
55	500							0.03	0.02	3	9.4	4.4	3
56	150	41.1	10.3	3	6.25	3.33	3	0.28	0.08	3	63.9	9.1	3
56	200	21.4	1.3	4	2.37	0.16	4	0.19	0.04	3	56.1	5.1	3
56	300	11.5	1.3	4	0.31	0.15	4	0.15	0.08	3	35.1	5.1	3
56	500	9.7	1.8	4	0.82	0.30	4	0.12	0.03	3	27.2	1.3	3
57	150	18.2	5.7	4	2.58	1.19	4	0.19	0.03	3	40.7	4.9	3
57	200	12.6	0.3	4	1.46	0.22	4	0.15	0.03	3	38.7	4.9	3
57	300	11.2	2.3	4	0.84	0.46	4	0.08	0.02	3	24.6	4.4	3
57	500	7.8	1.5	4	0.44	0.20	4	0.06	0.02	3	21.6	5.1	3
58	150	17.7	2.2	4	2.29	0.18	4	0.40	0.04	3	64.1	9.7	3
58	200	16.2	1.7	4	1.91	0.25	4	0.24	0.14	3	44.9	8.6	3
58	300	7.5	1.0	4	0.82	0.12	4	0.16	0.12	3	18.9	0.6	3
58	500	6.8	1.6	4	0.74	0.20	4	0.06	0.01	3	20.7	8.1	3

4.9. Inverted Echo Sounder Observations

Plots of dynamic height are presented in Figure 4.1. The IES records prior to 1994 were examined and reported in Tupas et al. (1994a). It was concluded that large events with time-scales from weeks to months dominate dynamic height to such an extent that there is no clearly defined annual cycle, for instance, the highest and lowest dynamic height in 1991 occurred within the space of about a month. These events are not well sampled with the monthly spacing of the HOT cruises.

4.10. Bottom Moored Sediment Traps

Initial results have been obtained from analyses of samples from ALOHA-I. The mass, particulate carbon, nitrogen and phosphorus time-series flux data all dsiplayed an unexpected and major export pulse in July-August 1992, during a period of time when the upper water column is well stratified (Figure 4.2). A second peak was also observed in late winter-early spring but this feature appears to be very different from the summer peak. The major particulate matter export event was recorded in the same collector cups (#'s 3 to 5) regardless of the water depth, suggesting a sinking rate of at least 200 m d^{-1}. Analysis of chlorophyll a by fluorometry and phytolankton pigments by HPLC reveal that the peak export event is coincident with the removal of pigmented cells. The summer event contained the full spectrum of plant pigments and most accessory pigments. Direct microscopic analyses show that this major export event was dominated by diatoms. It appears that this major export event occured once more during the ALOHA-II deployment, again in the late summer. Further analyses of ALOHA-I and ALOHA-II bottom sediment trap experiments are in progress.

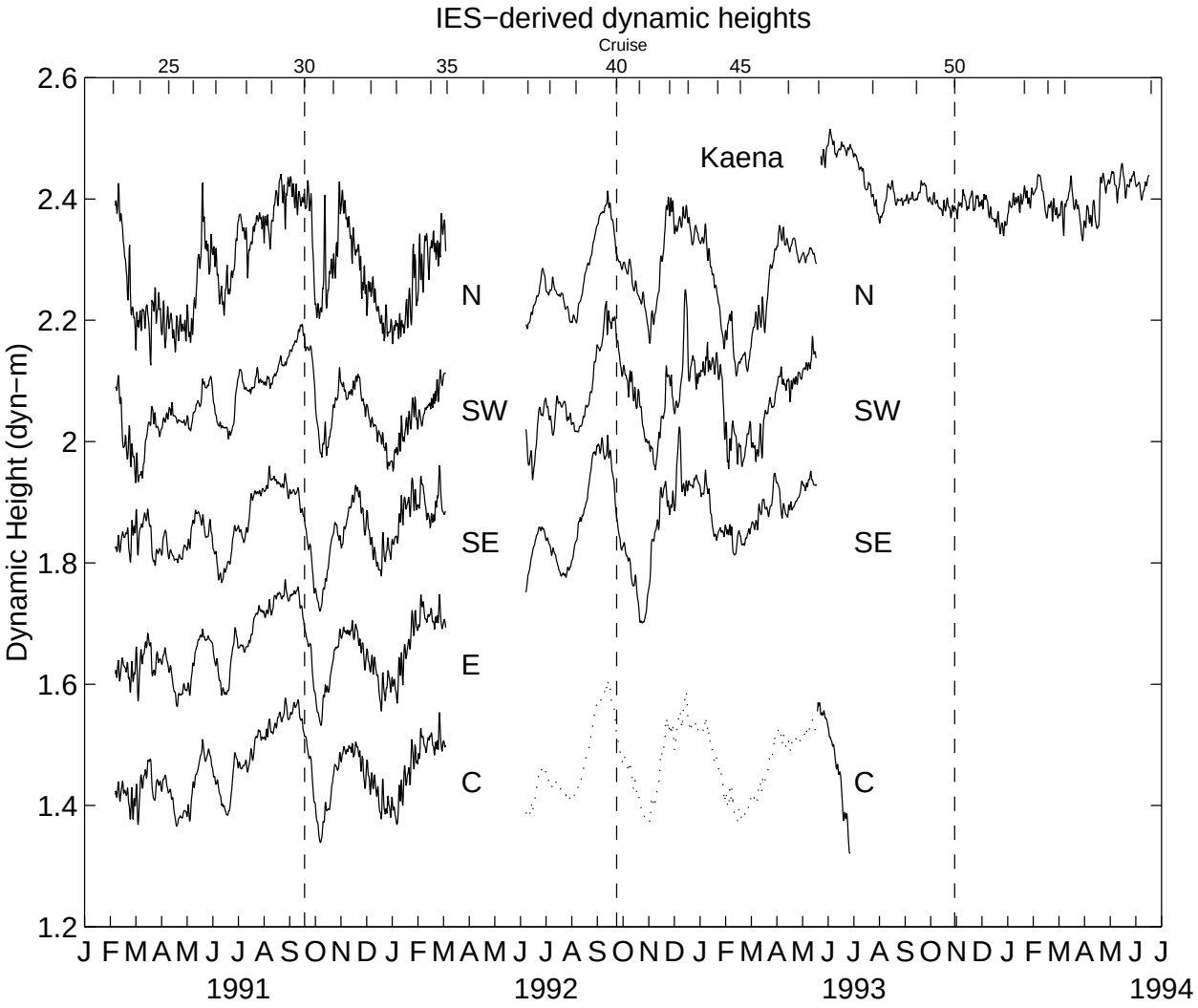

Figure 4.1: Dynamic height from the inverted echo sounders after removal of the semi-diurnal, diurnal tides and variability with time-scales less than one day. The plots are staggered at 0.2 dyn-m intervals (the curve labeled "C" corresponds to the y-scale). The dotted line is an average of the N, SW and SE records between June 1992 and May 1993. This and the 1991-1992 C-record have been calibrated from CTD casts at Station ALOHA made during 25 cruises. The horizontal axis above the plots shows the HOT cruise numbers. The deployed locations of the IESs are shown in Fig. 1.1. The locations of the deployments were changed in May 1993 (one IES was deployed at Station Kaena) in order to span the Hawaiian Ridge Current.

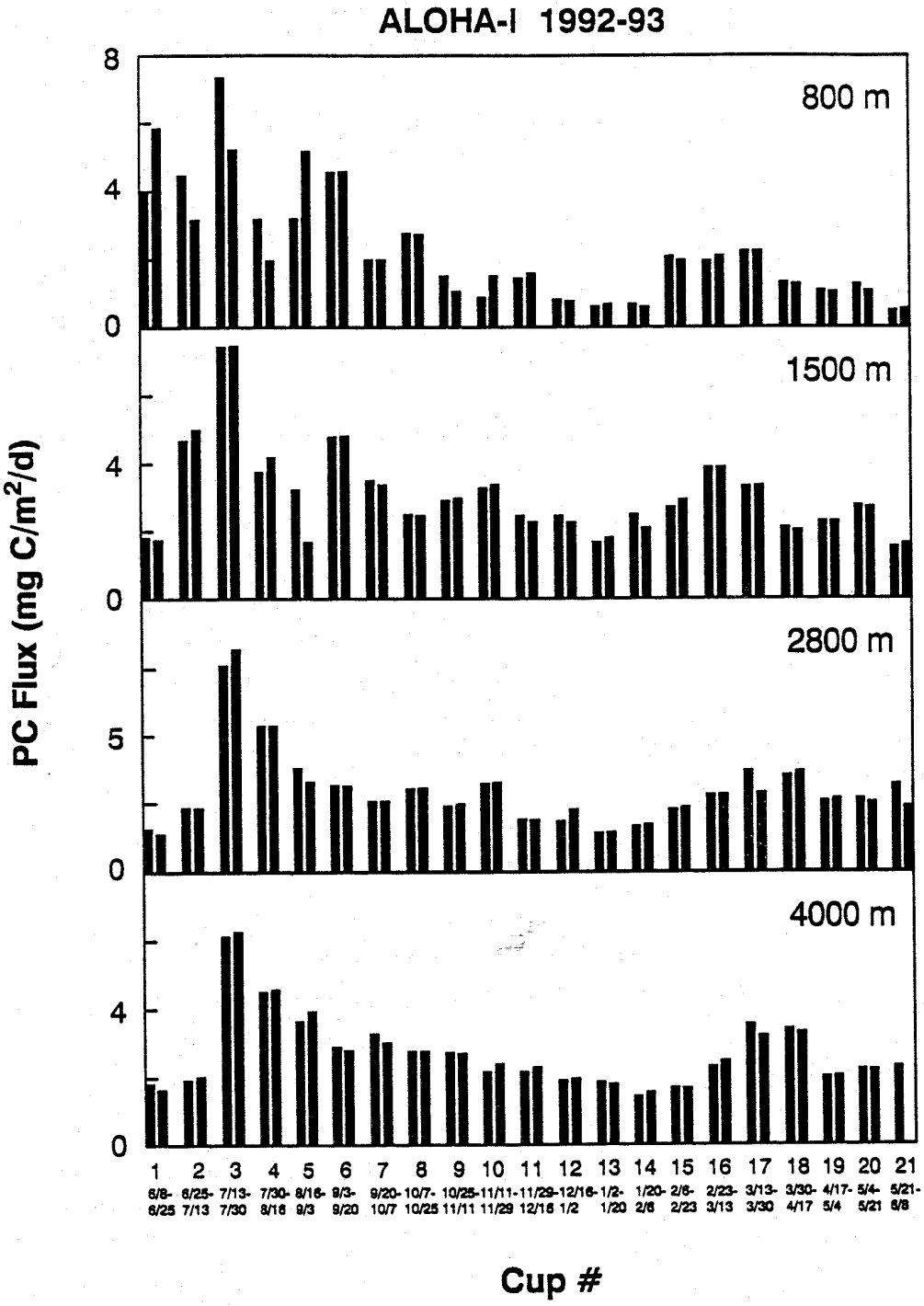

Figure 4.2: Time series record of total mass flux (not corrected for soluble constituents) for the period 6/8/92 to 6/8/93 (ALOHA-I).

5. References

Bidigare, R.R., J. Marra, T.J. Dickey, R. Iturriaga, K.S. Baker, R.C. Smith and H. Pak, 1990: Evidence for phytoplankton succession and chromatic adaptation in the Sargasso Sea during Spring 1985. *Marine Ecology Progress Series*, 60, 113-122.

Chiswell, S.M., E. Firing, D. Karl, R. Lukas, C. Winn, 1990: Hawaii Ocean Time-series Program Data Report 1, 1988-1989. School of Ocean and Earth Science and Technology, University of Hawaii, 269 pp.

Clayton, T.D. and R.H. Byrne, 1993: Spectrophotometric seawater pH measurements: total hydrogen ion concentration scale calibration of m-cresol purple and at-sea results. *Deep-Sea Research*, 40, 2115-2129.

Cox, R.D., 1980: Determination of nitrate at the parts per billion level by chemiluminescence. *Analytical Chemistry*, 52, 332-335.

Eppley, R.W. and B.J. Peterson, 1979: Particulate organic matter flux and planktonic new production in the deep ocean. *Nature*, 282, 677-680.

Garside, C., 1982: A chemiluminescent technique for the determination of nanomolar concentrations of nitrate and nitrite in seawater. *Marine Chemistry*, 11, 159-167.

Karl, D.M. and O. Holm-Hansen, 1978: Methodology and measurement of adenylate energy charge ratios in environmental samples. *Marine Biology*, 48, 185-197.

Karl, D. M., R. Letelier, D. V. Hebel, D. F. Bird and C. D. Winn, 1992: *Trichodesmium* blooms and new nitrogen in the North Pacific gyre. In: E. J. Carpenter et al. (eds.), Marine Pelagic Cyanobacteria: Trichodesmium and Other Diazotrophs, pp. 219-237. Kluwer Academic Publishers, Netherlands.

Karl, D.M. and G. Tien, 1992: MAGIC: A sensitive and precise method for measuring dissolved phosphorus in aquatic environments. *Limnology and Oceanography*, 37, 105-116.

Karl, D.M., C.D. Winn, D.V.W. Hebel and R. Letelier, 1990: Hawaii Ocean Time-series Program Field and Laboratory Protocols, September 1990.

Kennan, S.C. and R. Lukas: Saline intrusions in the intermediate waters north of Oahu, Hawaii. *Deep-Sea Research*, in press.

Knauer, G.A., D.G. Redalje, W.G. Harrison and D.M. Karl, 1990: New production at the VERTEX time-series site. *Deep-Sea Research*, 37, 1121-1134.

Laws, E.A., G.R. DiTullio, P.R. Betzer, D.M. Karl and R.L. Carder, 1989: Autotrophic production and elemental fluxes at 26^{o}N, 155^{o}W in the North Pacific subtropical gyre. *Deep-Sea Research*, 36, 103-120.

Lukas, R. and S. Chiswell, 1991: Submesoscale water mass variations in the salinity minimum of the north Pacific near Hawaii. *WOCE Notes*, 3(1), 1,6-8.

Martin, J.H., G.A. Knauer, D.M. Karl and W.W. Broenkow, 1987: VERTEX: Carbon cycling in the northeast Pacific. *Deep-Sea Research*, 34, 267-285.

Owens, W.B. and R.C. Millard, 1985: A new algorithm for CTD oxygen calibration. *Journal of Physical Oceanography*, 15, 621-631.

Ryther, J.H., 1969: Photosynthesis and fish production in the sea. The production of organic matter and its conversion to higher forms of life vary throughout the world ocean. *Science* 166, 72-76.

Strickland, J.D.H. and T.R. Parsons, 1972: A practical handbook of seawater analysis. Fisheries Research Board of Canada, 167 pp.

Tsuchiya, M., 1968: Upper waters of the intertropical Pacific Ocean. Johns Hopkins Oceanographic Studies, 4, 49 pp.

Tupas, L., F. Santiago-Mandujano, D. Hebel, E. Firing, F. Bingham, R. Lukas and D. Karl, 1994a: Hawaii Ocean Time-series Program Data Report 5, 1993. School of Ocean and Earth Science and Technology, University of Hawaii, 156 pp.

Tupas, L., F. Santiago-Mandujano, D. Hebel, R. Lukas, D. Karl and E. Firing, 1993: Hawaii Ocean Time-series Program Data Report 4, 1992. School of Ocean and Earth Science and Technology, University of Hawaii, 248 pp.

Tupas, L.M., B.N. Popp and D.M. Karl, 1994b: Dissolved organic carbon in oligotrophic waters: experiments on sample preservation, storage and analysis. *Marine Chemistry*, 48, 207-216.

UNESCO, 1981: Tenth report of the joint panel on oceanographic tables and standards. UNESCO Technical Papers in Marine Science, No. 36. UNESCO, Paris.

Weiss, R.F., R.A. Jahnke and C.D. Keeling, 1982: Seasonal effects of temperature and salinity on the partial pressure of CO_2 in seawater. *Nature*, 300, 511-513.

Winn, C.D., L. Campbell, J.R. Christian, R.M. Letelier, D.V. Hebel, J.E. Dore, L. Fujieki and D.M. Karl, 1995: Seasonal variability in the phytoplankton community of the North Pacific subtropical gyre. *Global Biogeochemical Cycles*, in press.

Winn, C., S.M. Chiswell, E. Firing, D. Karl, R. Lukas, 1991: Hawaii Ocean Time-series Program Data Report 2, 1990. School of Ocean and Earth Science and Technology, University of Hawaii, 175 pp.

Winn, C., R. Lukas, D. Karl, E. Firing, 1993: Hawaii Ocean Time-series Program Data Report 3, 1991. School of Ocean and Earth Science and Technology, University of Hawaii, 228 pp.

Woodroff, J., R.J. Slotz, R.L. Jenne and P.M. Steurer, 1987: A comprehensive ocean-atmosphere data set. *Bulletin of the American Meteorological Society*, 68, 1239-1250.

Wright, S.W., S.W. Jeffrey, R.F.C. Mantoura, C.A. Llewellyn, T. Bjornland, D. Repeta and N. Welschmeyer, 1991: Improved HPLC method for the analysis of chlorophylls and carotenoids from marine phytoplankton. *Marine Ecology Progress Series*, 77, 183-196.

6. Figures

6.1. CTD Station Locations and Sediment Trap Drift Tracks

Figure 6.1.1: CTD station locations on HOT-51 and 52. CTD stations represented by open circles relative to Station ALOHA. Solid lines connect casts taken in sequence and numbers show location of first and last casts. Dashed line shows area nominally defined as Station ALOHA. Drift track for the sediment trap array during the 72-hour deployment period is indicated by a solid line with the start point indicated by an S.

Figure 6.1.2: As in Figure 6.1.1, except for HOT-53 and 54.

Figure 6.1.3: As in Figure 6.1.1, except for HOT-55 and 56.

Figure 6.1.4: As in Figure 6.1.1, except for HOT-57 and 58.

Figure 6.1.5: As in Figure 6.1.1, except for HOT-59.

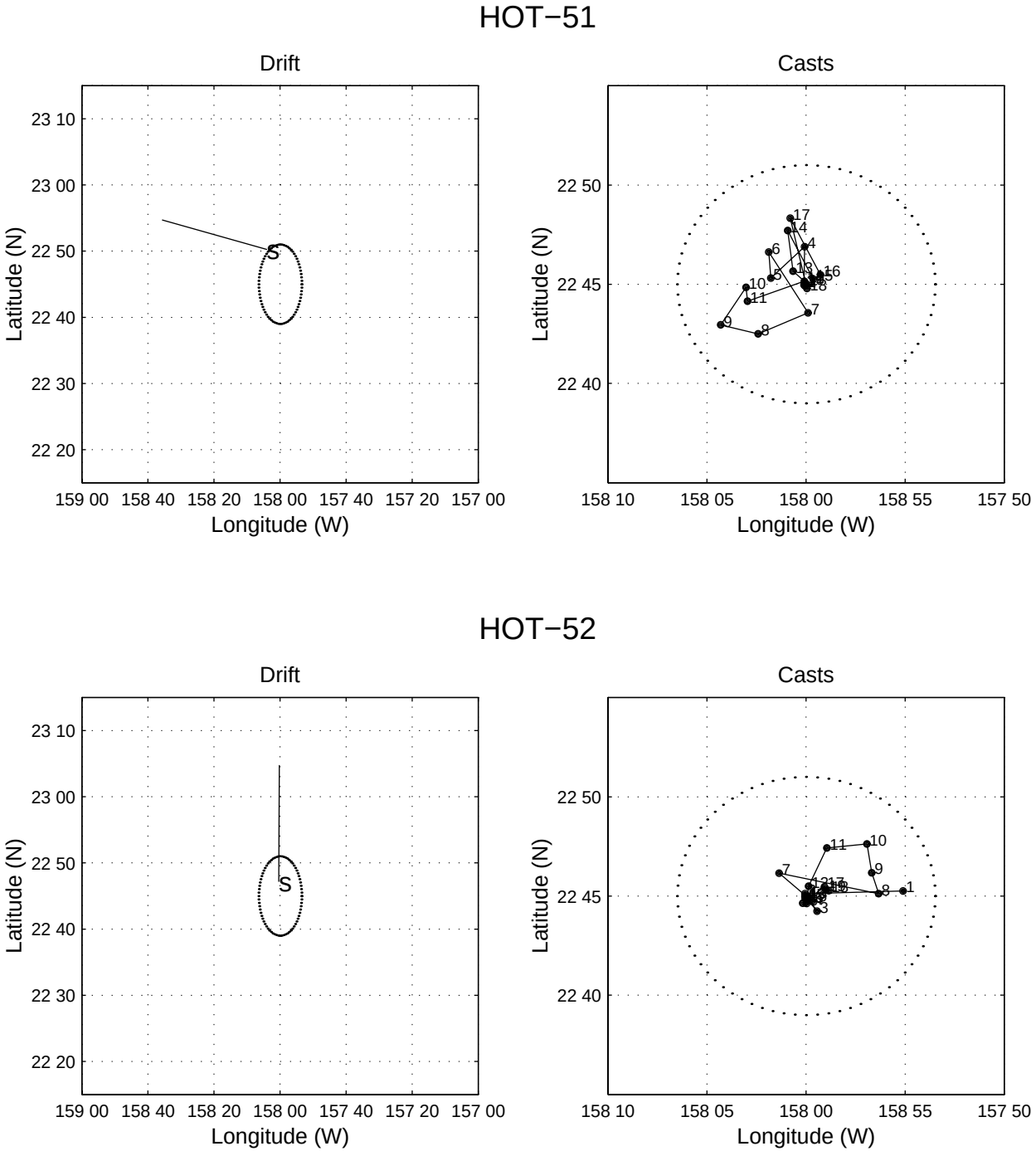
HOT−51
Drift
Casts
Latitude (N)
Longitude (W)
23 10
23 00
22 50
22 40
22 30
22 20
159 00
158 40
158 20
158 00
157 40
157 20
157 00
S
22 50
22 45
22 40
158 10
158 05
158 00
158 55
157 50
HOT−52
Drift
Casts
Latitude (N)
Longitude (W)
23 10
23 00
22 50
22 40
22 30
22 20
159 00
158 40
158 20
158 00
157 40
157 20
157 00
S
22 50
22 45
22 40
158 10
158 05
158 00
158 55
157 50

Figure 6.1.1

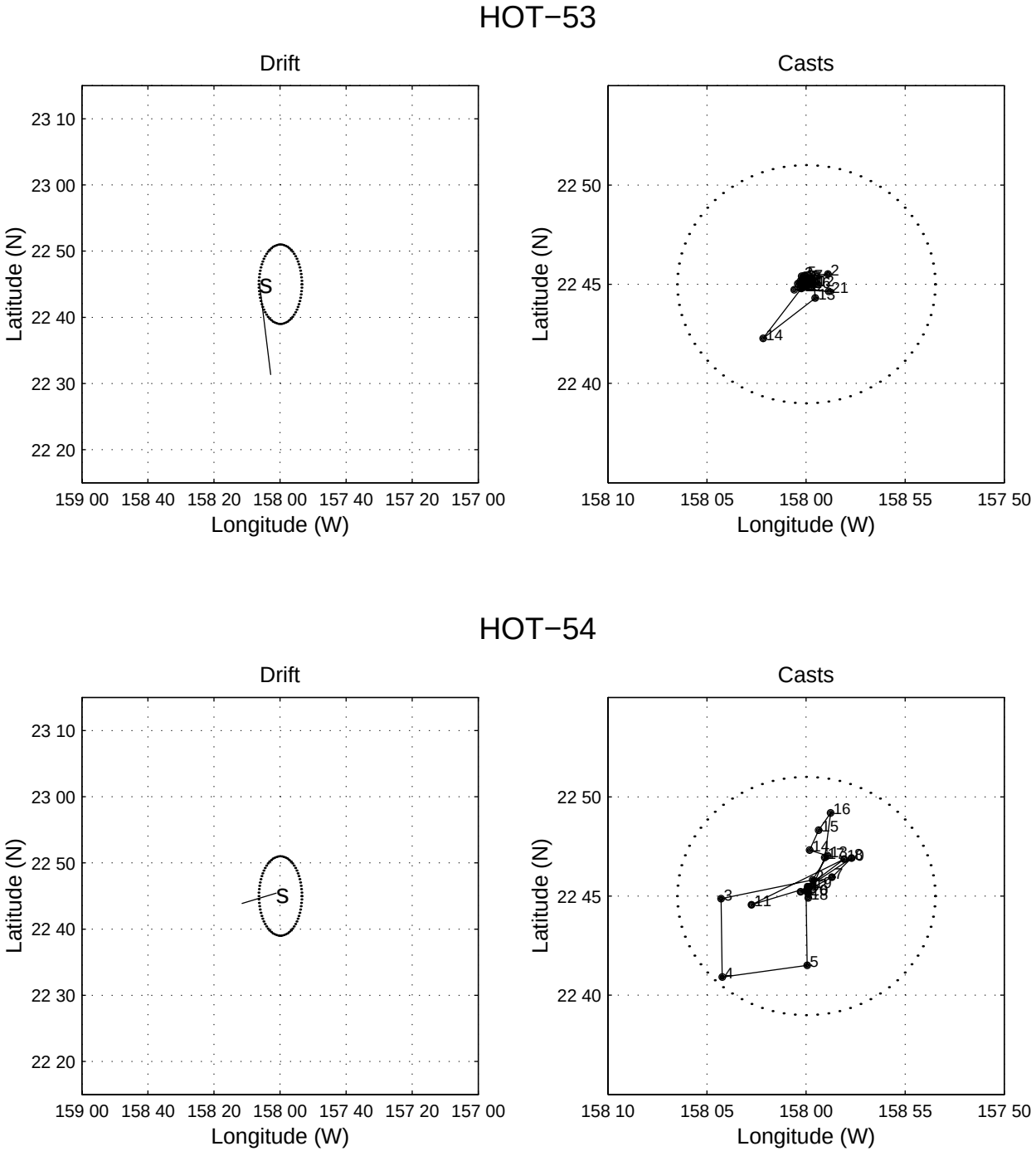
HOT−53
Drift
Casts
Latitude (N)
Longitude (W)
23 10
23 00
22 50
22 40
22 30
22 20
159 00
158 40
158 20
158 00
157 40
157 20
157 00
S
22 50
22 45
22 40
158 10
158 05
158 00
158 55
157 50
HOT−54
Drift
Casts
Latitude (N)
Longitude (W)
S

Figure 6.1.2

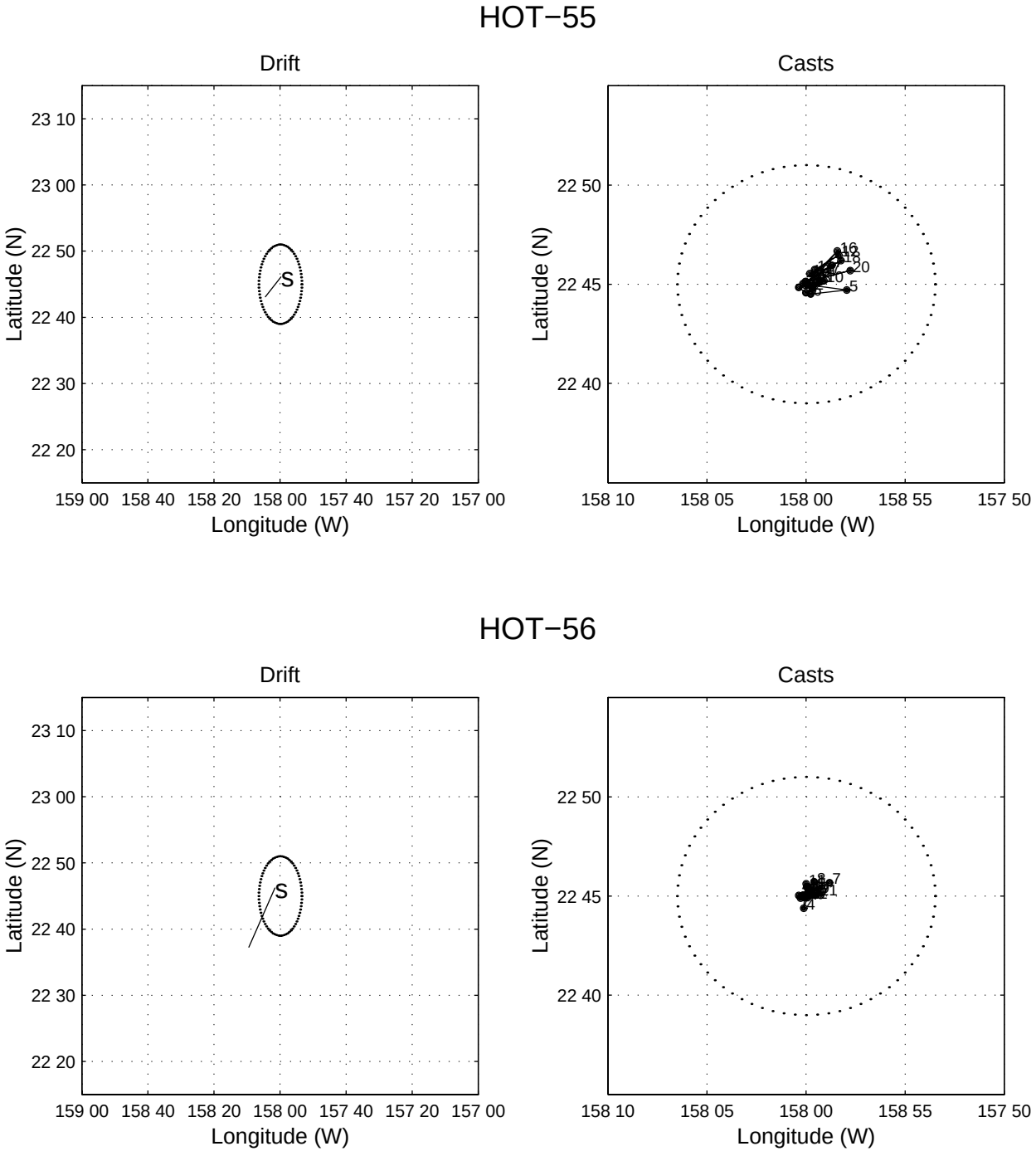
HOT−55
Drift
Casts
Latitude (N)
Longitude (W)
23 10
23 00
22 50
22 40
22 30
22 20
159 00
158 40
158 20
158 00
157 40
157 20
157 00
S
22 50
22 45
22 40
158 10
158 05
158 00
158 55
157 50
HOT−56
Drift
Casts
Latitude (N)
Longitude (W)
S

Figure 6.1.3

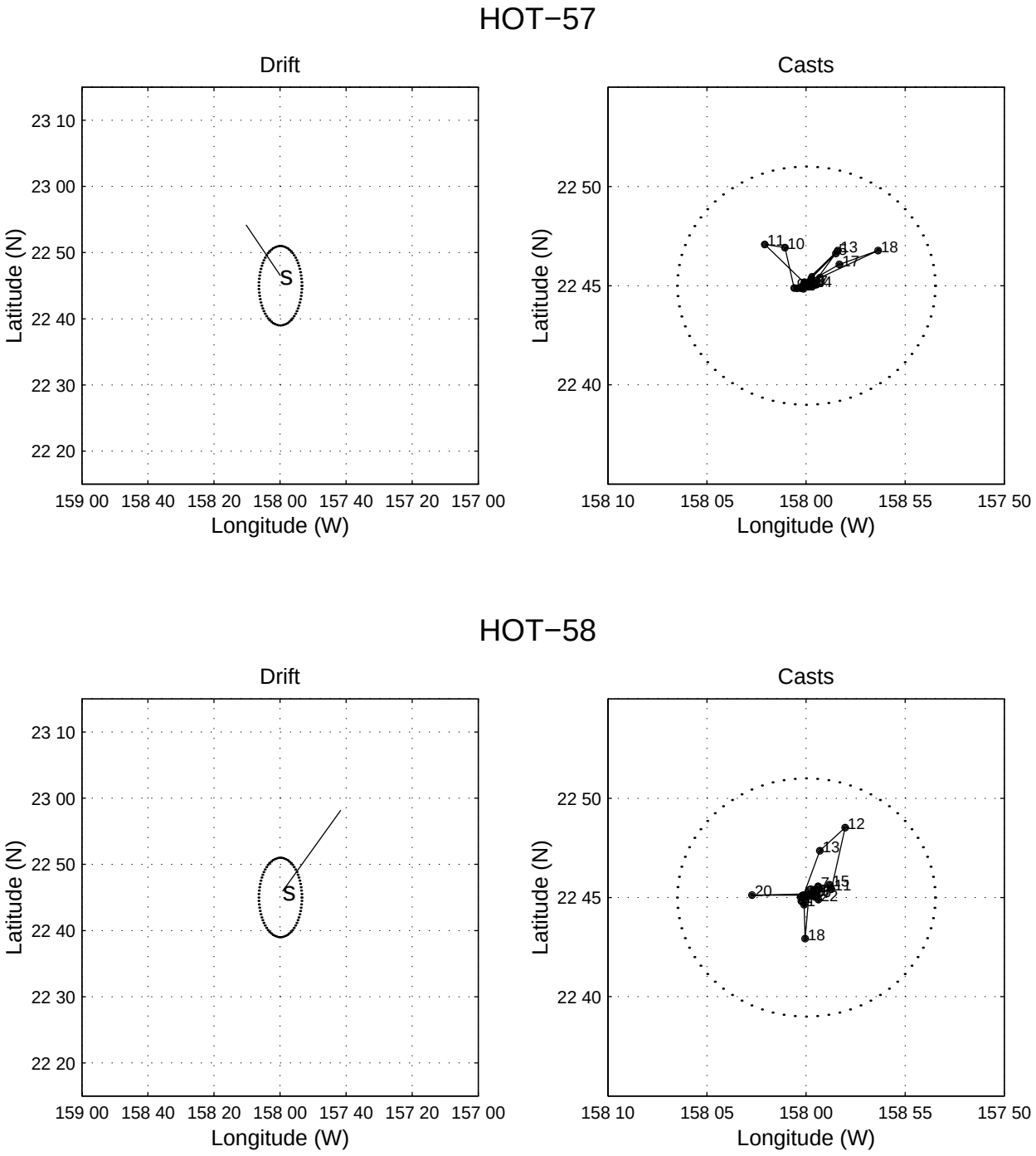
HOT−57
Drift
Casts
23 10
23 00
22 50
22 40
22 30
22 20
Latitude (N)
159 00 158 40 158 20 158 00 157 40 157 20 157 00
Longitude (W)
S
22 50
22 45
22 40
158 10 158 05 158 00 158 55 157 50
11 10 13 18 17
HOT−58
Drift
Casts
12 13 20 18
S

Figure 6.1.4

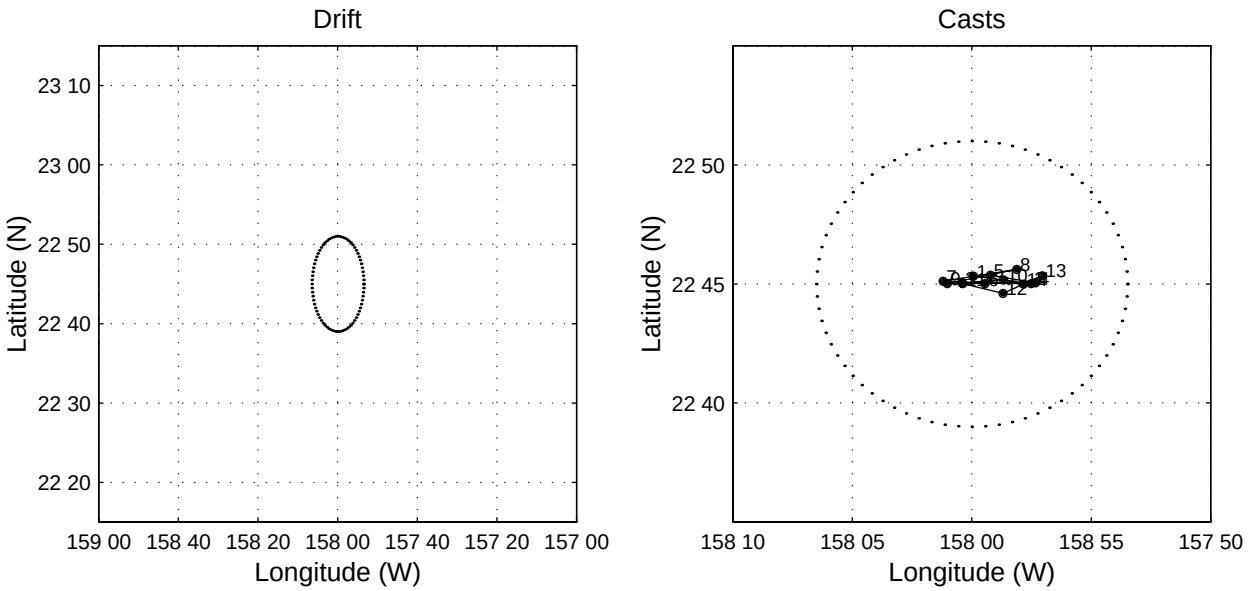
HOT−59
Drift
Casts
Latitude (N)
Longitude (W)
23 10
23 00
22 50
22 40
22 30
22 20
159 00
158 40
158 20
158 00
157 40
157 20
157 00
22 50
22 45
22 40
158 10
158 05
158 00
158 55
157 50

Figure 6.1.5

6.2. CTD Profiles

Figures 6.2.1a-i. Upper left panel: Temperature, salinity, oxygen and density ($\sigma\theta$) as a function of pressure for WOCE deep cast. Salinity and oxygen water bottle data are also plotted. Upper right panel: Nutrients (nitrate+nitrite, soluble reactive phosphate and silicate) and oxygen as a function of potential temperature for all water samples. Lower left panel: CTD temperature and salinity profiles plotted as a function of pressure. Lower right panel: Salinity and oxygen from CTD and water samples plotted as a function of potential temperature.

Figures 6.2.2a-i. Upper panel: Stack plots of potential temperature versus pressure to 1000 dbar. Offset is 2º C. Lower panel: Stack plots of salinity versus pressure to 1000 dbar. Offset is 0.1.

Figures 6.2.3a-i: As in 6.1.1 but for Station Kahe.

Figure 6.2.4. Upper panel: Potential temperature versus pressure for all deep casts in 1994. Lower panel: Potential temperature for all deep casts in 1994 plotted from 2500 dbar.

Figure 6.2.5. Upper panel: Potential temperature versus salinity for all deep casts collected during 1994. Lower panel: Potential temperature versus salinity on same casts in the 1-5 °C range.

Figure 6.2.6. Upper panel: Oxygen values derived from calibrated CTD sensor data versus potential temperature for all deep casts collected during 1994. Lower panel: Oxygen versus potential temperature for 1994 deep casts within the 1-5 °C range.

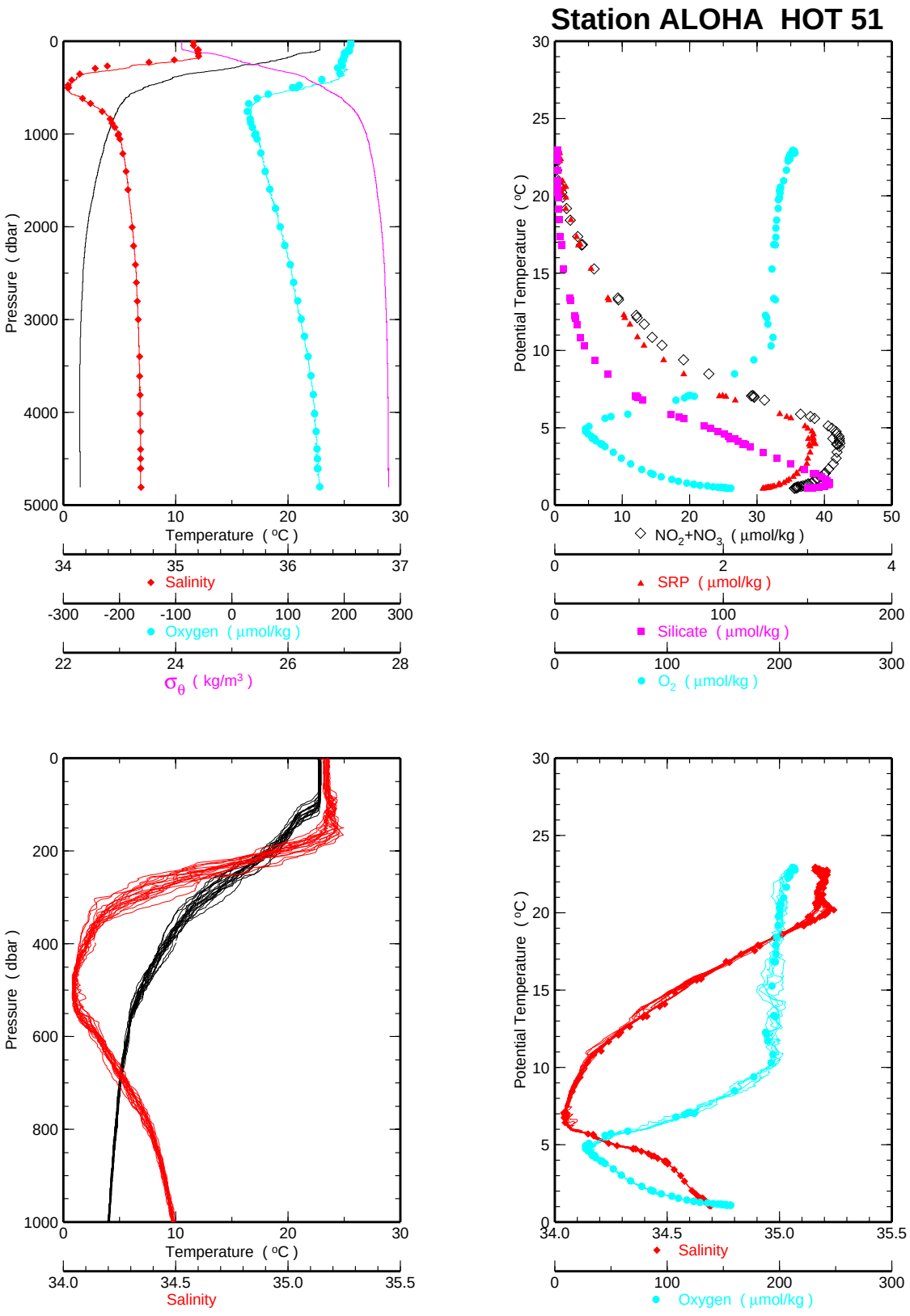
Station ALOHA HOT 51
Pressure (dbar)
Temperature (ºC)
Salinity
Oxygen (µmol/kg)
σθ (kg/m³)
Potential Temperature (ºC)
NO2+NO3 (µmol/kg)
SRP (µmol/kg)
Silicate (µmol/kg)
O2 (µmol/kg)

Figure 6.2.1a

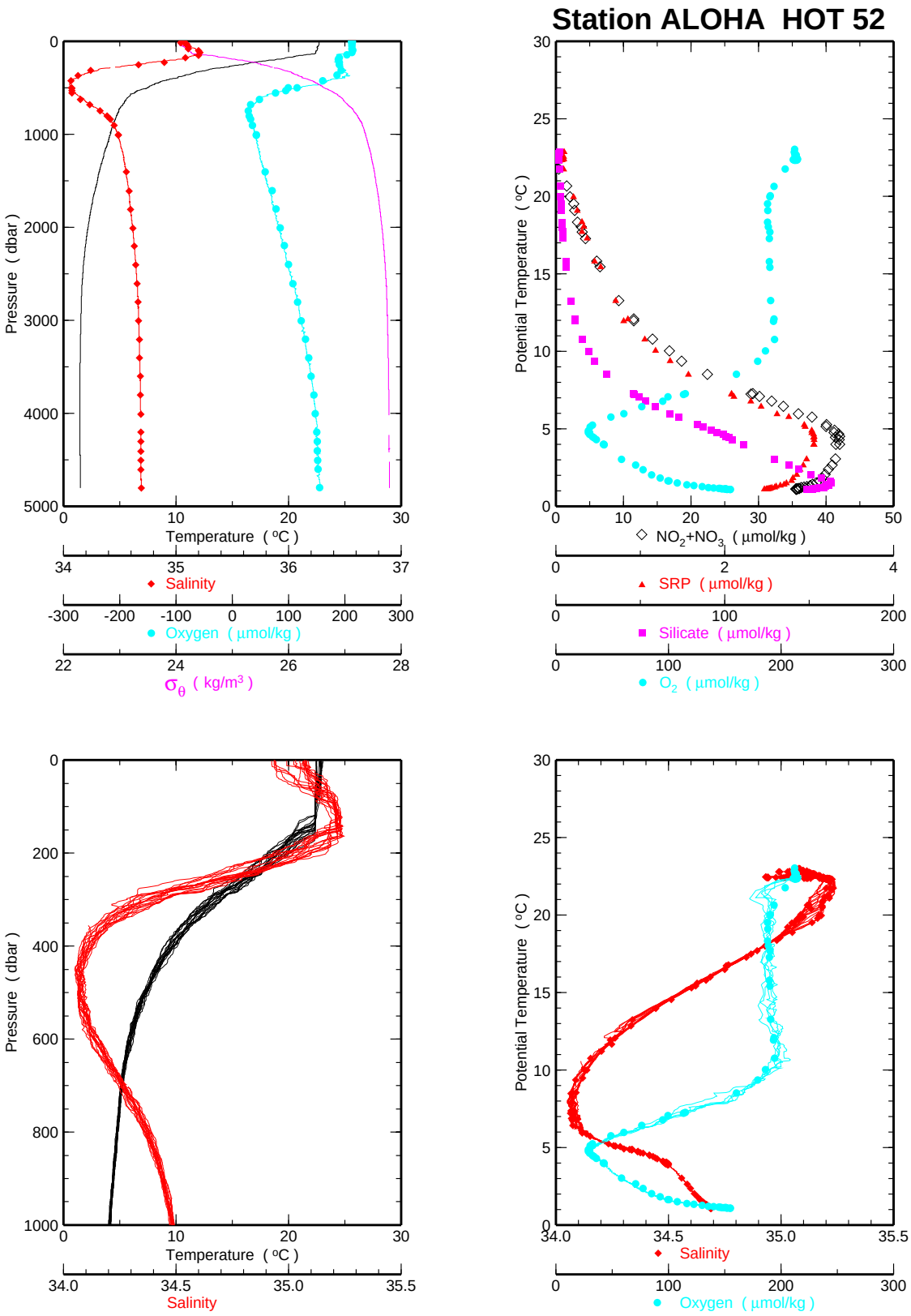
Station ALOHA HOT 52
Pressure (dbar)
Temperature (ºC)
Salinity
Oxygen (µmol/kg)
σθ (kg/m³)
Potential Temperature (ºC)
NO2+NO3 (µmol/kg)
SRP (µmol/kg)
Silicate (µmol/kg)
O2 (µmol/kg)

Figure 6.2.1b

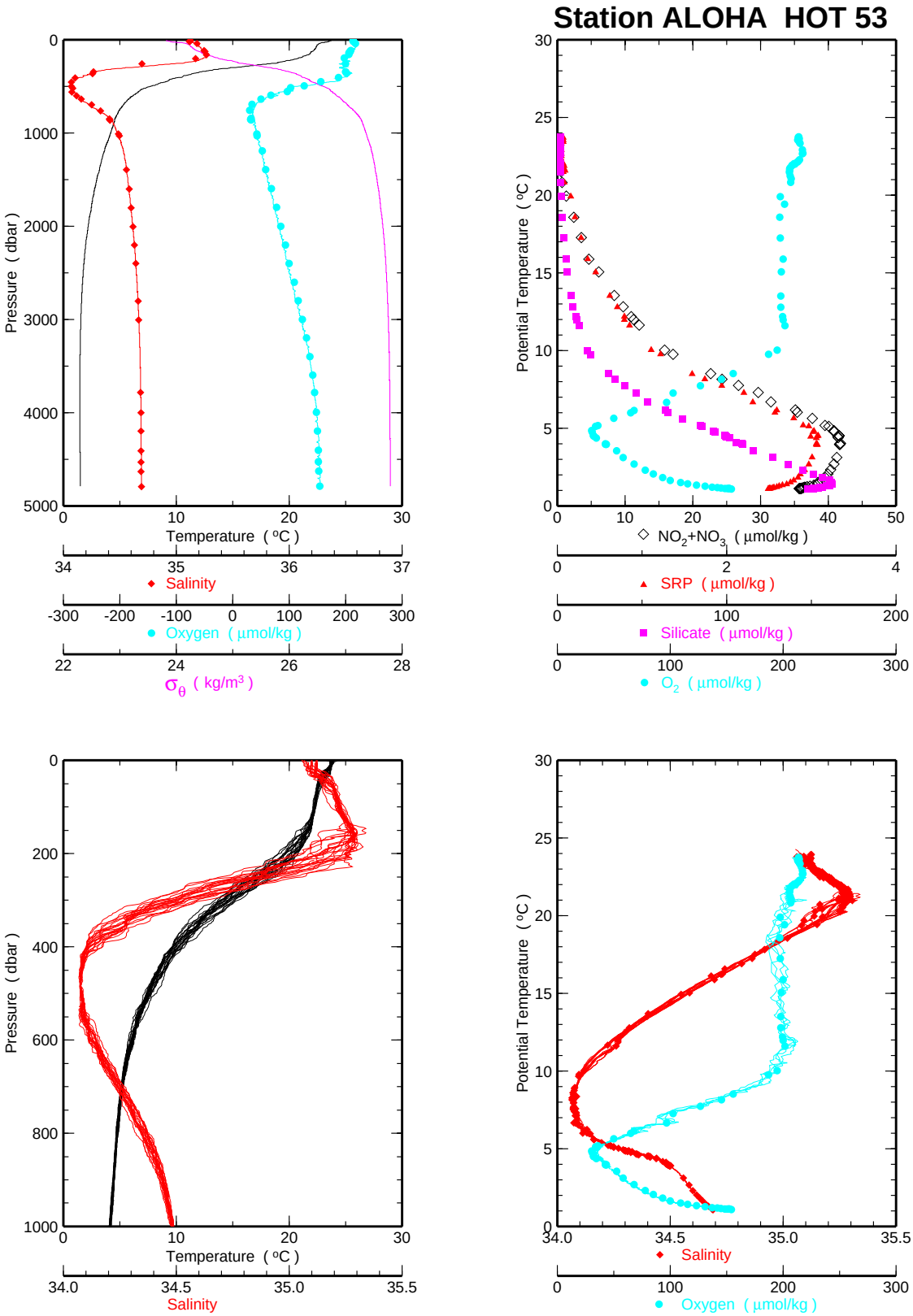
Station ALOHA HOT 53
Pressure (dbar)
Temperature (°C)
Salinity
Oxygen (µmol/kg)
σθ (kg/m³)
Potential Temperature (°C)
NO2+NO3 (µmol/kg)
SRP (µmol/kg)
Silicate (µmol/kg)
O2 (µmol/kg)

Figure 6.2.1c

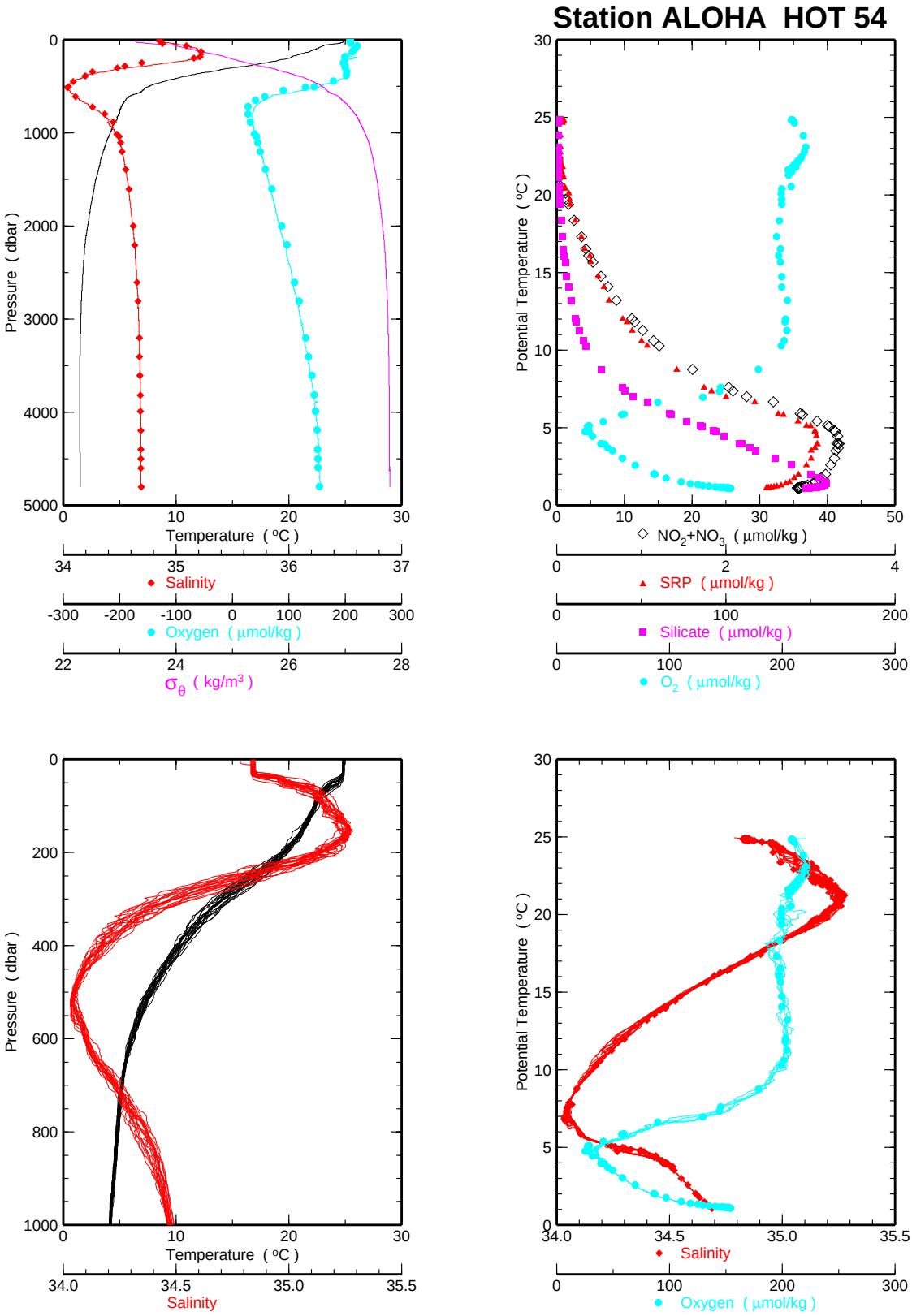
Station ALOHA HOT 54
Pressure (dbar)
Temperature (°C)
Salinity
Oxygen (µmol/kg)
σθ (kg/m³)
Potential Temperature (°C)
NO2+NO3 (µmol/kg)
SRP (µmol/kg)
Silicate (µmol/kg)
O2 (µmol/kg)

Figure 6.2.1d

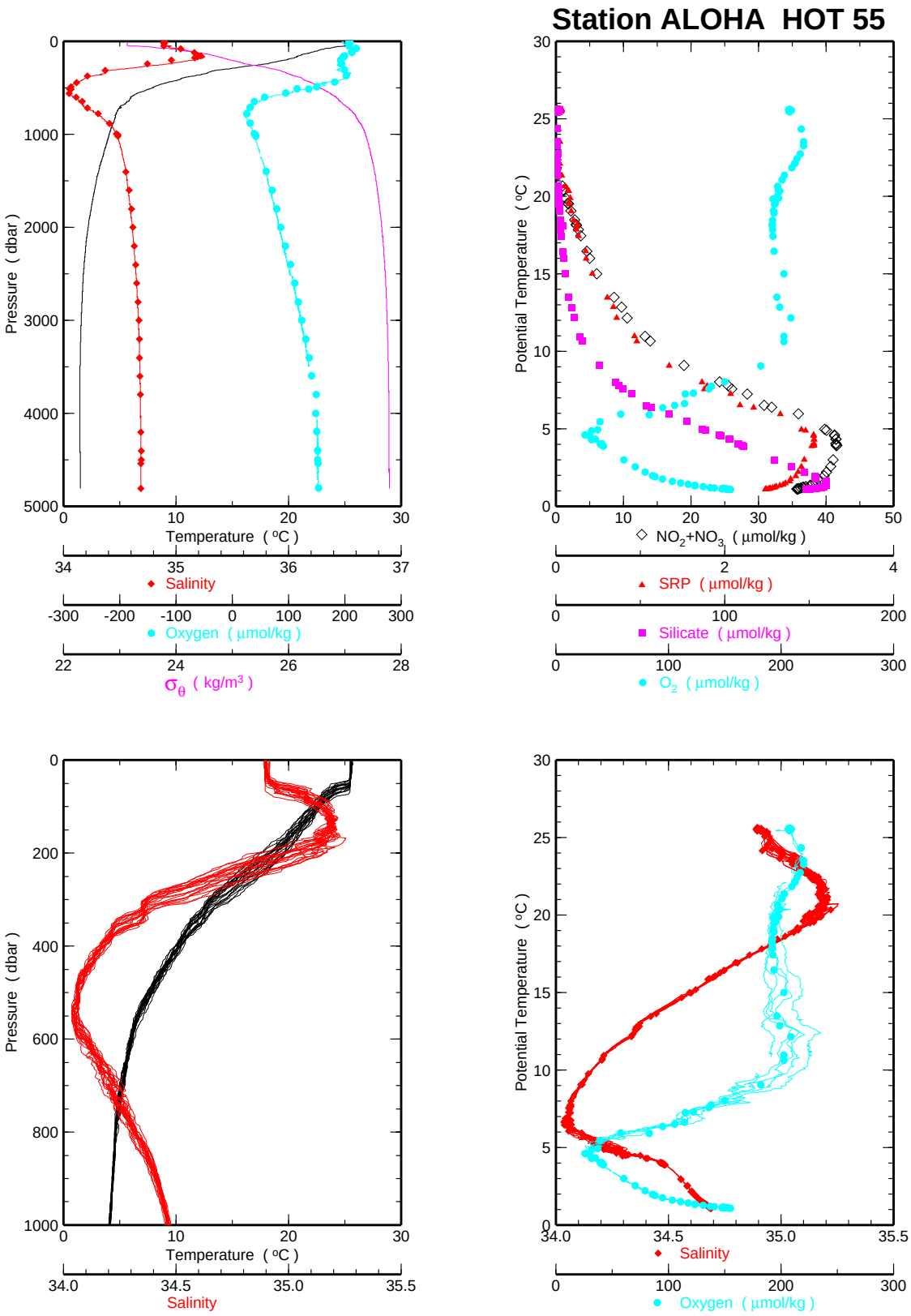
Station ALOHA HOT 55
Pressure (dbar)
Temperature (ºC)
Salinity
Oxygen (µmol/kg)
σθ (kg/m³)
Potential Temperature (ºC)
NO2+NO3 (µmol/kg)
SRP (µmol/kg)
Silicate (µmol/kg)
O2 (µmol/kg)

Figure 6.2.1e

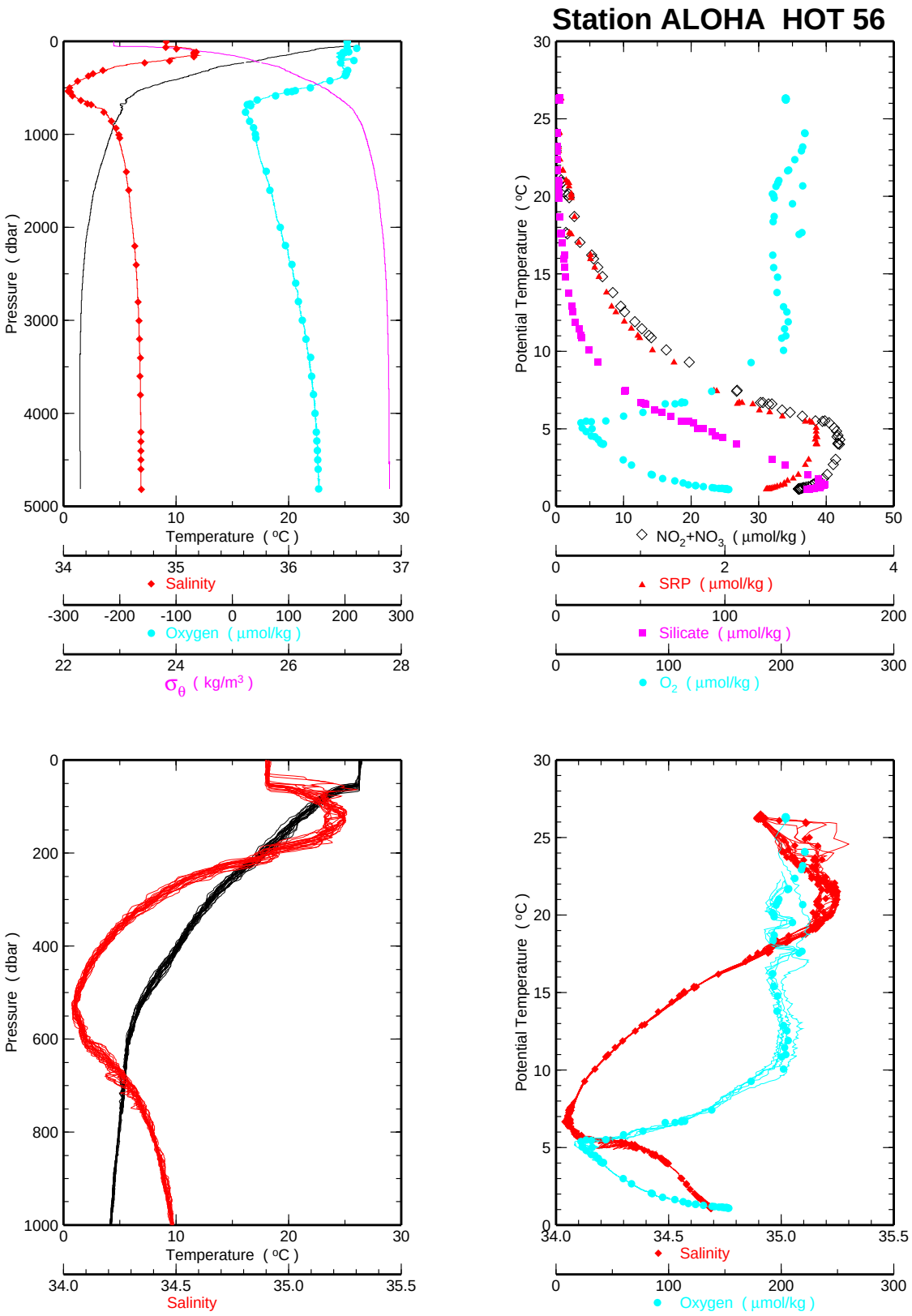
Station ALOHA HOT 56
Pressure (dbar)
Temperature (ºC)
Salinity
Oxygen (µmol/kg)
σθ (kg/m³)
Potential Temperature (ºC)
NO2+NO3 (µmol/kg)
SRP (µmol/kg)
Silicate (µmol/kg)
O2 (µmol/kg)

Figure 6.2.1f

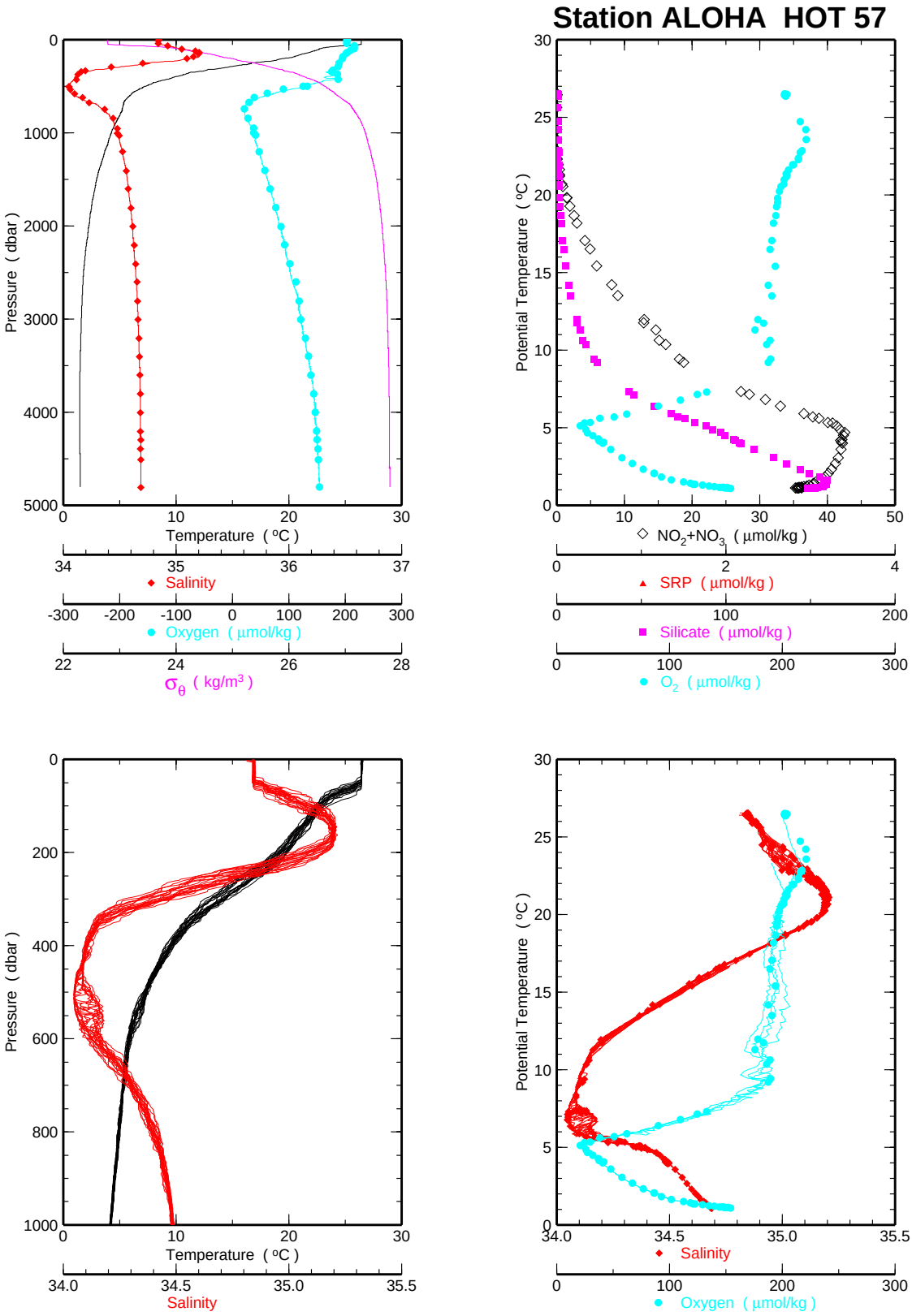
Station ALOHA HOT 57
Pressure (dbar)
Temperature (°C)
Salinity
Oxygen (µmol/kg)
σθ (kg/m³)
Potential Temperature (°C)
NO2+NO3 (µmol/kg)
SRP (µmol/kg)
Silicate (µmol/kg)
O2 (µmol/kg)

Figure 6.2.1g

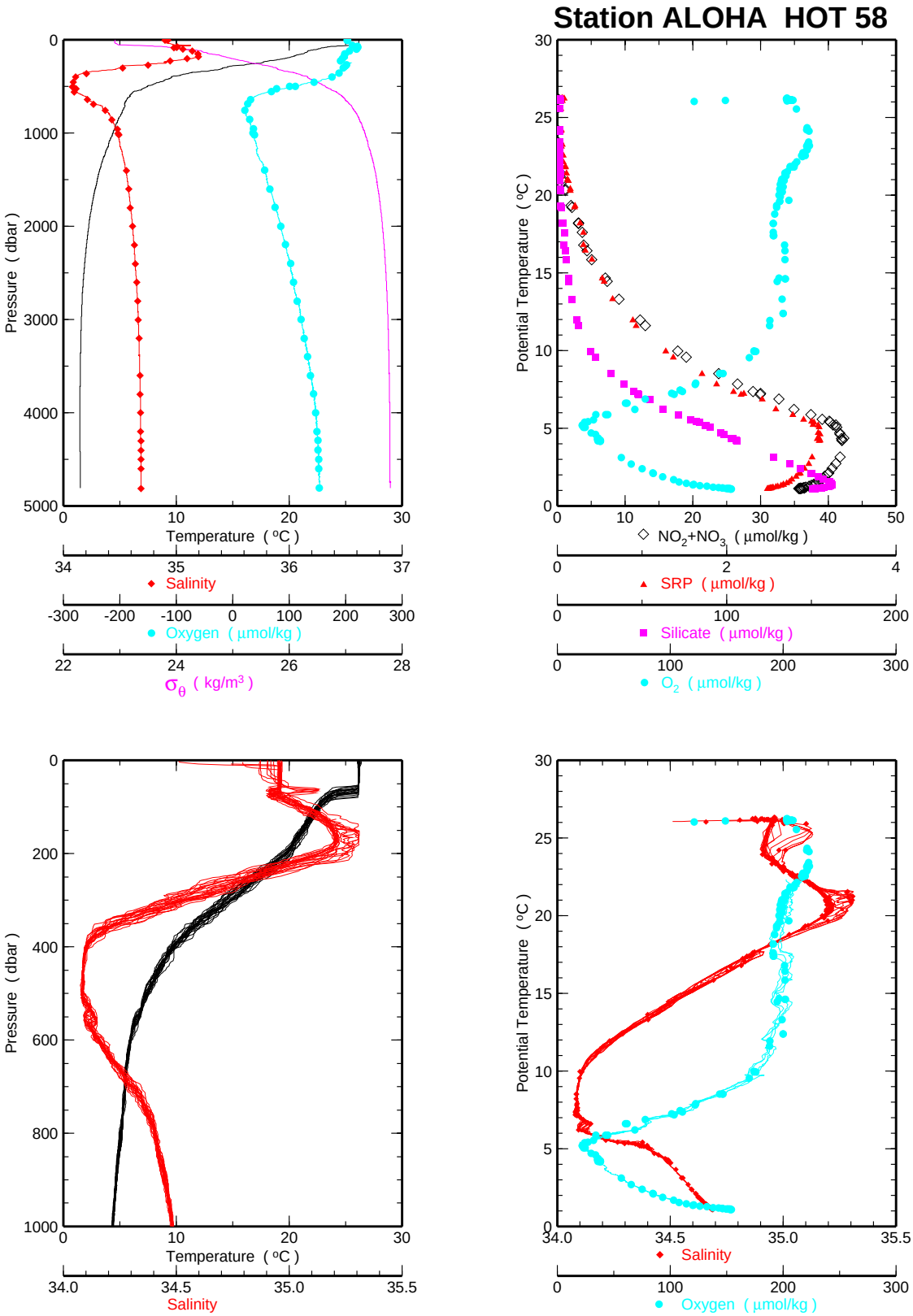
Station ALOHA HOT 58
Pressure (dbar)
Temperature (°C)
Salinity
Oxygen (µmol/kg)
σθ (kg/m³)
Potential Temperature (°C)
NO2+NO3 (µmol/kg)
SRP (µmol/kg)
Silicate (µmol/kg)
O2 (µmol/kg)

Figure 6.2.1h

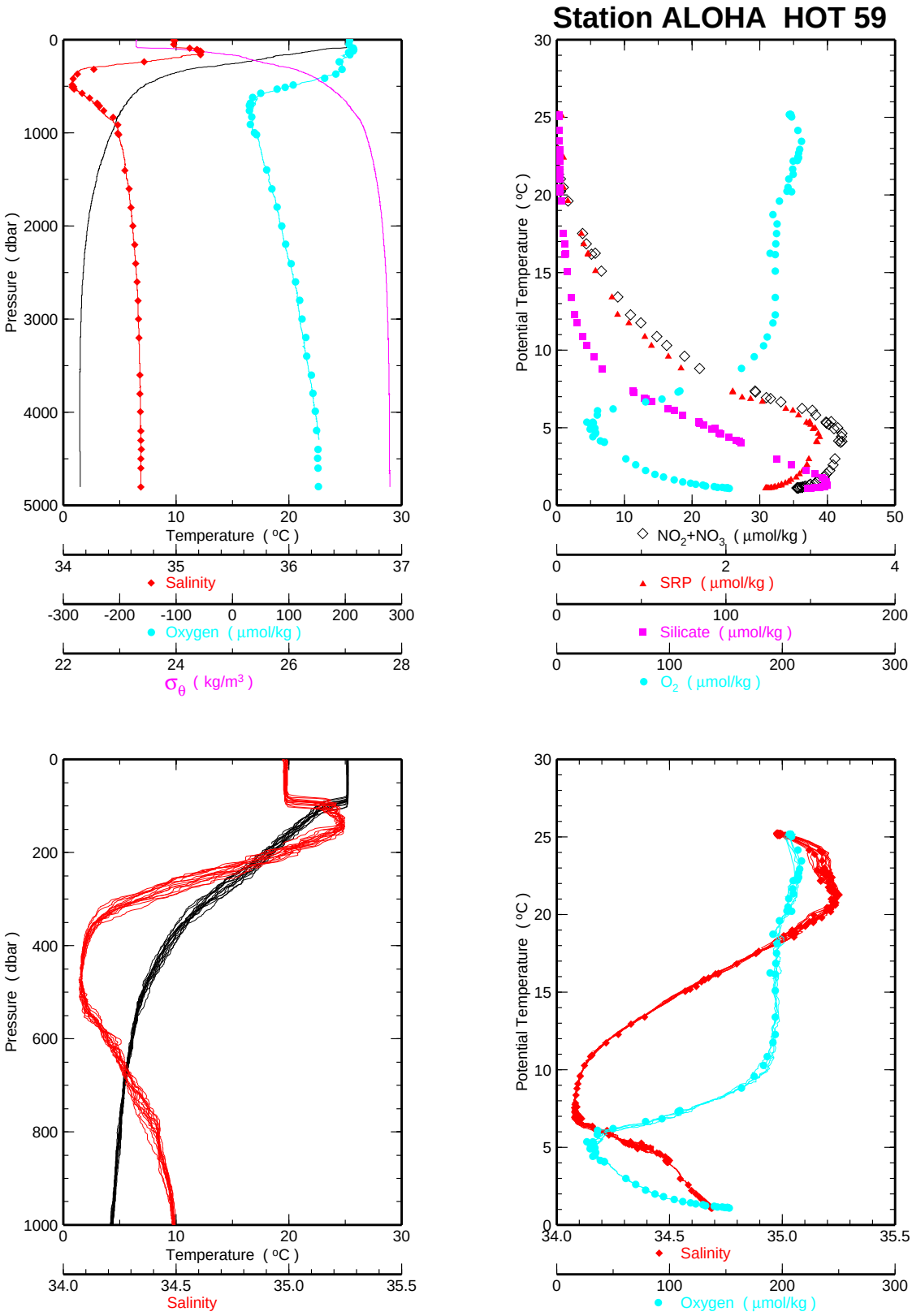
Station ALOHA HOT 59
Pressure (dbar)
Temperature (°C)
Salinity
Oxygen (µmol/kg)
σθ (kg/m³)
Potential Temperature (°C)
NO2+NO3 (µmol/kg)
SRP (µmol/kg)
Silicate (µmol/kg)
O2 (µmol/kg)

Figure 6.2.1i

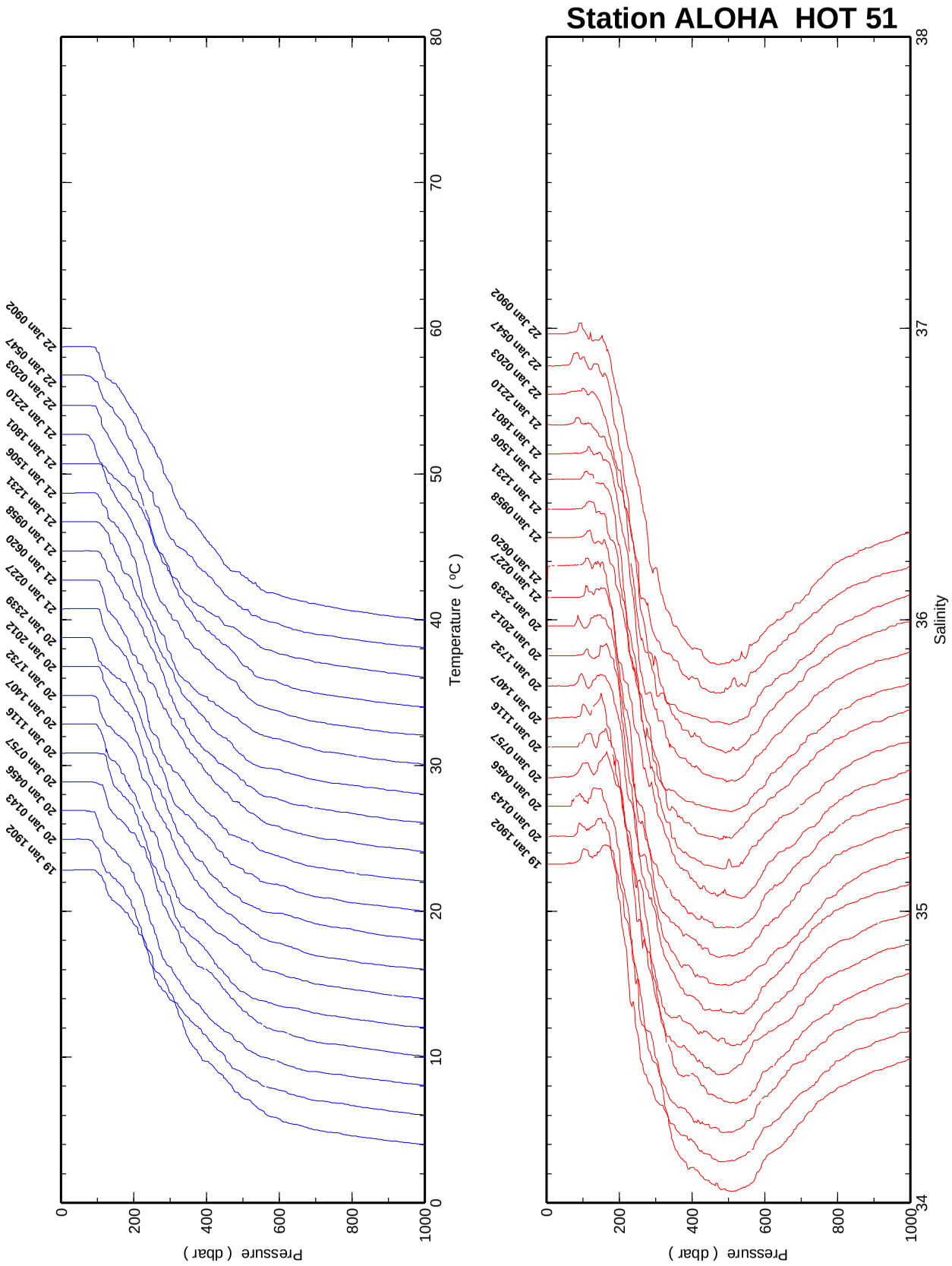
Station ALOHA HOT 51
Pressure (dbar)
Temperature (°C)
Salinity
22 Jan 0902
22 Jan 0547
22 Jan 0203
21 Jan 2210
21 Jan 1801
21 Jan 1506
21 Jan 1231
21 Jan 0958
21 Jan 0620
21 Jan 0227
20 Jan 2339
20 Jan 2012
20 Jan 1732
20 Jan 1407
20 Jan 1116
20 Jan 0757
20 Jan 0456
20 Jan 0143
19 Jan 1902

Figure 6.2.2a

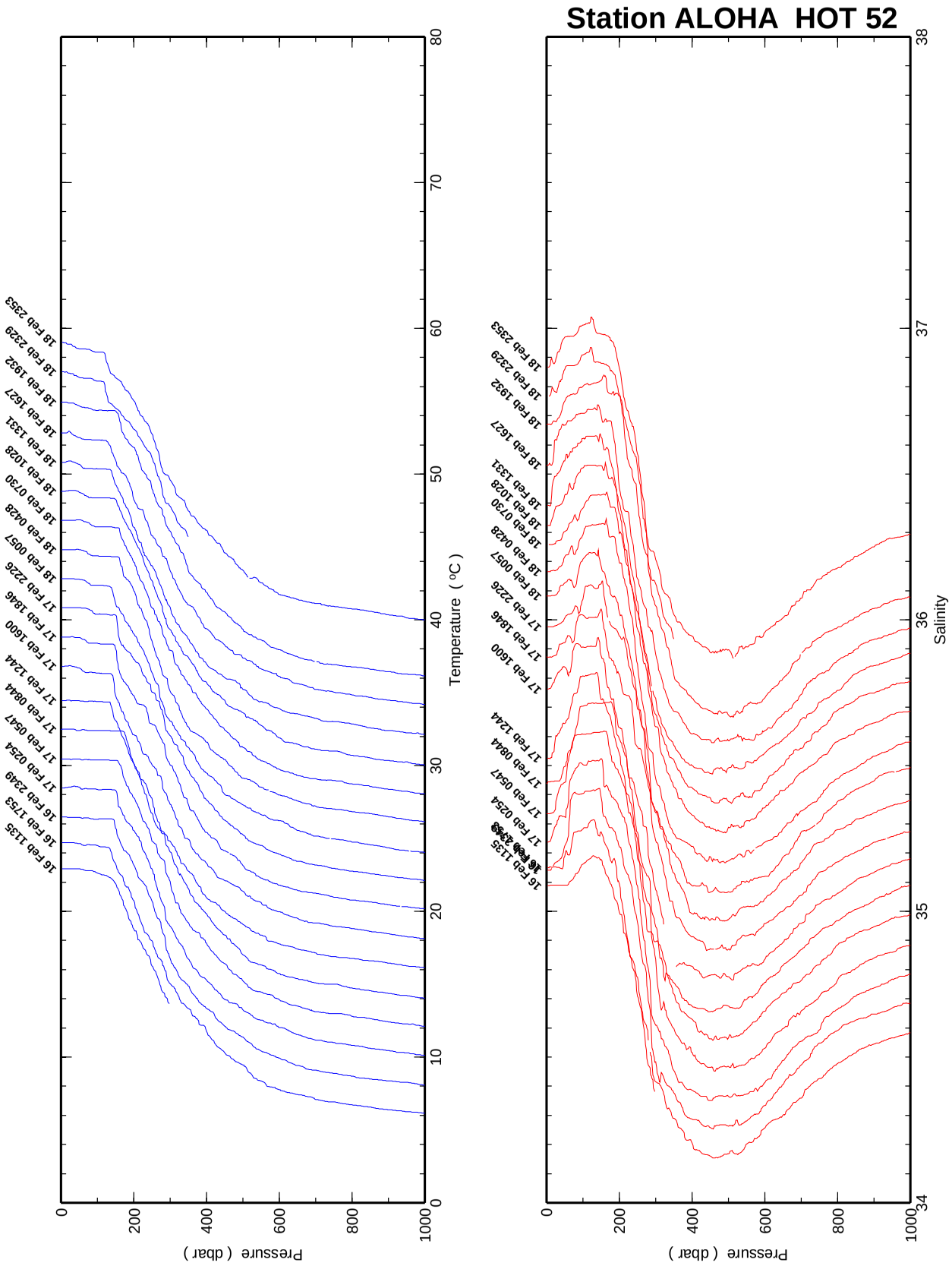
Station ALOHA HOT 52
Temperature (°C)
Salinity
Pressure (dbar)
Pressure (dbar)
18 Feb 2353
18 Feb 2329
18 Feb 1932
18 Feb 1627
18 Feb 1331
18 Feb 1028
18 Feb 0730
18 Feb 0428
18 Feb 0057
17 Feb 2226
17 Feb 1846
17 Feb 1600
17 Feb 1244
17 Feb 0844
17 Feb 0547
17 Feb 0254
16 Feb 2349
16 Feb 1753
16 Feb 1135

Figure 6.2.2b

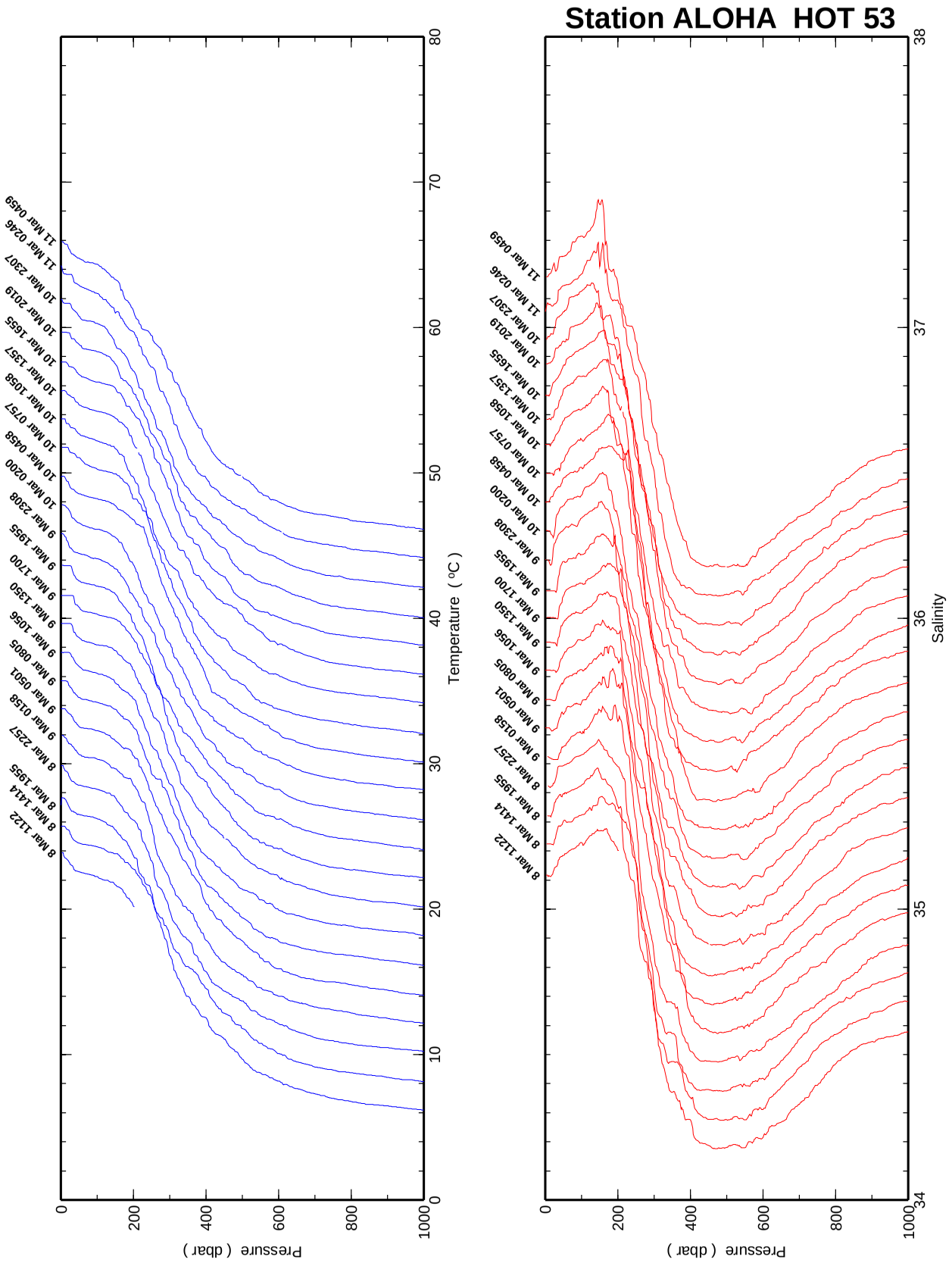
Station ALOHA HOT 53
Temperature (°C)
Salinity
Pressure (dbar)
Pressure (dbar)
11 Mar 0459
11 Mar 0246
10 Mar 2307
10 Mar 2019
10 Mar 1655
10 Mar 1357
10 Mar 1058
10 Mar 0757
10 Mar 0458
10 Mar 0200
9 Mar 2308
9 Mar 1955
9 Mar 1700
9 Mar 1350
9 Mar 1056
9 Mar 0805
9 Mar 0501
9 Mar 0158
8 Mar 2257
8 Mar 1955
8 Mar 1414
8 Mar 1122

Figure 6.2.2c

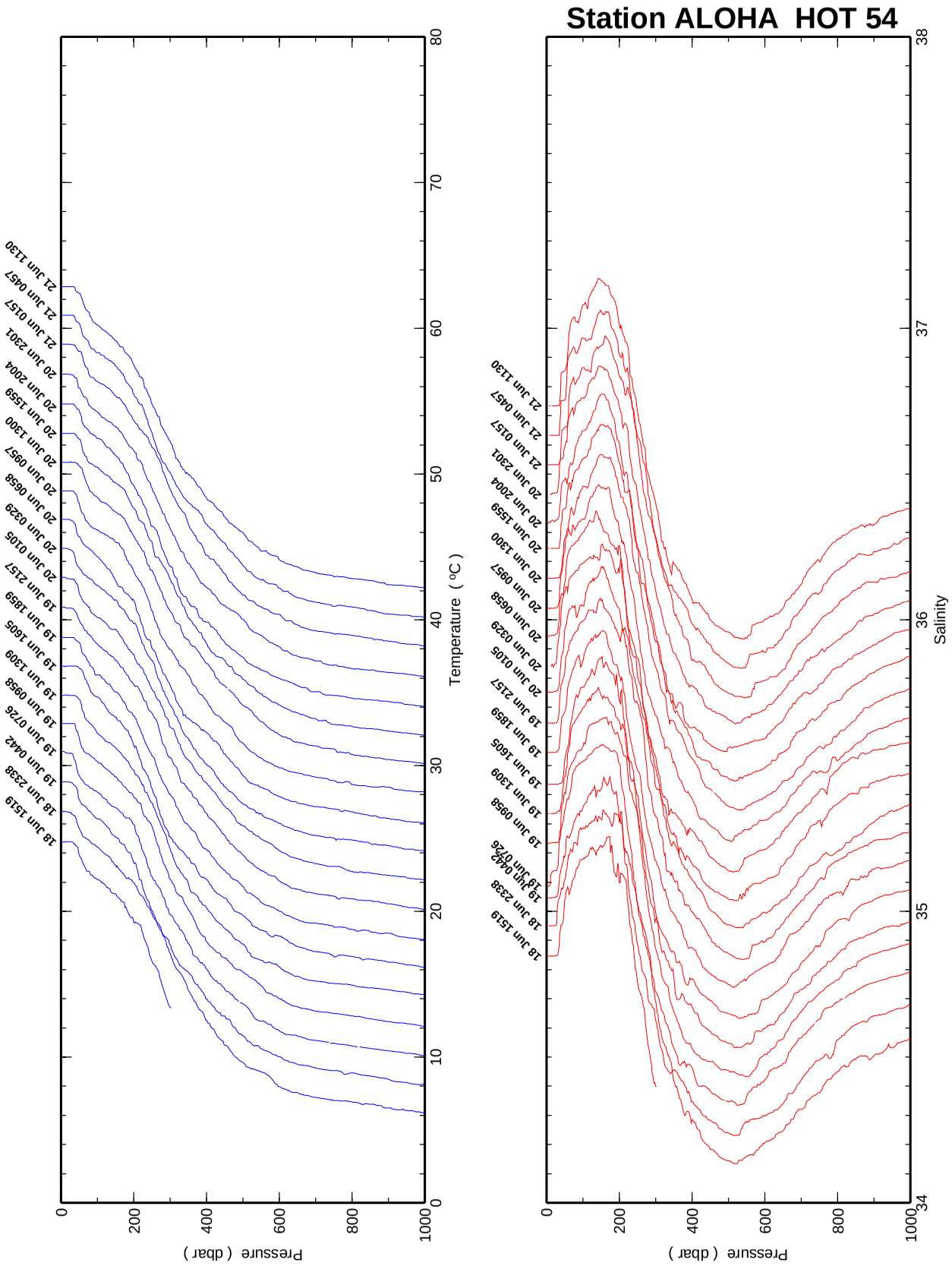
Station ALOHA HOT 54
Temperature (°C)
Salinity
Pressure (dbar)
Pressure (dbar)
18 Jun 1519
18 Jun 2338
19 Jun 0442
19 Jun 0726
19 Jun 0958
19 Jun 1309
19 Jun 1605
19 Jun 1859
19 Jun 2157
20 Jun 0105
20 Jun 0329
20 Jun 0658
20 Jun 0957
20 Jun 1300
20 Jun 1559
20 Jun 2004
20 Jun 2301
21 Jun 0157
21 Jun 0457
21 Jun 1130

Figure 6.2.2d

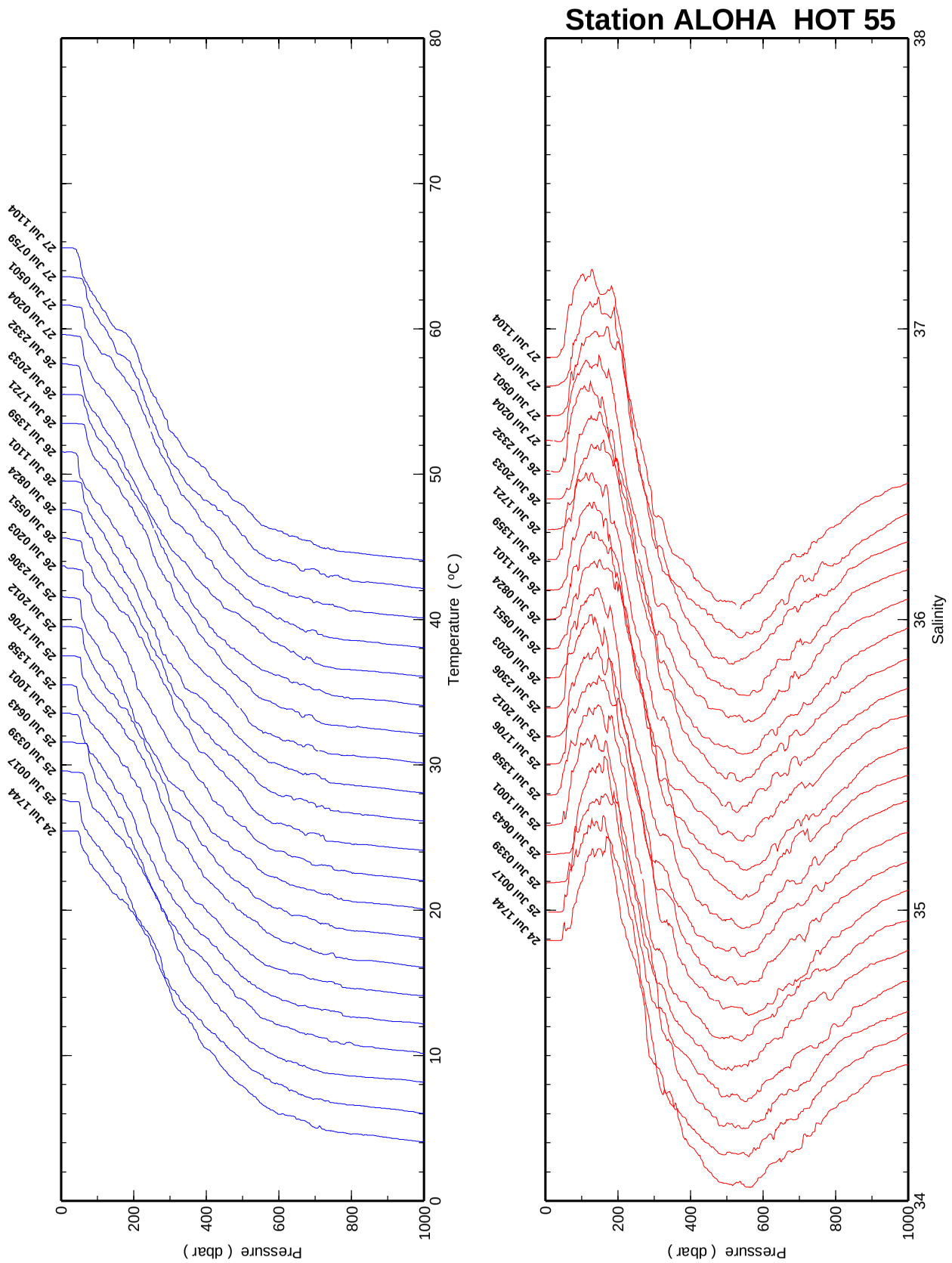
Station ALOHA HOT 55
Temperature (°C)
Salinity
Pressure (dbar)
Pressure (dbar)
27 Jul 1104
27 Jul 0759
27 Jul 0501
27 Jul 0204
26 Jul 2332
26 Jul 2033
26 Jul 1721
26 Jul 1359
26 Jul 1101
26 Jul 0824
26 Jul 0551
26 Jul 0203
25 Jul 2306
25 Jul 2012
25 Jul 1706
25 Jul 1358
25 Jul 1001
25 Jul 0643
25 Jul 0339
25 Jul 0017
24 Jul 1744

Figure 6.2.2e

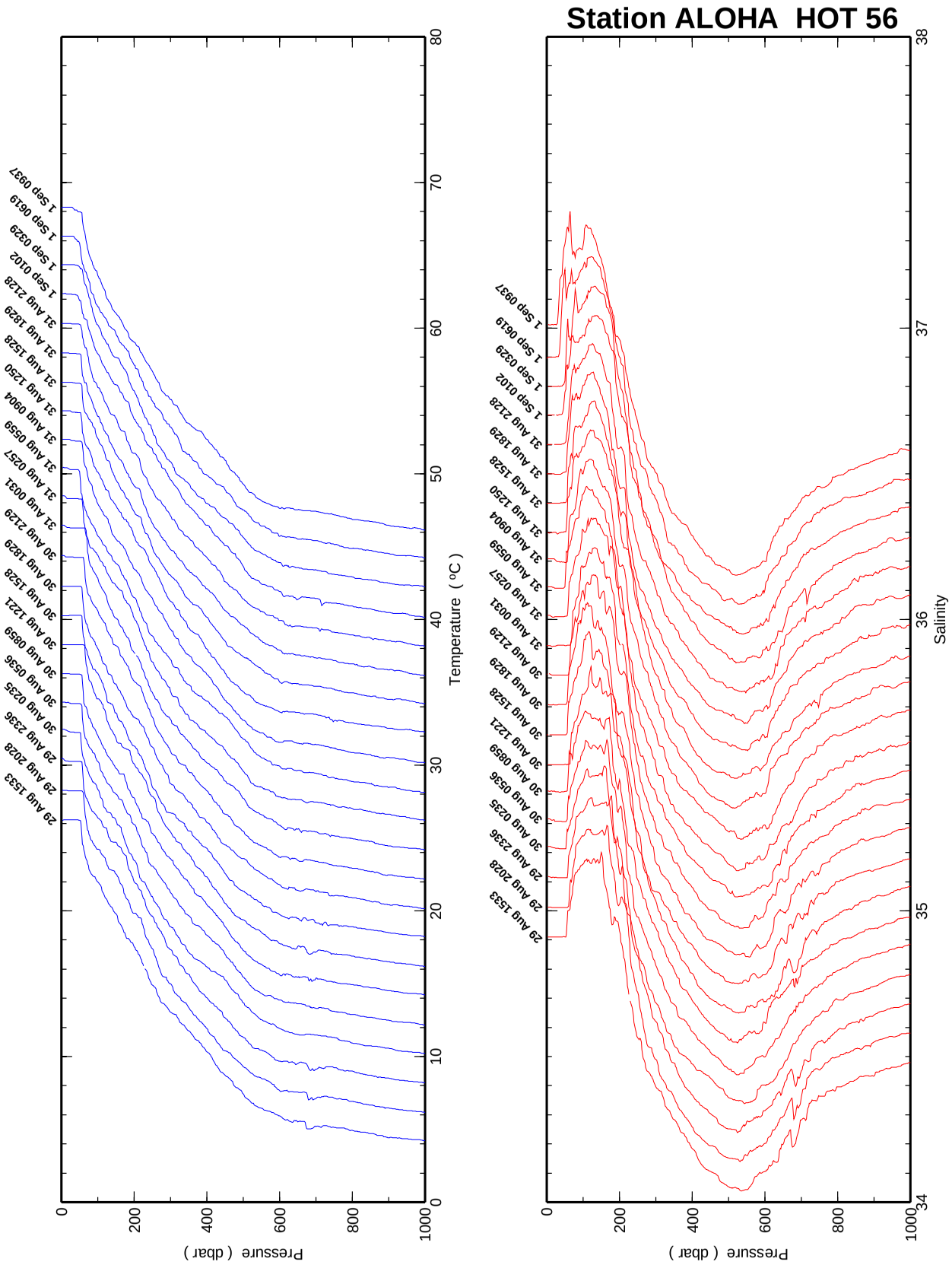
Station ALOHA HOT 56
Temperature (°C)
Salinity
Pressure (dbar)
Pressure (dbar)
1 Sep 0937
1 Sep 0619
1 Sep 0329
1 Sep 0102
31 Aug 2128
31 Aug 1829
31 Aug 1528
31 Aug 1250
31 Aug 0904
31 Aug 0559
31 Aug 0257
31 Aug 0031
30 Aug 2129
30 Aug 1829
30 Aug 1528
30 Aug 1221
30 Aug 0859
30 Aug 0536
30 Aug 0235
29 Aug 2336
29 Aug 2028
29 Aug 1533

Figure 6.2.2f

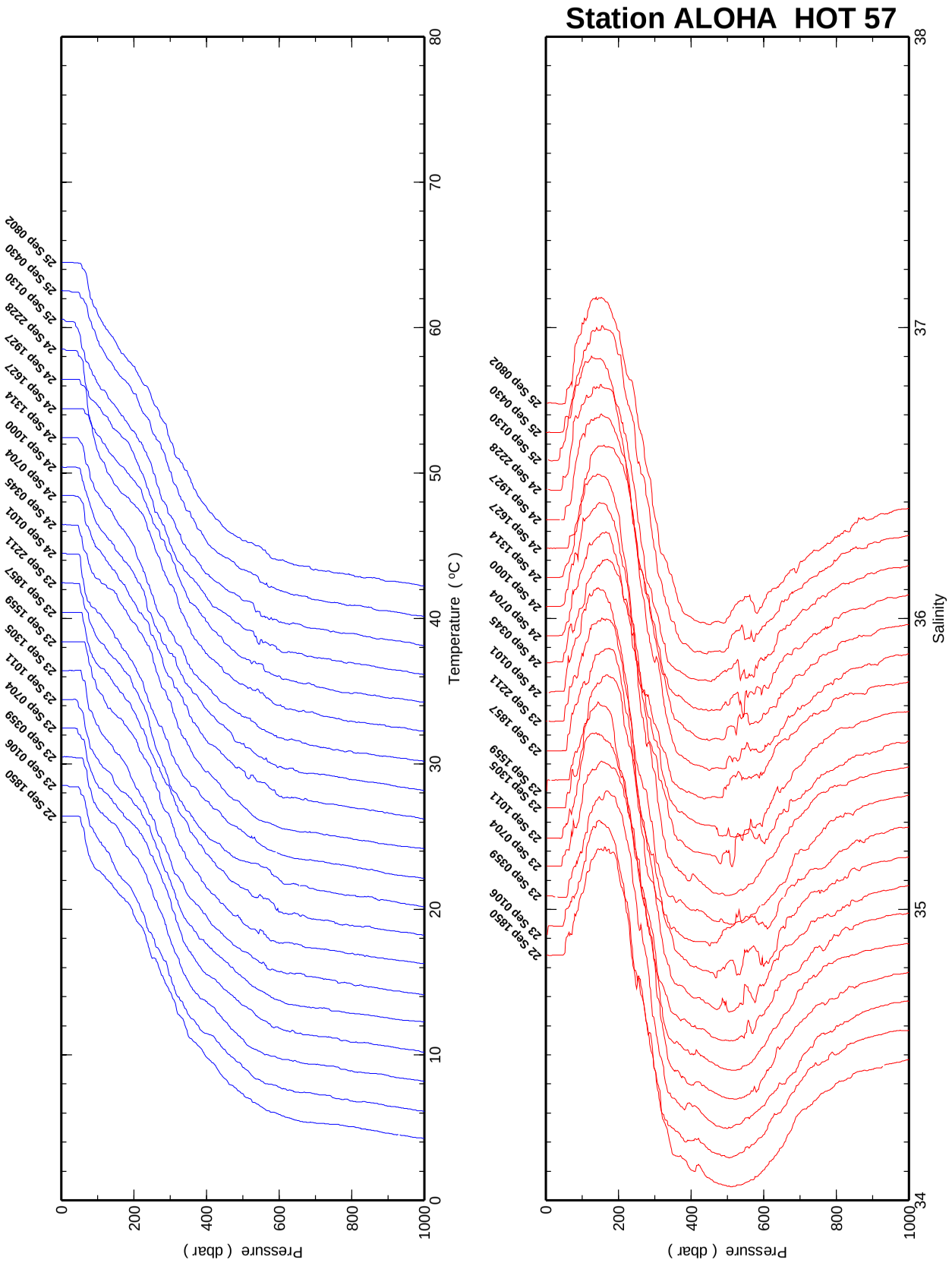
Station ALOHA HOT 57
Temperature (°C)
Salinity
Pressure (dbar)
Pressure (dbar)
22 Sep 1850
23 Sep 0106
23 Sep 0359
23 Sep 0704
23 Sep 1011
23 Sep 1305
23 Sep 1559
23 Sep 1857
24 Sep 2211
24 Sep 0101
24 Sep 0345
24 Sep 0704
24 Sep 1000
24 Sep 1314
24 Sep 1627
24 Sep 1927
25 Sep 2228
25 Sep 0130
25 Sep 0430
25 Sep 0802

Figure 6.2.2g

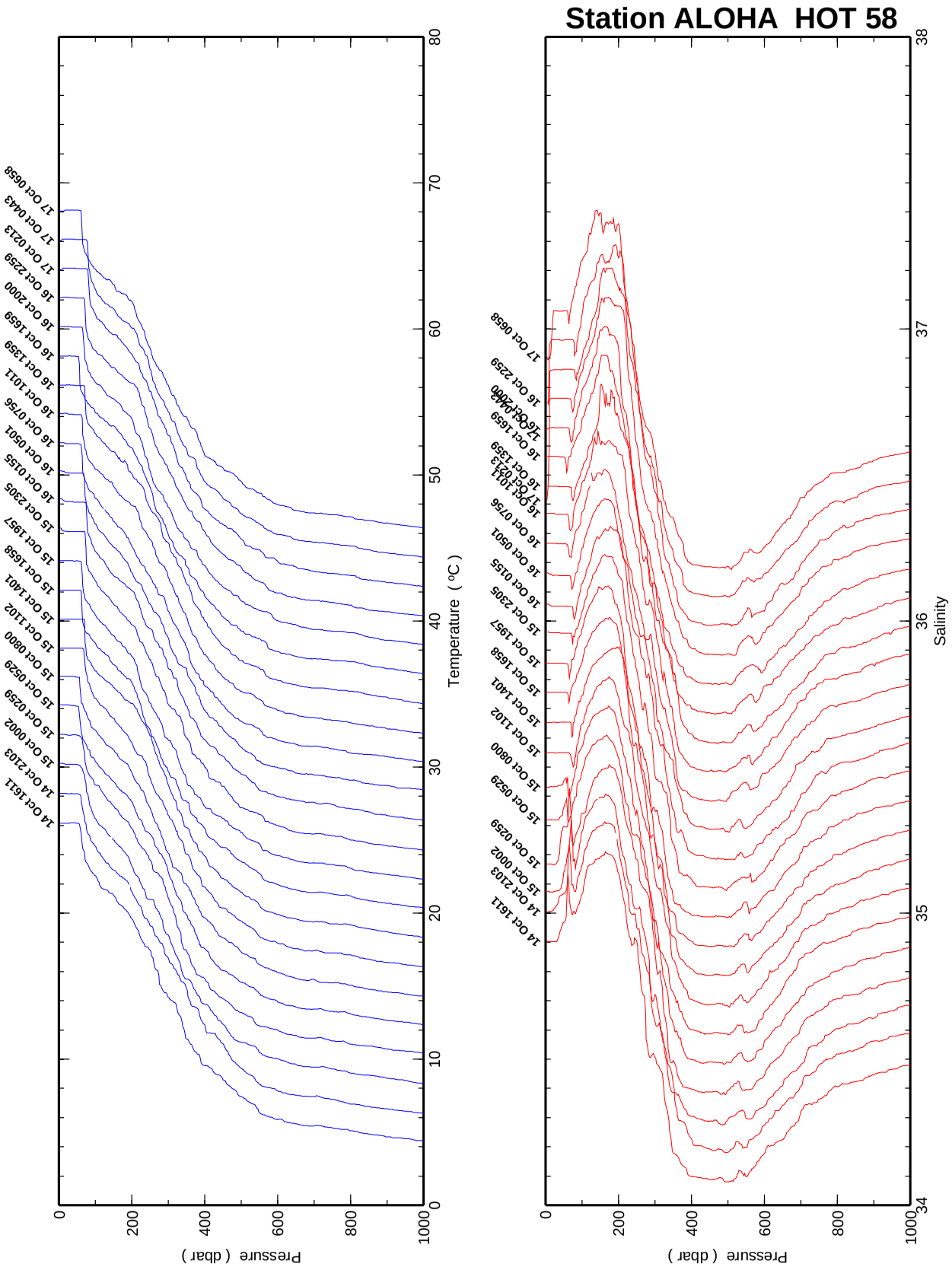
Station ALOHA HOT 58
Temperature (°C)
Salinity
Pressure (dbar)
Pressure (dbar)
14 Oct 1611
14 Oct 2103
15 Oct 0002
15 Oct 0259
15 Oct 0529
15 Oct 0800
15 Oct 1102
15 Oct 1401
15 Oct 1658
15 Oct 1957
15 Oct 2305
16 Oct 0155
16 Oct 0501
16 Oct 0756
16 Oct 1011
16 Oct 1359
16 Oct 1659
16 Oct 2000
16 Oct 2259
17 Oct 0213
17 Oct 0443
17 Oct 0658

Figure 6.2.2h

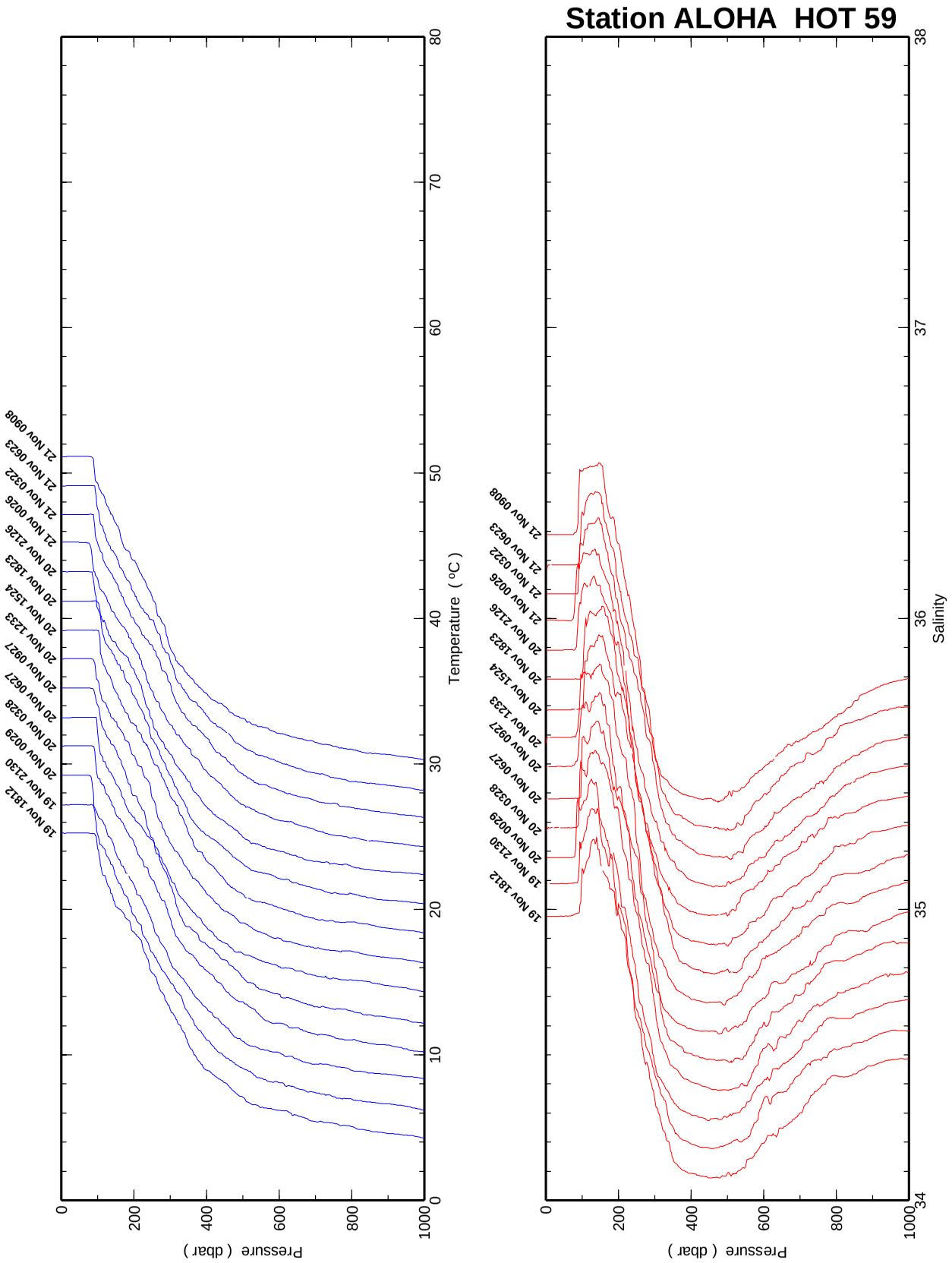
Station ALOHA HOT 59
Temperature (°C)
Salinity
Pressure (dbar)
Pressure (dbar)
19 Nov 1812
19 Nov 2130
20 Nov 0029
20 Nov 0328
20 Nov 0627
20 Nov 0927
20 Nov 1233
20 Nov 1524
20 Nov 1823
20 Nov 2126
21 Nov 0026
21 Nov 0322
21 Nov 0623
21 Nov 0908

Figure 6.2.2i

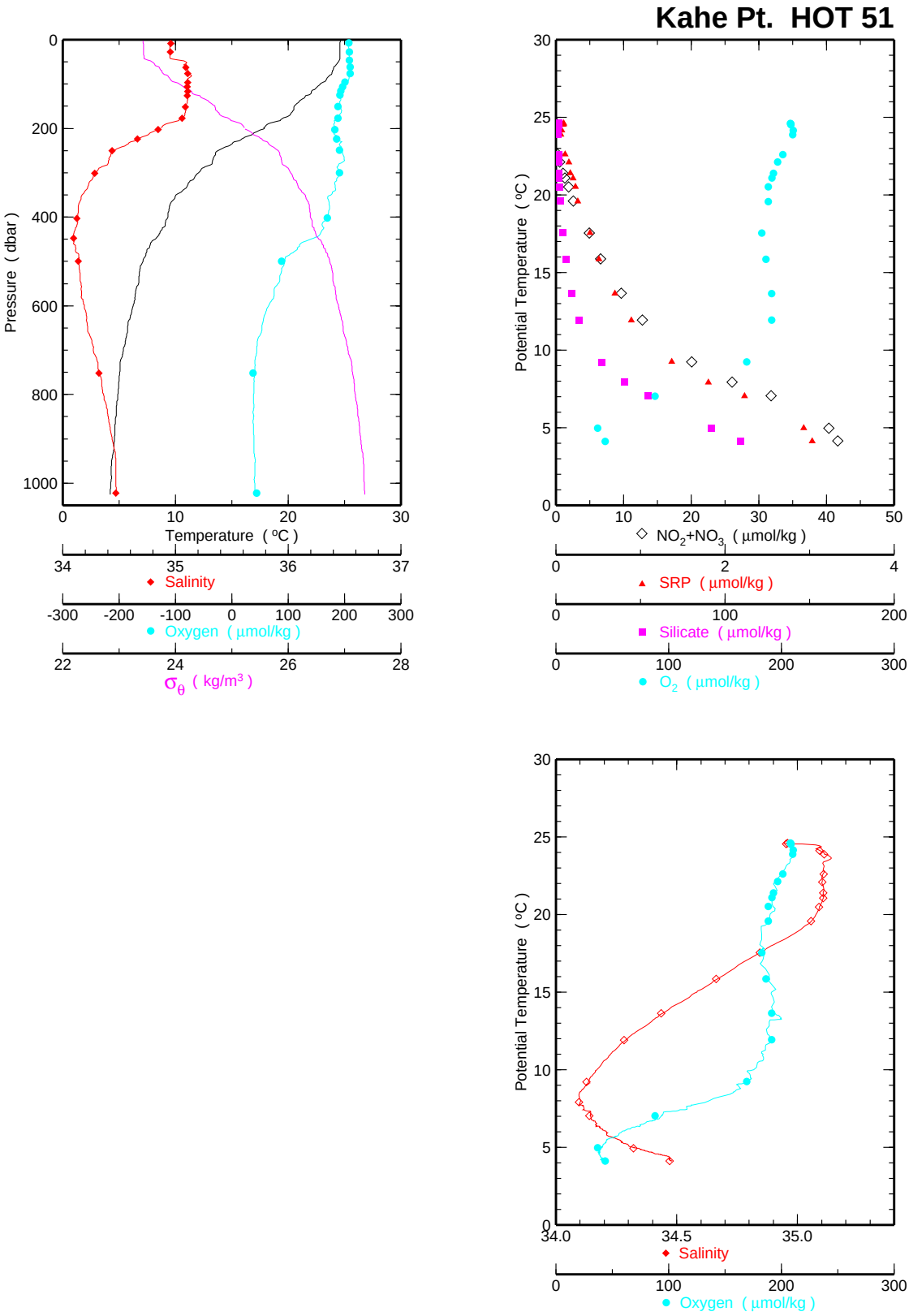
Kahe Pt. HOT 51
Pressure (dbar)
Temperature (ºC)
Salinity
Oxygen (µmol/kg)
σθ (kg/m³)
Potential Temperature (ºC)
NO2+NO3 (µmol/kg)
SRP (µmol/kg)
Silicate (µmol/kg)
O2 (µmol/kg)
Potential Temperature (ºC)
Salinity
Oxygen (µmol/kg)

Figure 6.2.3a

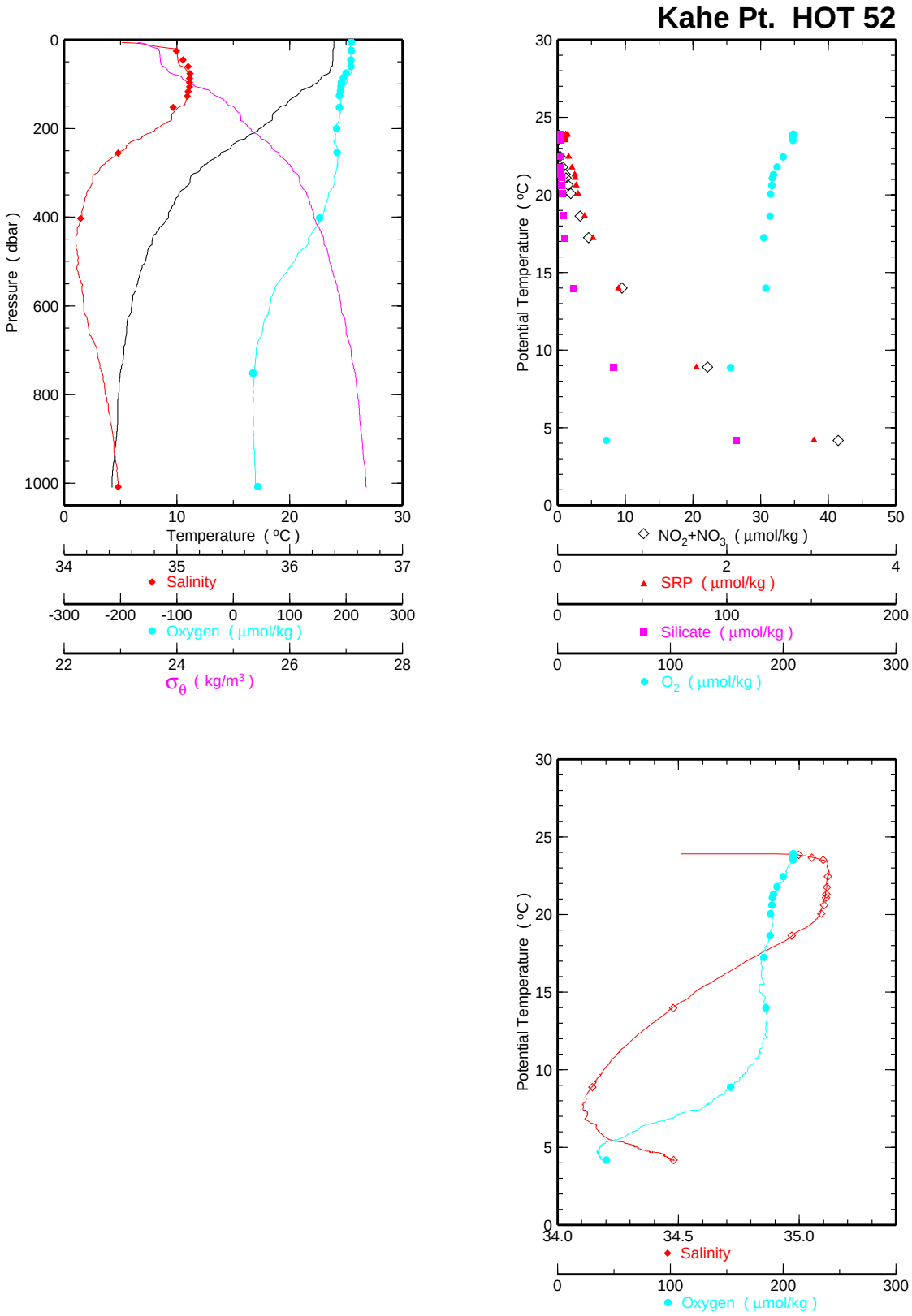
Kahe Pt. HOT 52
Pressure (dbar)
Temperature (°C)
Salinity
Oxygen (µmol/kg)
σθ (kg/m3)
Potential Temperature (°C)
NO2+NO3 (µmol/kg)
SRP (µmol/kg)
Silicate (µmol/kg)
O2 (µmol/kg)
Potential Temperature (°C)
Salinity
Oxygen (µmol/kg)

Figure 6.2.3b

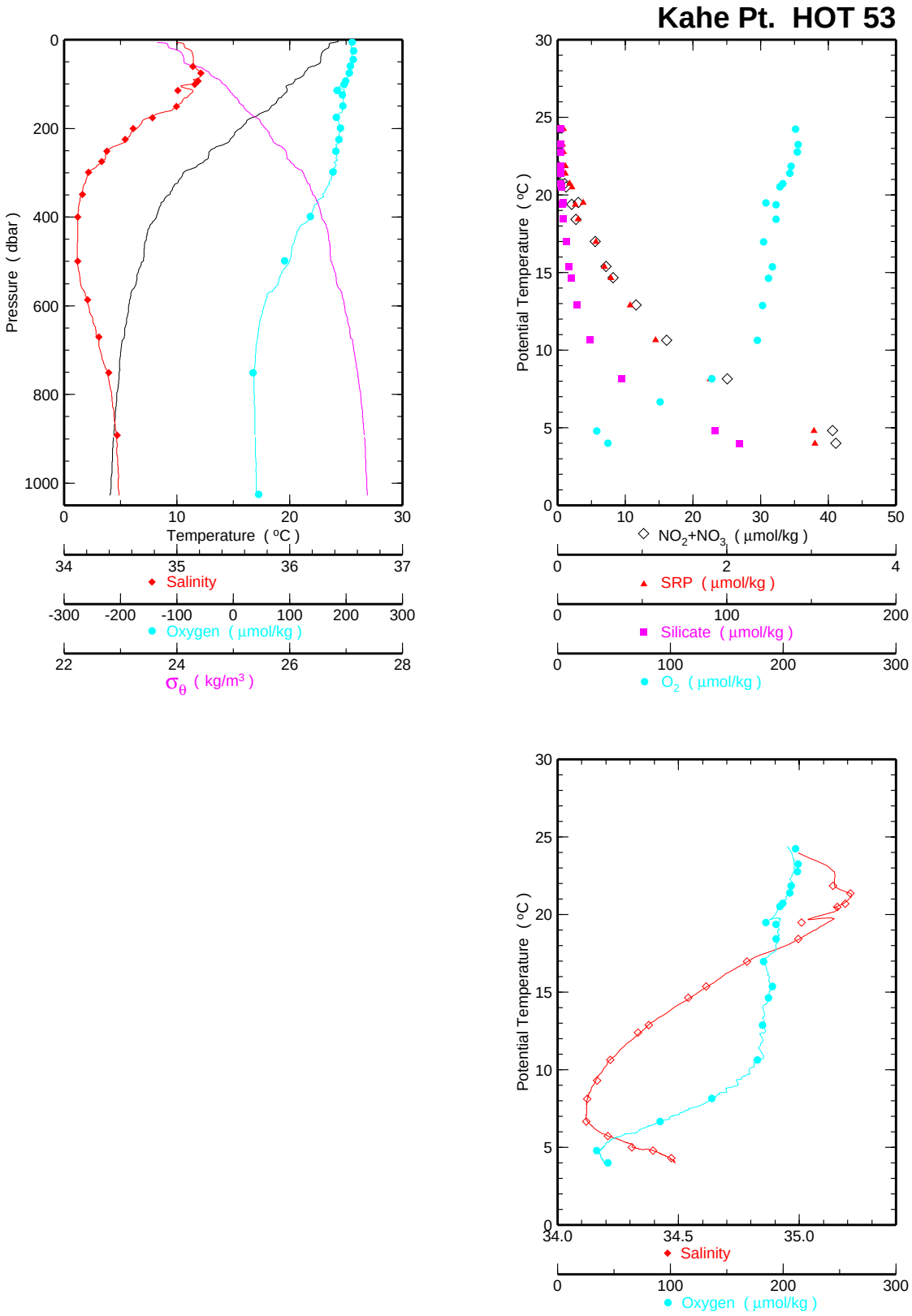
Kahe Pt. HOT 53
Pressure (dbar)
Temperature (°C)
Salinity
Oxygen (µmol/kg)
σθ (kg/m3)
Potential Temperature (°C)
NO2+NO3 (µmol/kg)
SRP (µmol/kg)
Silicate (µmol/kg)
O2 (µmol/kg)
Potential Temperature (°C)
Salinity
Oxygen (µmol/kg)

Figure 6.2.3c

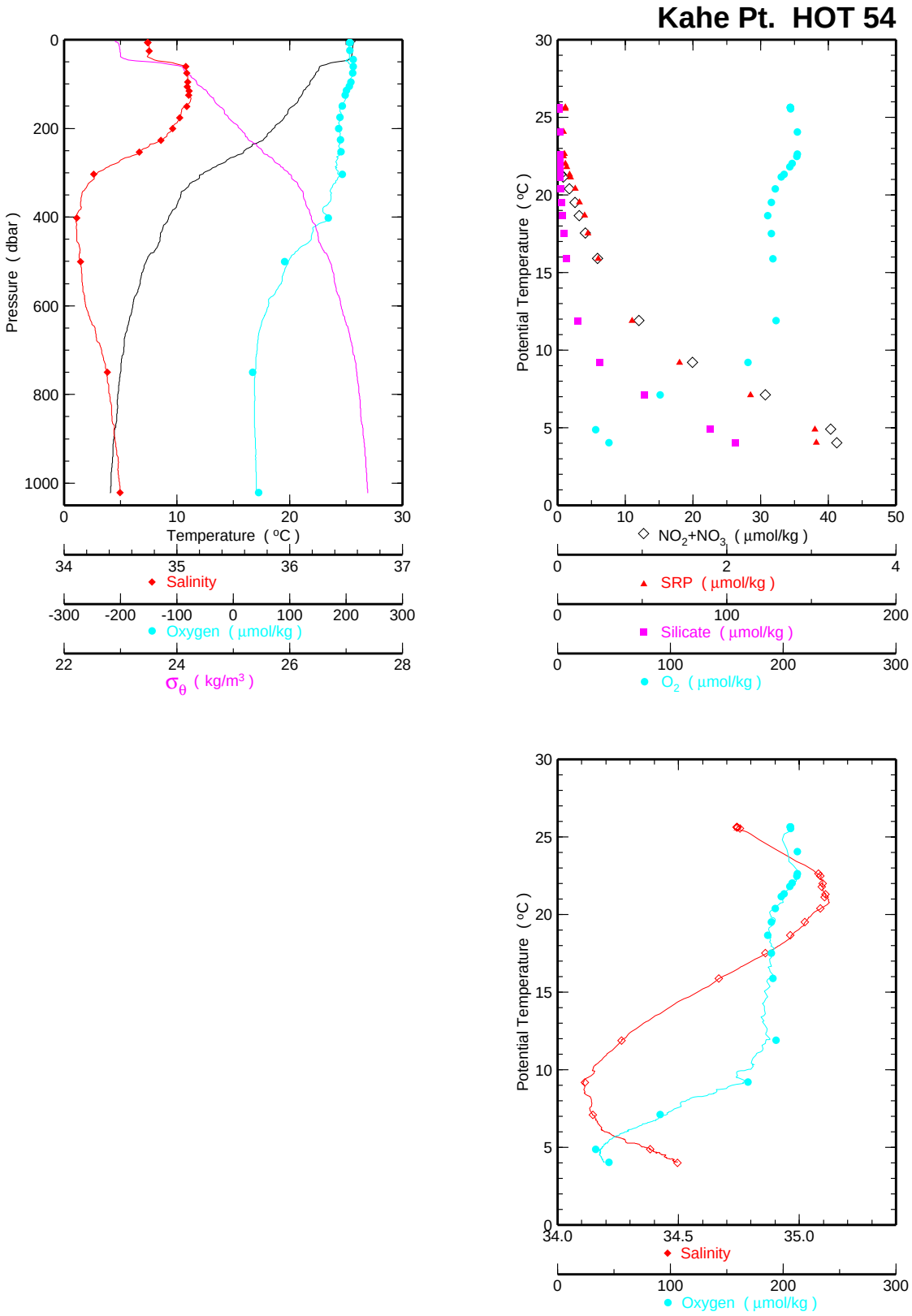
Kahe Pt. HOT 54
Pressure (dbar)
Temperature (°C)
Salinity
Oxygen (µmol/kg)
σθ (kg/m3)
Potential Temperature (°C)
NO2+NO3 (µmol/kg)
SRP (µmol/kg)
Silicate (µmol/kg)
O2 (µmol/kg)
Potential Temperature (°C)
Salinity
Oxygen (µmol/kg)

Figure 6.2.3d

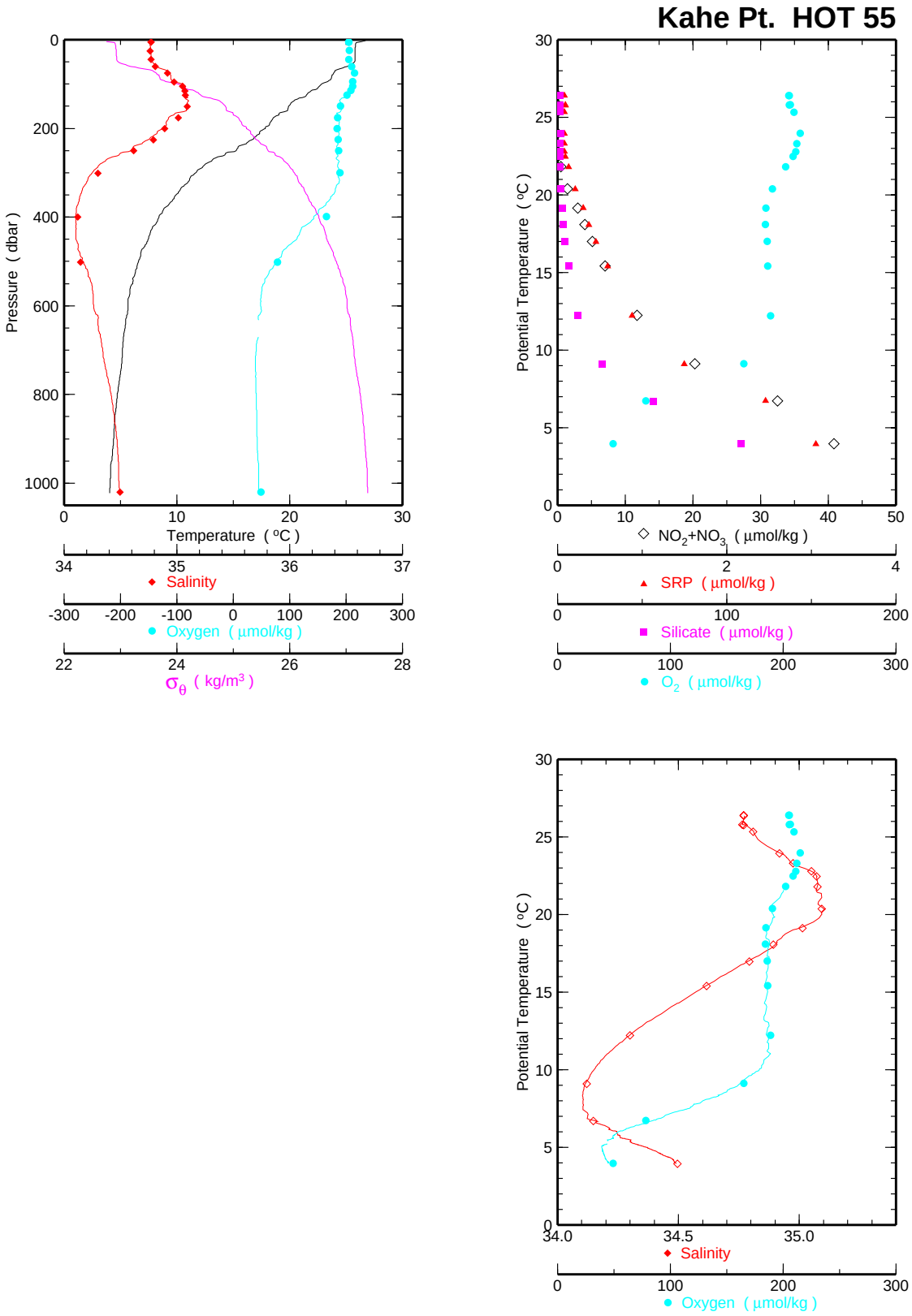
Kahe Pt. HOT 55
Pressure (dbar)
Temperature (°C)
Salinity
Oxygen (µmol/kg)
σθ (kg/m3)
Potential Temperature (°C)
NO2+NO3 (µmol/kg)
SRP (µmol/kg)
Silicate (µmol/kg)
O2 (µmol/kg)
Potential Temperature (°C)
Salinity
Oxygen (µmol/kg)

Figure 6.2.3e

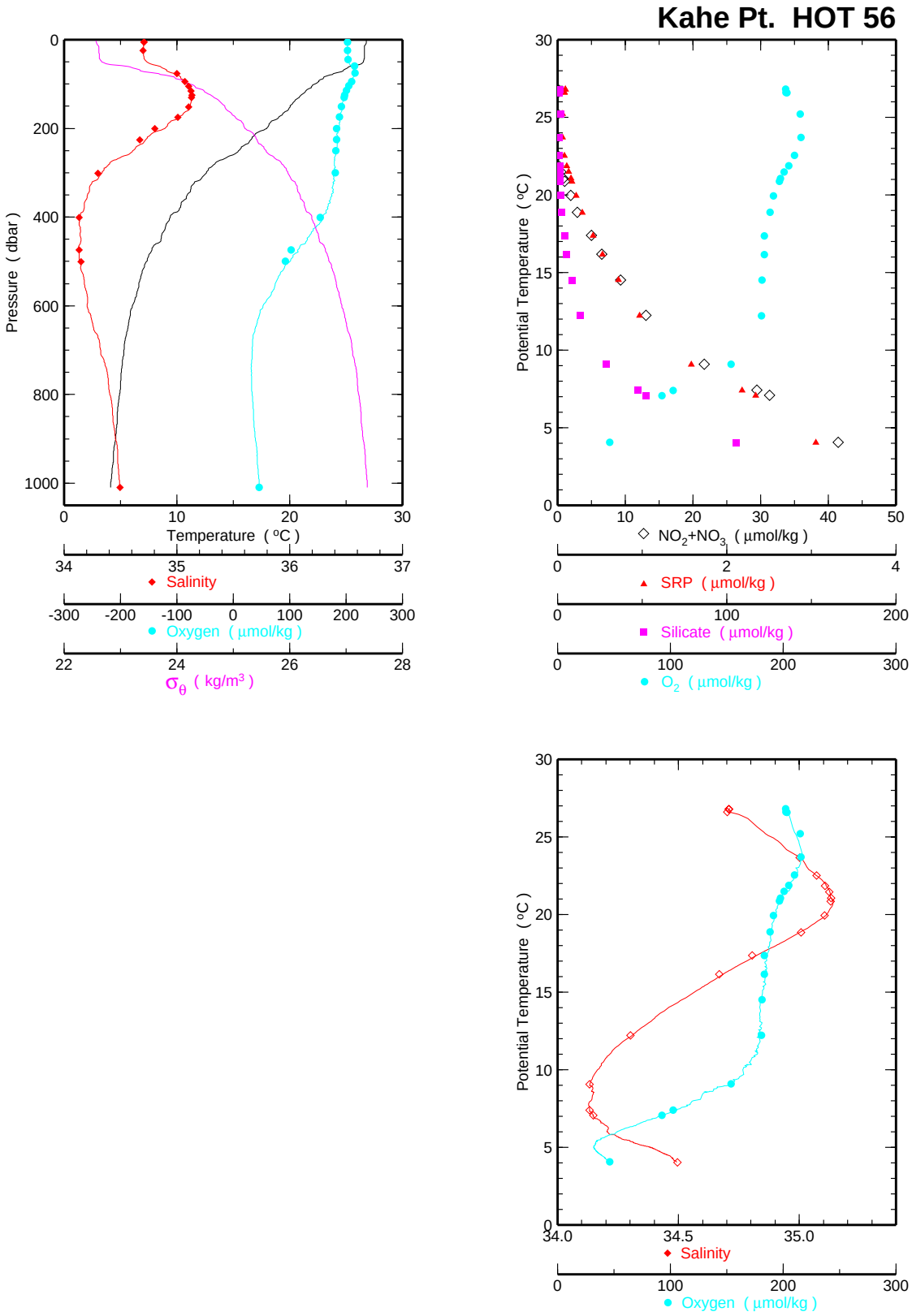
Kahe Pt. HOT 56
Pressure (dbar)
Temperature (°C)
Salinity
Oxygen (µmol/kg)
σθ (kg/m3)
Potential Temperature (°C)
NO2+NO3 (µmol/kg)
SRP (µmol/kg)
Silicate (µmol/kg)
O2 (µmol/kg)
Potential Temperature (°C)
Salinity
Oxygen (µmol/kg)

Figure 6.2.3f

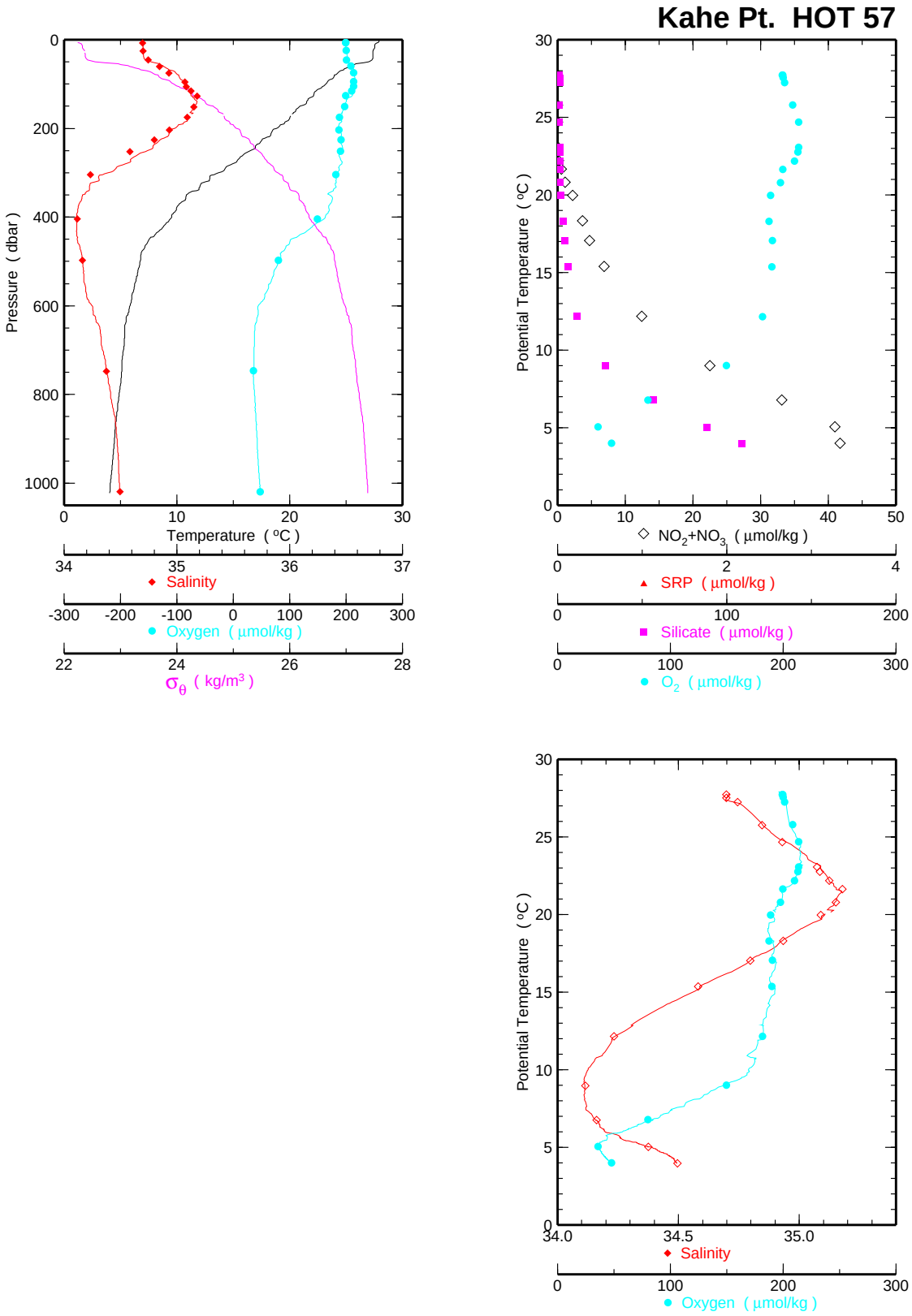
Kahe Pt. HOT 57
Pressure (dbar)
Temperature (°C)
Salinity
Oxygen (µmol/kg)
σθ (kg/m3)
Potential Temperature (°C)
NO2+NO3 (µmol/kg)
SRP (µmol/kg)
Silicate (µmol/kg)
O2 (µmol/kg)
Potential Temperature (°C)
Salinity
Oxygen (µmol/kg)

Figure 6.2.3g

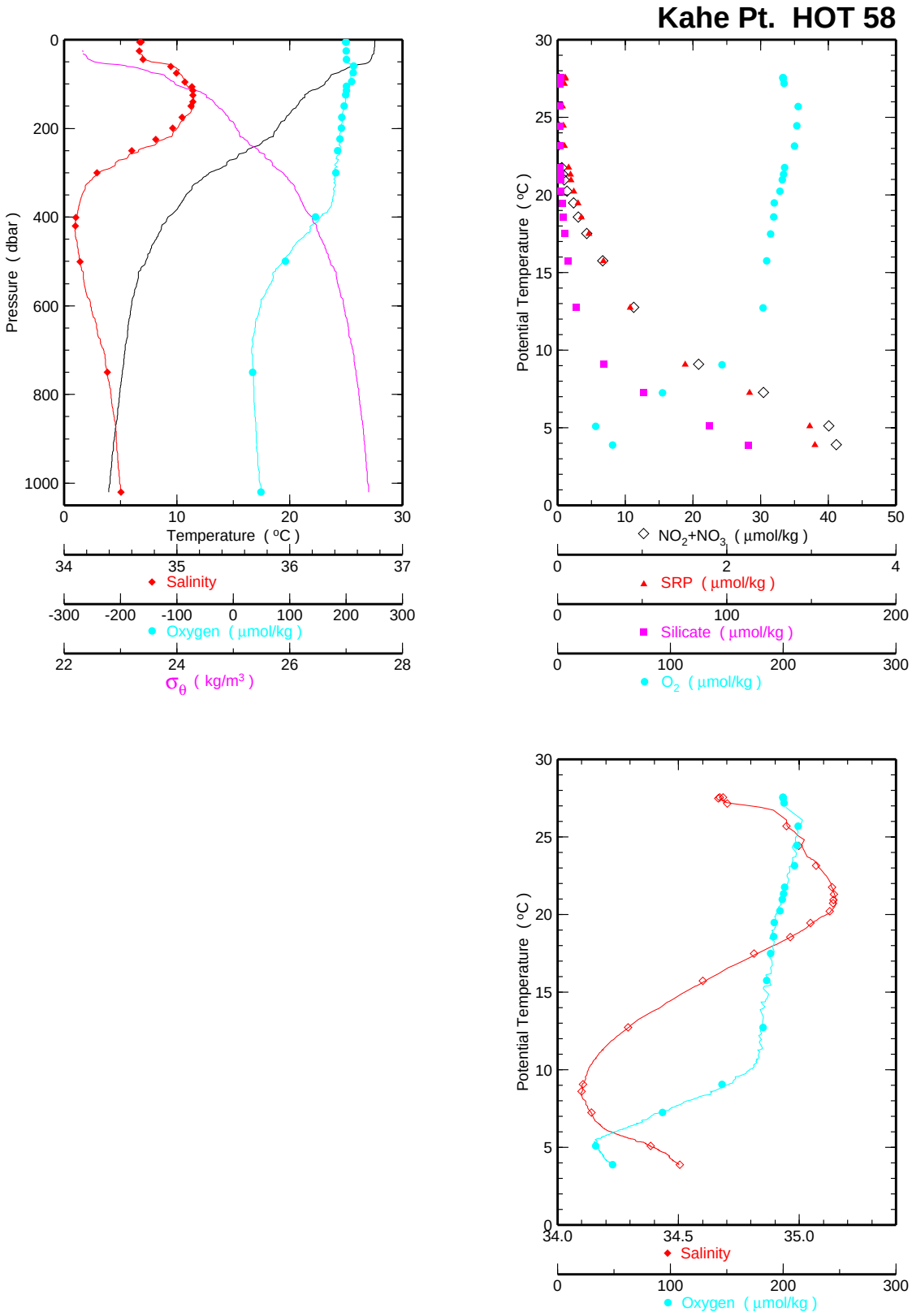
Kahe Pt. HOT 58
Pressure (dbar)
Temperature (°C)
Salinity
Oxygen (µmol/kg)
σθ (kg/m3)
Potential Temperature (°C)
NO2+NO3 (µmol/kg)
SRP (µmol/kg)
Silicate (µmol/kg)
O2 (µmol/kg)
Potential Temperature (°C)
Salinity
Oxygen (µmol/kg)

Figure 6.2.3h

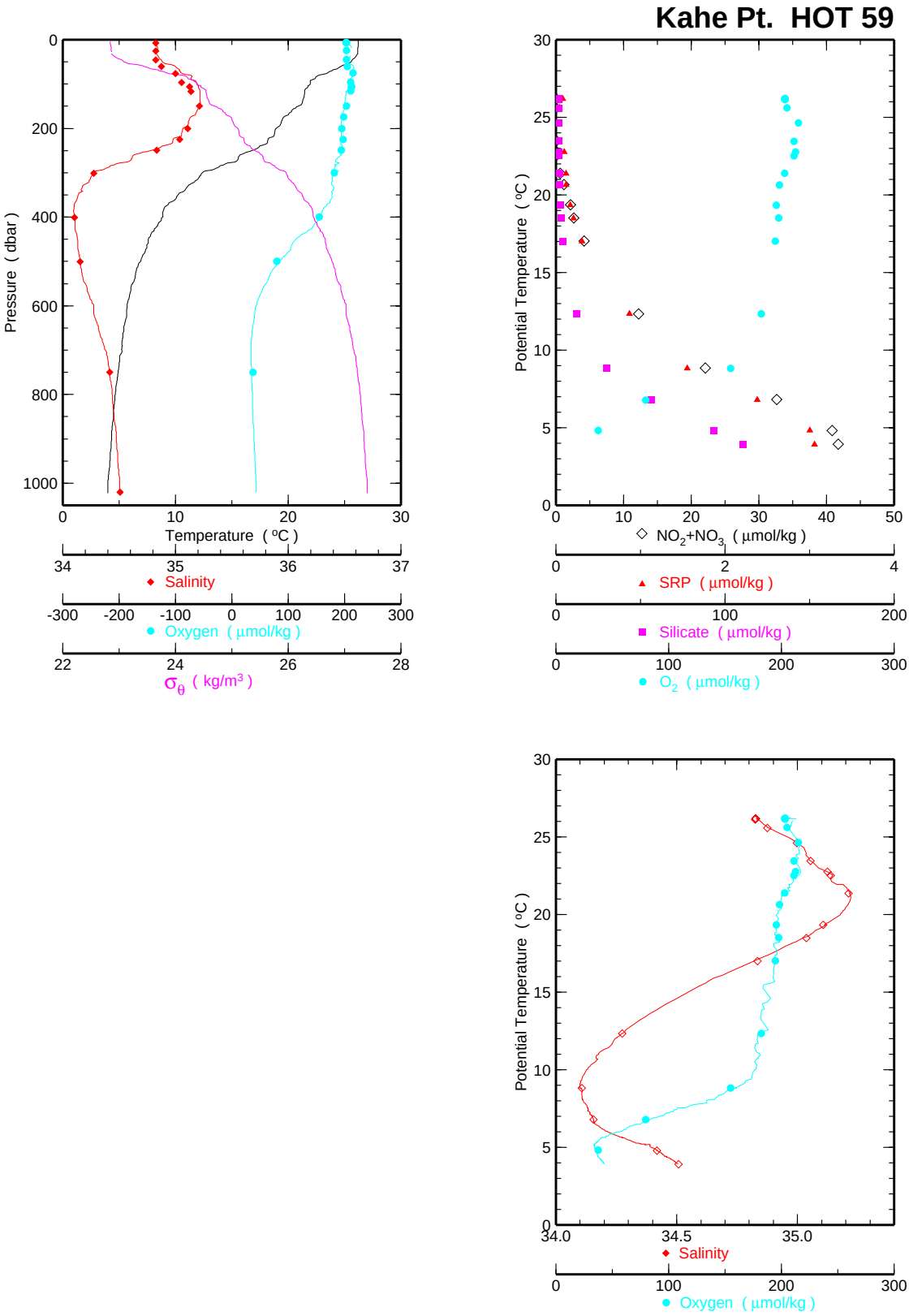
Kahe Pt. HOT 59
Pressure (dbar)
Temperature (ºC)
Salinity
Oxygen (µmol/kg)
σθ (kg/m³)
Potential Temperature (ºC)
NO2+NO3 (µmol/kg)
SRP (µmol/kg)
Silicate (µmol/kg)
O2 (µmol/kg)
Potential Temperature (ºC)
Salinity
Oxygen (µmol/kg)

Figure 6.2.3i

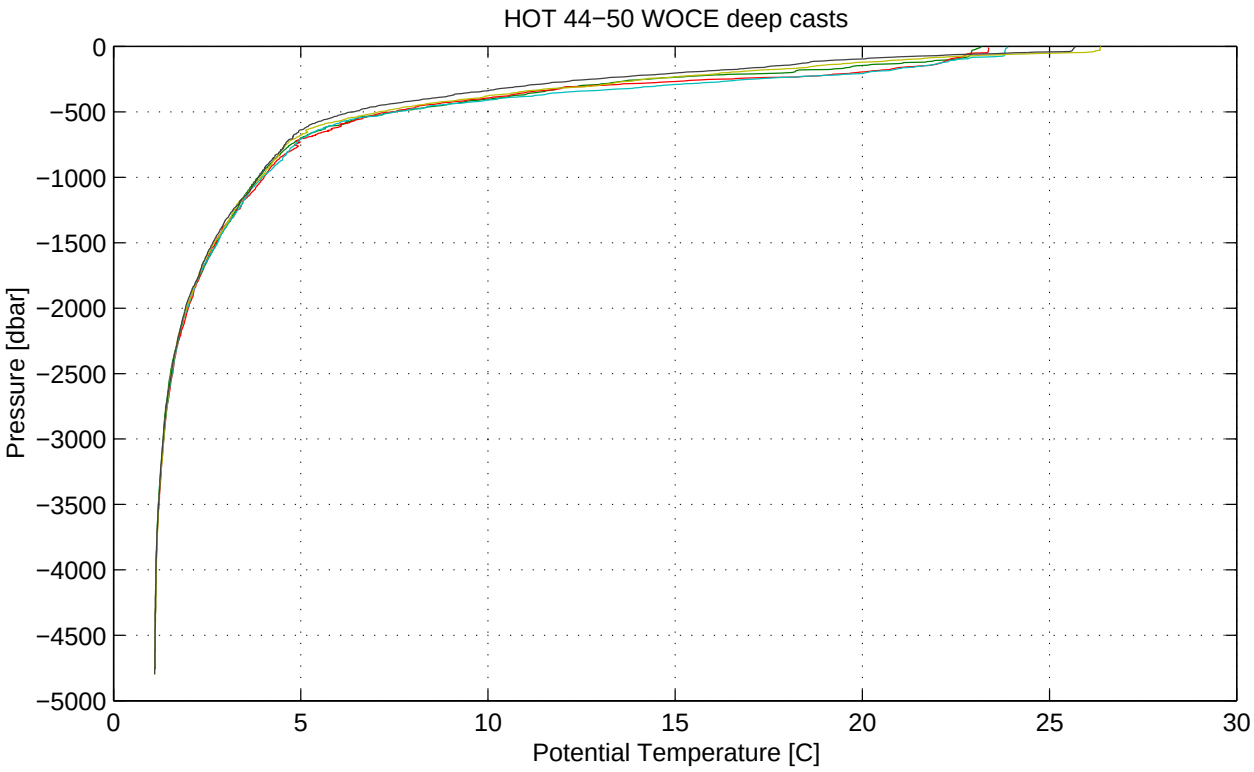
HOT 44−50 WOCE deep casts
Pressure [dbar]
Potential Temperature [C]
0
−500
−1000
−1500
−2000
−2500
−3000
−3500
−4000
−4500
−5000
0
5
10
15
20
25
30

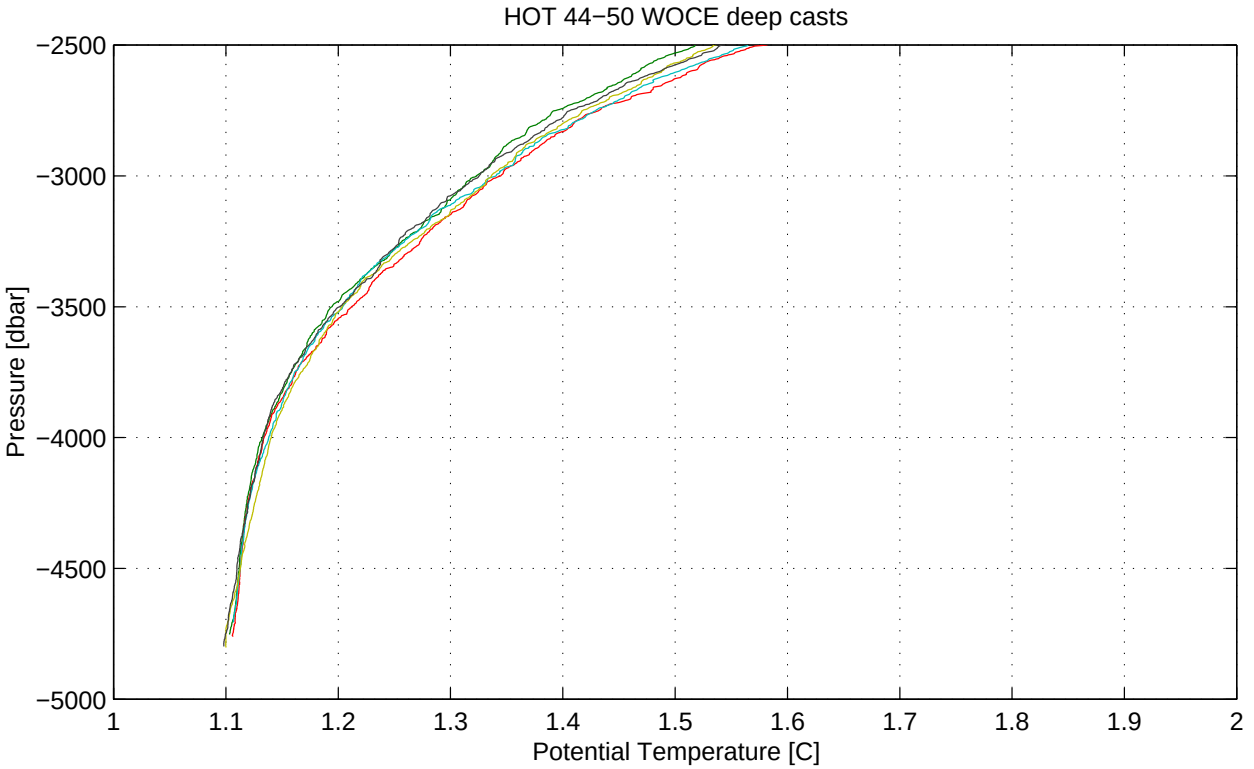
HOT 44−50 WOCE deep casts
Pressure [dbar]
Potential Temperature [C]
−2500
−3000
−3500
−4000
−4500
−5000
1
1.1
1.2
1.3
1.4
1.5
1.6
1.7
1.8
1.9
2

Figure 6.2.4

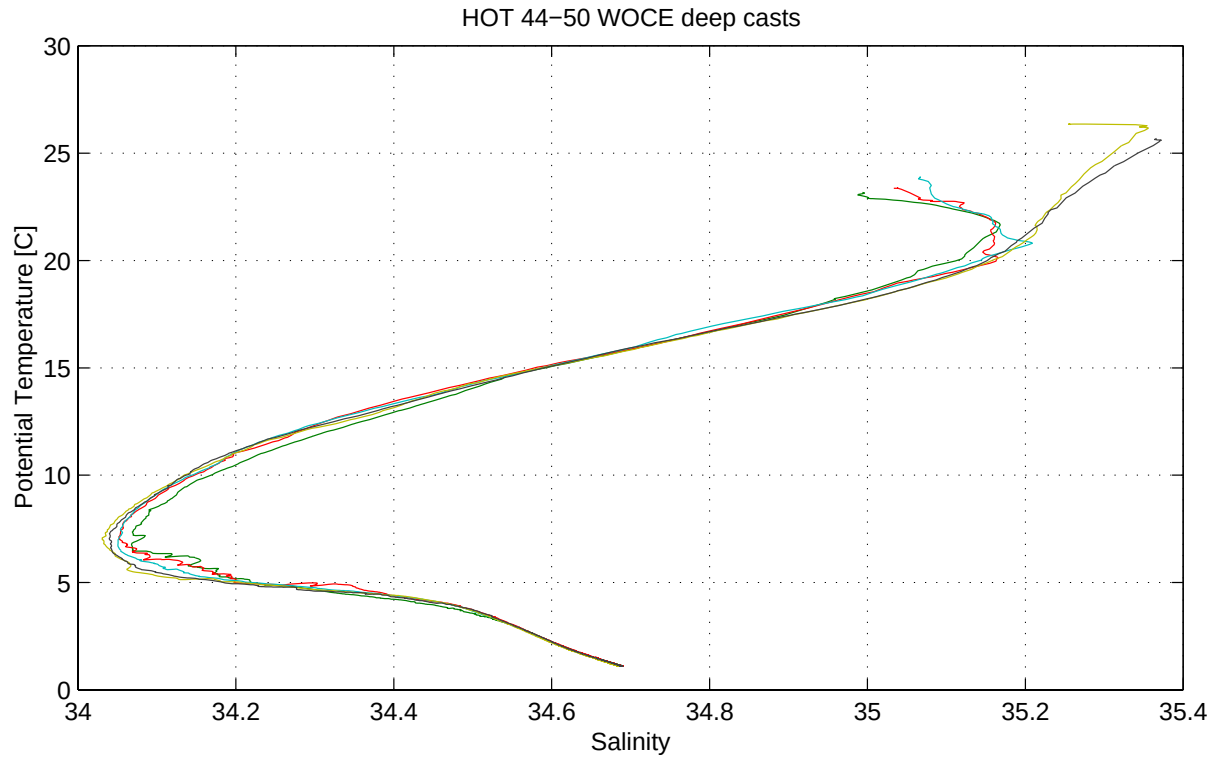
HOT 44−50 WOCE deep casts
Potential Temperature [C]
Salinity
30
25
20
15
10
5
0
34
34.2
34.4
34.6
34.8
35
35.2
35.4

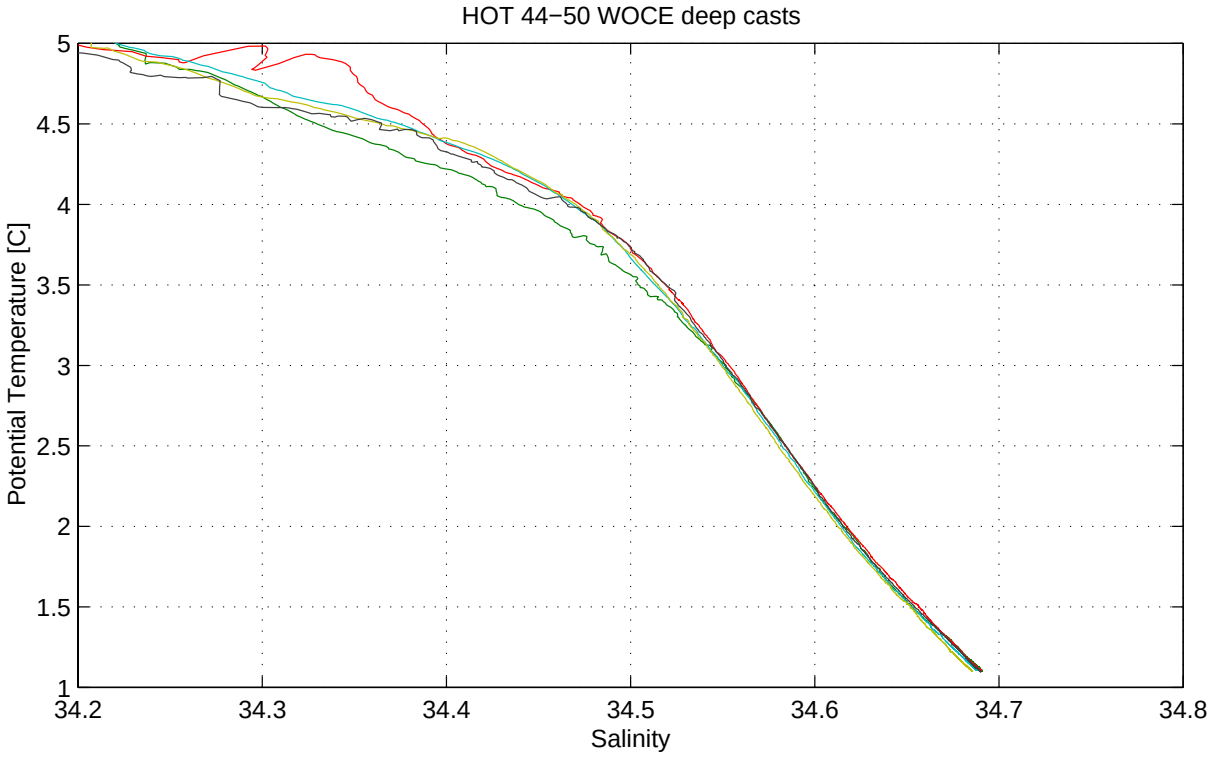
HOT 44−50 WOCE deep casts
Potential Temperature [C]
Salinity
5
4.5
4
3.5
3
2.5
2
1.5
1
34.2
34.3
34.4
34.5
34.6
34.7
34.8

Figure 6.2.5

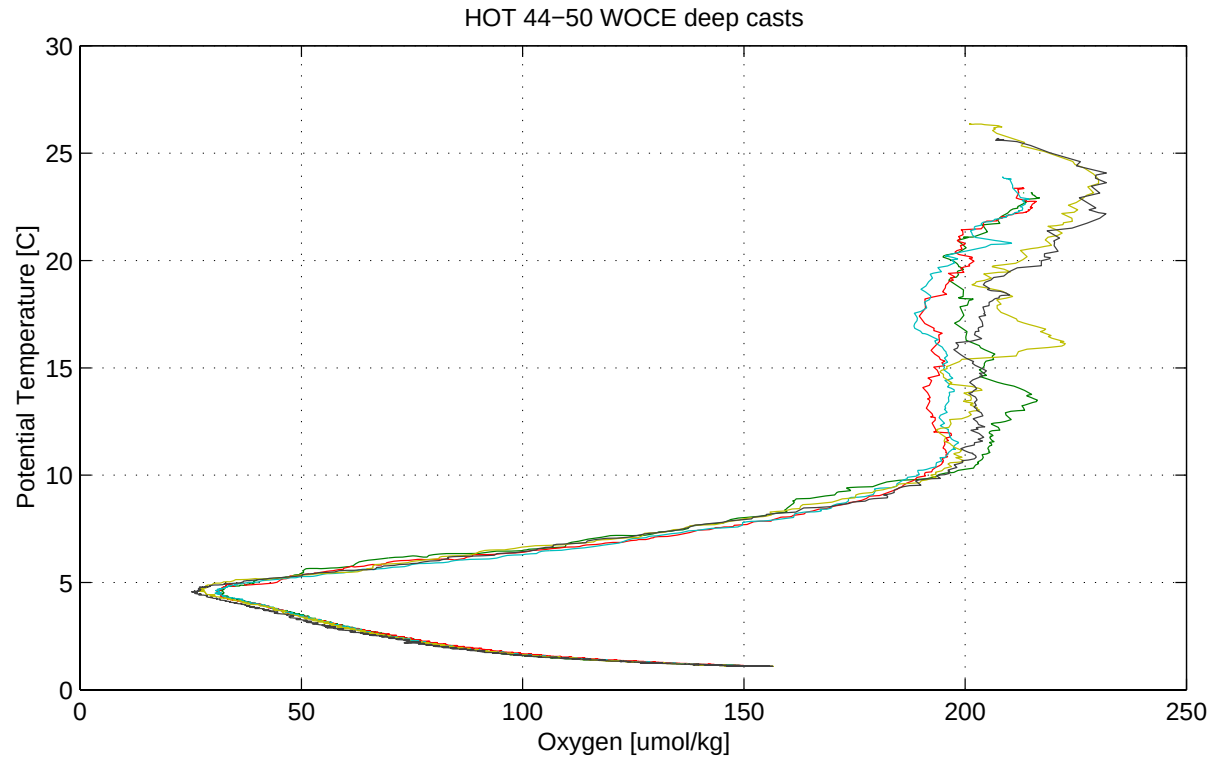
HOT 44−50 WOCE deep casts
Potential Temperature [C]
Oxygen [umol/kg]
0
5
10
15
20
25
30
0
50
100
150
200
250

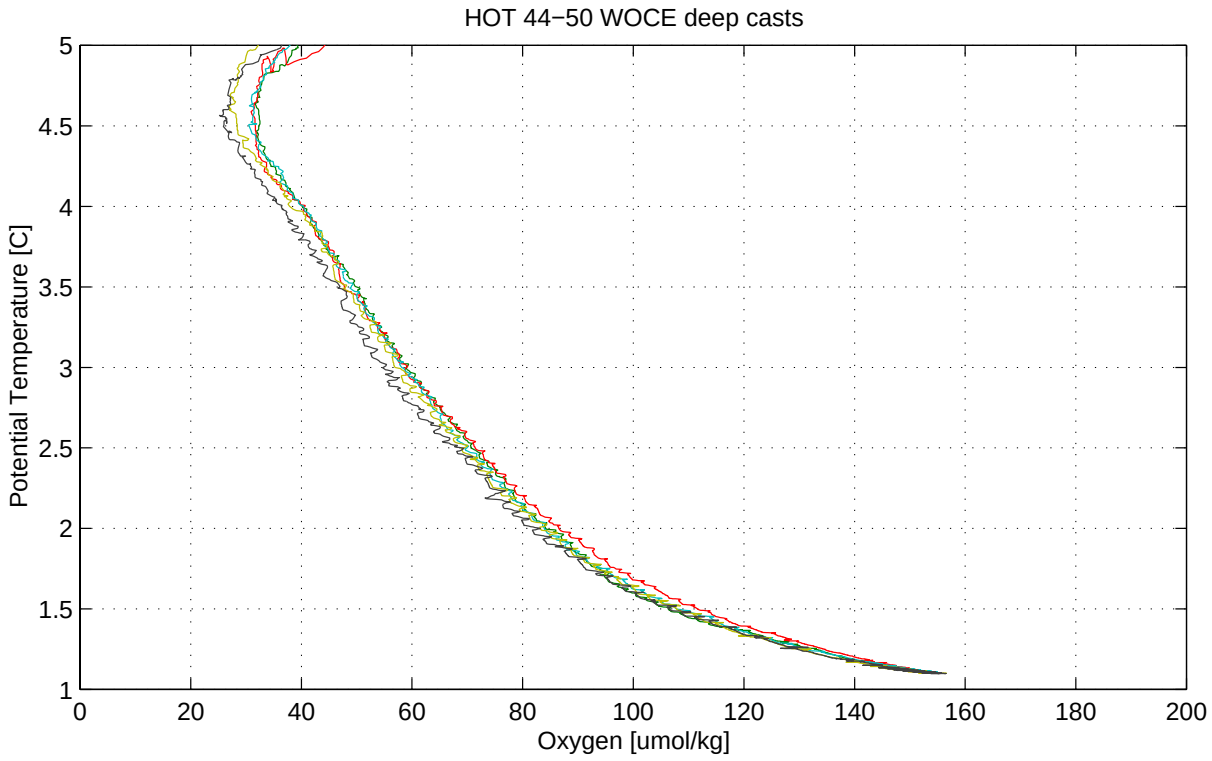
HOT 44−50 WOCE deep casts
Potential Temperature [C]
Oxygen [umol/kg]
1
1.5
2
2.5
3
3.5
4
4.5
5
0
20
40
60
80
100
120
140
160
180
200

Figure 6.2.6

6.3. Contour Plots

Figures 6.3.1 to 14 show data from HOT 1-59. Cruise is indicated by a diamond symbol along the time axis. Data are the average of all casts for each cruise.

Figure 6.3.1: Potential temperature measured by CTD versus pressure.

Figure 6.3.2: Potential density, calculated from CTD measurements of pressure, temperature and salinity versus pressure.

Figure 6.3.3: Salinity measured by CTD plotted versus pressure.

Figure 6.3.4: Salinity measured by CTD versus potential density. The average density of the sea surface for each cruise is connected by a heavy line.

Figure 6.3.5: Salinity from discrete water samples plotted versus pressure. Locations of bottle closures are indicated by solid circles.

Figure 6.3.6: Salinity from discrete water samples plotted versus potential density. The average density of the sea surface for each cruise is connected by a heavy line. Locations of bottle closures are indicated by solid circles.

Figure 6.3.7: Oxygen from discrete water samples plotted versus pressure. Locations of bottle closures are indicated by solid circles.

Figure 6.3.8: Oxygen from discrete water samples plotted versus potential density. The average density of the sea surface for each cruise is connected by a heavy line. Locations of bottle closures are indicated by solid circles.

Figure 6.3.9: Nitrate plus nitrite from discrete water samples plotted versus pressure. Locations of bottle closures are indicated by solid circles.

Figure 6.3.10: Nitrate plus nitrite from discrete water samples plotted versus potential density. The average density of the sea surface for each cruise is connected by a heavy line. Locations of bottle closures are indicated by solid circles.

Figure 6.3.11: Soluble reactive phosphate from discrete water samples plotted versus pressure. Locations of bottle closures are indicated by solid circles.

Figure 6.3.12: Soluble reactive phosphate from discrete water samples plotted versus potential density. The average density of the sea surface for each cruise is connected by a heavy line. Locations of bottle closures are indicated by solid circles.

Figure 6.3.13: Silicate from discrete water samples plotted versus pressure. Locations of bottle closures are indicated by solid circles.

Figure 6.3.14: Silicate from discrete water samples plotted versus potential density. The average density of the sea surface for each cruise is connected by a heavy line. Locations of bottle closures are indicated by solid circles.

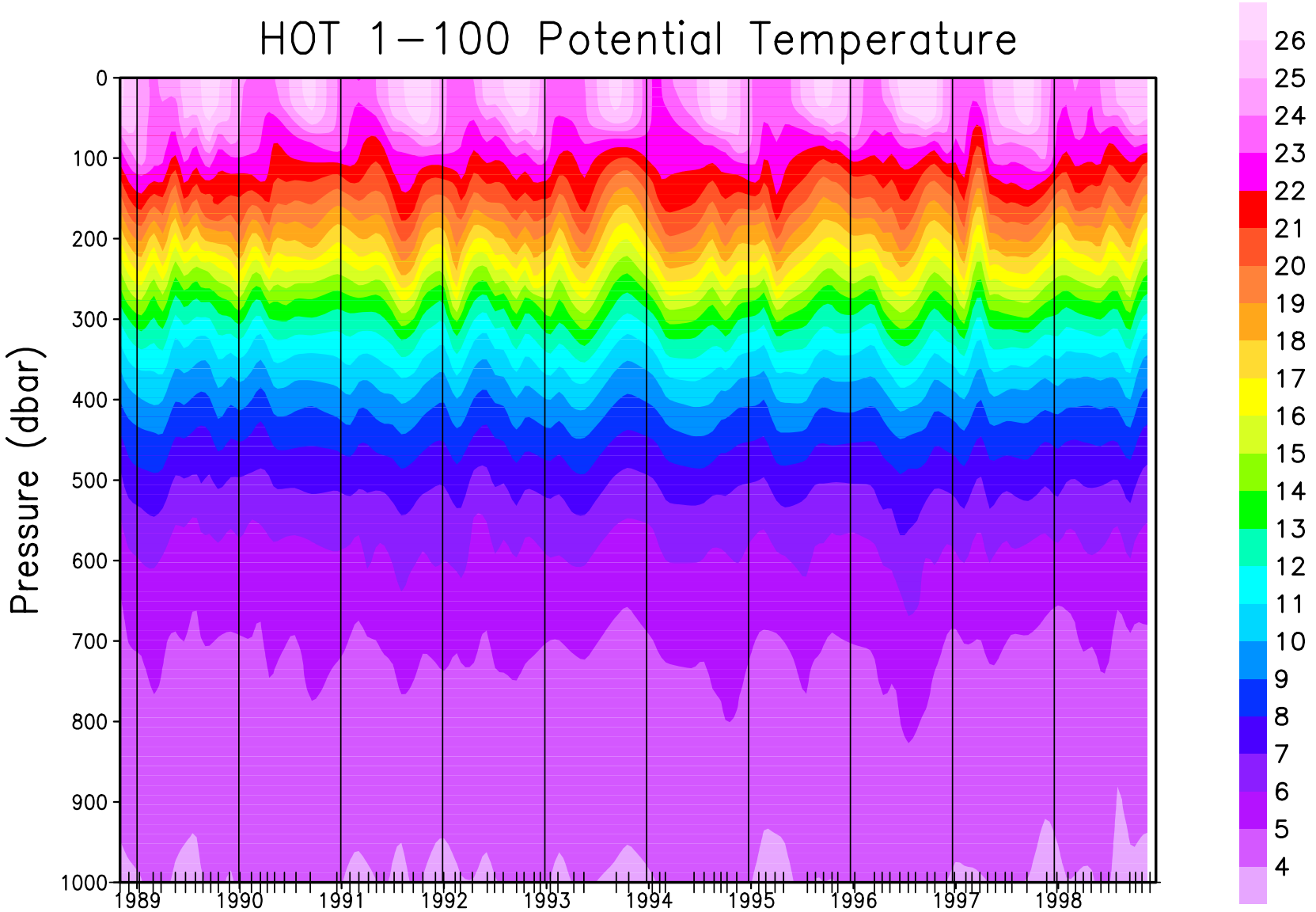

Figure 6.3.1: Contour plot of CTD potential temperature versus pressure

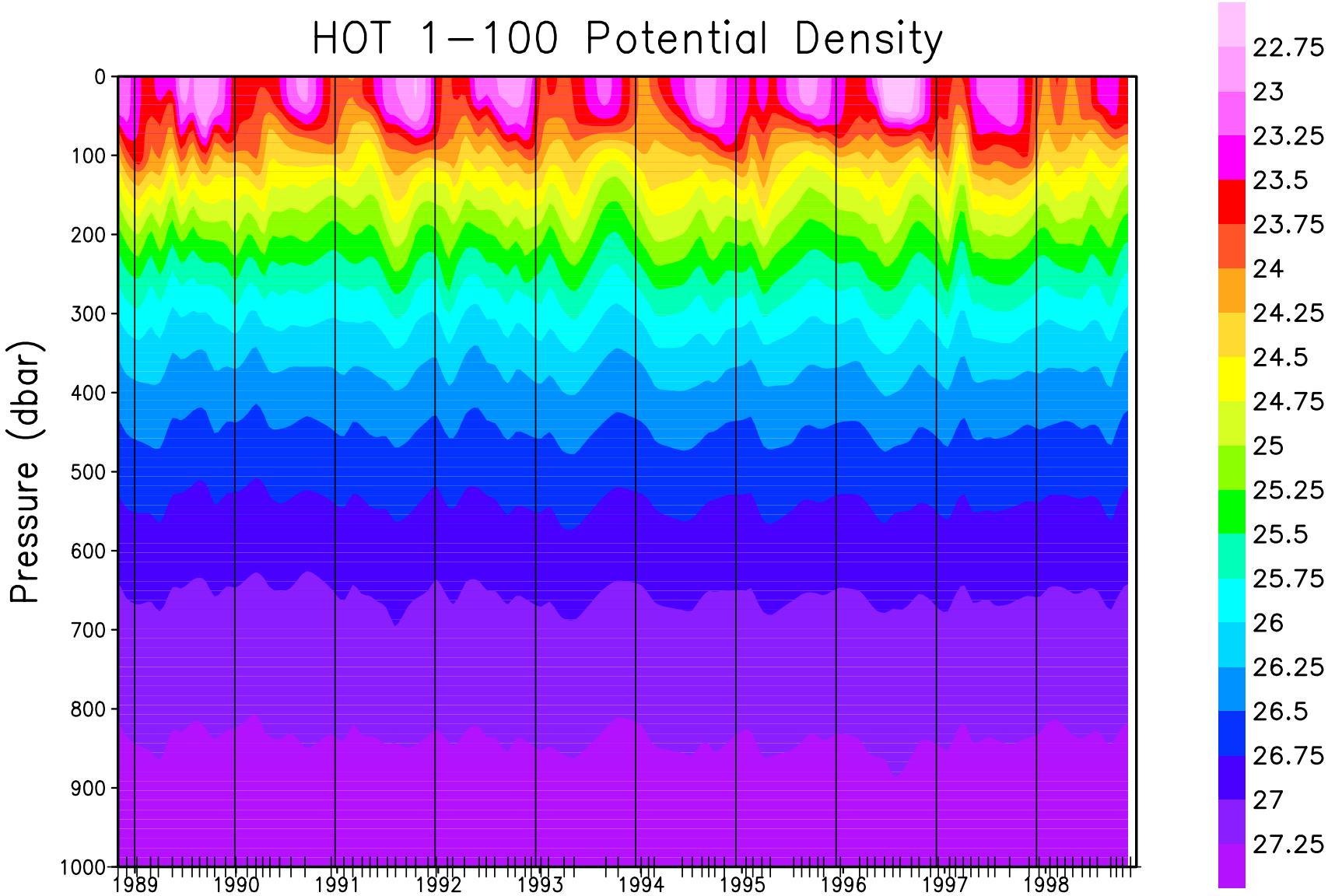

Figure 6.3.2: Contour plot of potential density (σ_θ), calculated from CTD pressure, temperature and salinity, versus pressure for HOT cruises 1-100.

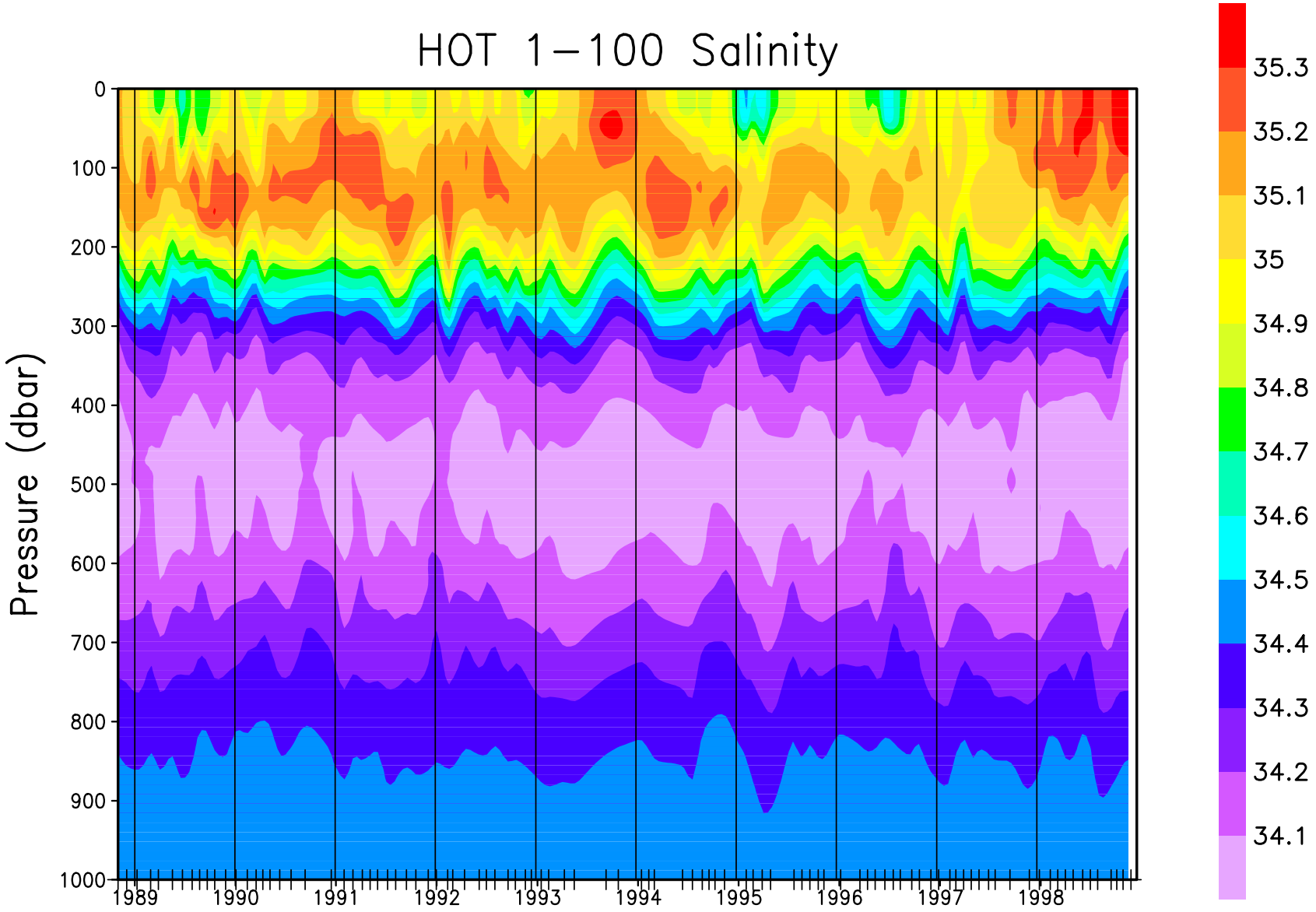

Figure 6.3.3: Contour plot of CTD salinity versus pressure for HOT cruises 1-100.

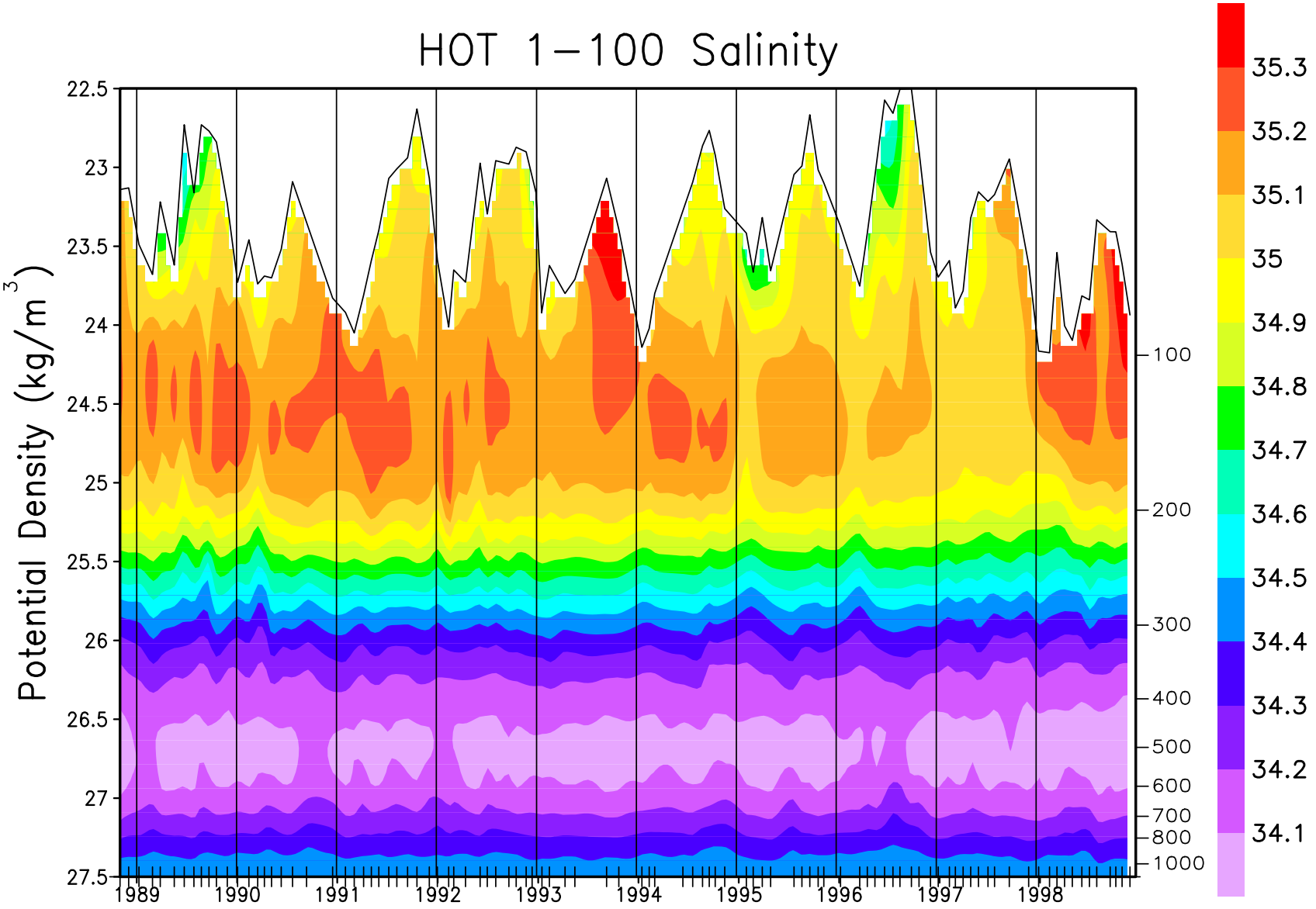

Figure 6.3.4: Contour plot of CTD salinity versus potential density (σ_θ) to 27.5 kg m^{-3} for HOT cruises 1-100. The average density of the sea surface is connected by the heavy line.

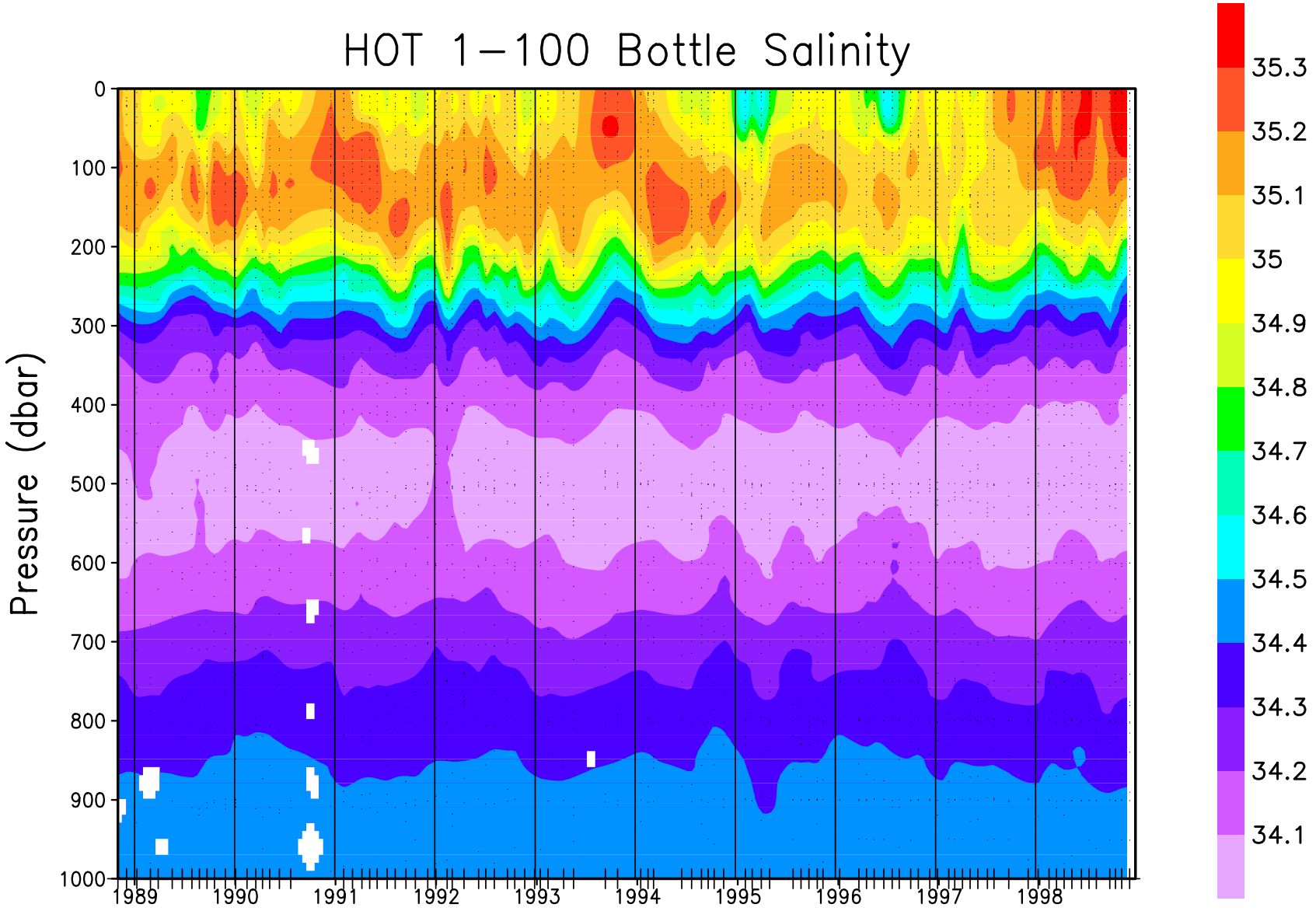

Figure 6.3.5: Contour plot of bottle salinity versus pressure for HOT cruises 1-100. Location of samples in the water column are indicated by the solid circles.

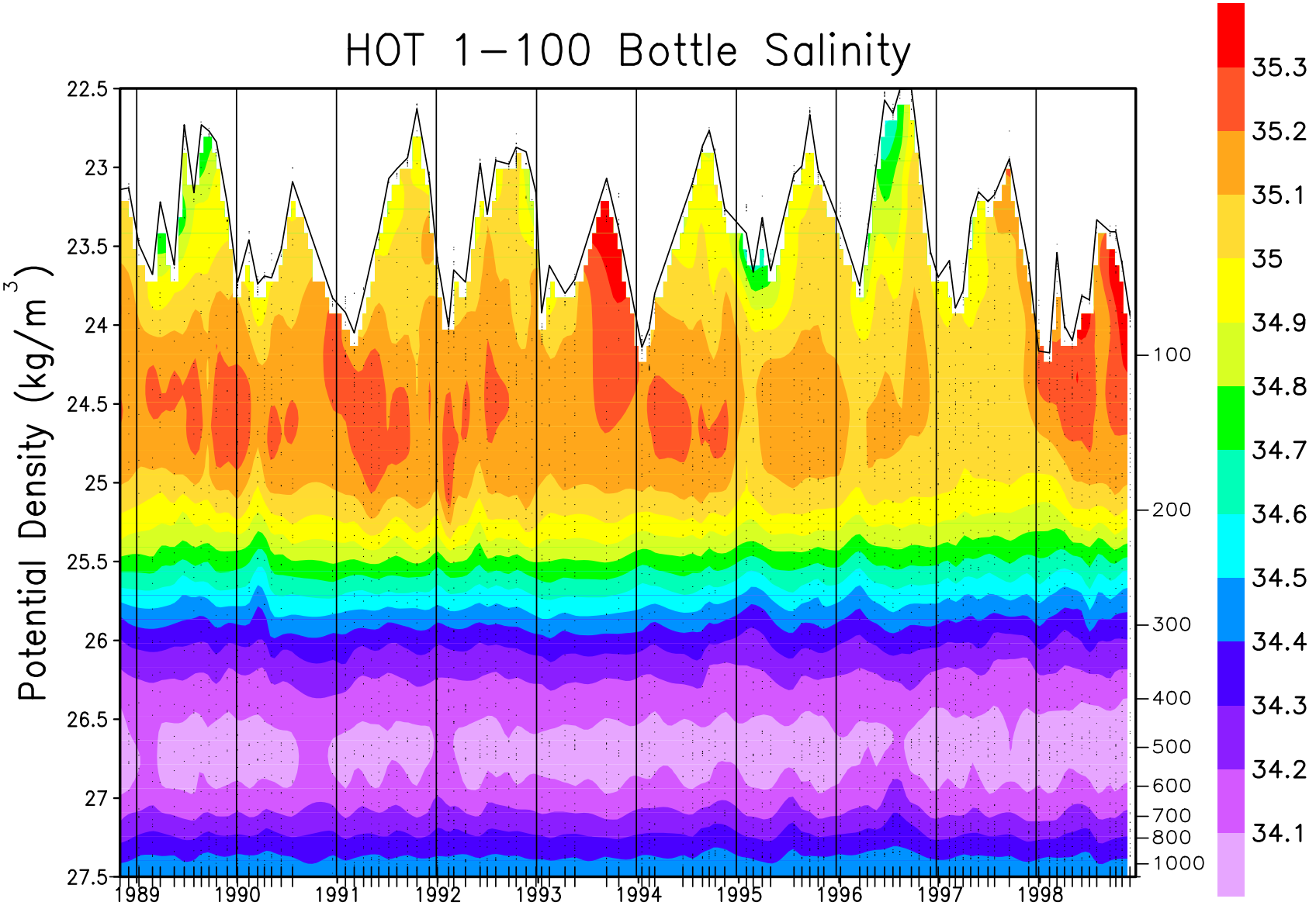

Figure 6.3.6: Contour plot of bottle salinity versus potential density (σ_θ)to 27.5 kg m^{-3} for HOT cruises 1-100. The average density of the sea surface is connected by the heavy line.

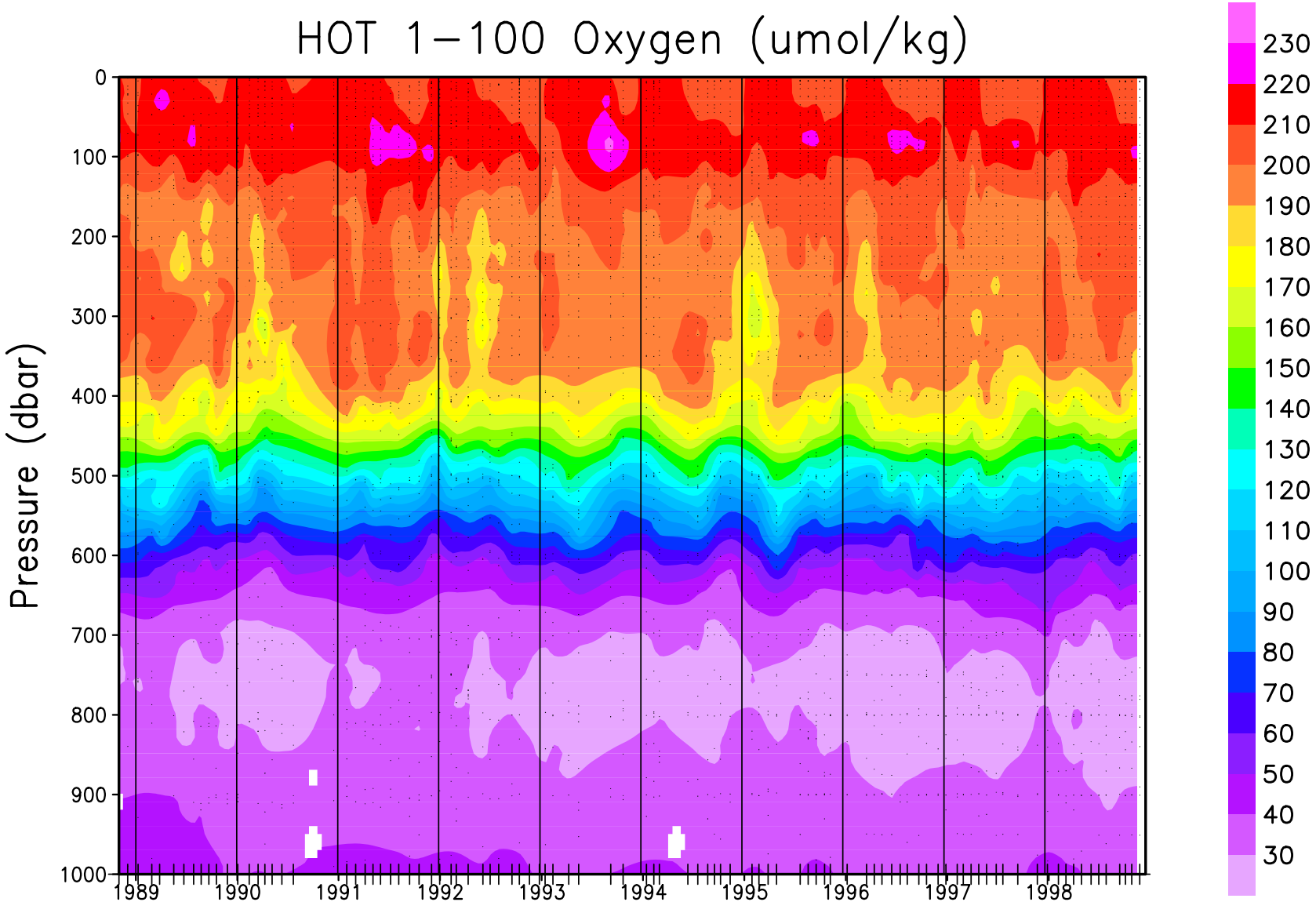

Figure 6.3.7: Contour plot of bottle oxygen versus pressure for HOT cruises 1-100. Location of samples in the water column are indicated by the solid circles.

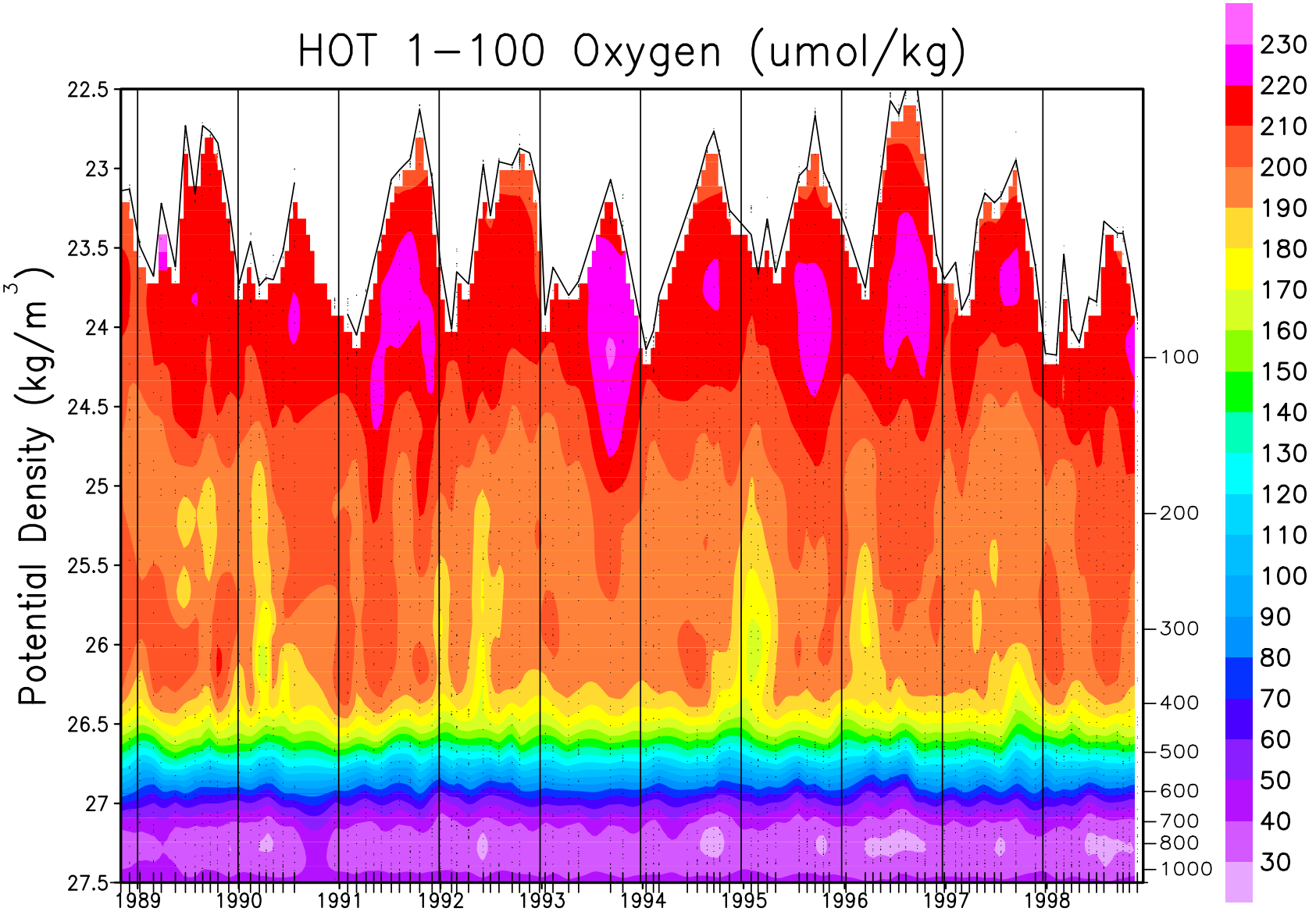

Figure 6.3.8: Contour plot of bottle oxygen versus potential density (σ_θ) to 27.5 kg m^{-3} for HOT cruises 1-100. The average density of the sea surface is connected by the heavy line.

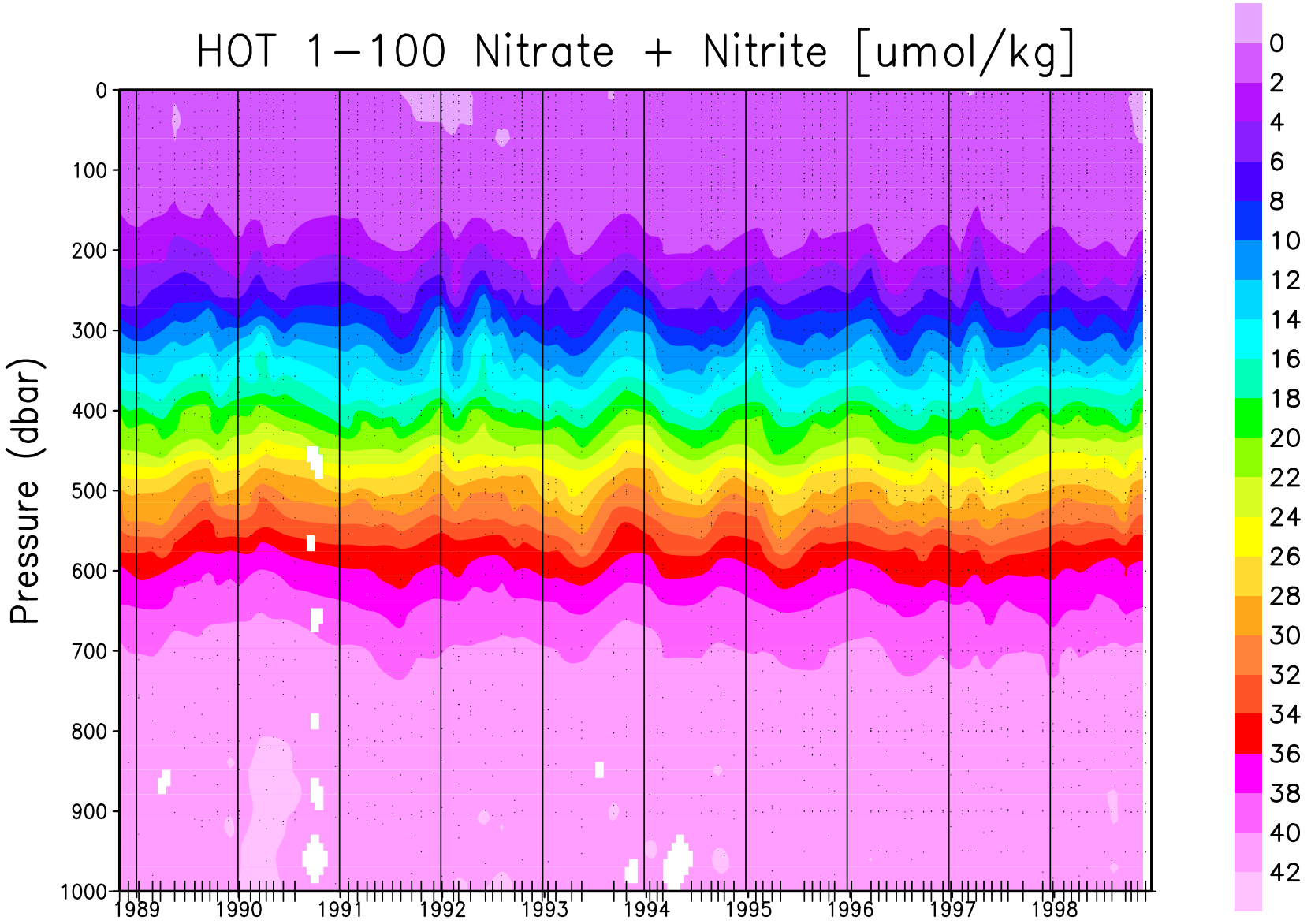

Figure 6.3.9: Contour plot of [nitrate + nitrite] versus pressure for HOT cruises 1-100. Location of samples in the water column are indicated by the solid circles.

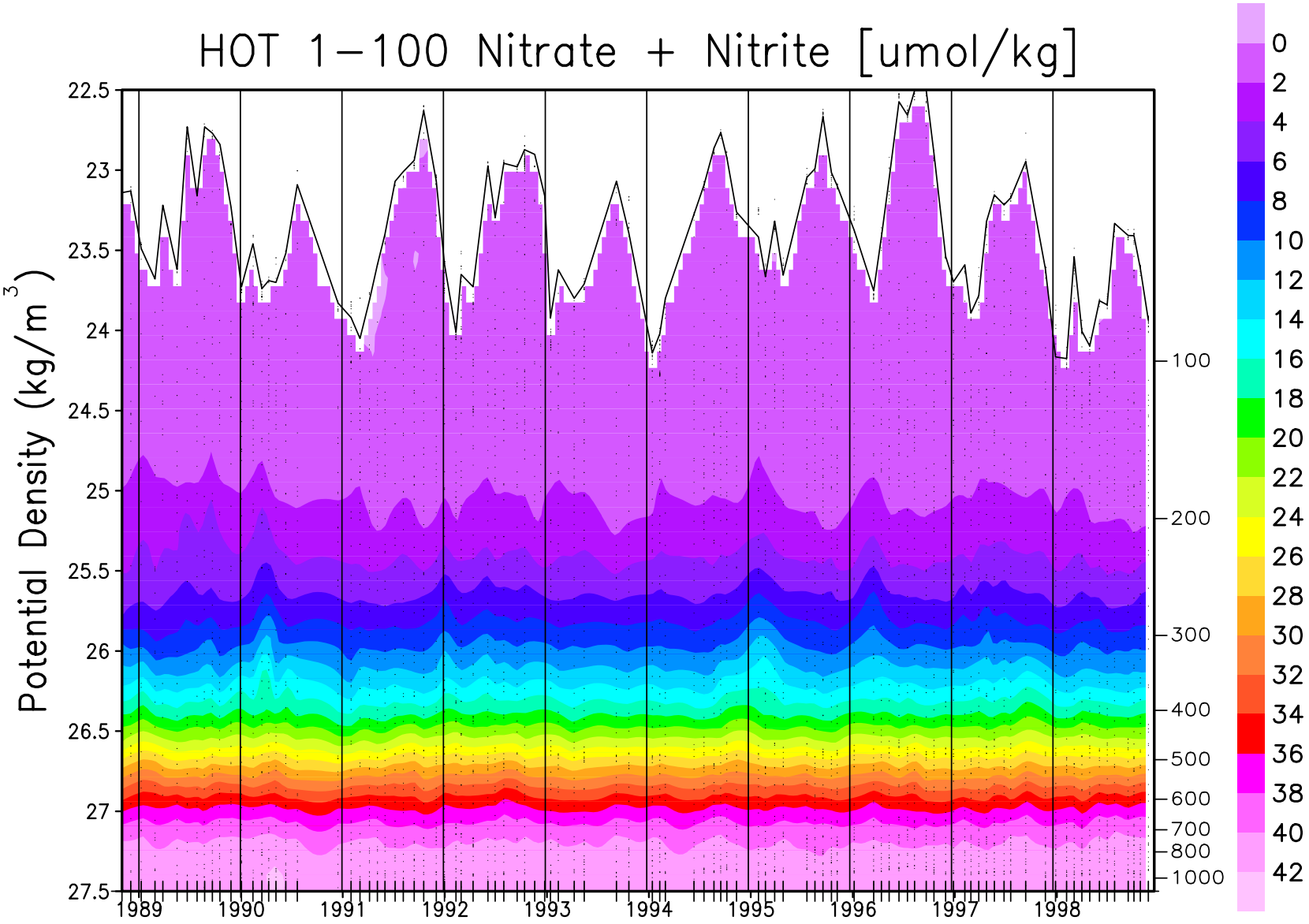

Figure 6.3.10: Contour plot of [nitrate + nitrite] versus potential density (σ_θ) to 27.5 kg m^{-3} for HOT cruises 1-100. The average density of the sea surface is connected by the heavy line.

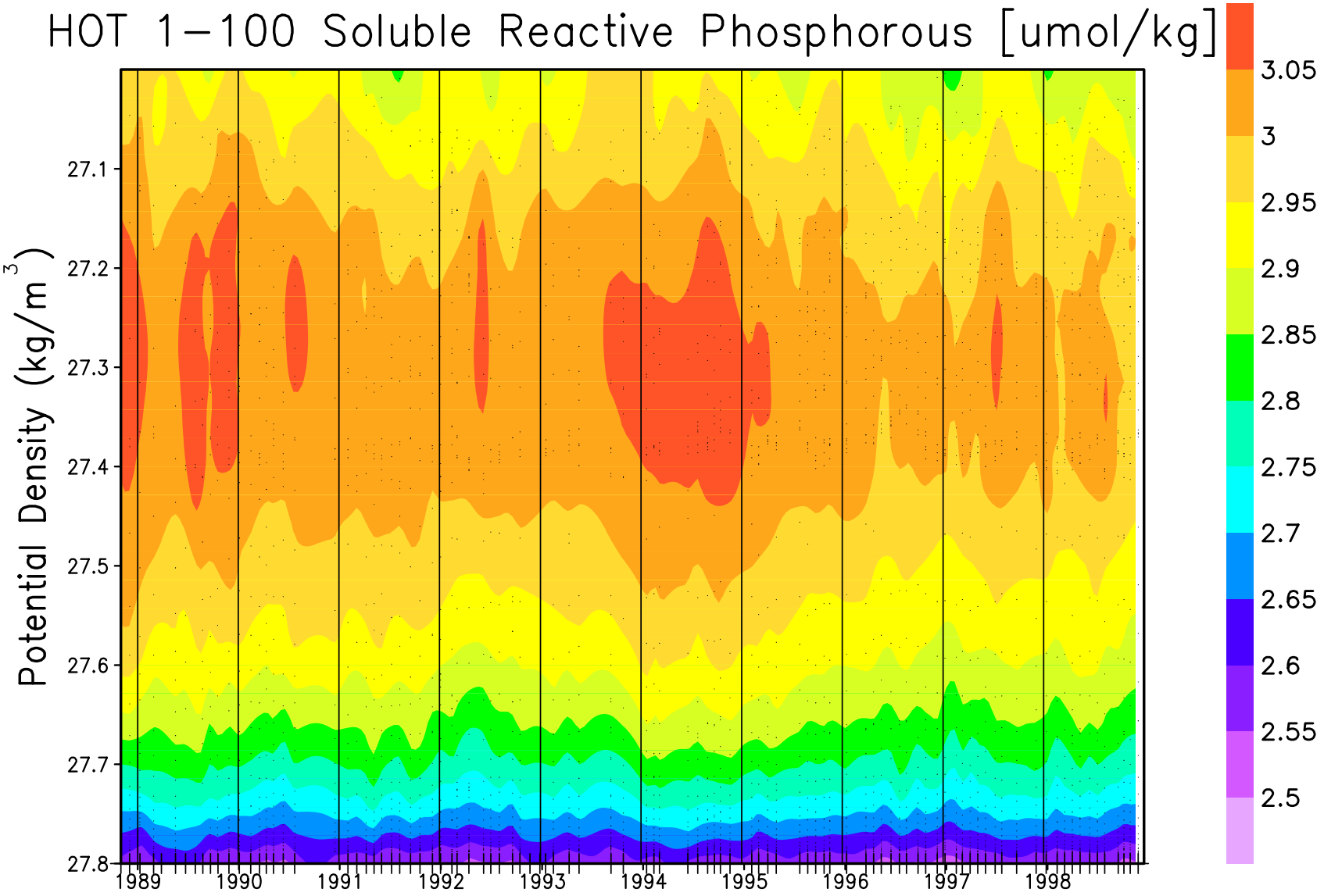

Figure 6.3.11: Contour plot of soluble reactive phosphate versus pressure for HOT cruises 1-100. Location of samples in the water column are indicated by the solid circles.

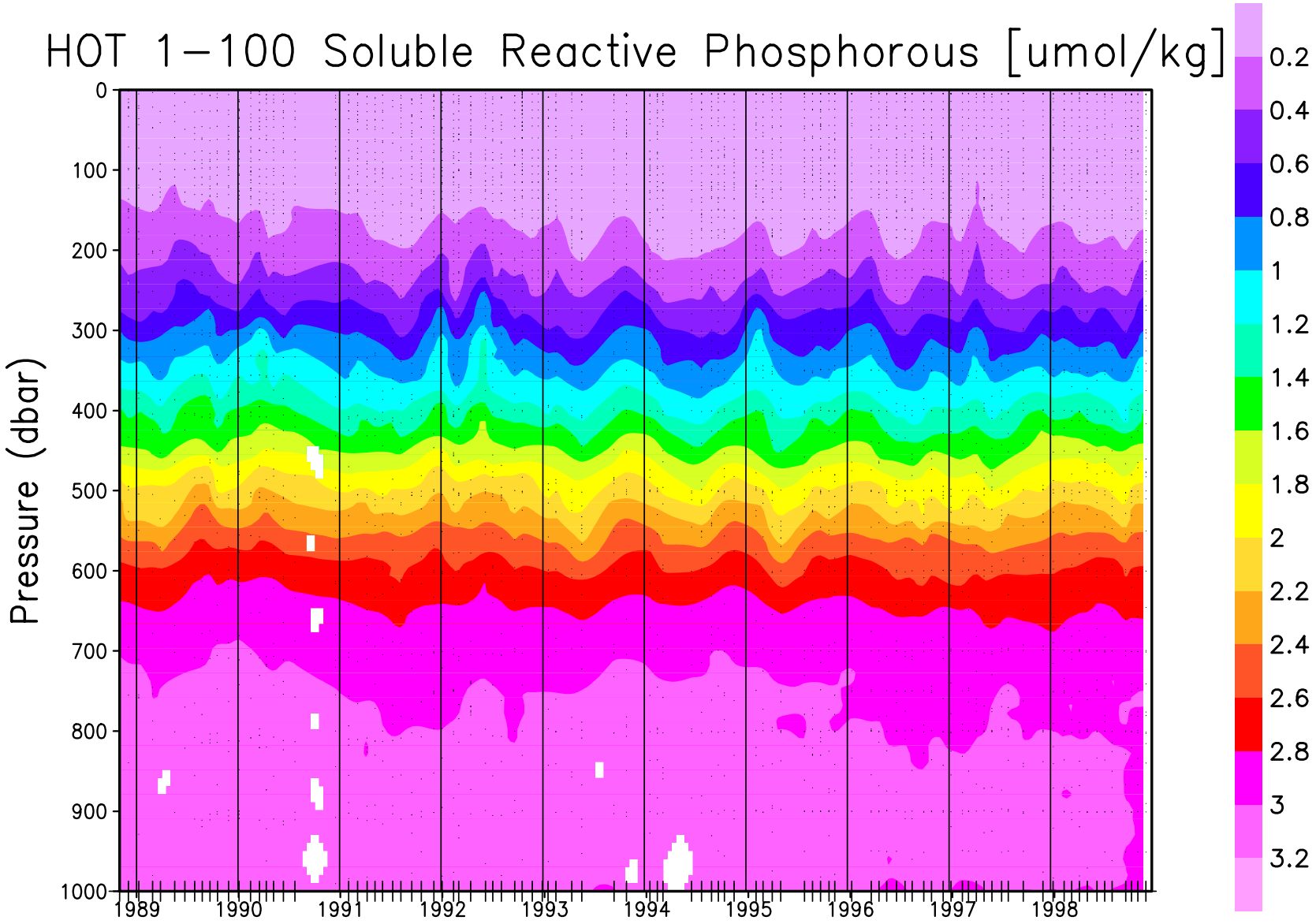

Figure 6.3.12: Contour plot of soluble reactive phosphate versus potential density (σ_θ) to 27.5 kg m^{-3} for HOT cruises 1-100. The average density of the sea surface is connected by the heavy line.

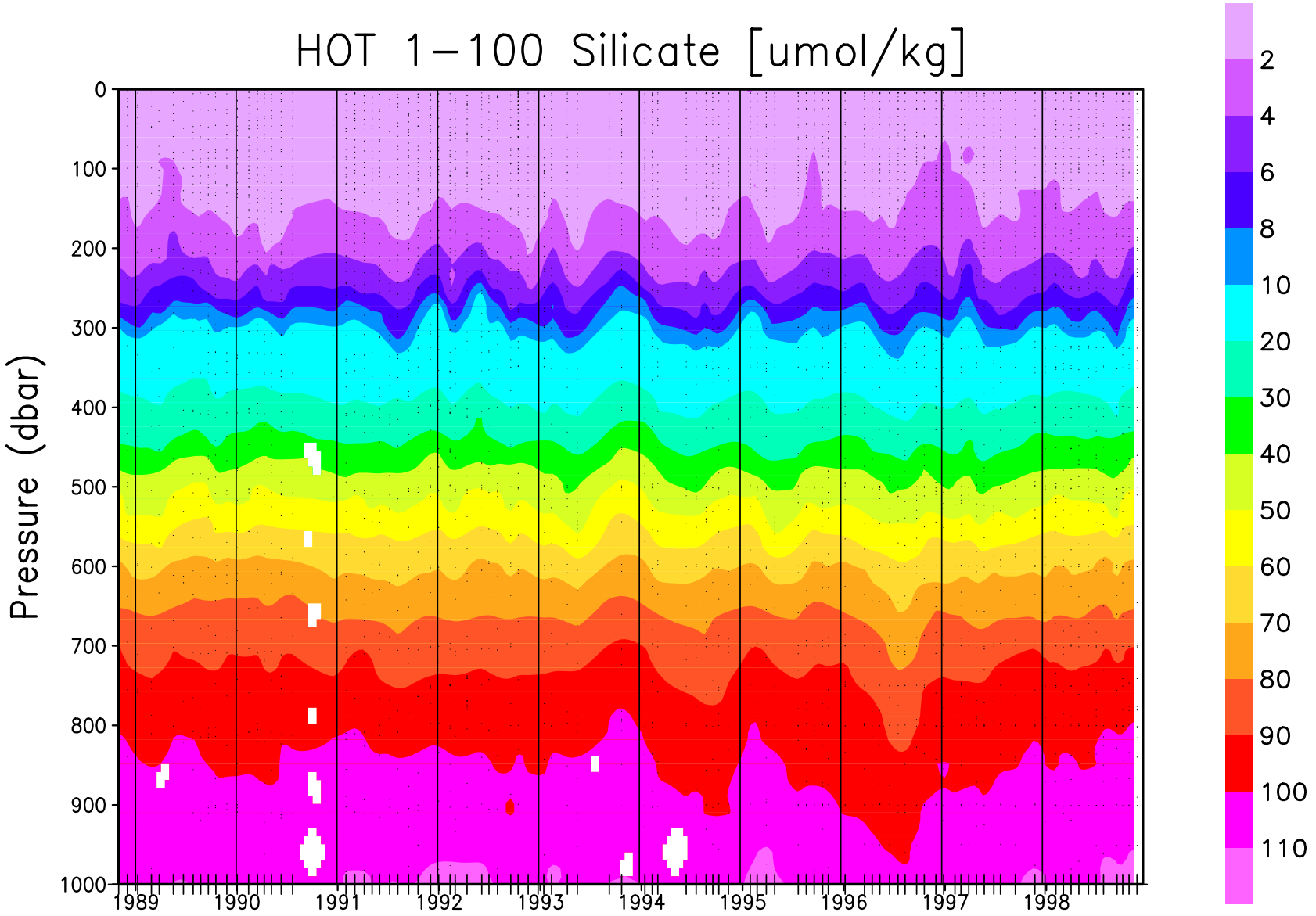

Figure 6.3.13: Contour plot of silicate versus pressure for HOT cruises 1-100. Location of samples in the water column are indicated by the solid circles.

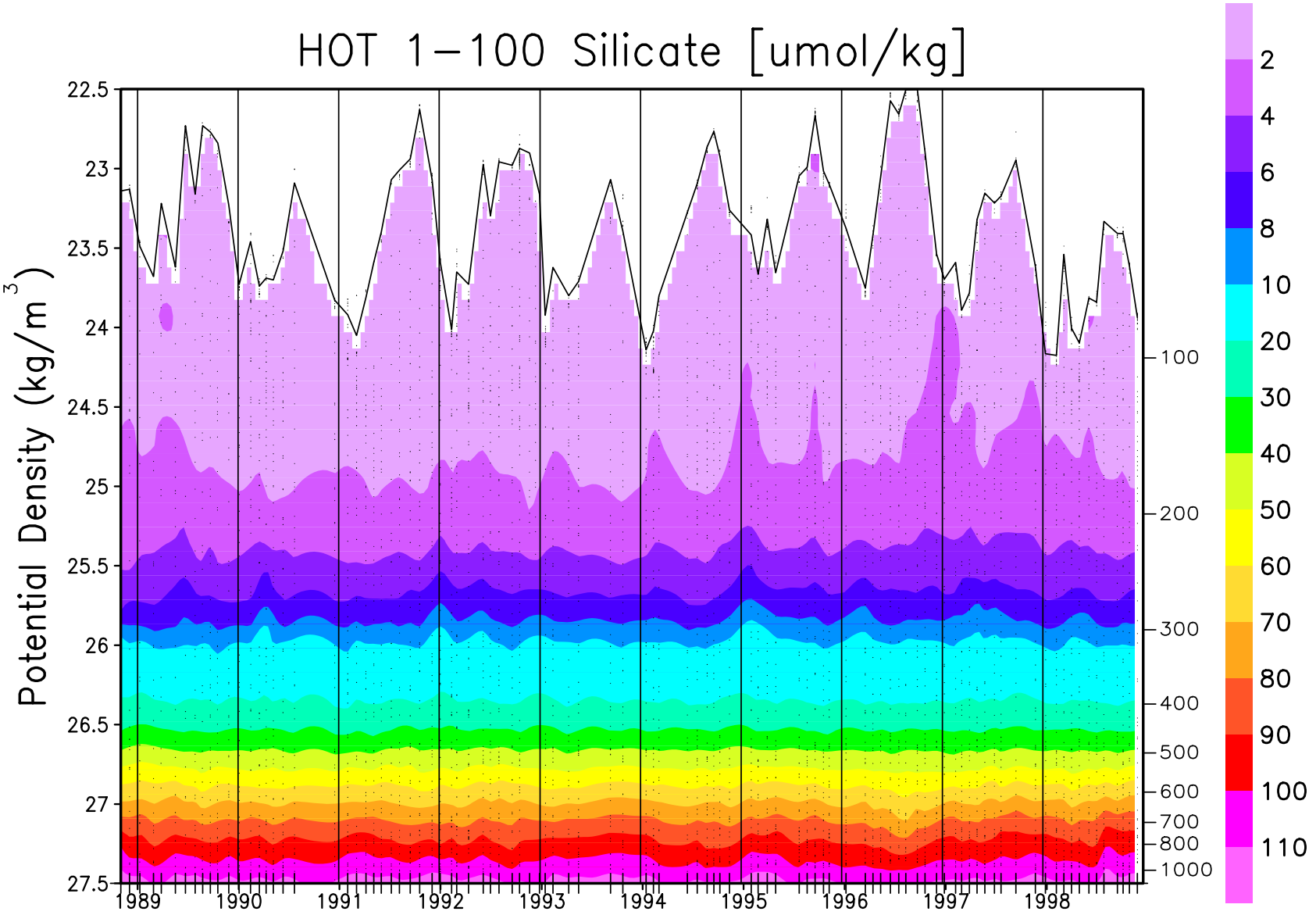

Figure 6.3.14: Contour plot of silicate versus potential density (σ_θ) to 27.5 kg m^{-3} for HOT cruises 1-100. The average density of the sea surface is connected by the heavy line.

6.4. Flash Fluorescence and Beam Transmission

Figures 6.4.1 to 9: Stack plots of flash fluorescence and beam transmission (when available) collected at Station ALOHA on HOT 51 to 59. Upper two panels show flash fluorescence data collected on each cruise plotted versus pressure to 250 dbar and potential density at 26 s_q. Offset is 20 mvolts. Lower two panels show % transmittance data collected on each cruise plotted versus pressure to 250 dbar and potential density at 26 s_q. Offset is 33%.

Figure 6.4.10: Stack plots of averaged night-time fluorescence profiles plotted versus pressure to 250 dbar collected on each HOT cruise from 1988 through 1994. The HOT cruise number is shown at the top of each panel.

Figure 6.4.11: As in 6.4.10, except profiles are plotted versus potential density at 26 σ_θ.

Figure 6.4.12: Stack plots of averaged beam transmission profiles collected in 1991-1994. Upper panel shows profiles plotted versus pressure to 250 dbar. Lower panel shows profiles plotted versus potential density at 26 σ_θ. The HOT cruise number is shown at the top of each panel.

Figure 6.4.13: As in 6.3.12, except profiles are plotted versus potential density at 26 σ_θ.

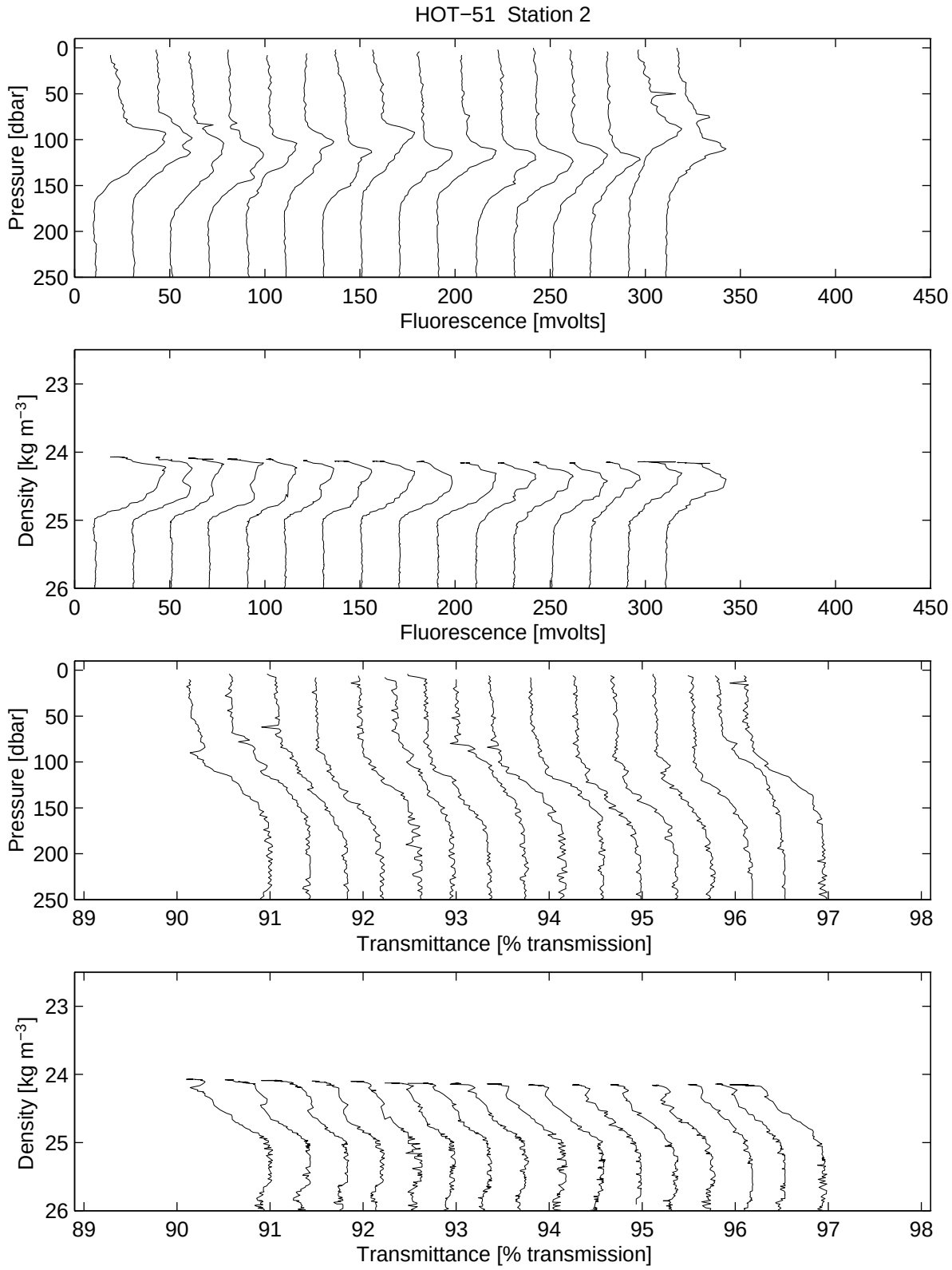
HOT−51 Station 2
Pressure [dbar]
Fluorescence [mvolts]
Density [kg m^{-3}]
Fluorescence [mvolts]
Pressure [dbar]
Transmittance [% transmission]
Density [kg m^{-3}]
Transmittance [% transmission]

Figure 6.4.1

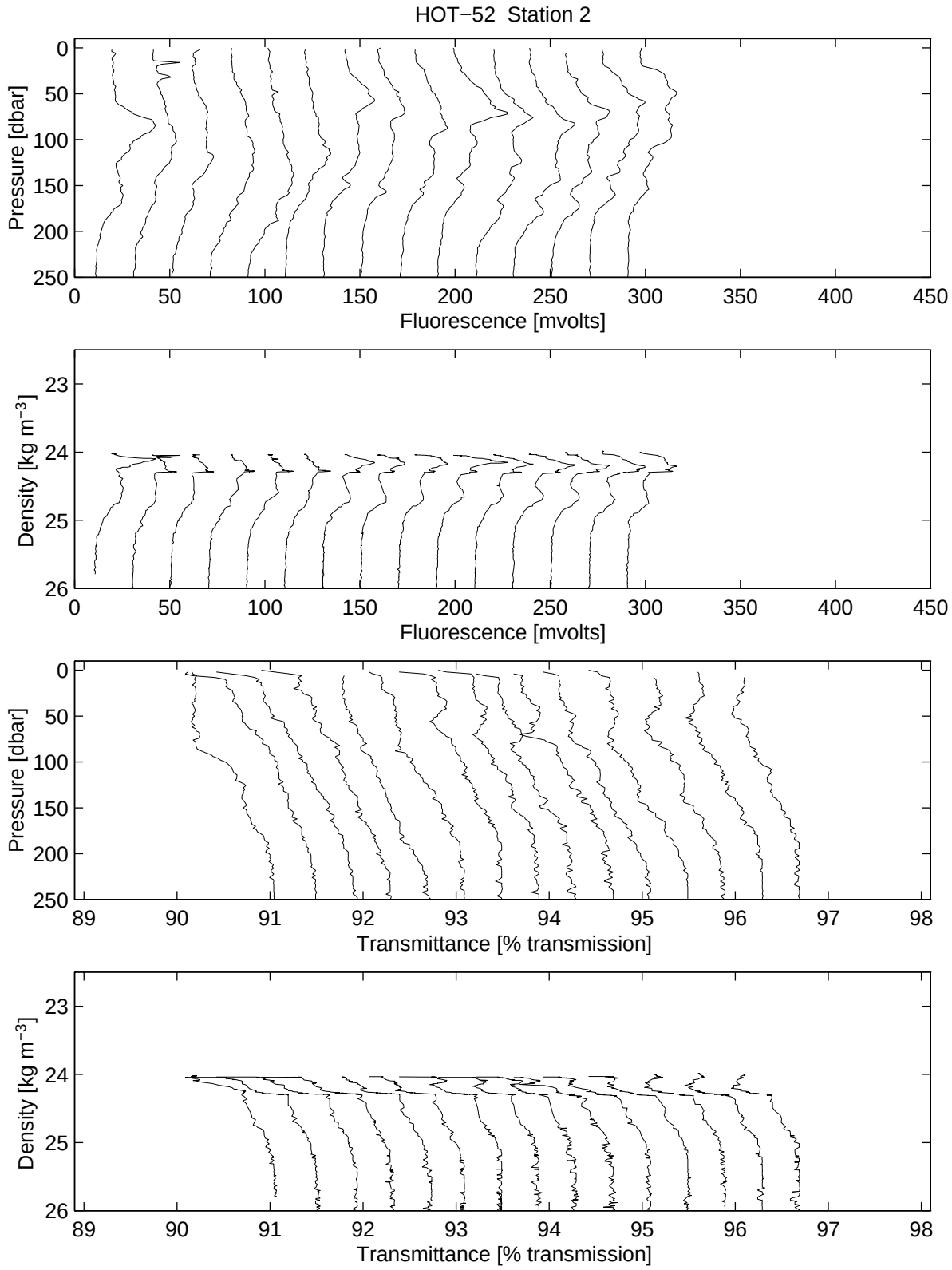
HOT−52 Station 2
Pressure [dbar]
Fluorescence [mvolts]
Density [kg m^{-3}]
Fluorescence [mvolts]
Pressure [dbar]
Transmittance [% transmission]
Density [kg m^{-3}]
Transmittance [% transmission]

Figure 6.4.2

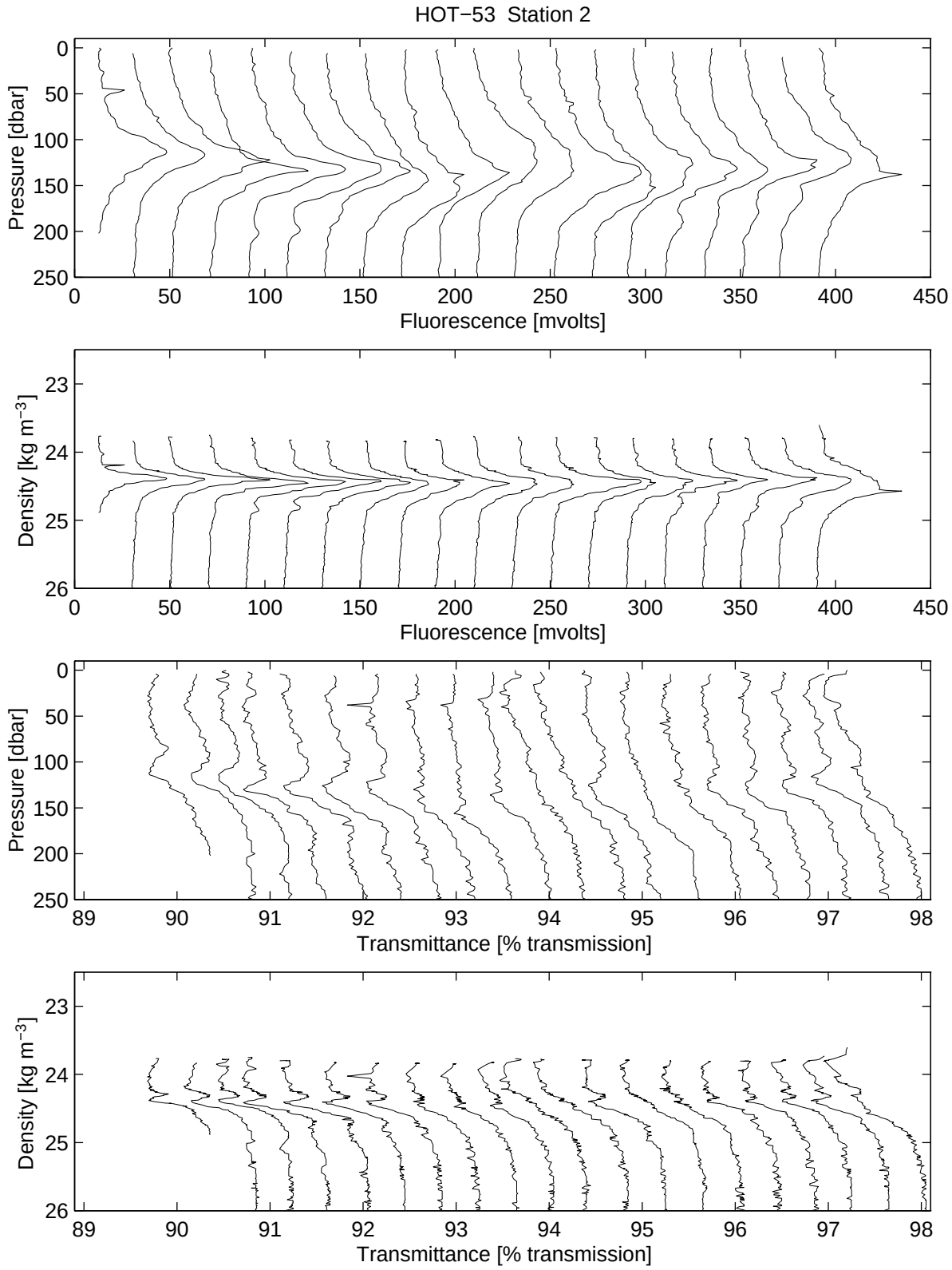
HOT−53 Station 2
Pressure [dbar]
Fluorescence [mvolts]
Density [kg m−3]
Fluorescence [mvolts]
Pressure [dbar]
Transmittance [% transmission]
Density [kg m−3]
Transmittance [% transmission]

Figure 6.4.3

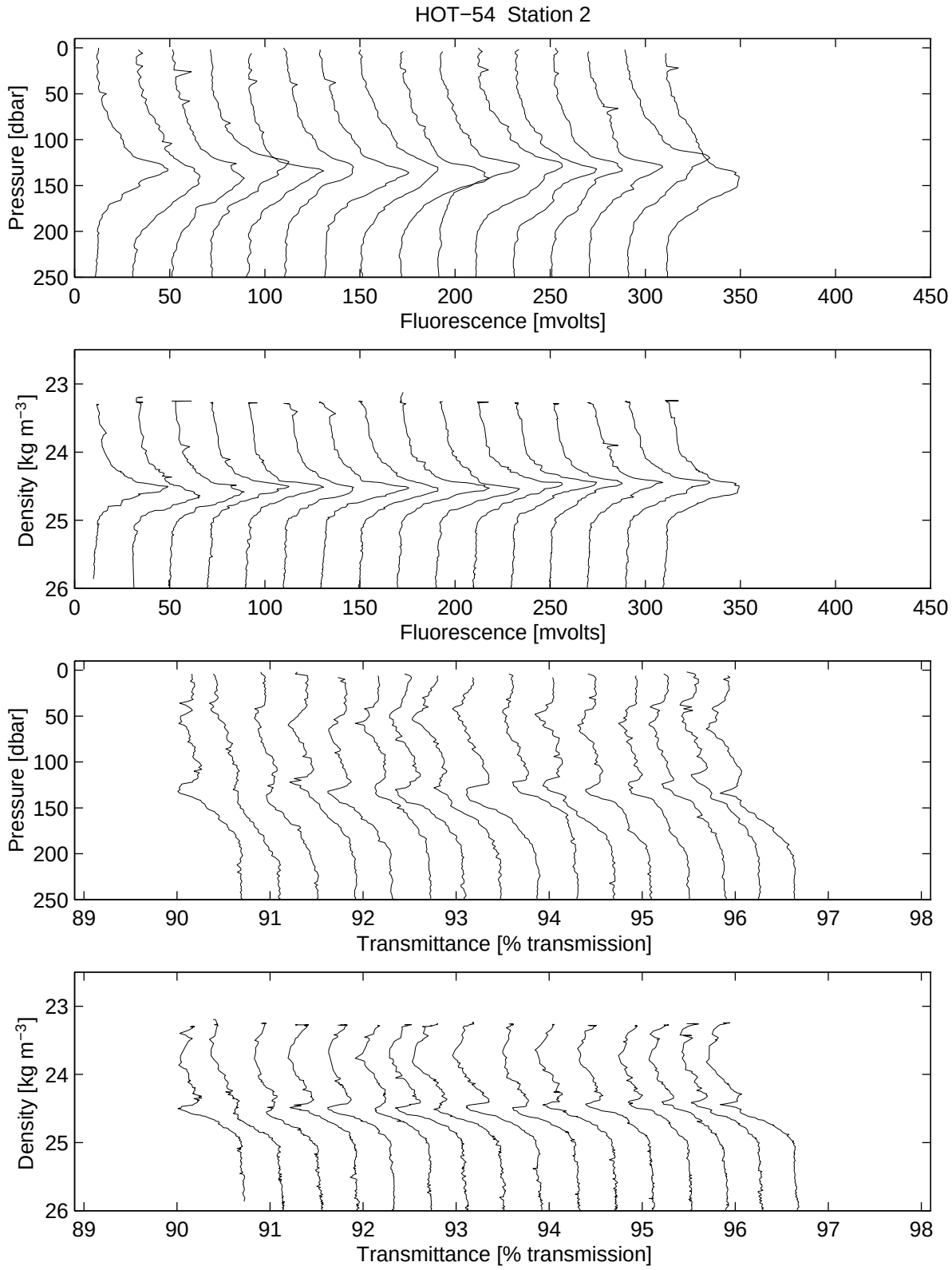
HOT−54 Station 2
Pressure [dbar]
Fluorescence [mvolts]
Density [kg m−3]
Fluorescence [mvolts]
Pressure [dbar]
Transmittance [% transmission]
Density [kg m−3]
Transmittance [% transmission]

Figure 6.4.4

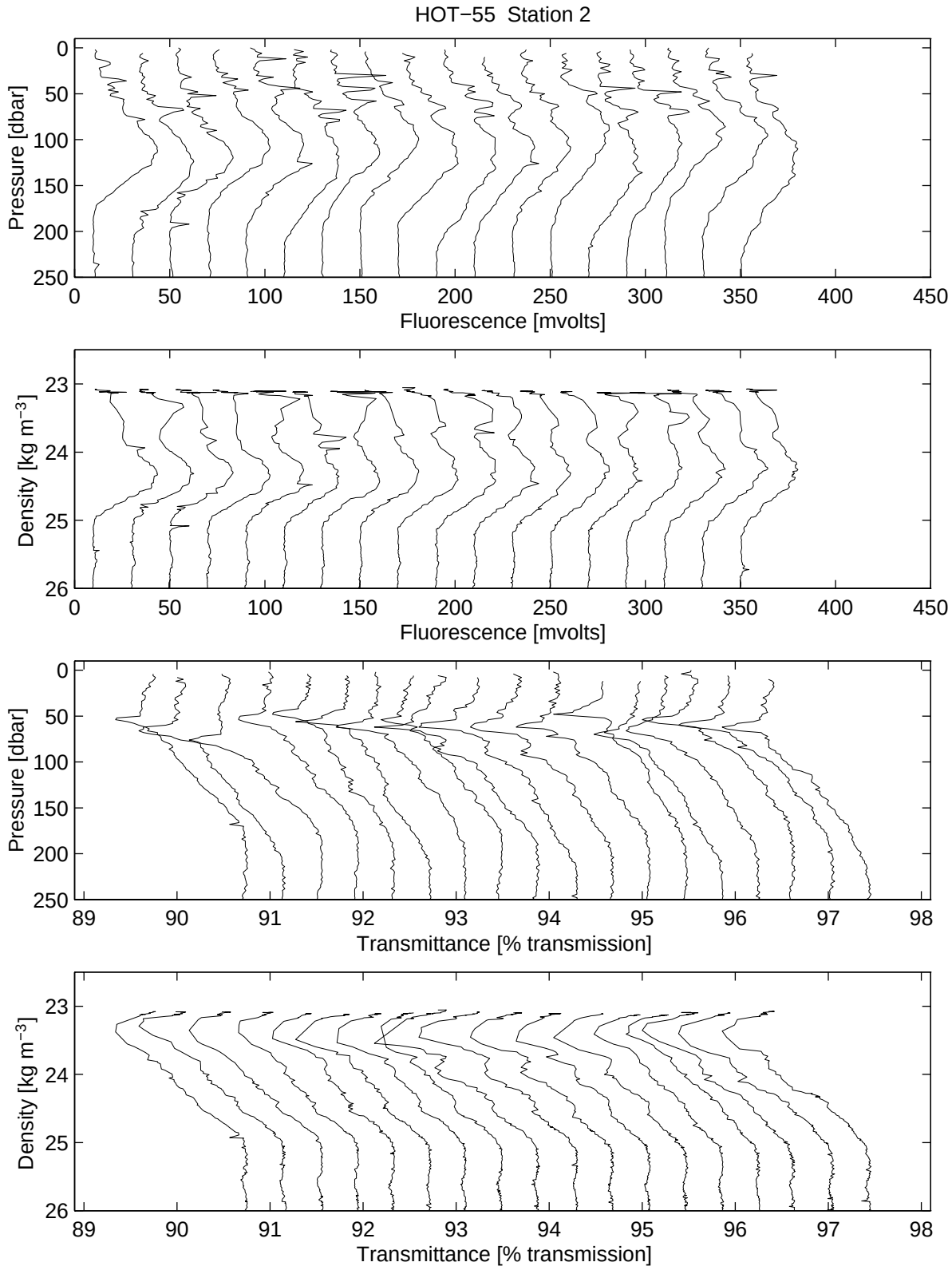
HOT−55 Station 2
Pressure [dbar]
Fluorescence [mvolts]
Density [kg m^{-3}]
Fluorescence [mvolts]
Pressure [dbar]
Transmittance [% transmission]
Density [kg m^{-3}]
Transmittance [% transmission]

Figure 6.4.5

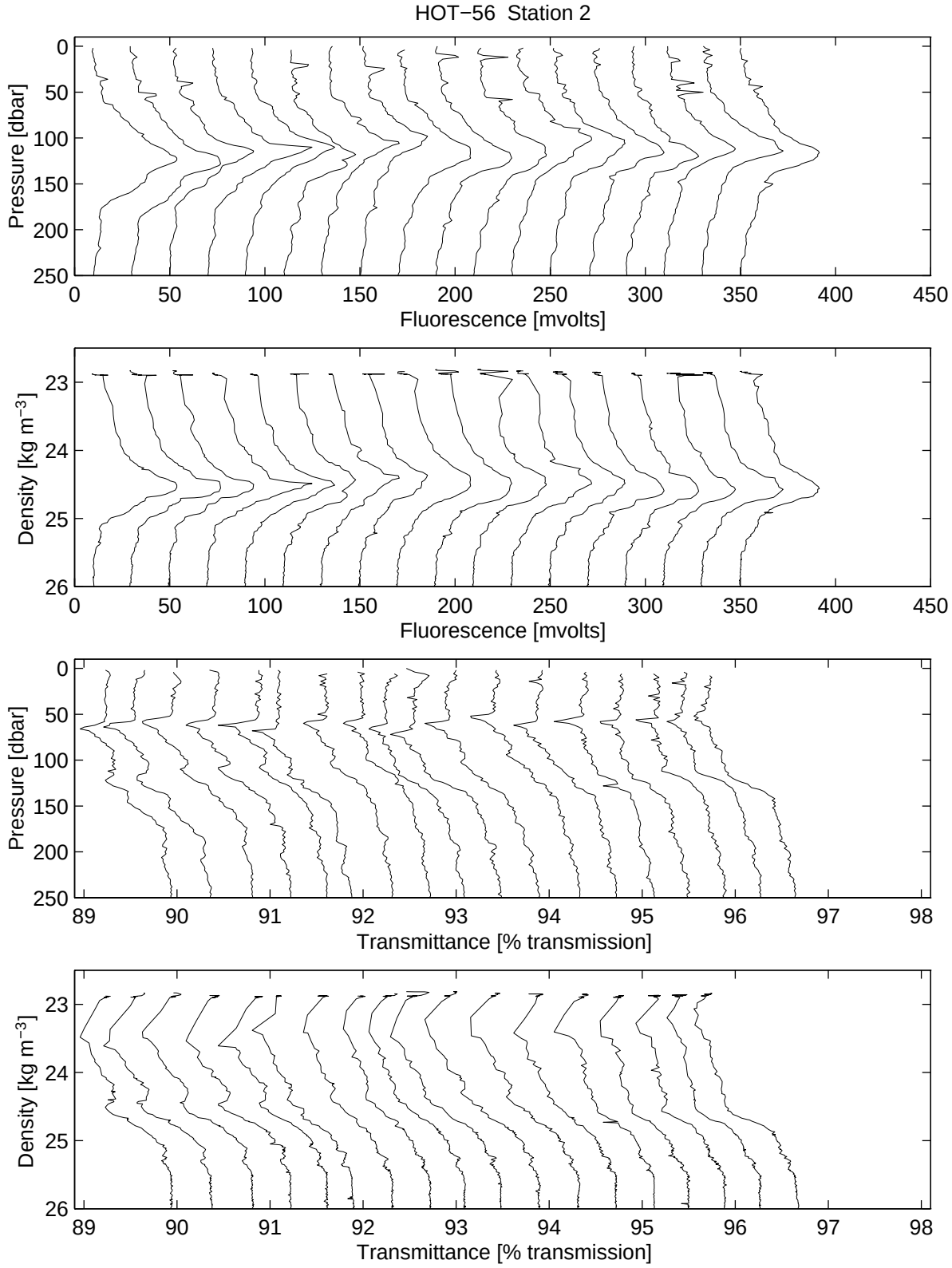
HOT−56 Station 2
Pressure [dbar]
Fluorescence [mvolts]
Density [kg m−3]
Fluorescence [mvolts]
Pressure [dbar]
Transmittance [% transmission]
Density [kg m−3]
Transmittance [% transmission]

Figure 6.4.6

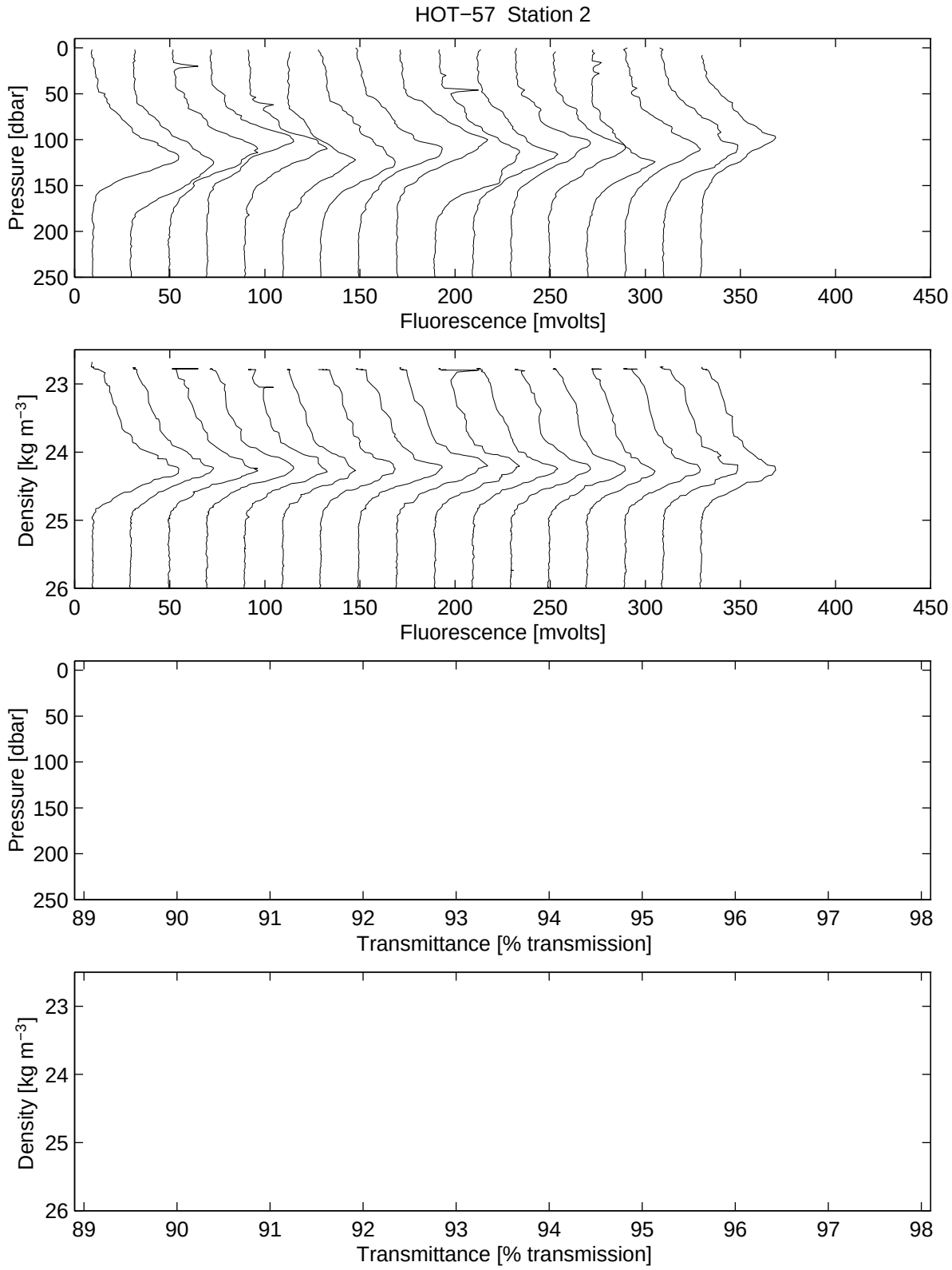
HOT−57 Station 2
Pressure [dbar]
Fluorescence [mvolts]
Density [kg m−3]
Fluorescence [mvolts]
Pressure [dbar]
Transmittance [% transmission]
Density [kg m−3]
Transmittance [% transmission]

Figure 6.4.7

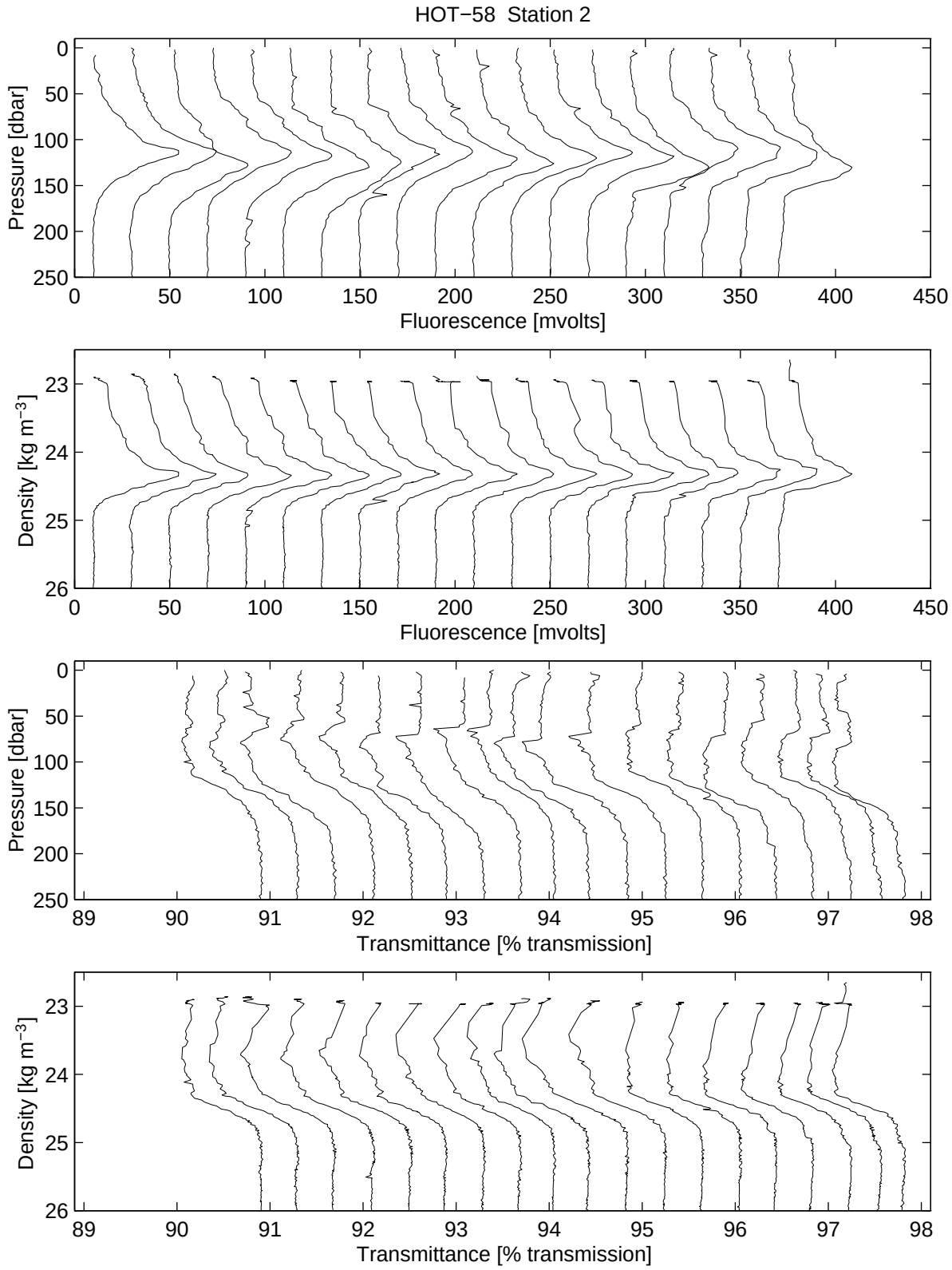
HOT−58 Station 2
Pressure [dbar]
Fluorescence [mvolts]
Density [kg m−3]
Fluorescence [mvolts]
Pressure [dbar]
Transmittance [% transmission]
Density [kg m−3]
Transmittance [% transmission]

Figure 6.4.8

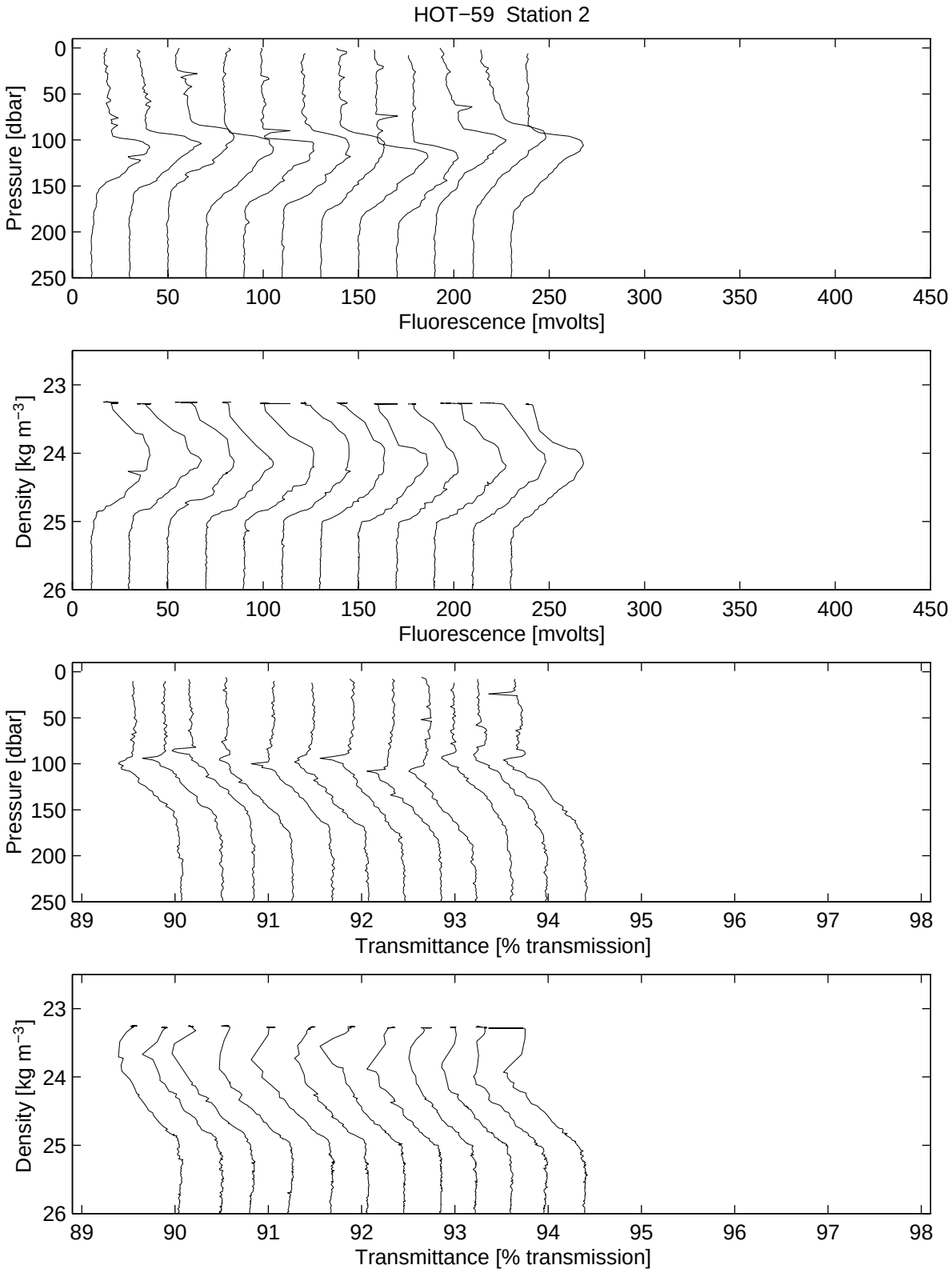
HOT−59 Station 2
Pressure [dbar]
Fluorescence [mvolts]
Density [kg m−3]
Fluorescence [mvolts]
Pressure [dbar]
Transmittance [% transmission]
Density [kg m−3]
Transmittance [% transmission]

Figure 6.4.9

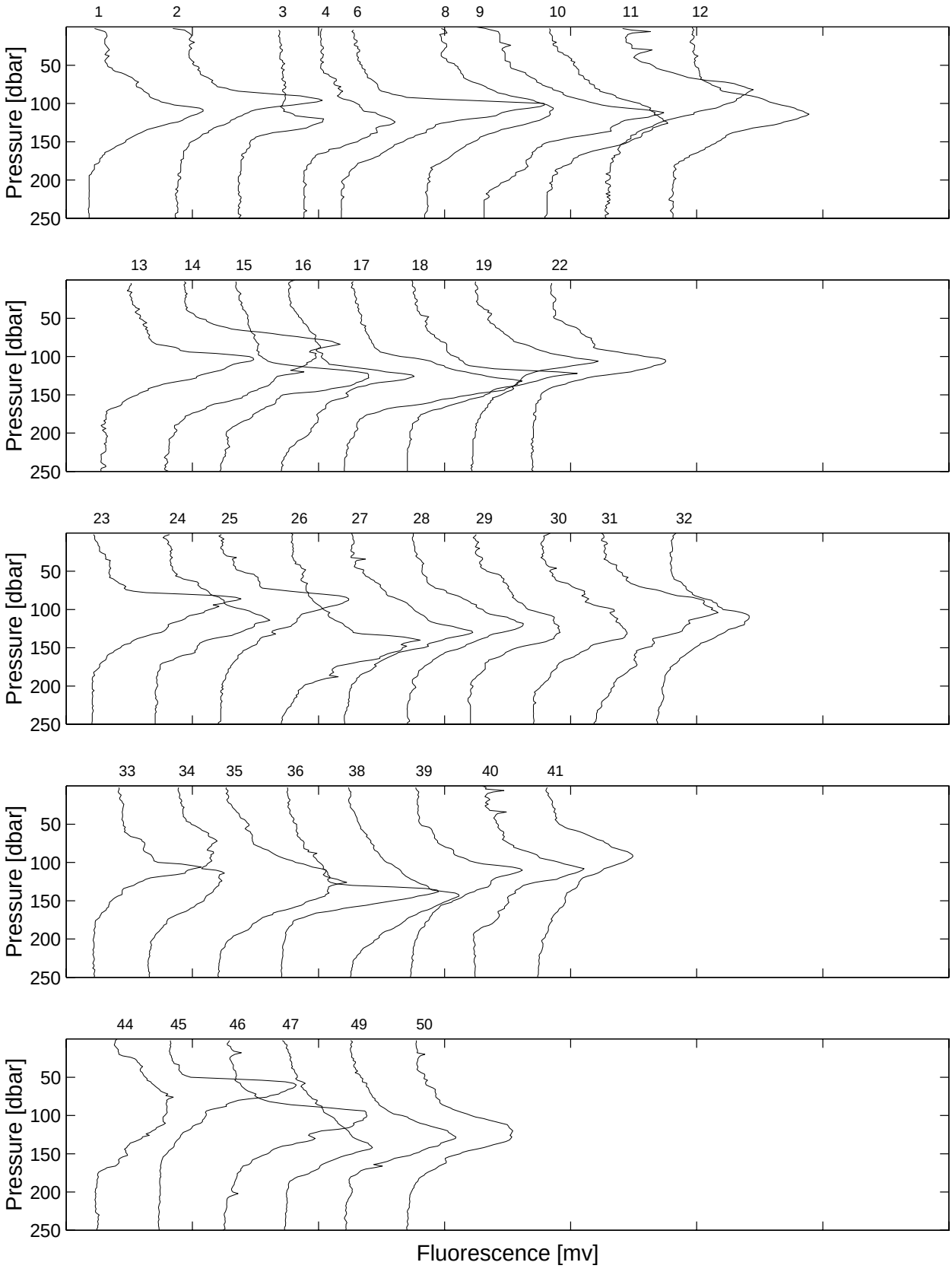
1 2 3 4 6 8 9 10 11 12
13 14 15 16 17 18 19 22
23 24 25 26 27 28 29 30 31 32
33 34 35 36 38 39 40 41
44 45 46 47 49 50
Pressure [dbar]
50
100
150
200
250
Fluorescence [mv]

Figure 6.4.10

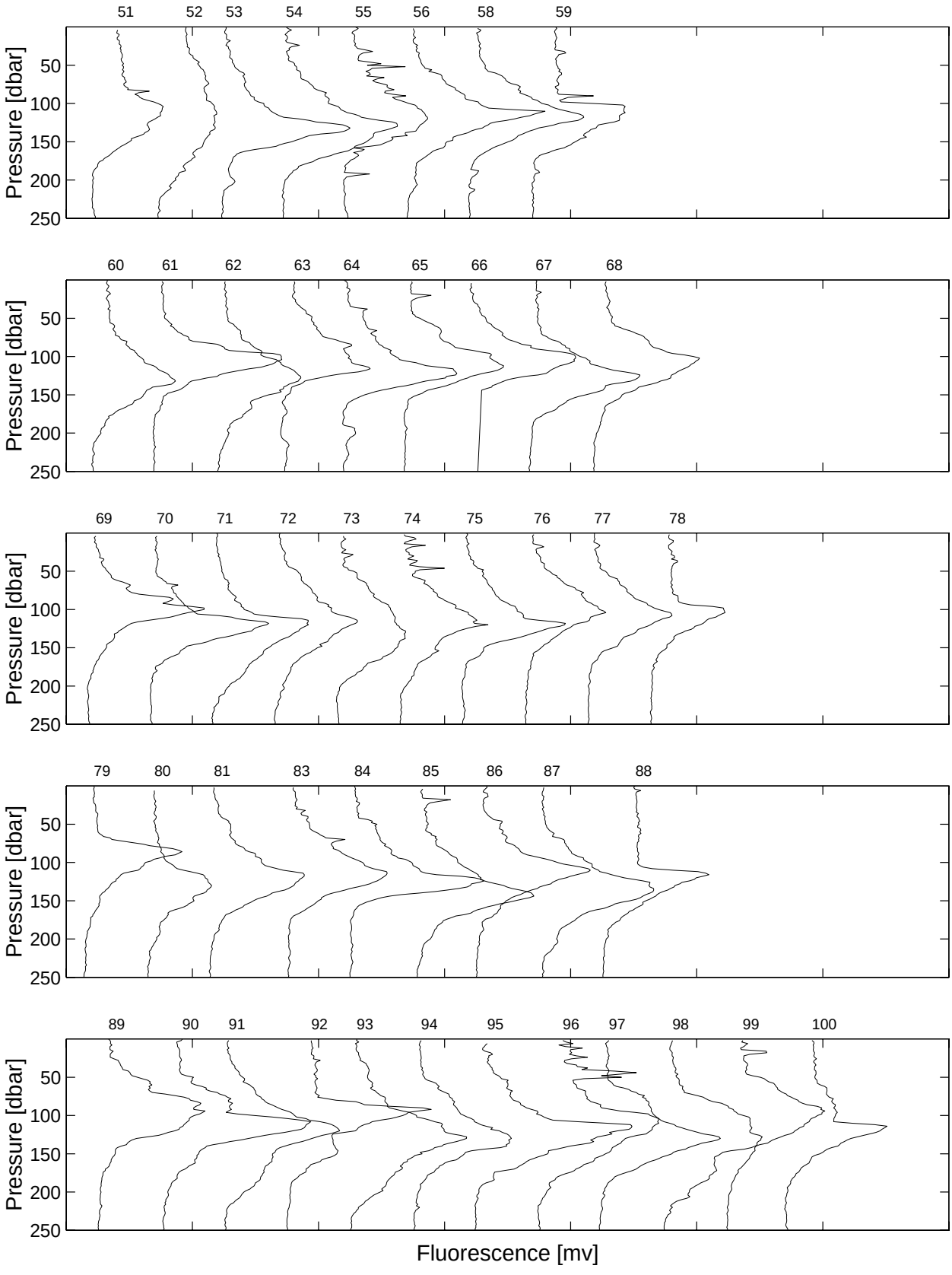
51 52 53 54 55 56 58 59
60 61 62 63 64 65 66 67 68
69 70 71 72 73 74 75 76 77 78
79 80 81 83 84 85 86 87 88
89 90 91 92 93 94 95 96 97 98 99 100
Pressure [dbar]
50
100
150
200
250
Fluorescence [mv]

Figure 6.4.11

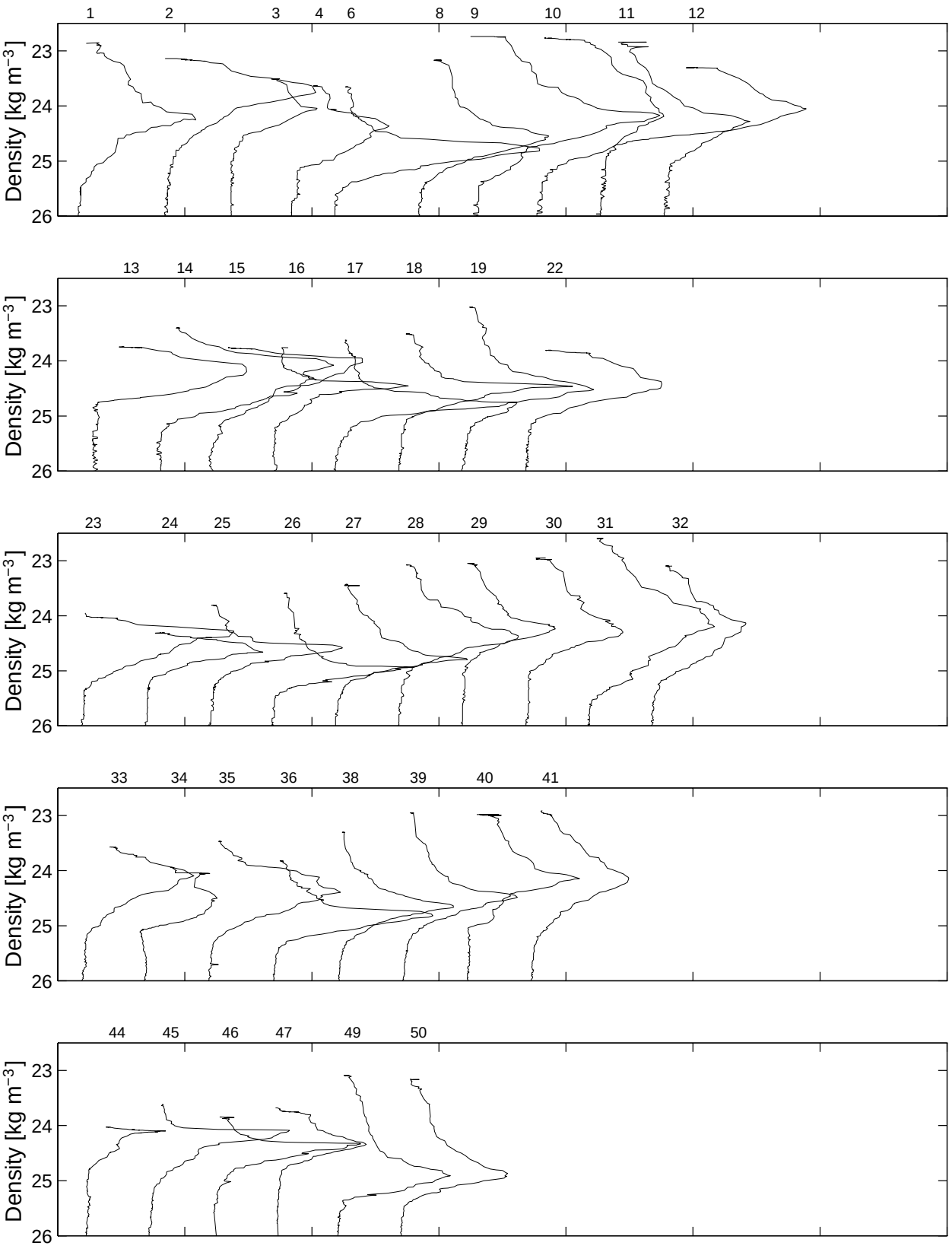
1 2 3 4 6 8 9 10 11 12
13 14 15 16 17 18 19 22
23 24 25 26 27 28 29 30 31 32
33 34 35 36 38 39 40 41
44 45 46 47 49 50
Density [kg m⁻³]
23
24
25
26
Fluorescence [mv]

Figure 6.4.12

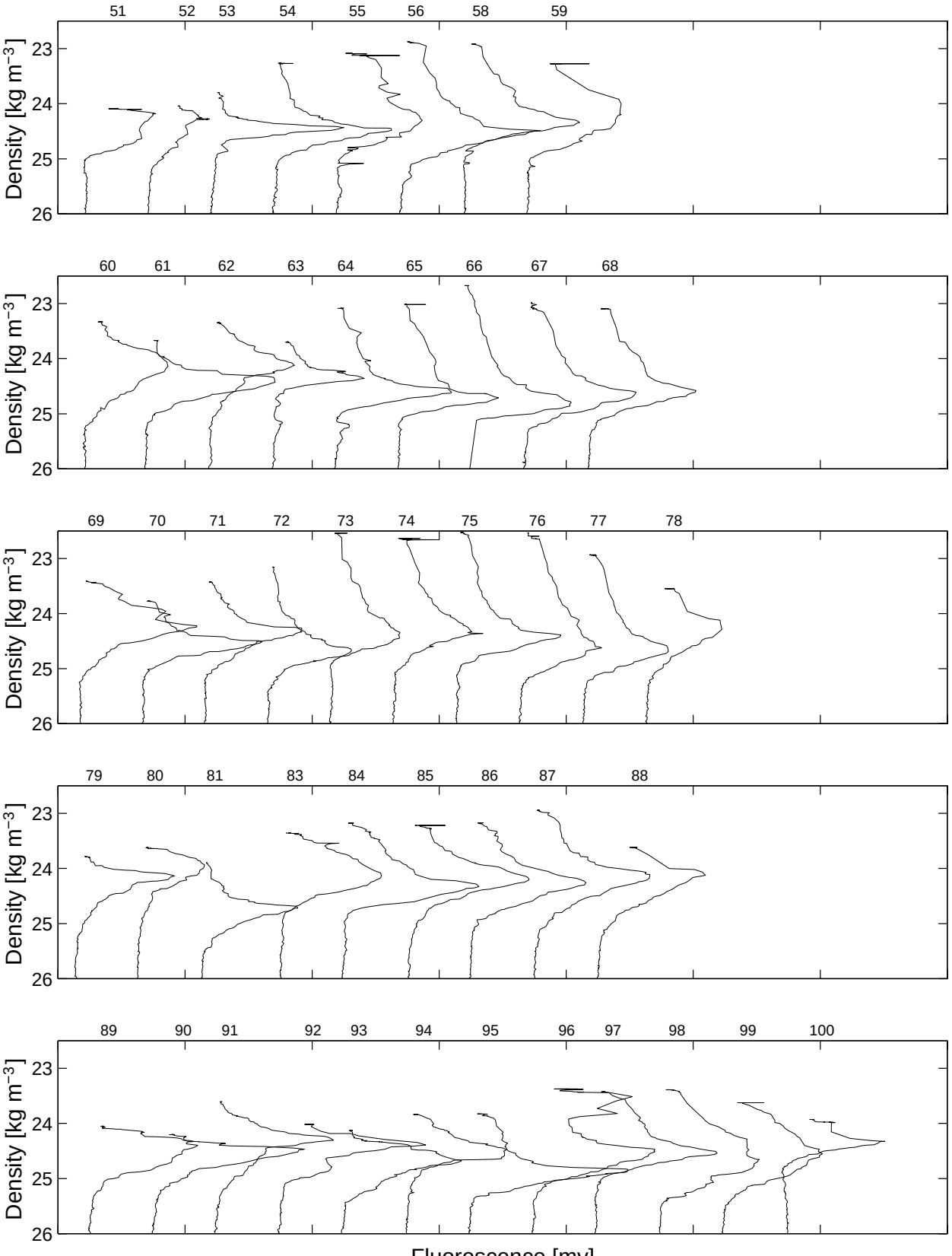
51 52 53 54 55 56 58 59
60 61 62 63 64 65 66 67 68
69 70 71 72 73 74 75 76 77 78
79 80 81 83 84 85 86 87 88
89 90 91 92 93 94 95 96 97 98 99 100
Density [kg m⁻³]
23
24
25
26
Fluorescence [mv]

Figure 6.4.13

6.5. Biogeochemistry

Figure 6.5.1: Contoured time-series of DIC in the upper 1000 dbar at Station ALOHA normalized to 35 ppt salinity. Location of bottle closure is indicated by solid circle.

Figure 6.5.2: Contoured time-series of titration alkalinity in the upper 1000 dbar at Station ALOHA normalized to 35 ppt salinity. Location of bottle closure is indicated by solid circle.

Figure 6.5.3: Mean titration alkalinity and DIC in surface waters (0-50 dbars) at Station ALOHA. Upper Panel: Titration alkalinity plotted versus time for all HOT cruises. Error bars represent standard deviation of pooled samples collected between 0 and 50 dbar. Lower panel: As in upper panel except for DIC.

Figure 6.5.4: Soluble reactive phosphorus measured by the MAGIC procedure in the upper 250 dbar at Station ALOHA in 1994.

Figure 6.5.5: Nitrate plus nitrite measured by chemiluminescence in the upper 250 dbar at Station ALOHA in 1994.

Figure 6.5.6: Contoured time-series of fluorometric chlorophyll *a* in the upper 200 dbar for all HOT cruises.

Figure 6.5.7: Particulate carbon at Station ALOHA on all HOT cruises. Upper panel: Mean particulate carbon concentration in the upper 50 dbar. Error bar represents the standard deviation of pooled samples collected between 0 and 50 dbar. Lower panel: As in upper panel but for 50 to 100 dbar.

Figure 6.5.8: As in Figure 6.5.7 except for particulate nitrogen.

Figure 6.5.9: As in Figure 6.5.7 except for particulate phosphorus.

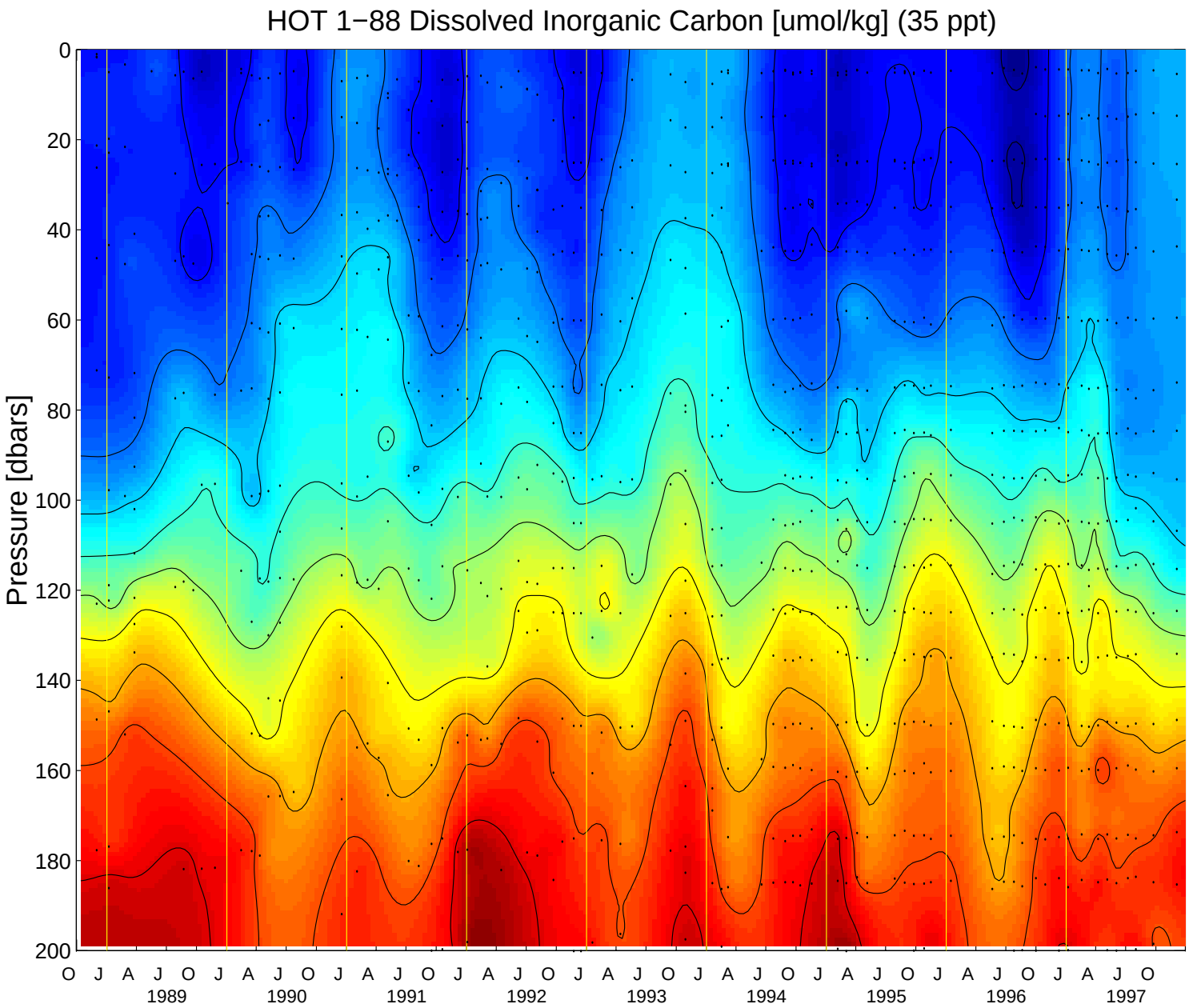
HOT 1−88 Dissolved Inorganic Carbon [umol/kg] (35 ppt)
Pressure [dbars]
0
20
40
60
80
100
120
140
160
180
200
O J A J O J A J O J A J O J A J O J A J O J A J O J A J O J A J O J A J O J A J O J A J O J A J O
1989
1990
1991
1992
1993
1994
1995
1996
1997

Figure 6.5.1

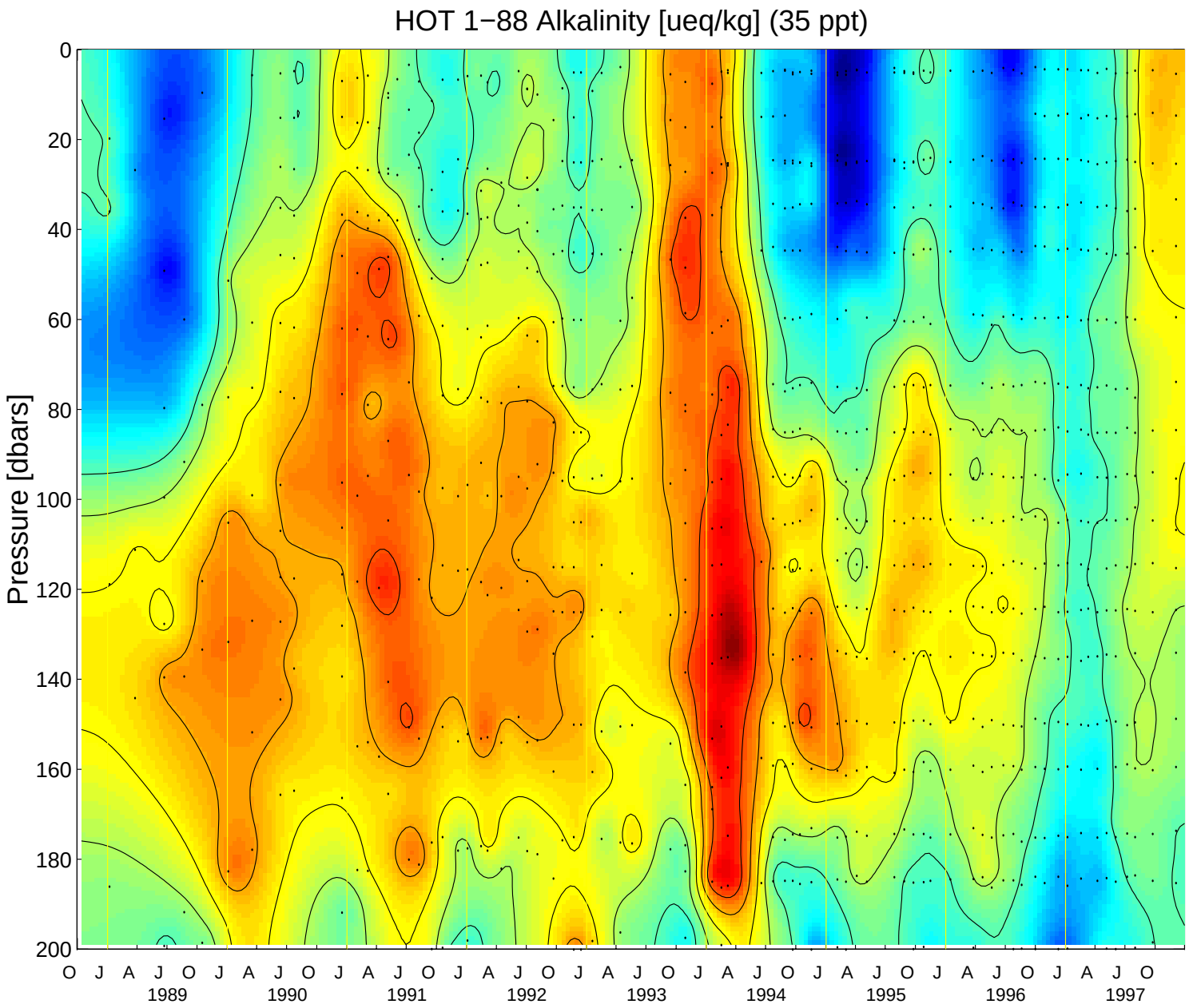
HOT 1−88 Alkalinity [ueq/kg] (35 ppt)
Pressure [dbars]
0
20
40
60
80
100
120
140
160
180
200
O J A J O J A J O J A J O J A J O J A J O J A J O J A J O J A J O J A J O J A J O J A J O
1989
1990
1991
1992
1993
1994
1995
1996
1997

Figure 6.5.2

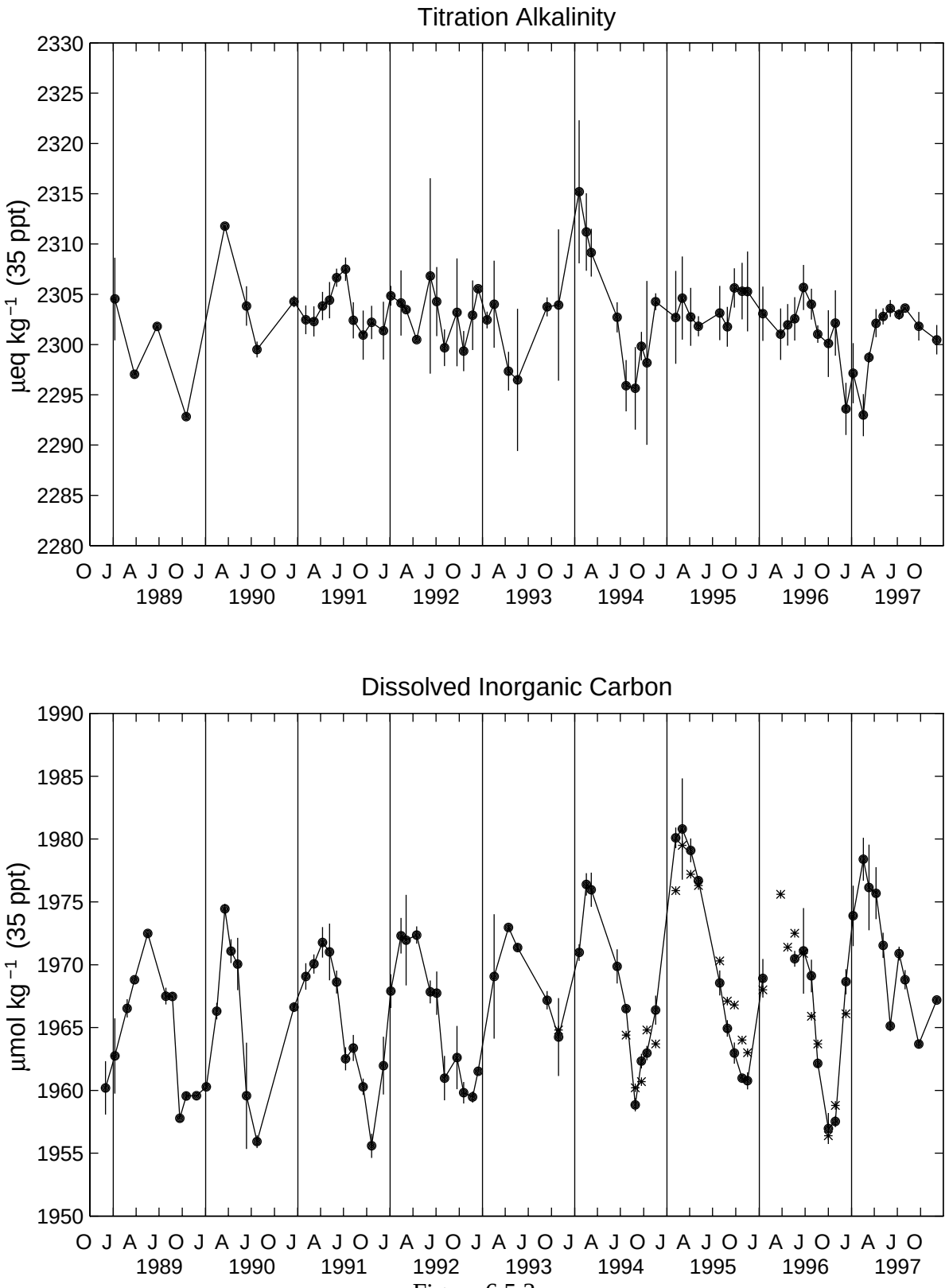
Titration Alkalinity
µeq kg⁻¹ (35 ppt)
2330
2325
2320
2315
2310
2305
2300
2295
2290
2285
2280
O J A J O J A J O J A J O J A J O J A J O J A J O J A J O J A J O J A J O J A J O
1989
1990
1991
1992
1993
1994
1995
1996
1997
Dissolved Inorganic Carbon
µmol kg⁻¹ (35 ppt)
1990
1985
1980
1975
1970
1965
1960
1955
1950
O J A J O J A J O J A J O J A J O J A J O J A J O J A J O J A J O J A J O J A J O
1989
1990
1991
1992
1993
1994
1995
1996
1997
Figure 6.5.3

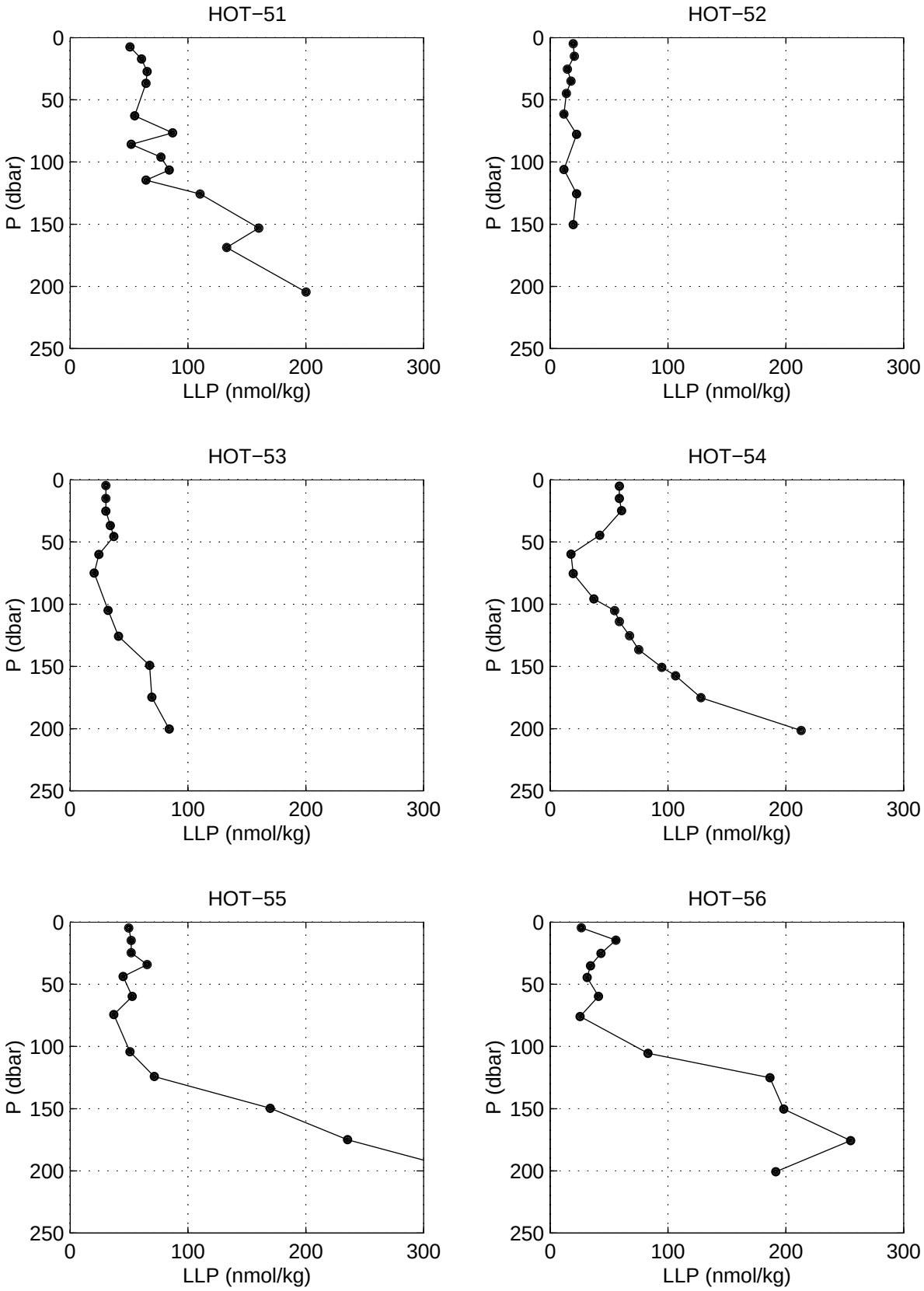
HOT−51
HOT−52
HOT−53
HOT−54
HOT−55
HOT−56
P (dbar)
LLP (nmol/kg)
0
50
100
150
200
250
300

Figure 6.5.4

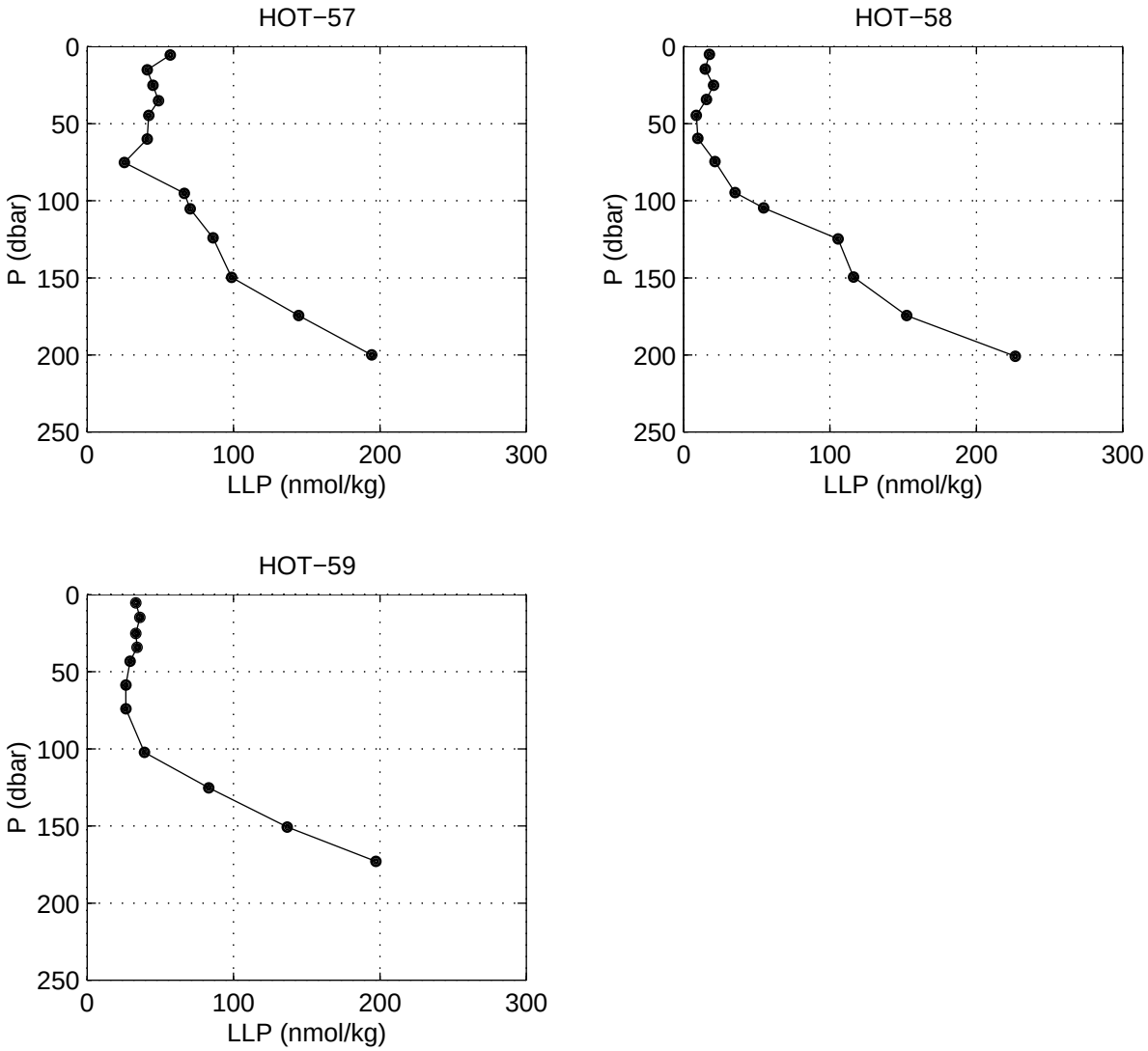

Figure 6.5.4 continued

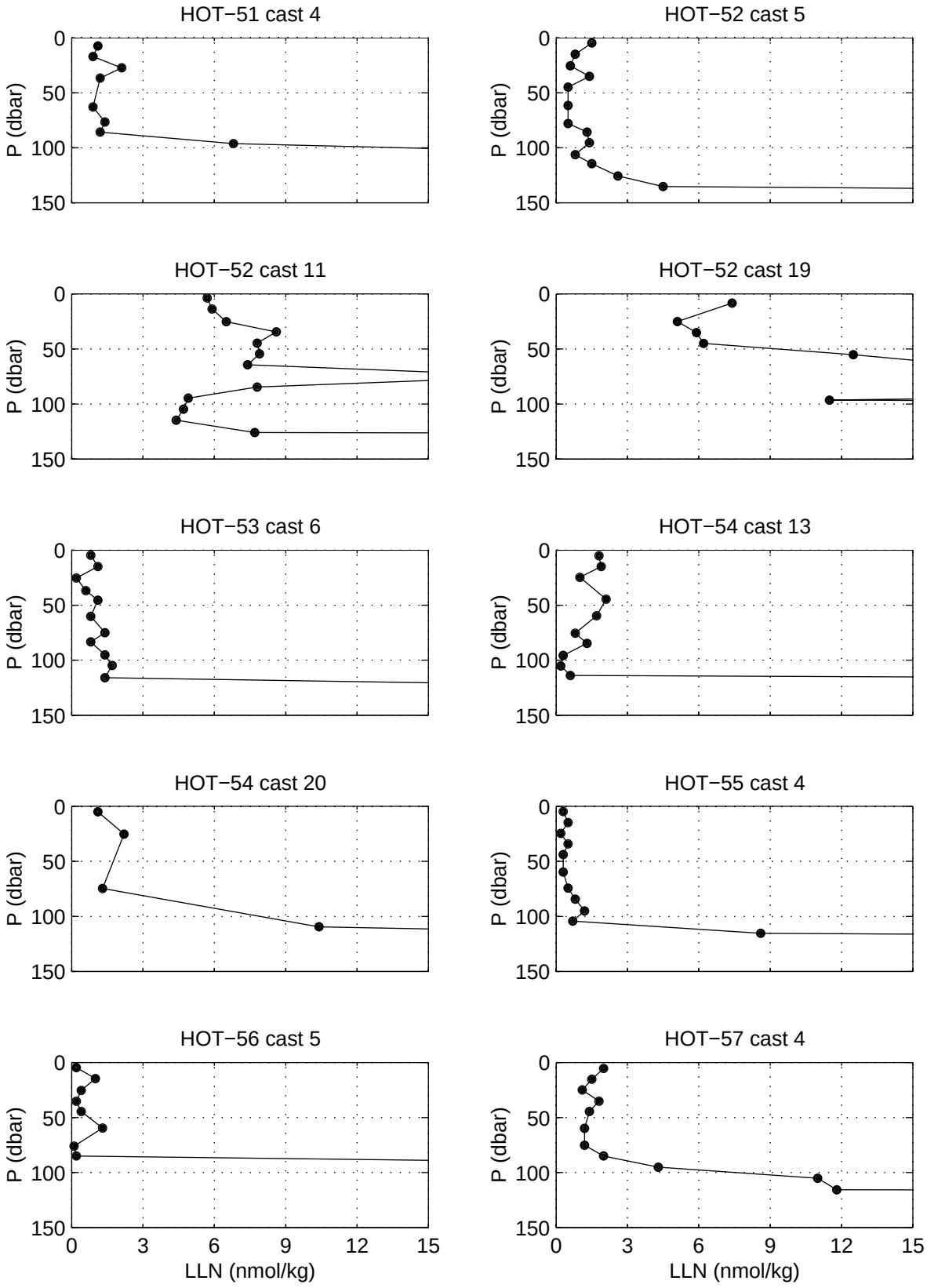
HOT−51 cast 4
HOT−52 cast 5
HOT−52 cast 11
HOT−52 cast 19
HOT−53 cast 6
HOT−54 cast 13
HOT−54 cast 20
HOT−55 cast 4
HOT−56 cast 5
HOT−57 cast 4
P (dbar)
0
50
100
150
0
3
6
9
12
15
LLN (nmol/kg)

Figure 6.5.5

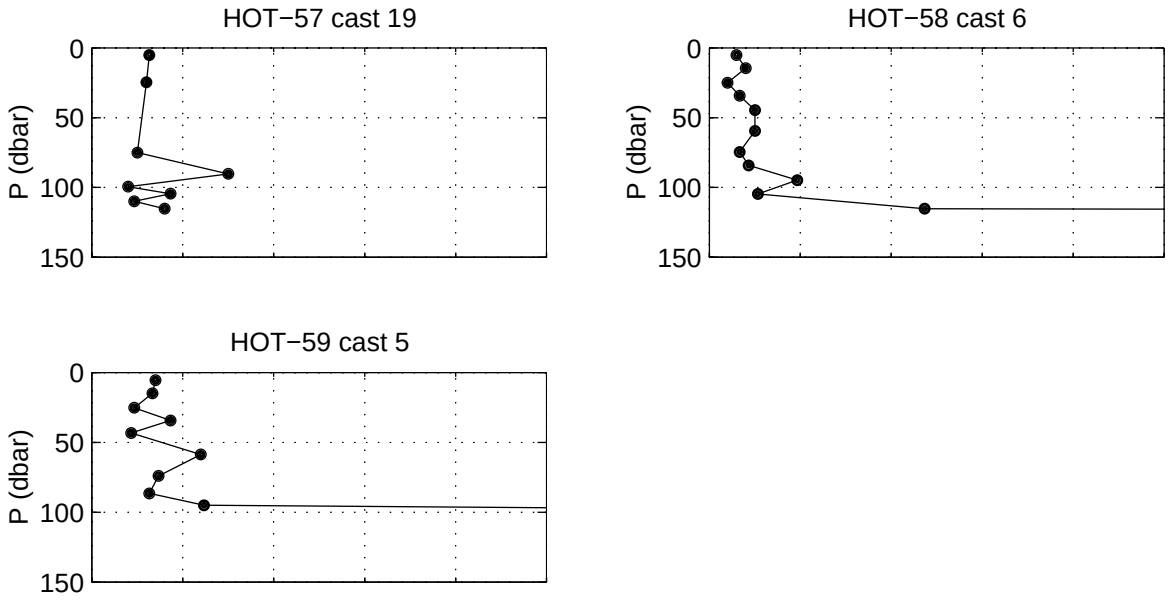

Figure 6.5.5 continued

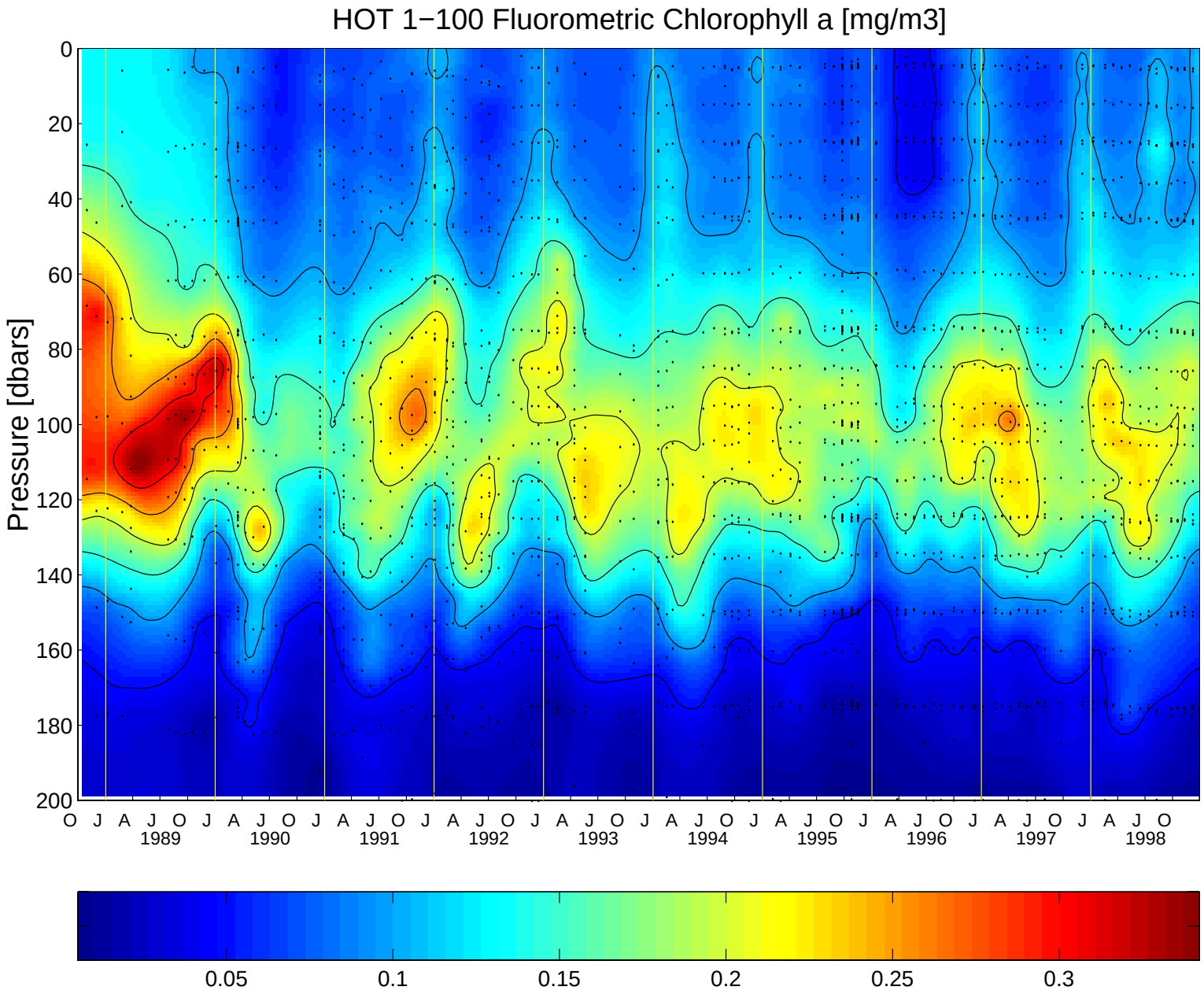
HOT 1−100 Fluorometric Chlorophyll a [mg/m3]
Pressure [dbars]
0
20
40
60
80
100
120
140
160
180
200
O J A J O J A J O J A J O J A J O J A J O J A J O J A J O J A J O J A J O J A J O J A J O
1989
1990
1991
1992
1993
1994
1995
1996
1997
1998
0.05
0.1
0.15
0.2
0.25
0.3

Figure 6.5.6

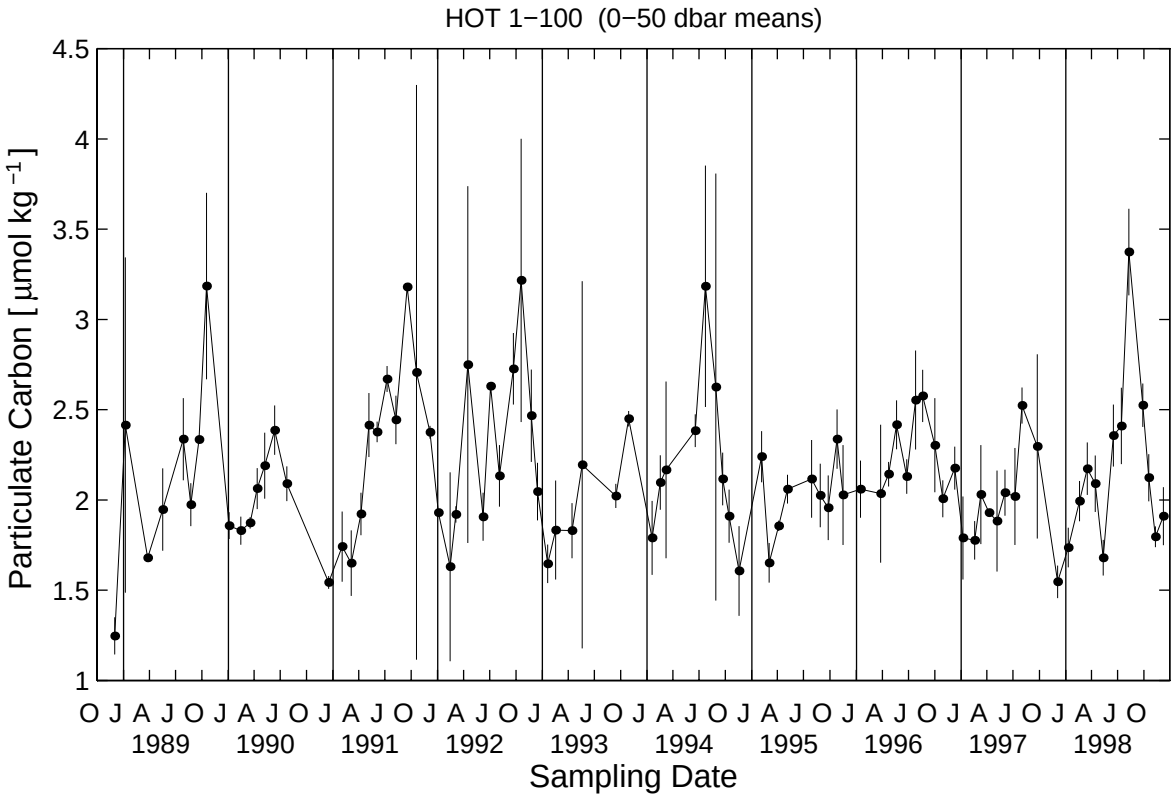
HOT 1−100 (0−50 dbar means)
Particulate Carbon [µmol kg −1]
4.5
4
3.5
3
2.5
2
1.5
1
O J A J O J A J O J A J O J A J O J A J O J A J O J A J O J A J O J A J O
1989 1990 1991 1992 1993 1994 1995 1996 1997 1998
Sampling Date

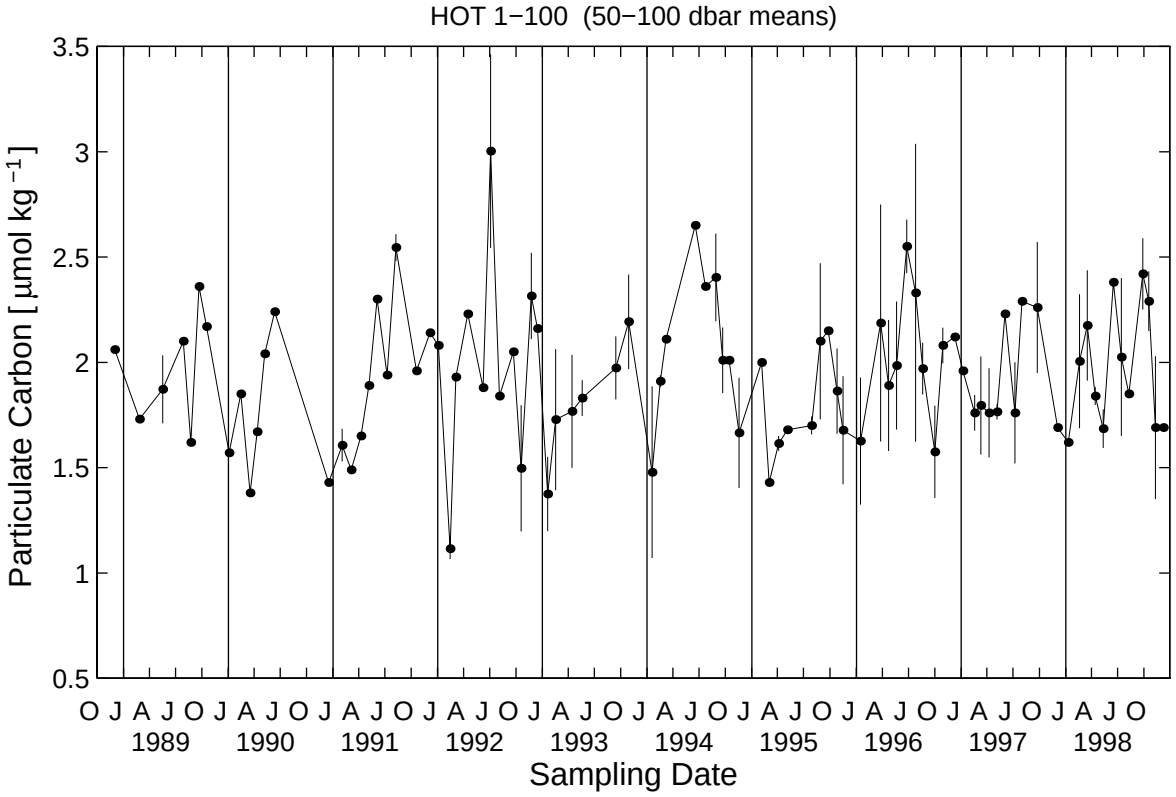
HOT 1−100 (50−100 dbar means)
Particulate Carbon [µmol kg −1]
3.5
3
2.5
2
1.5
1
0.5
O J A J O J A J O J A J O J A J O J A J O J A J O J A J O J A J O J A J O
1989 1990 1991 1992 1993 1994 1995 1996 1997 1998
Sampling Date

Figure 6.5.7

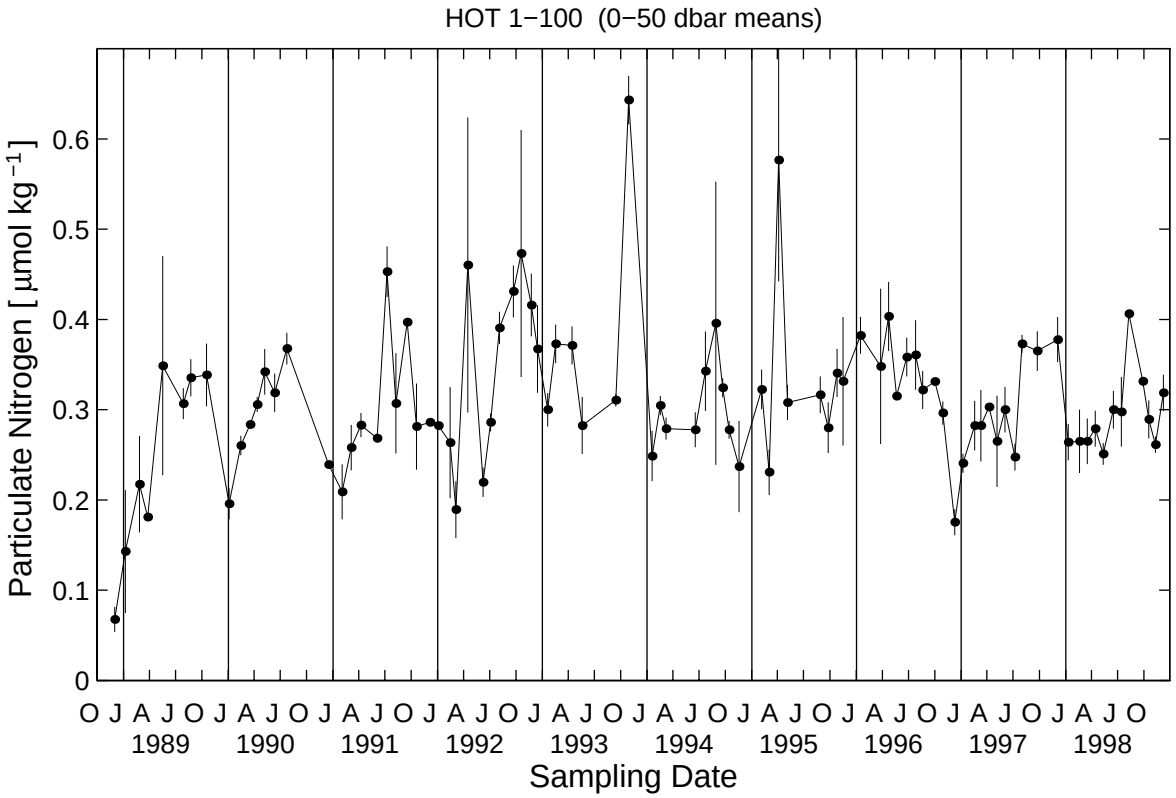
HOT 1−100 (0−50 dbar means)
Particulate Nitrogen [µmol kg⁻¹]
0
0.1
0.2
0.3
0.4
0.5
0.6
O J A J O J A J O J A J O J A J O J A J O J A J O J A J O J A J O J A J O J A J O
1989
1990
1991
1992
1993
1994
1995
1996
1997
1998
Sampling Date

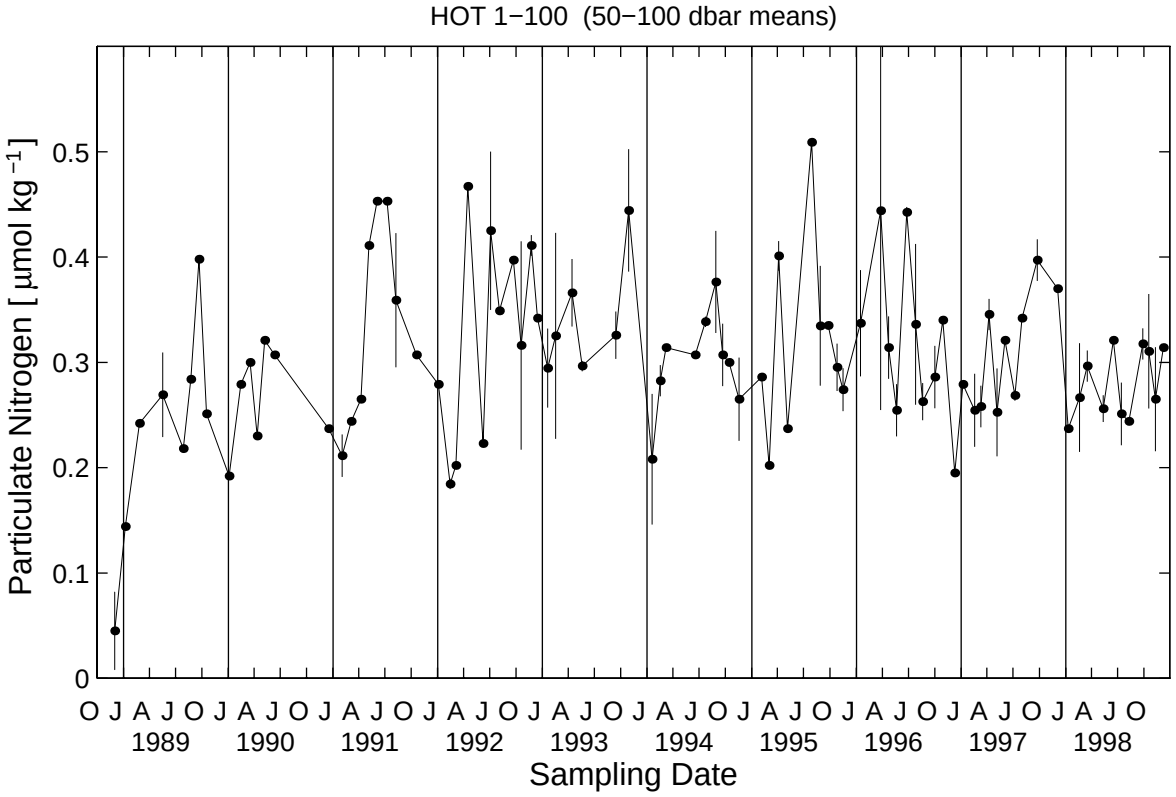
HOT 1−100 (50−100 dbar means)
Particulate Nitrogen [µmol kg⁻¹]
0
0.1
0.2
0.3
0.4
0.5
O J A J O J A J O J A J O J A J O J A J O J A J O J A J O J A J O J A J O J A J O
1989
1990
1991
1992
1993
1994
1995
1996
1997
1998
Sampling Date

Figure 6.5.8

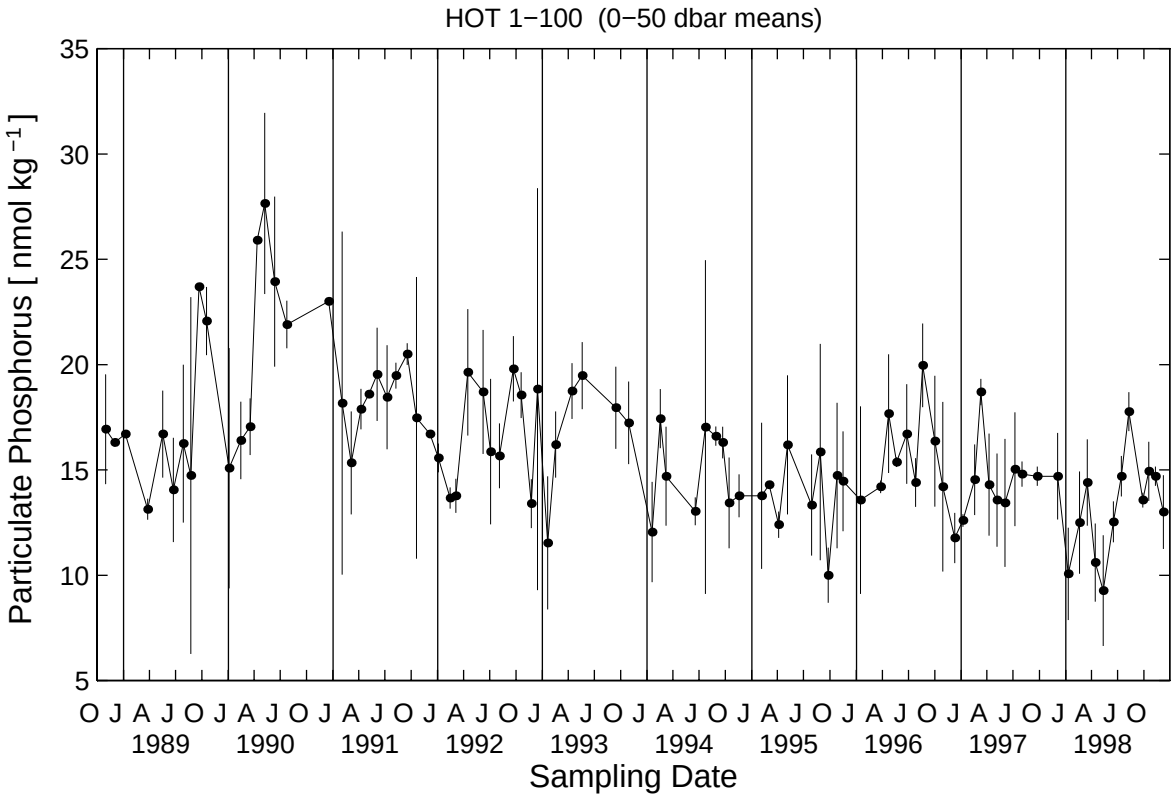
HOT 1−100 (0−50 dbar means)
Particulate Phosphorus [nmol kg⁻¹]
35
30
25
20
15
10
5
O J A J O J A J O J A J O J A J O J A J O J A J O J A J O J A J O J A J O J A J O
1989
1990
1991
1992
1993
1994
1995
1996
1997
1998
Sampling Date

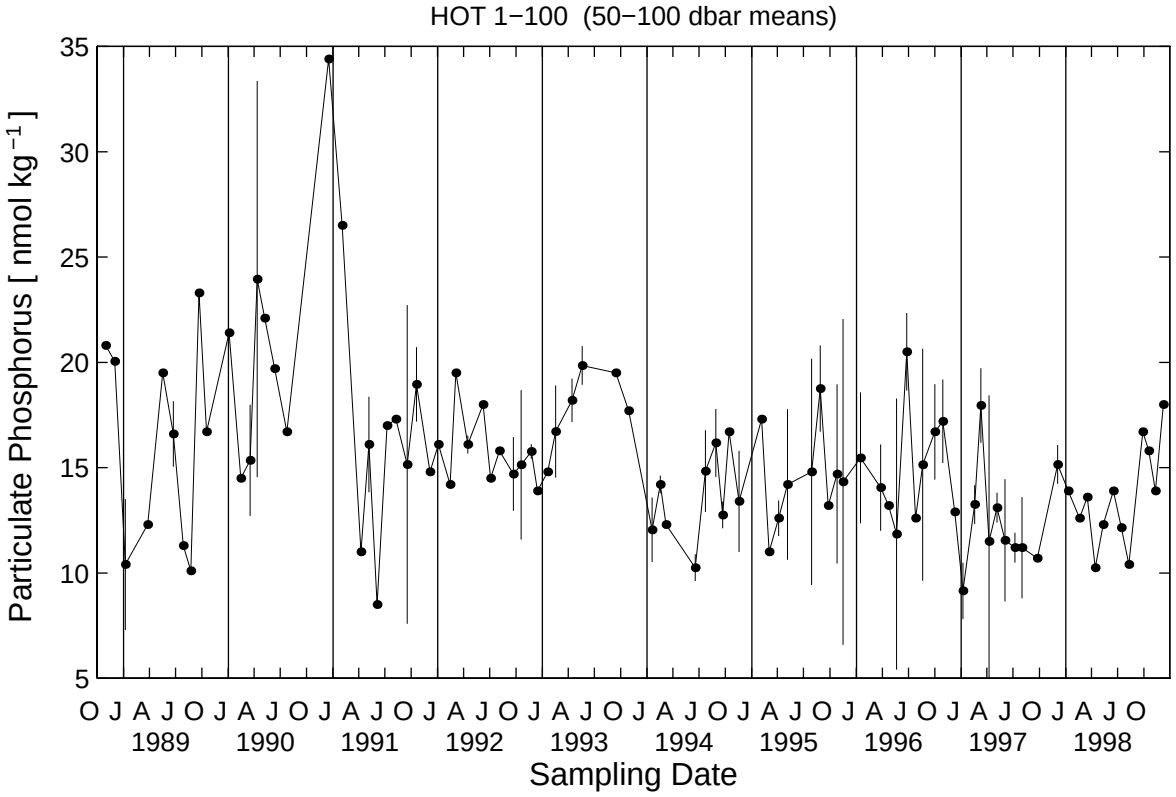
HOT 1−100 (50−100 dbar means)
Particulate Phosphorus [nmol kg⁻¹]
35
30
25
20
15
10
5
O J A J O J A J O J A J O J A J O J A J O J A J O J A J O J A J O J A J O J A J O
1989
1990
1991
1992
1993
1994
1995
1996
1997
1998
Sampling Date

Figure 6.5.9

6.6. Primary Production and Particle Flux

Figure 6.6.1: Integrated (0-200 m) primary production rates measured on all HOT cruises. Data for both in situ and on-deck incubations are presented. On HOT-15 (March 1990) primary production was measured on three consecutive days.

Figure 6.6.2: Carbon flux at 150 m measured on all HOT cruises from 1988 through 1994. Error bars represent the standard deviation of replicate determinations.

Figure 6.6.3: Same as 6.6.2 but for nitrogen.

Figure 6.6.4: Same as 6.6.2 but for phosphorus.

Figure 6.6.5: Same as 6.6.2 but for total mass

.

Figure 6.6.6: Contour plot of carbon flux for all cruises from 1988 through 1994.

Figure 6.6.7: Same as 6.6.6 but for nitrogen.

Figure 6.6.8: Same as 6.6.6 but for phosphorus.

Figure 6.6.9: Same as 6.6.6 but for total mass.

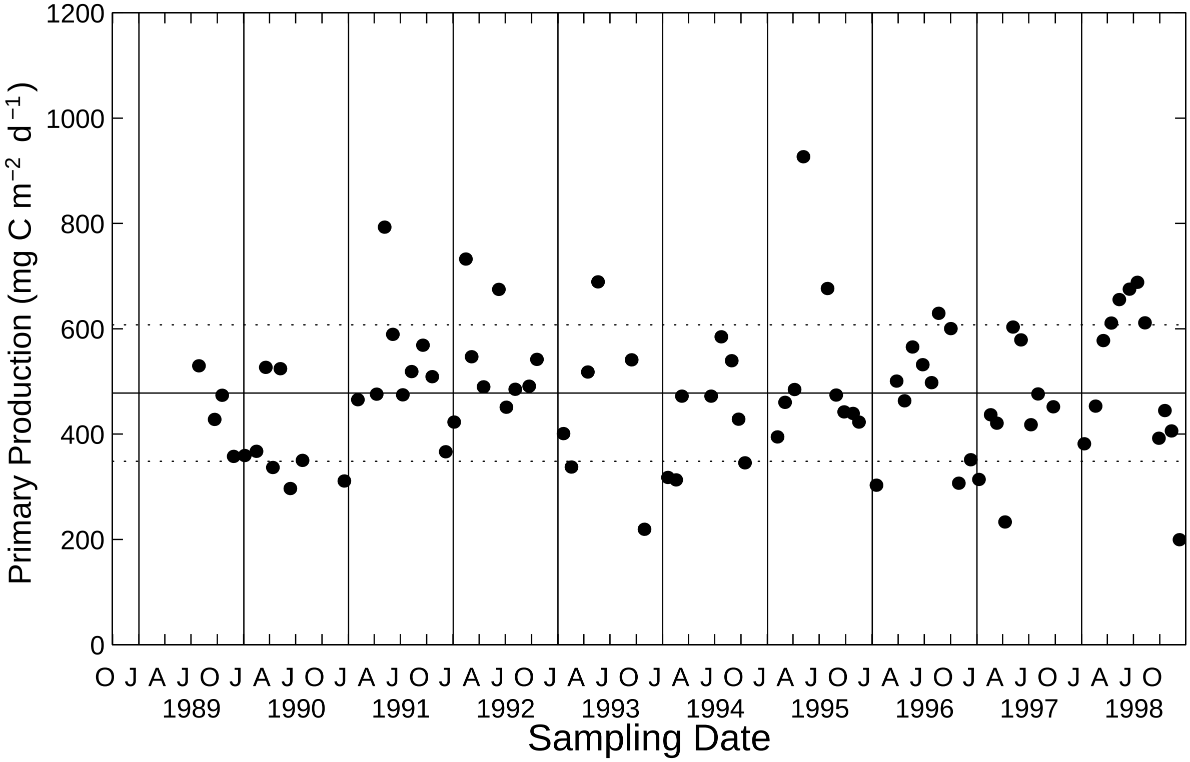
1200
1000
800
600
400
200
0
Primary Production (mg C m−2 d−1)
O J A J O J A J O J A J O J A J O J A J O J A J O J A J O J A J O J A J O J A J O
1989
1990
1991
1992
1993
1994
1995
1996
1997
1998
Sampling Date

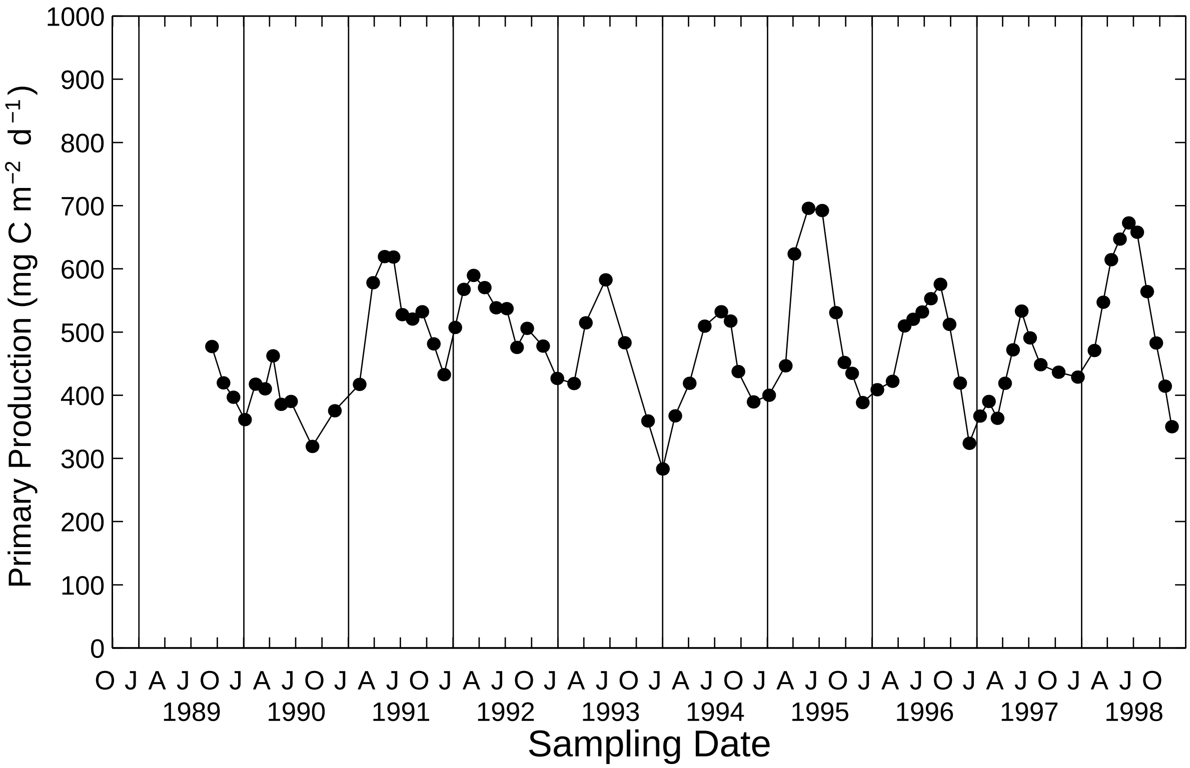
1000
900
800
700
600
500
400
300
200
100
0
Primary Production (mg C m−2 d−1)
O J A J O J A J O J A J O J A J O J A J O J A J O J A J O J A J O J A J O J A J O
1989
1990
1991
1992
1993
1994
1995
1996
1997
1998
Sampling Date

Figure 6.6.1

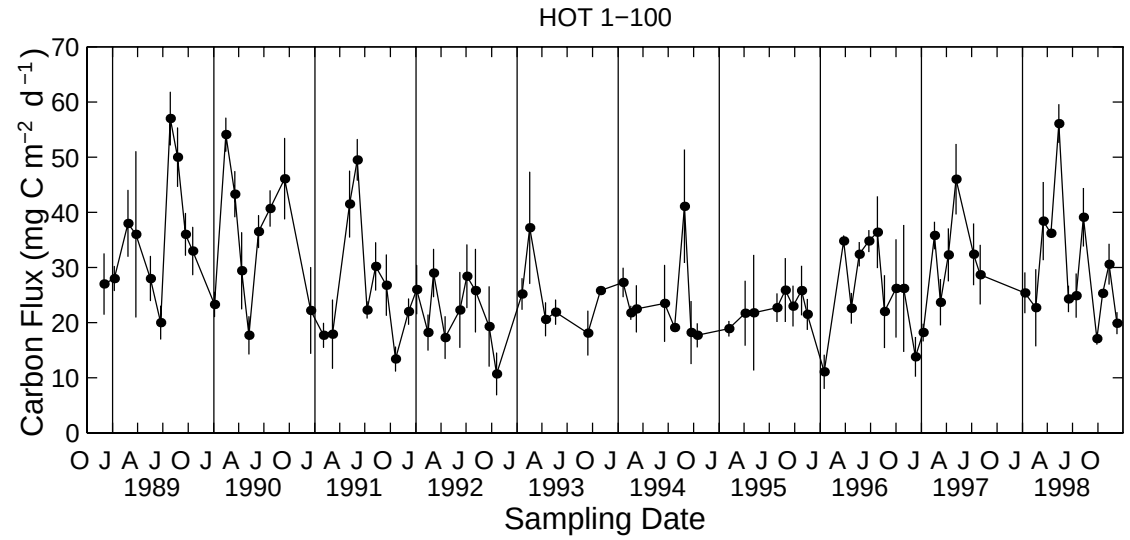

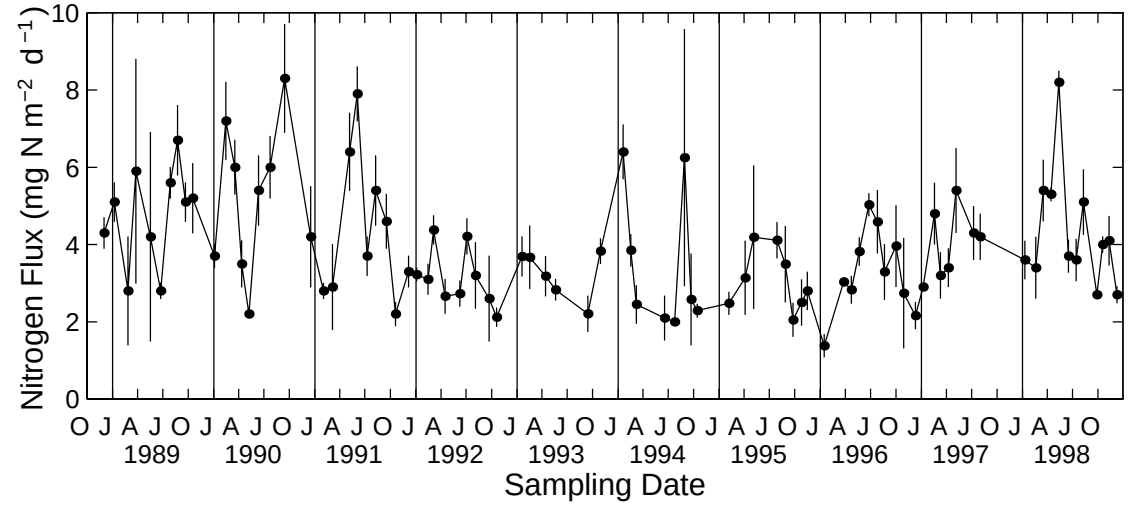

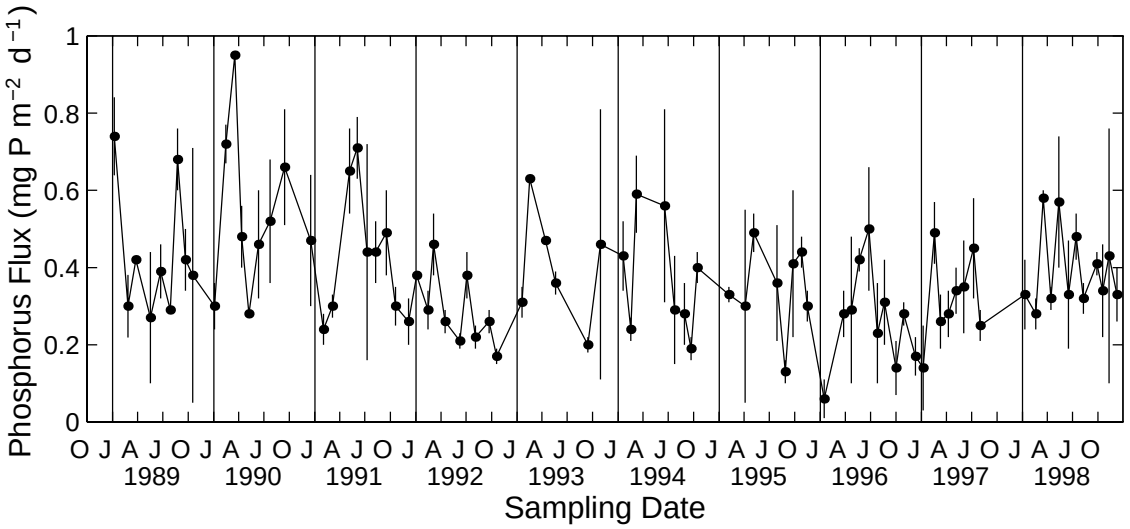

Figure 6.6.2, 6.6.3, 6.6.4

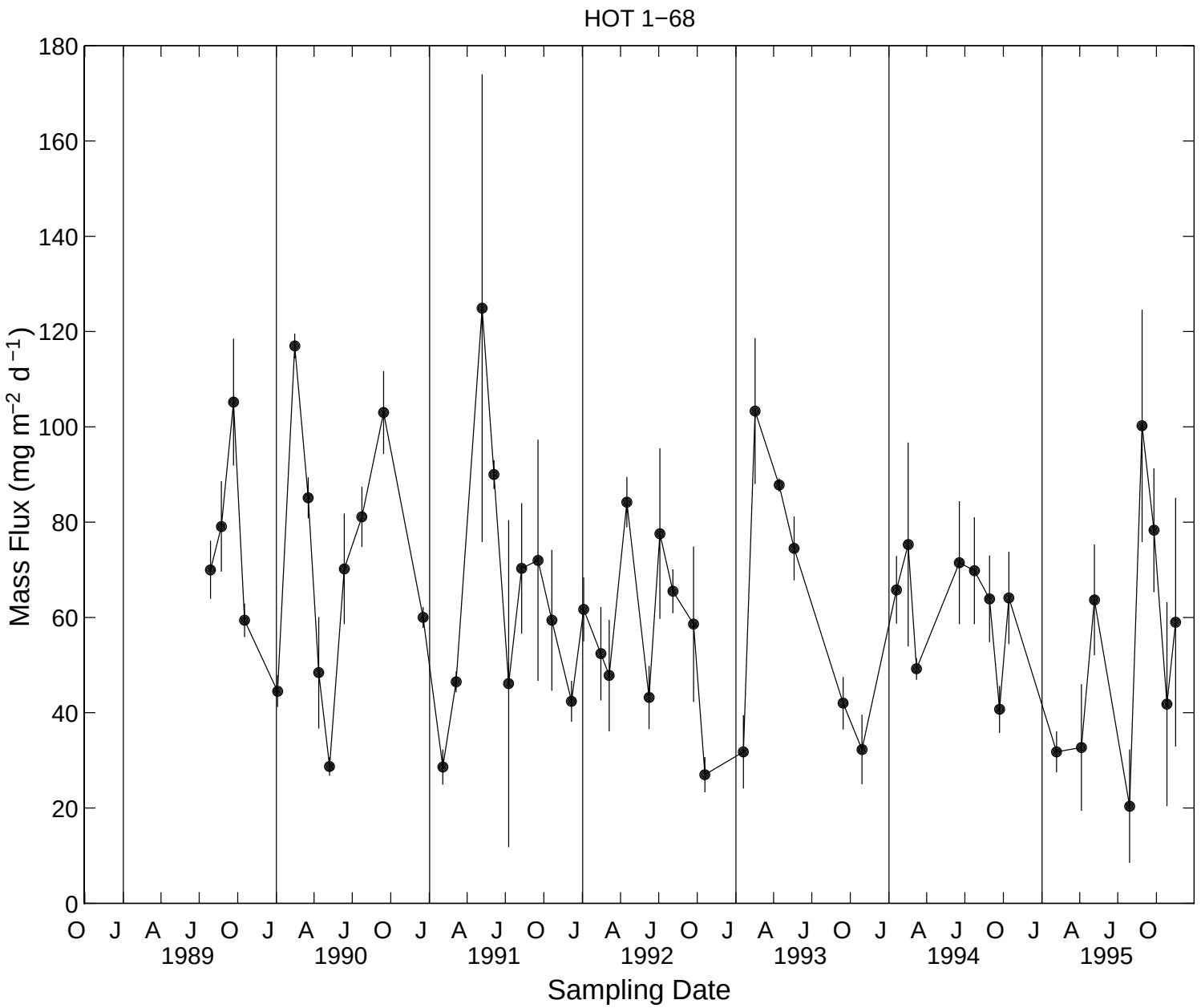
HOT 1−68
Mass Flux (mg m−2 d −1)
0
20
40
60
80
100
120
140
160
180
O J A J O J A J O J A J O J A J O J A J O J A J O J A J O J A J O
1989
1990
1991
1992
1993
1994
1995
Sampling Date

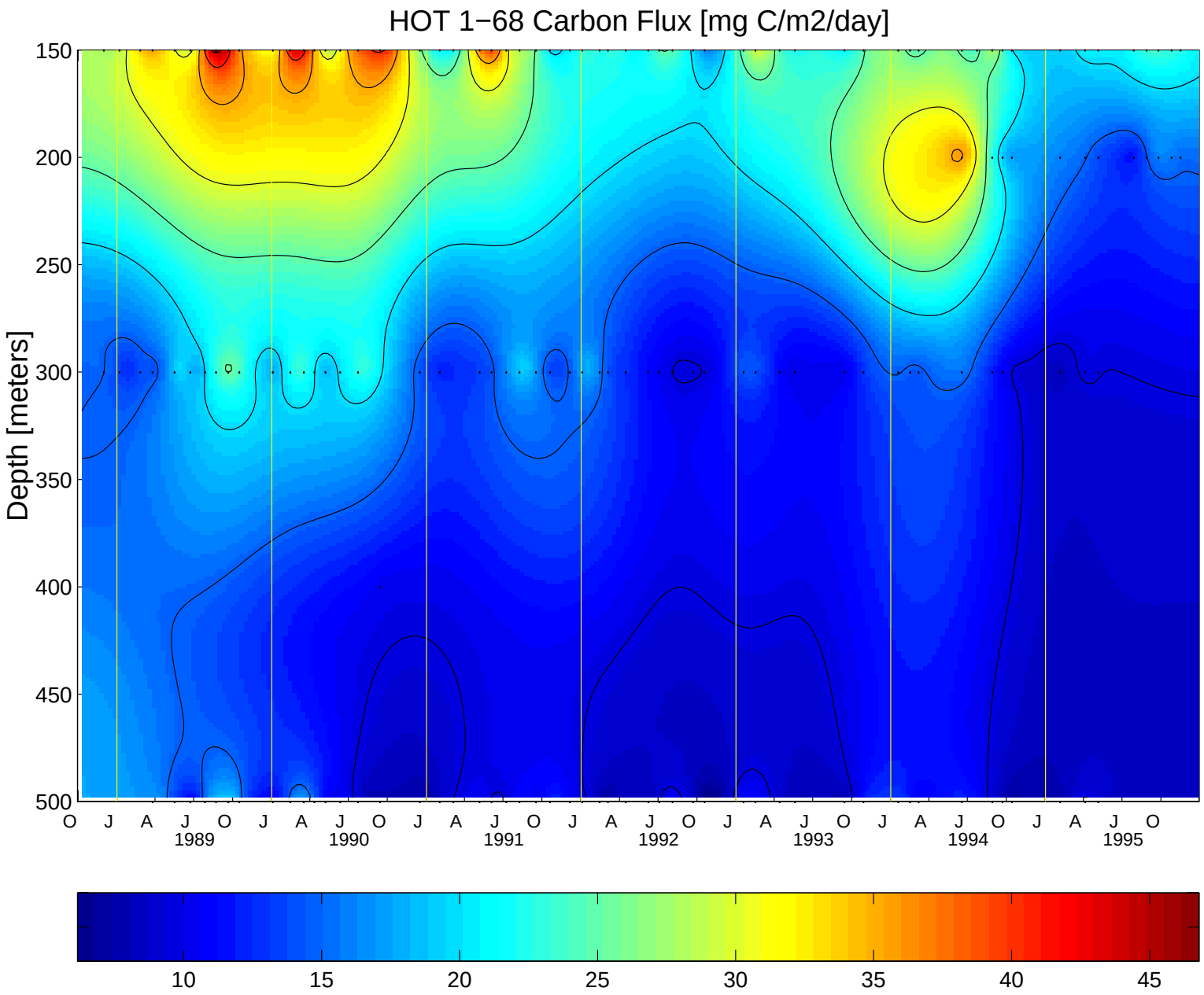
HOT 1−68 Carbon Flux [mg C/m2/day]
Depth [meters]
150
200
250
300
350
400
450
500
O J A J O J A J O J A J O J A J O J A J O J A J O J A J O J A J O
1989
1990
1991
1992
1993
1994
1995
10
15
20
25
30
35
40
45

Figure 6.6.6

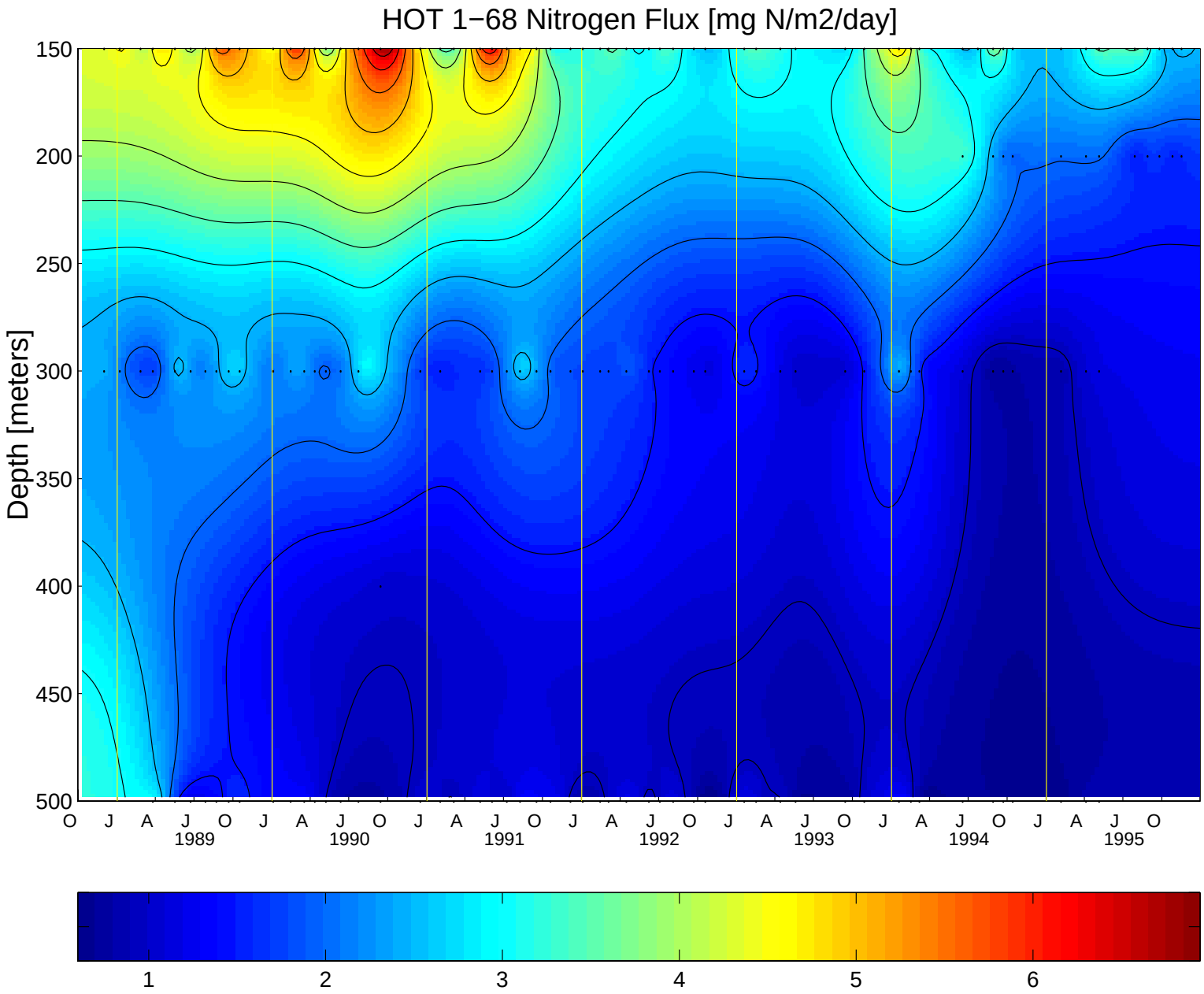
HOT 1−68 Nitrogen Flux [mg N/m2/day]
Depth [meters]
150
200
250
300
350
400
450
500
O J A J O J A J O J A J O J A J O J A J O J A J O J A J O J A J O
1989
1990
1991
1992
1993
1994
1995
1
2
3
4
5
6

Figure 6.6.7

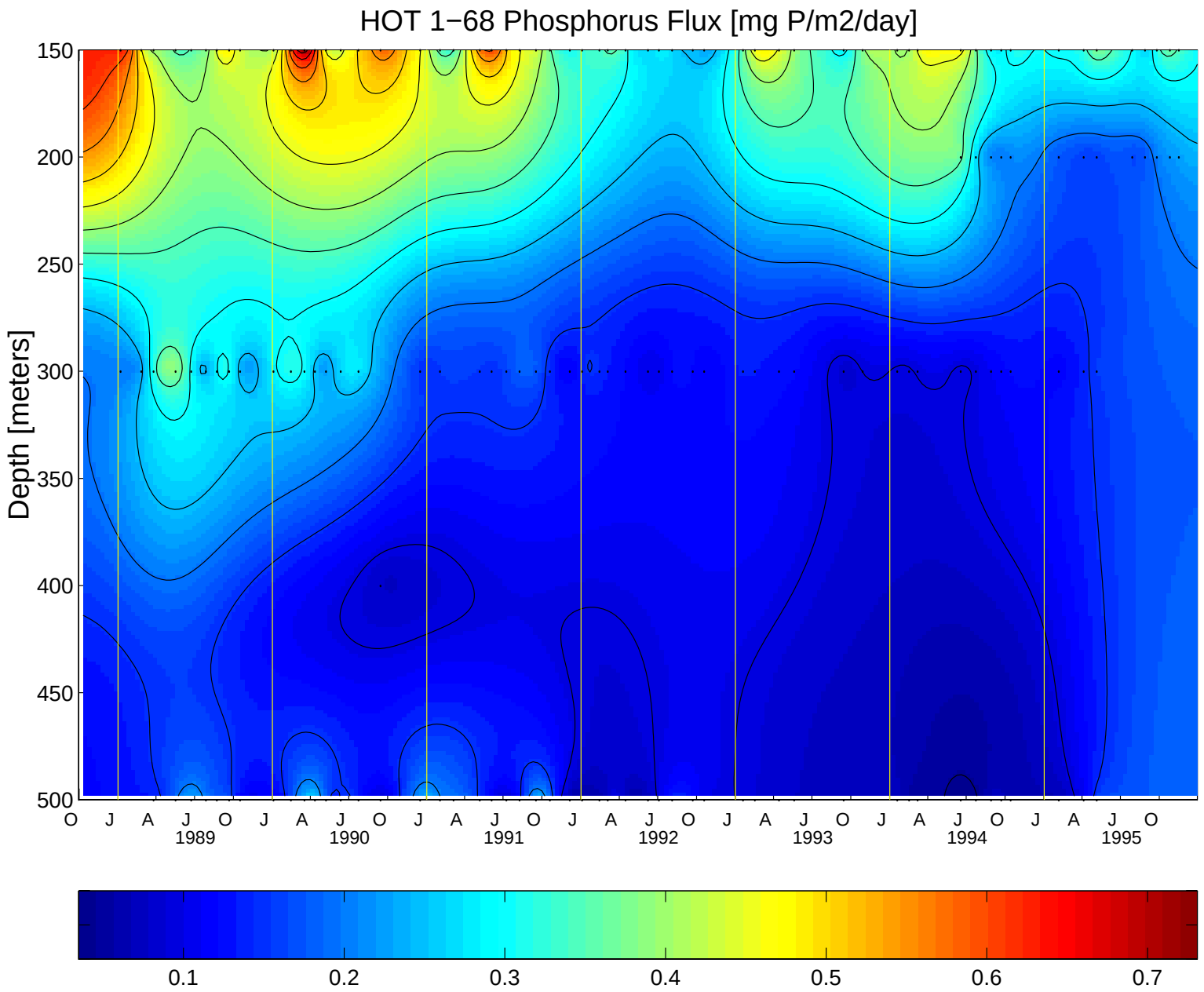
HOT 1−68 Phosphorus Flux [mg P/m2/day]
Depth [meters]
150
200
250
300
350
400
450
500
O J A J O J A J O J A J O J A J O J A J O J A J O J A J O J A J O
1989
1990
1991
1992
1993
1994
1995
0.1
0.2
0.3
0.4
0.5
0.6
0.7

Figure 6.6.8

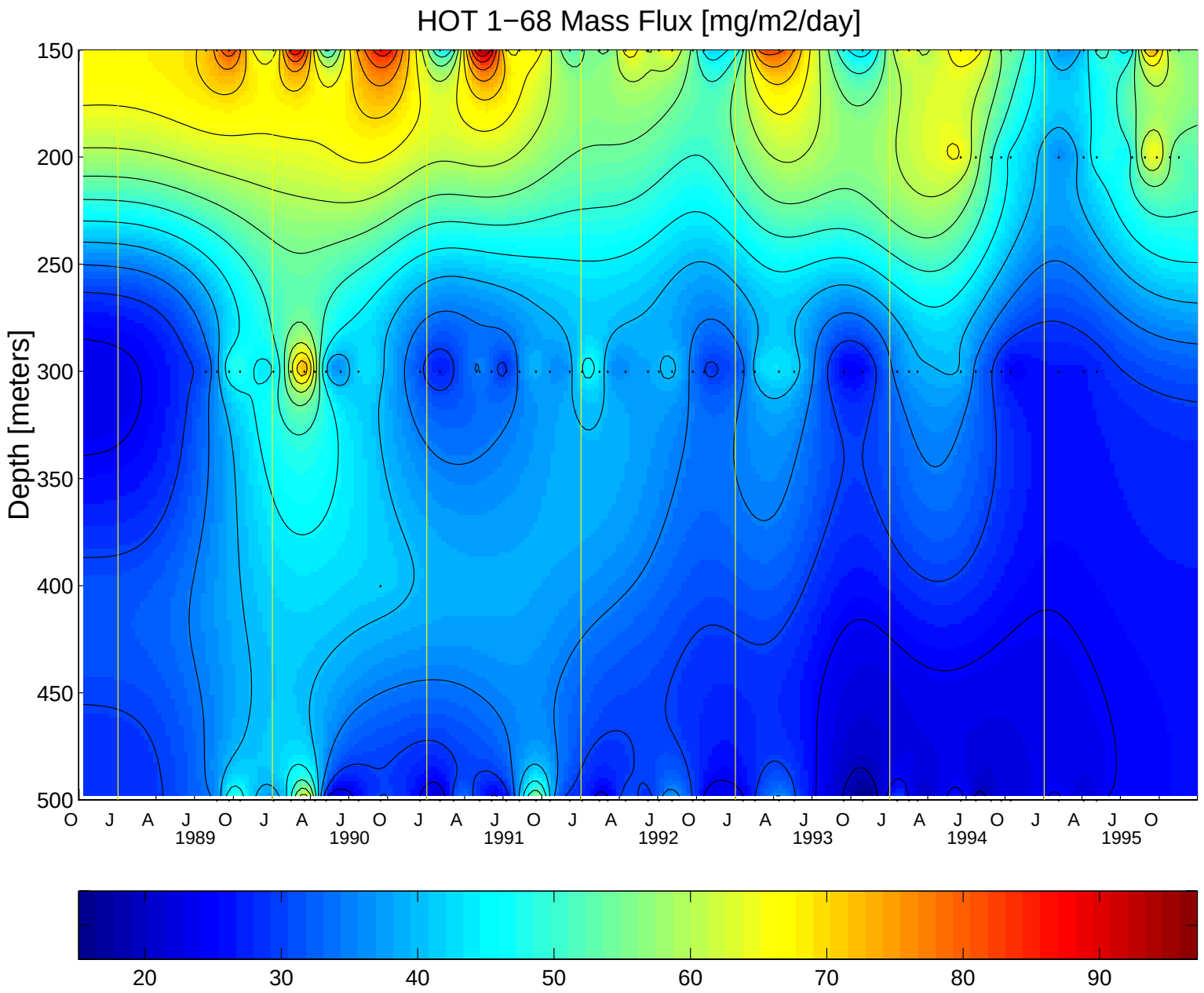
HOT 1−68 Mass Flux [mg/m2/day]
Depth [meters]
150
200
250
300
350
400
450
500
O J A J O J A J O J A J O J A J O J A J O J A J O J A J O J A J O
1989
1990
1991
1992
1993
1994
1995
20
30
40
50
60
70
80
90

Figure 6.6.9

6.7. ADCP Measurements

For each cruise with shipboard ADCP, the following figures are provided:

Figures 6.7.1a-j: Velocity fields at Station ALOHA. Top panel shows hourly averages at 20-m depth intervals while the ship was at Station ALOHA. The orientation of each stick gives the direction of the current: up is northward, to the right is eastward. The bottom panel shows the results of a least-squares fit of the hourly averages to a mean, trend, semidiurnal and diurnal tides and an inertial cycle. In the first column, the arrow shows the mean current, and the headless stick shows the sum of the mean plus the trend at the end of the station. For each harmonic, the current ellipse is shown in the first column. The orientation of the stick in the second column shows the direction of that harmonic component of the current at the beginning of the station, and the arrowhead at the end of the stick shows the direction of rotation of the current vector around the ellipse.

Figures 6.7.2a-j: Velocity field on the transits to and from the Station ALOHA. Velocity is shown as a function of latitude, averaged in 10-minute time intervals. Because HOT-58 was conducted in two segments, ADCP data are available for both legs on this cruise.

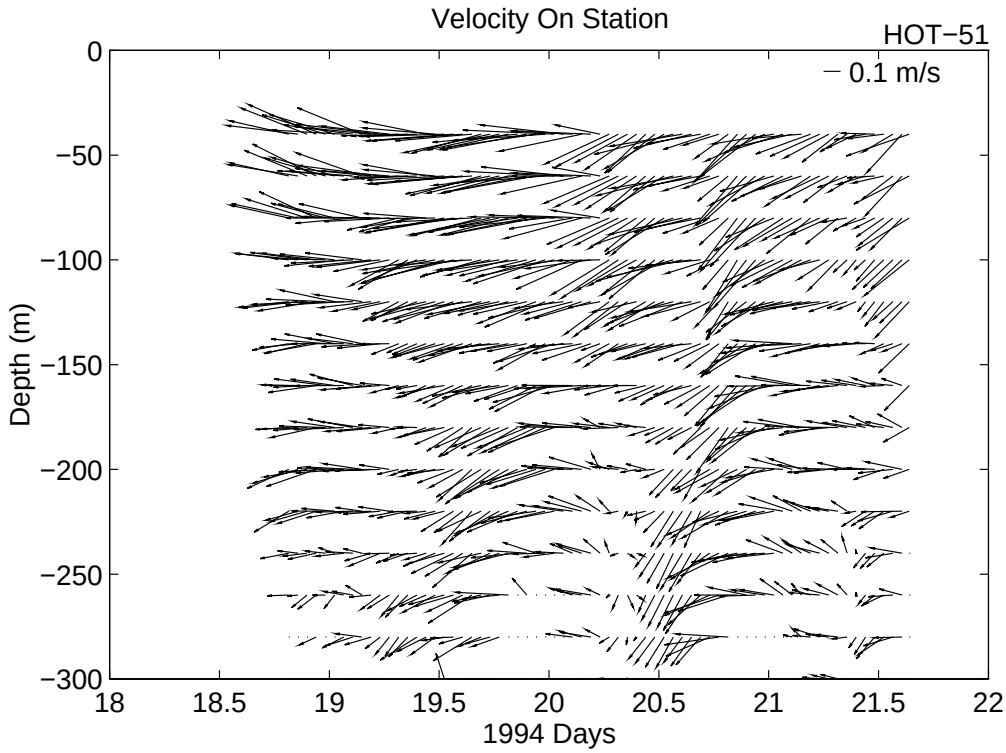
Velocity On Station
HOT−51
− 0.1 m/s
0
−50
−100
−150
−200
−250
−300
Depth (m)
18
18.5
19
19.5
20
20.5
21
21.5
22
1994 Days

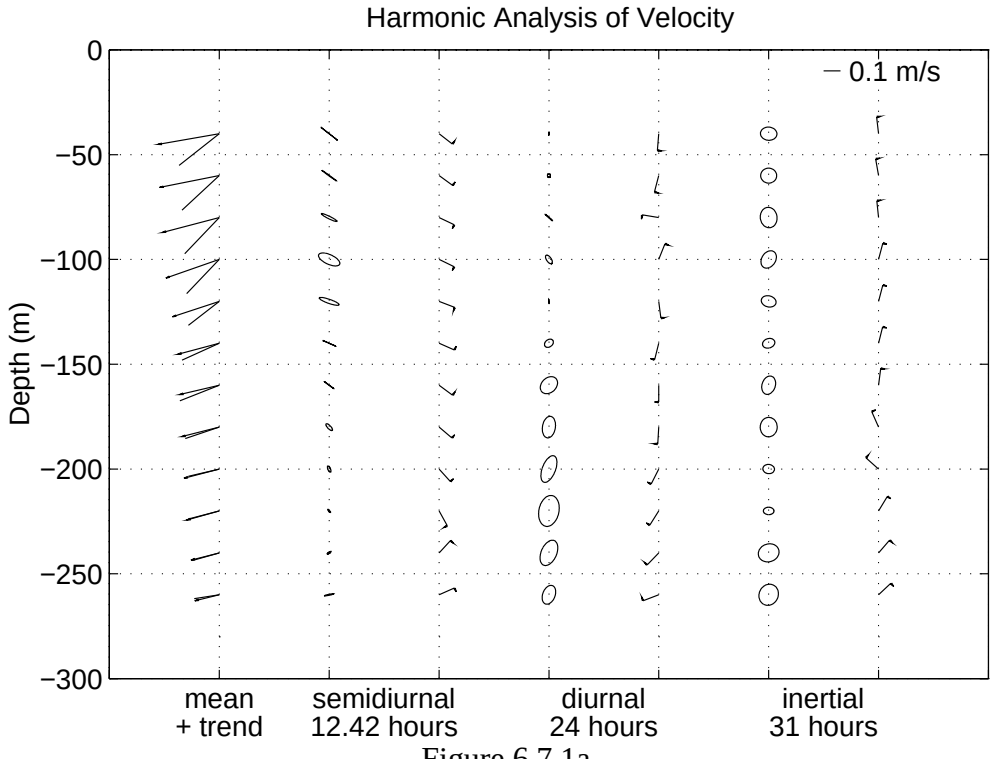
Harmonic Analysis of Velocity
− 0.1 m/s
0
−50
−100
−150
−200
−250
−300
Depth (m)
mean
+ trend
semidiurnal
12.42 hours
diurnal
24 hours
inertial
31 hours

Figure 6.7.1a

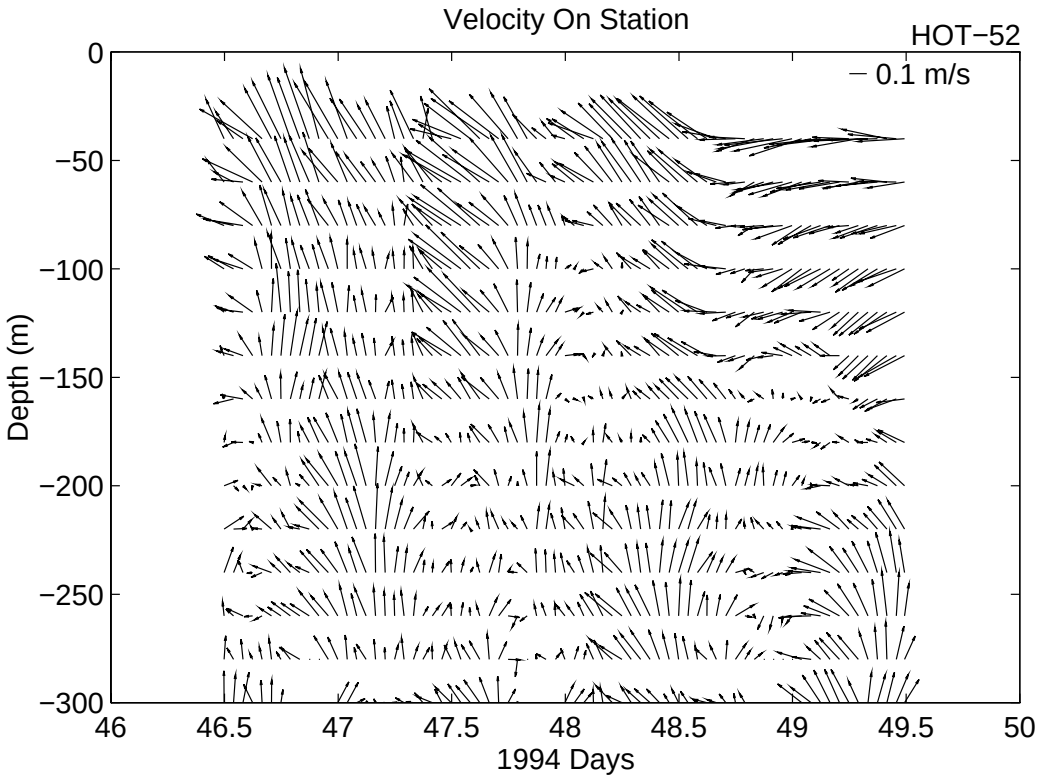
Velocity On Station
HOT−52
− 0.1 m/s
Depth (m)
0
−50
−100
−150
−200
−250
−300
46
46.5
47
47.5
48
48.5
49
49.5
50
1994 Days

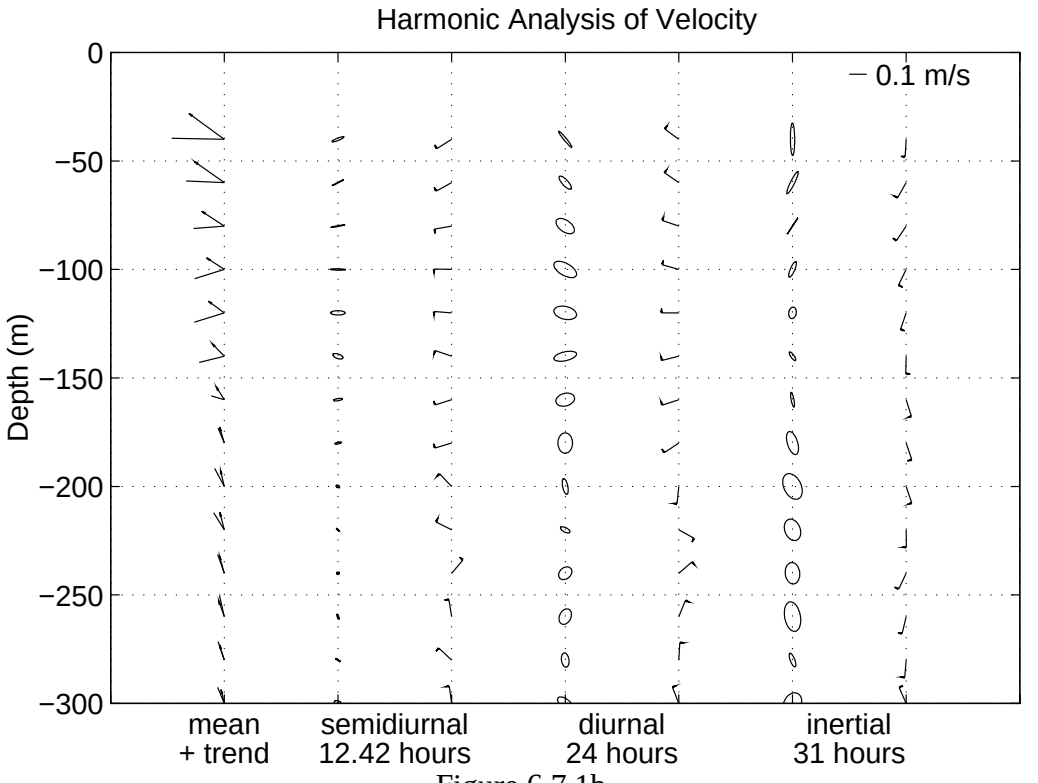
Harmonic Analysis of Velocity
− 0.1 m/s
Depth (m)
0
−50
−100
−150
−200
−250
−300
mean
+ trend
semidiurnal
12.42 hours
diurnal
24 hours
inertial
31 hours

Figure 6.7.1b

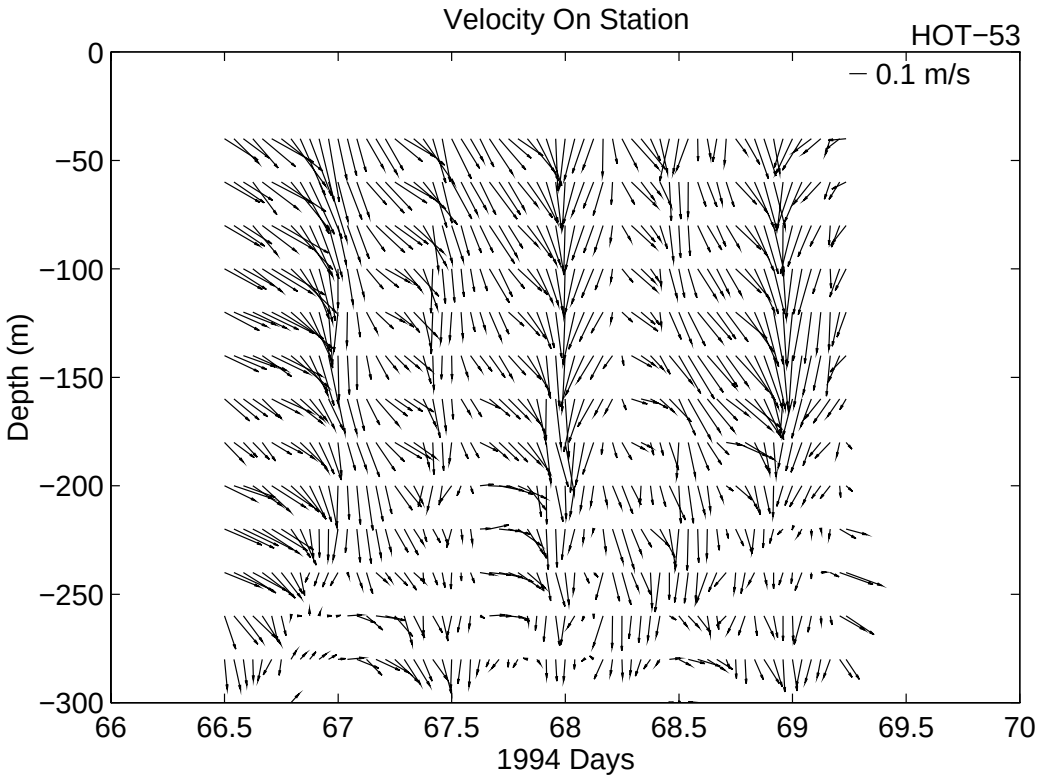
Velocity On Station
HOT−53
− 0.1 m/s
Depth (m)
0
−50
−100
−150
−200
−250
−300
66
66.5
67
67.5
68
68.5
69
69.5
70
1994 Days

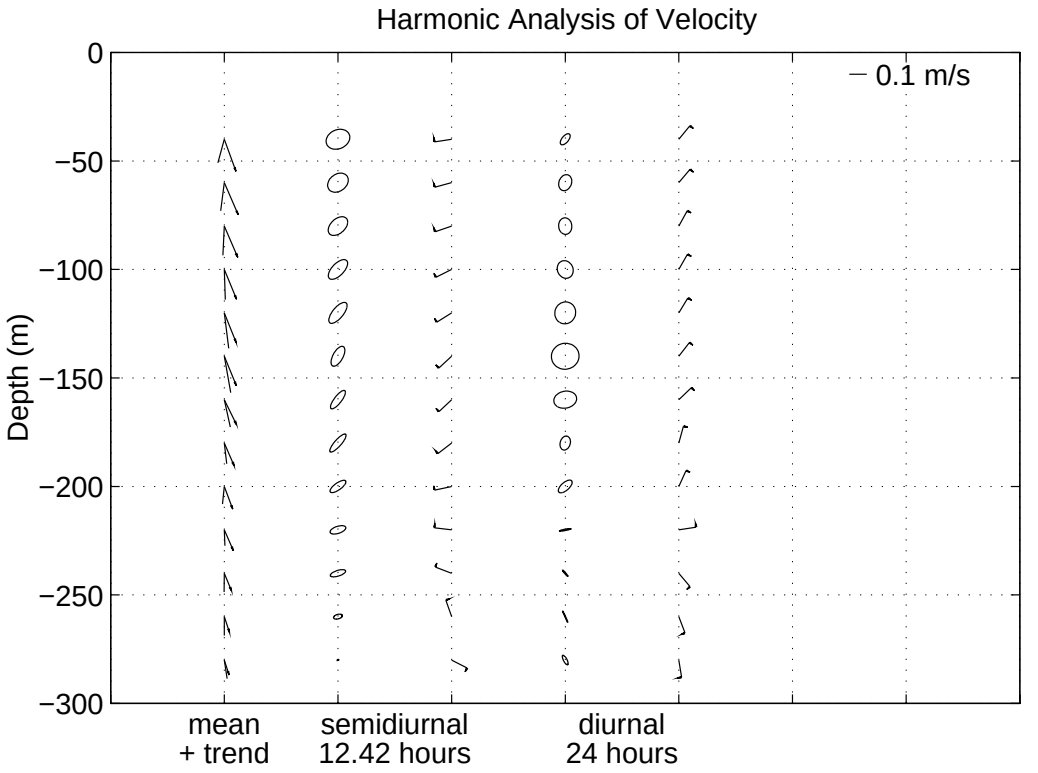
Harmonic Analysis of Velocity
− 0.1 m/s
Depth (m)
0
−50
−100
−150
−200
−250
−300
mean
+ trend
semidiurnal
12.42 hours
diurnal
24 hours

Figure 6.7.1c

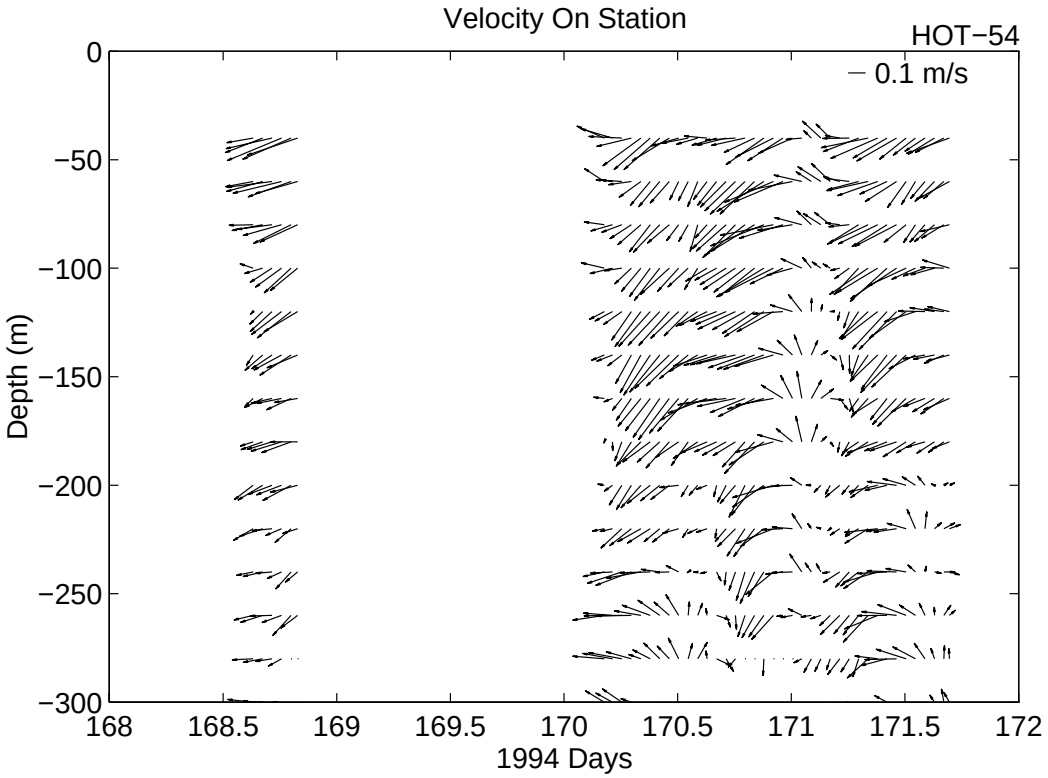
Velocity On Station
HOT−54
− 0.1 m/s
0
−50
−100
−150
−200
−250
−300
Depth (m)
168
168.5
169
169.5
170
170.5
171
171.5
172
1994 Days

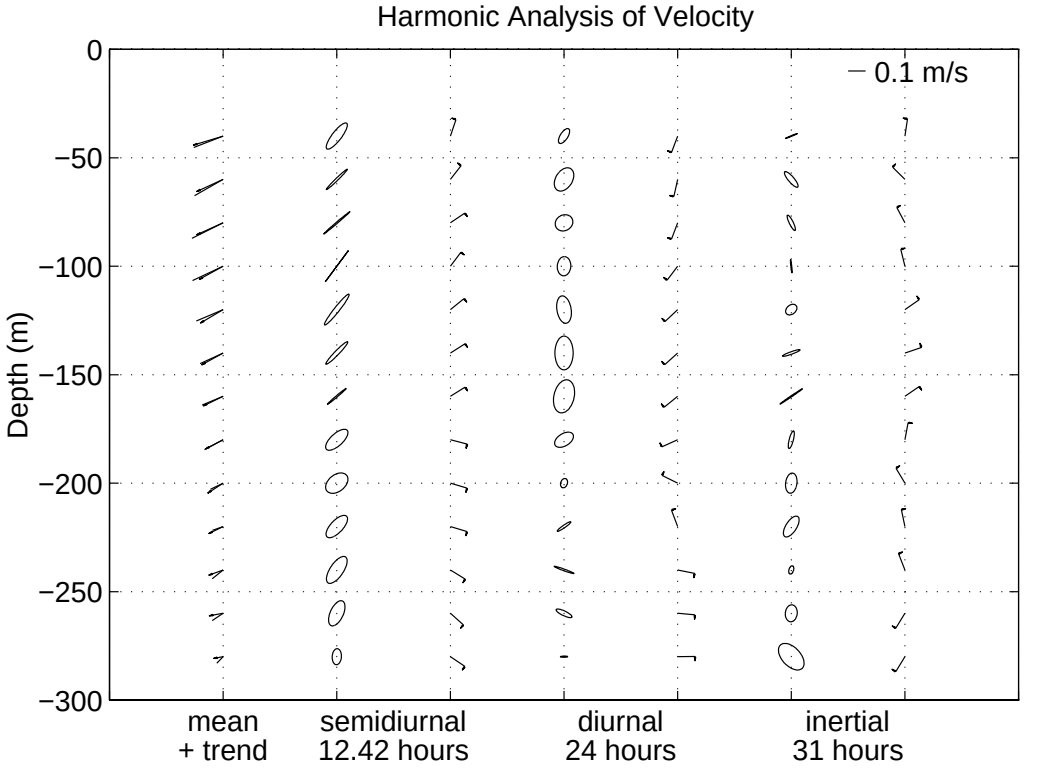
Harmonic Analysis of Velocity
− 0.1 m/s
0
−50
−100
−150
−200
−250
−300
Depth (m)
mean
+ trend
semidiurnal
12.42 hours
diurnal
24 hours
inertial
31 hours

Figure 6.7.1d

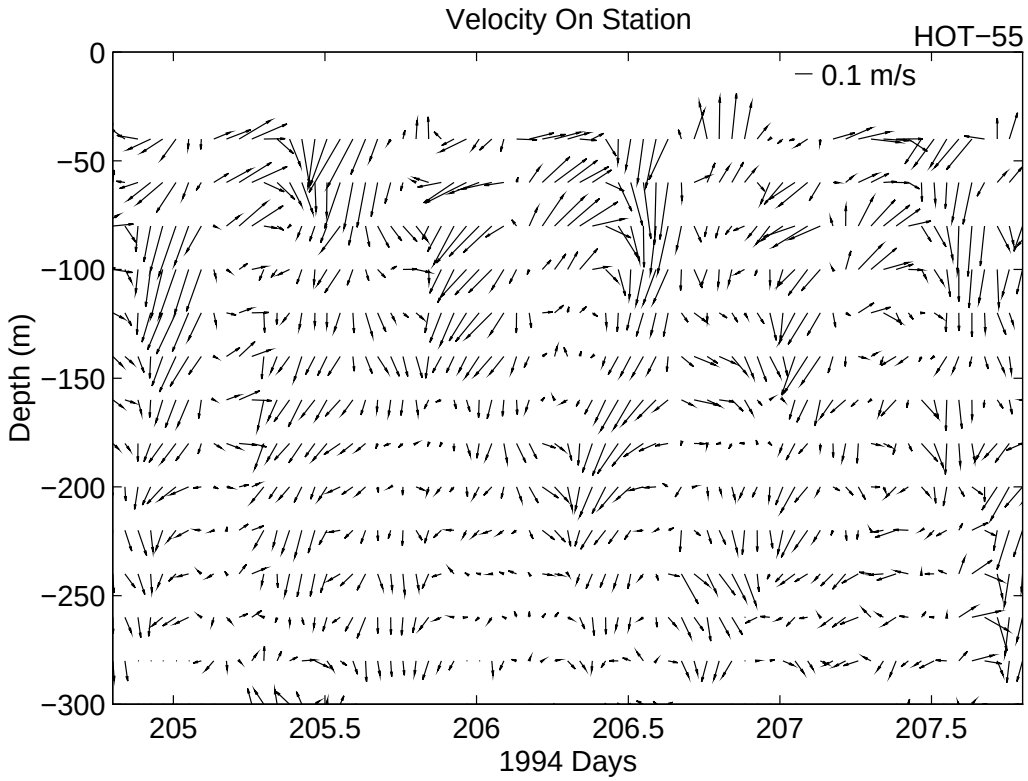
Velocity On Station
HOT−55
0.1 m/s
0
−50
−100
−150
−200
−250
−300
Depth (m)
205
205.5
206
206.5
207
207.5
1994 Days

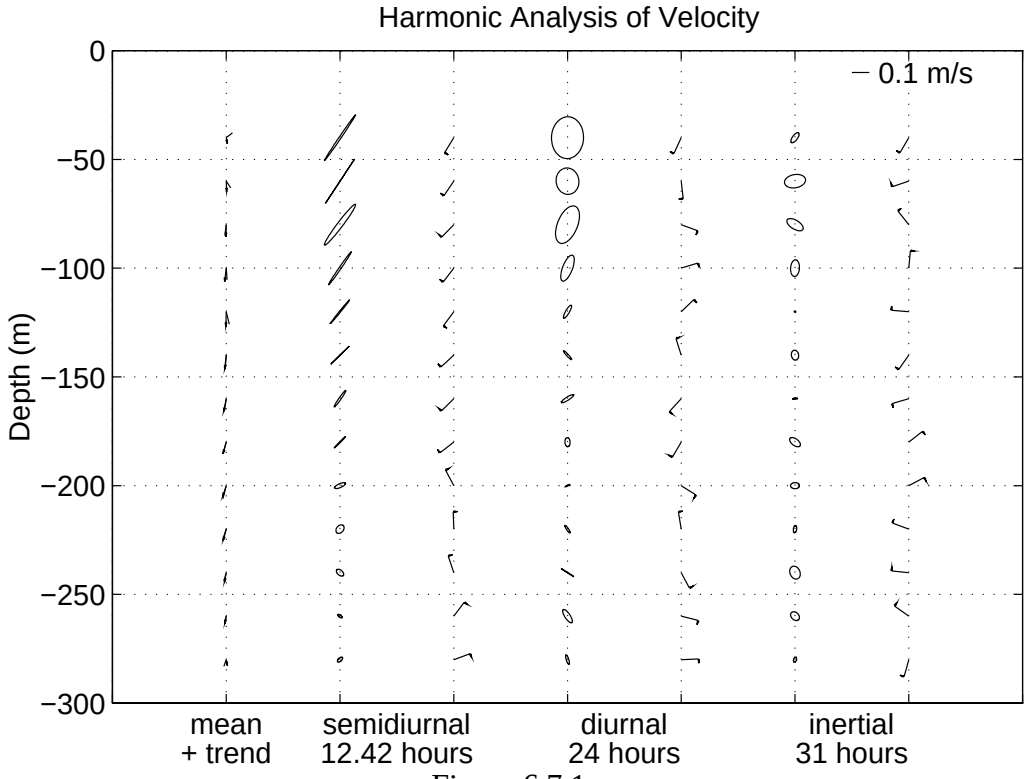
Harmonic Analysis of Velocity
0.1 m/s
0
−50
−100
−150
−200
−250
−300
Depth (m)
mean
+ trend
semidiurnal
12.42 hours
diurnal
24 hours
inertial
31 hours

Figure 6.7.1e

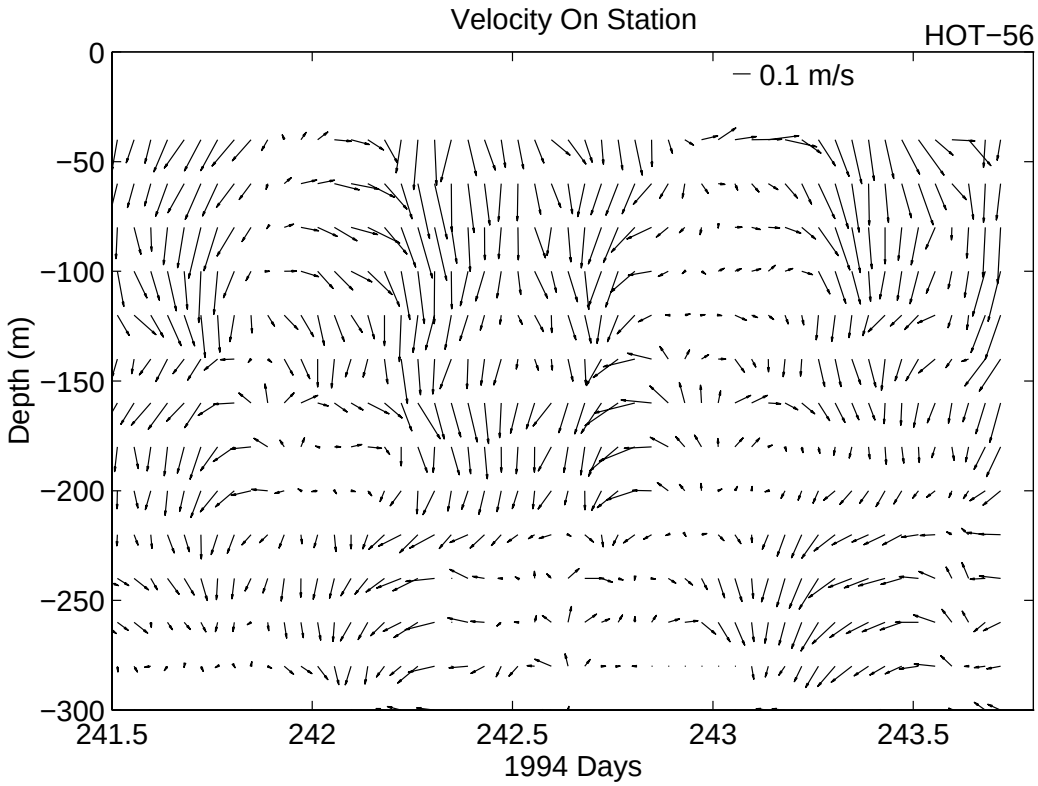
Velocity On Station
HOT−56
0.1 m/s
0
−50
−100
−150
−200
−250
−300
Depth (m)
241.5
242
242.5
243
243.5
1994 Days

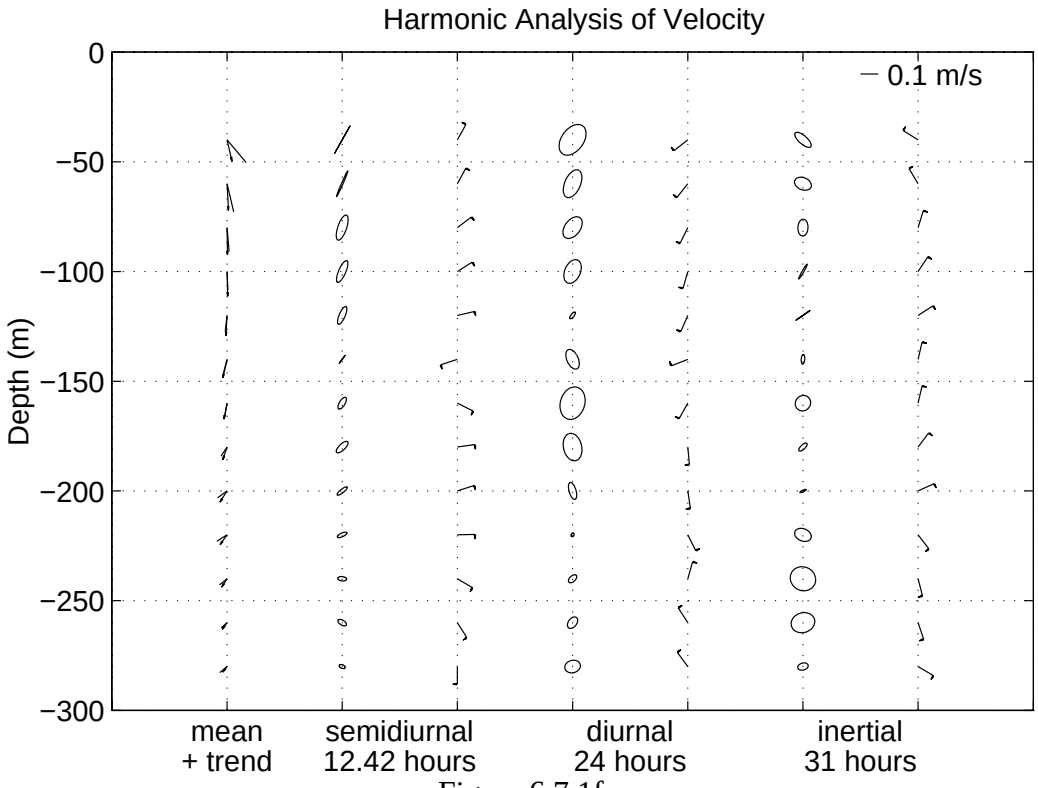
Harmonic Analysis of Velocity
0.1 m/s
0
−50
−100
−150
−200
−250
−300
Depth (m)
mean
+ trend
semidiurnal
12.42 hours
diurnal
24 hours
inertial
31 hours

Figure 6.7.1f

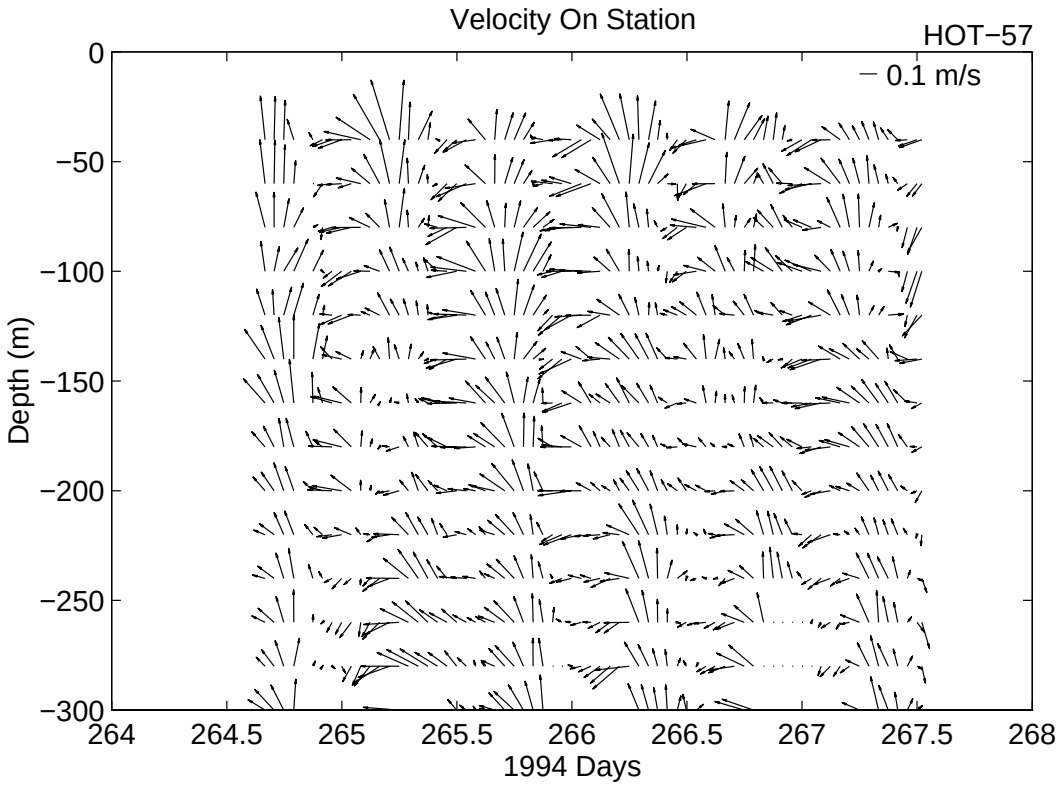
Velocity On Station
HOT−57
0.1 m/s
0
−50
−100
−150
−200
−250
−300
Depth (m)
264
264.5
265
265.5
266
266.5
267
267.5
268
1994 Days

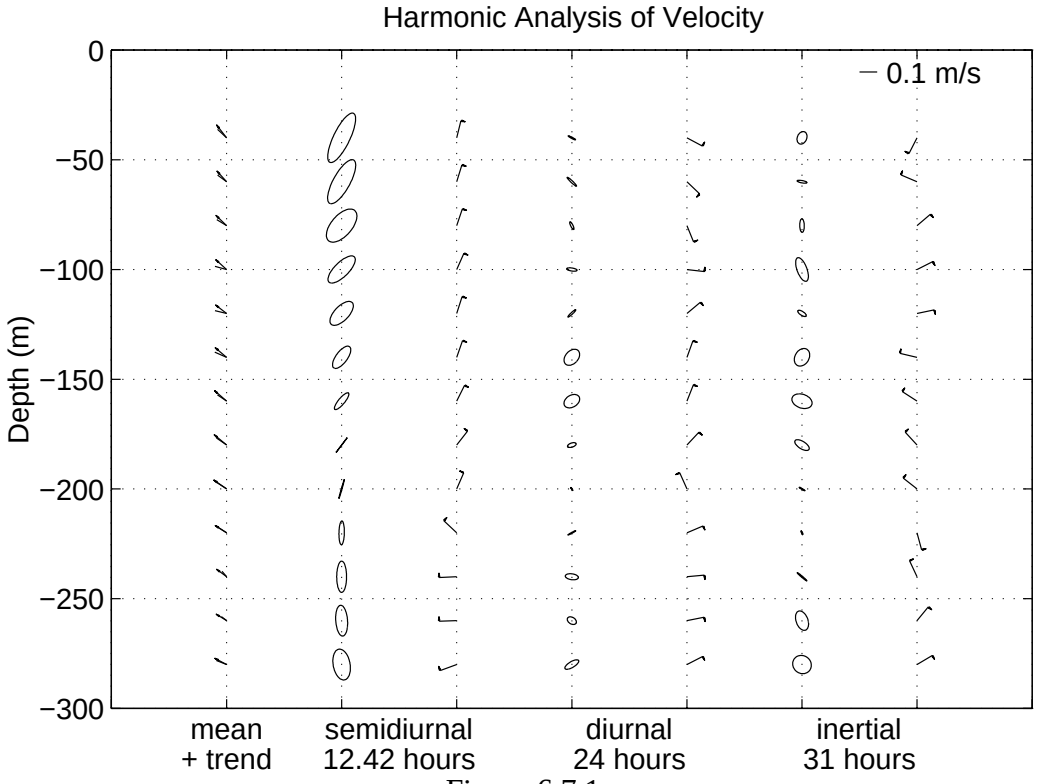
Harmonic Analysis of Velocity
0.1 m/s
0
−50
−100
−150
−200
−250
−300
Depth (m)
mean
+ trend
semidiurnal
12.42 hours
diurnal
24 hours
inertial
31 hours

Figure 6.7.1g

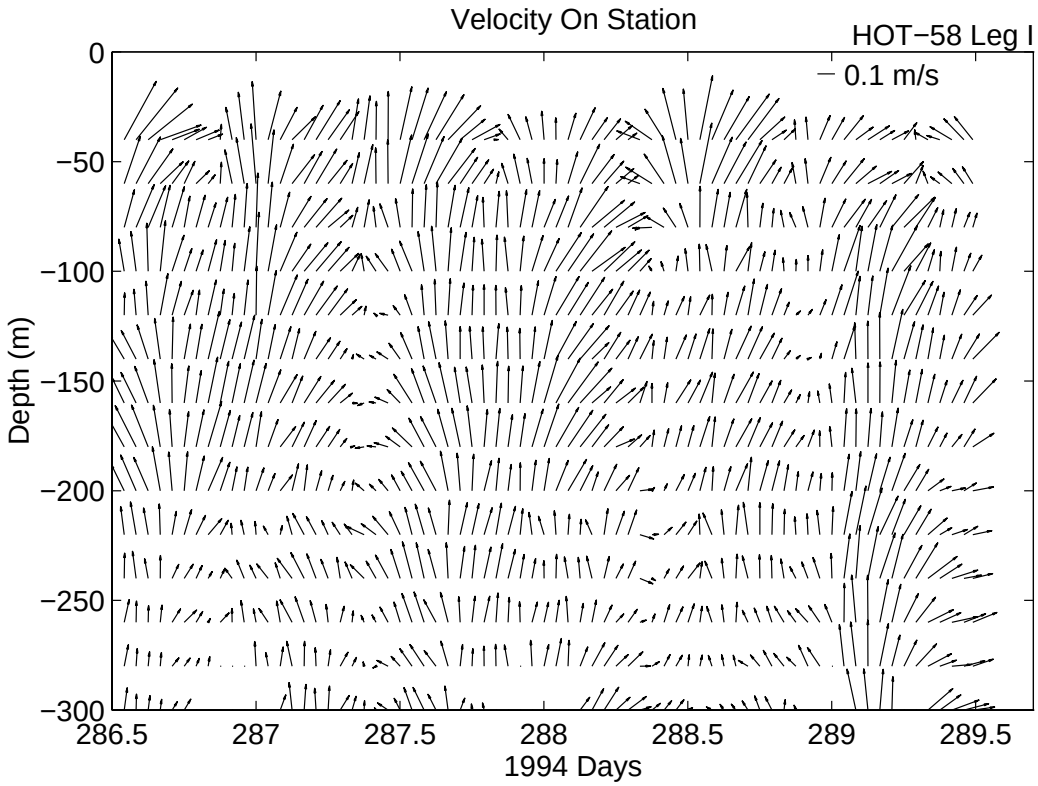
Velocity On Station
HOT−58 Leg I
0.1 m/s
Depth (m)
0
−50
−100
−150
−200
−250
−300
286.5
287
287.5
288
288.5
289
289.5
1994 Days

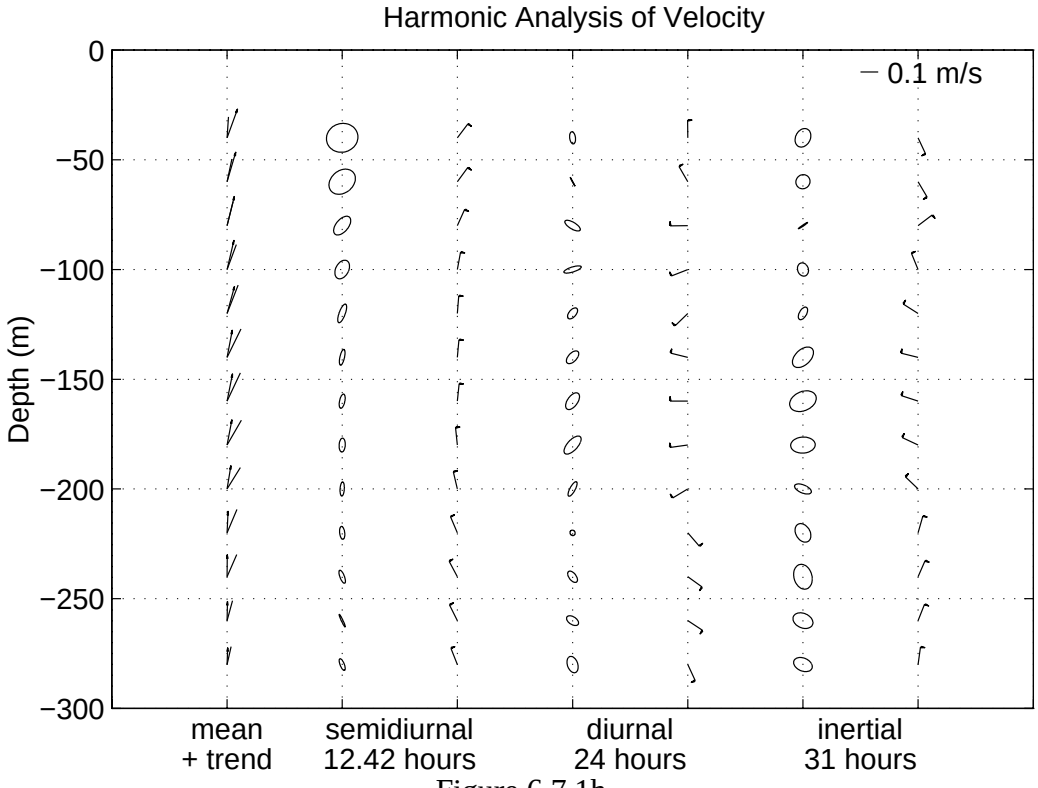
Harmonic Analysis of Velocity
0.1 m/s
Depth (m)
0
−50
−100
−150
−200
−250
−300
mean
+ trend
semidiurnal
12.42 hours
diurnal
24 hours
inertial
31 hours

Figure 6.7.1h

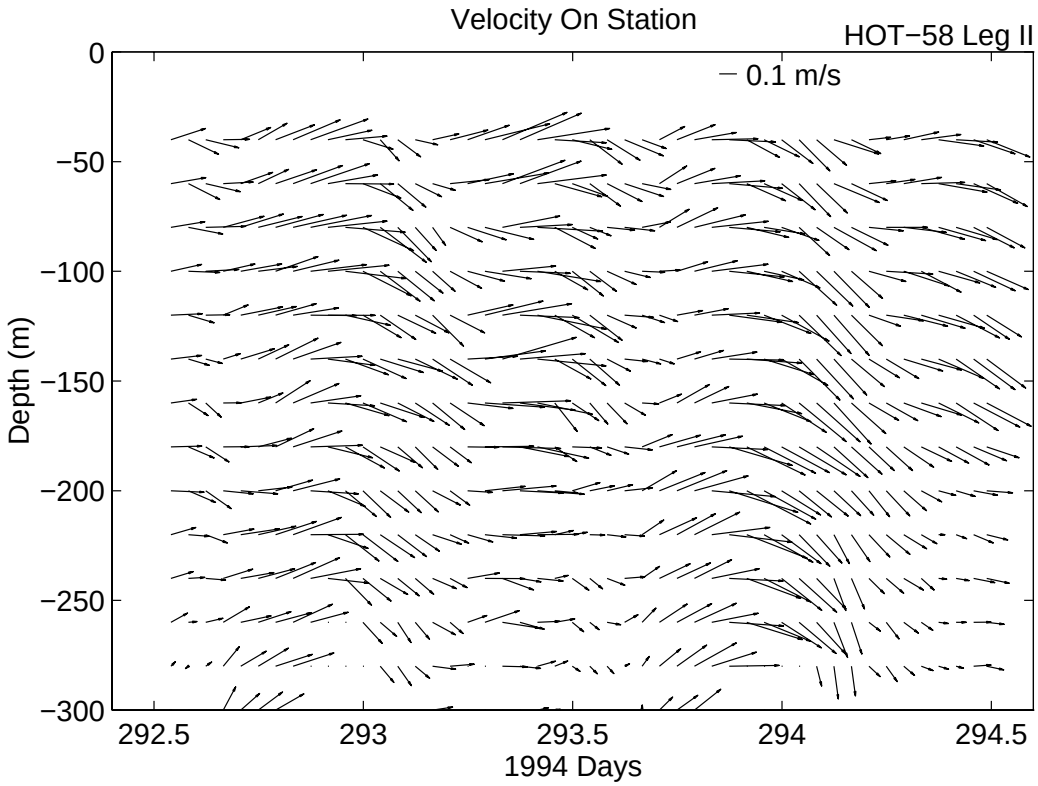
Velocity On Station
HOT−58 Leg II
0.1 m/s
0
−50
−100
−150
−200
−250
−300
Depth (m)
292.5
293
293.5
294
294.5
1994 Days

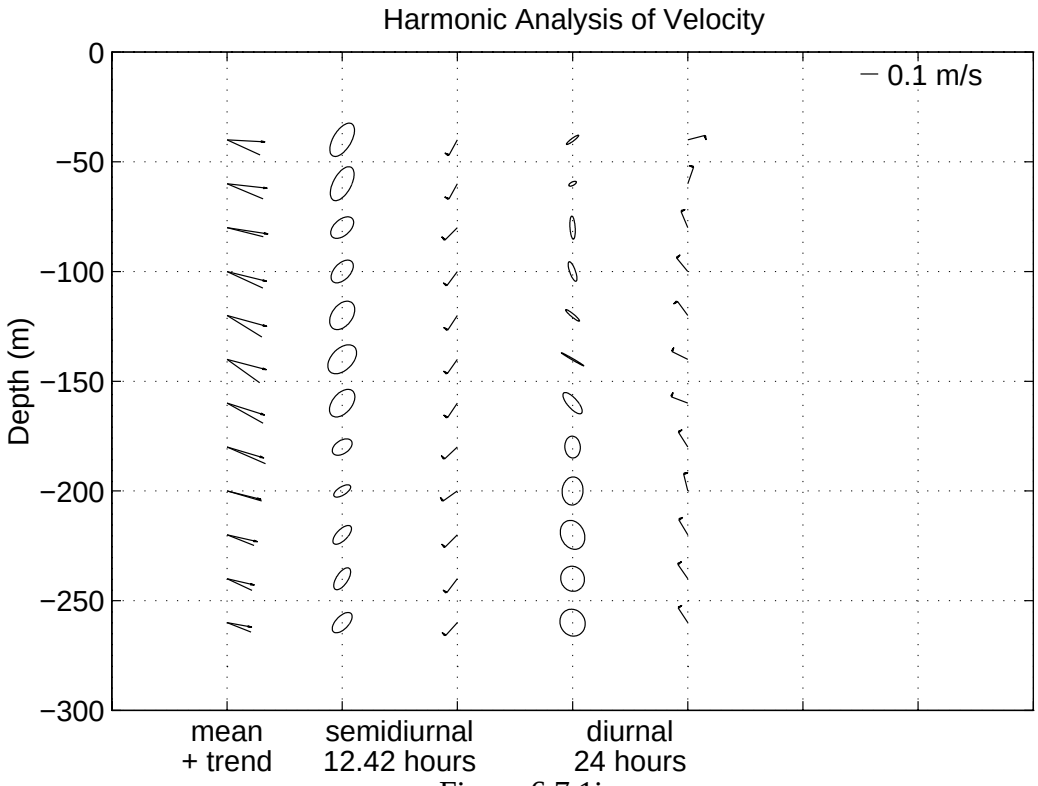
Harmonic Analysis of Velocity
0.1 m/s
0
−50
−100
−150
−200
−250
−300
Depth (m)
mean
+ trend
semidiurnal
12.42 hours
diurnal
24 hours

Figure 6.7.1i

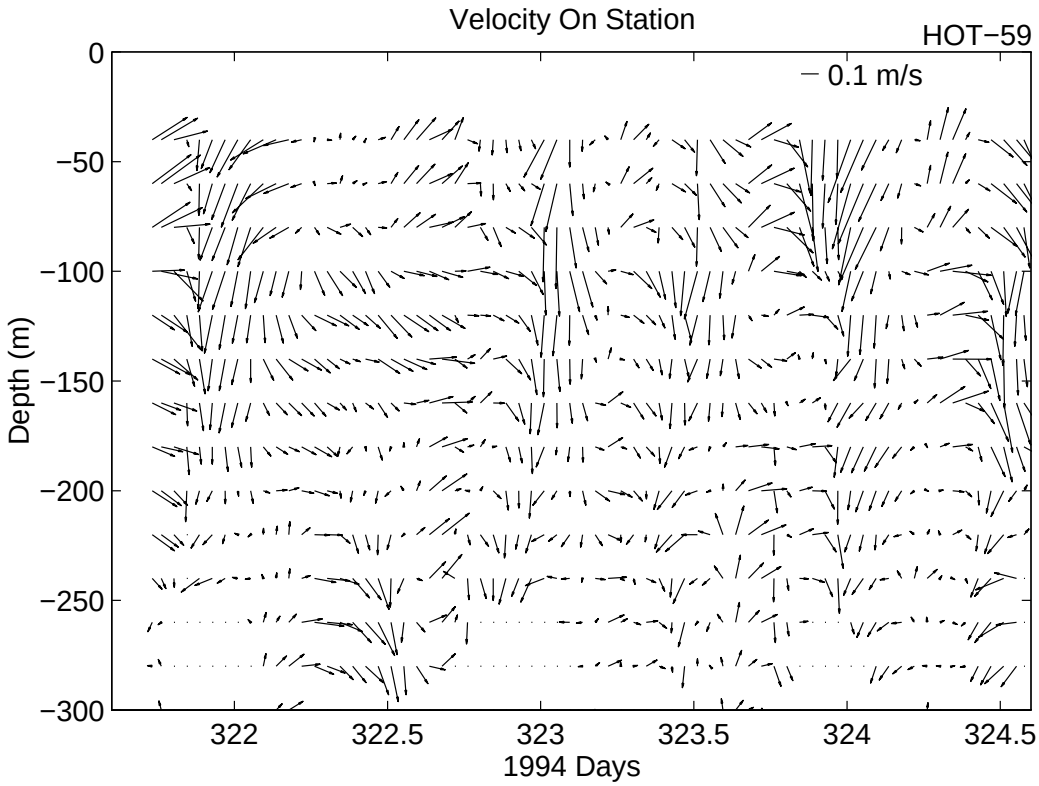
Velocity On Station
HOT−59
0.1 m/s
0
−50
−100
−150
−200
−250
−300
Depth (m)
322
322.5
323
323.5
324
324.5
1994 Days

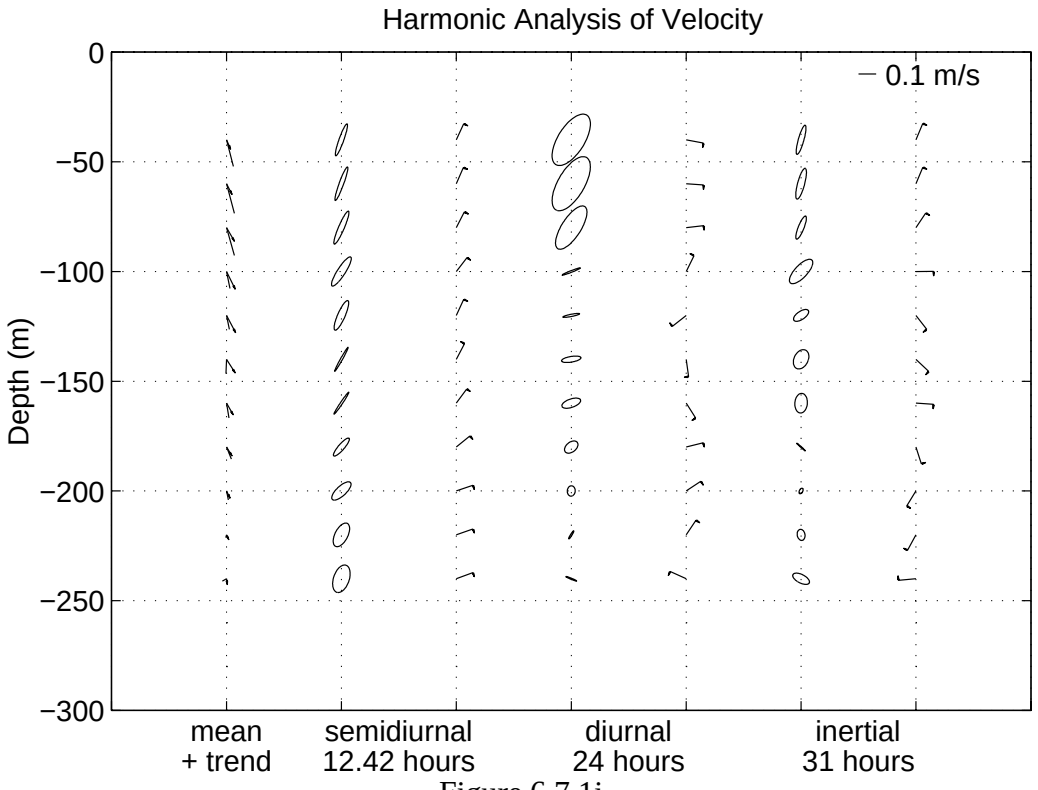
Harmonic Analysis of Velocity
0.1 m/s
0
−50
−100
−150
−200
−250
−300
Depth (m)
mean
+ trend
semidiurnal
12.42 hours
diurnal
24 hours
inertial
31 hours

Figure 6.7.1j

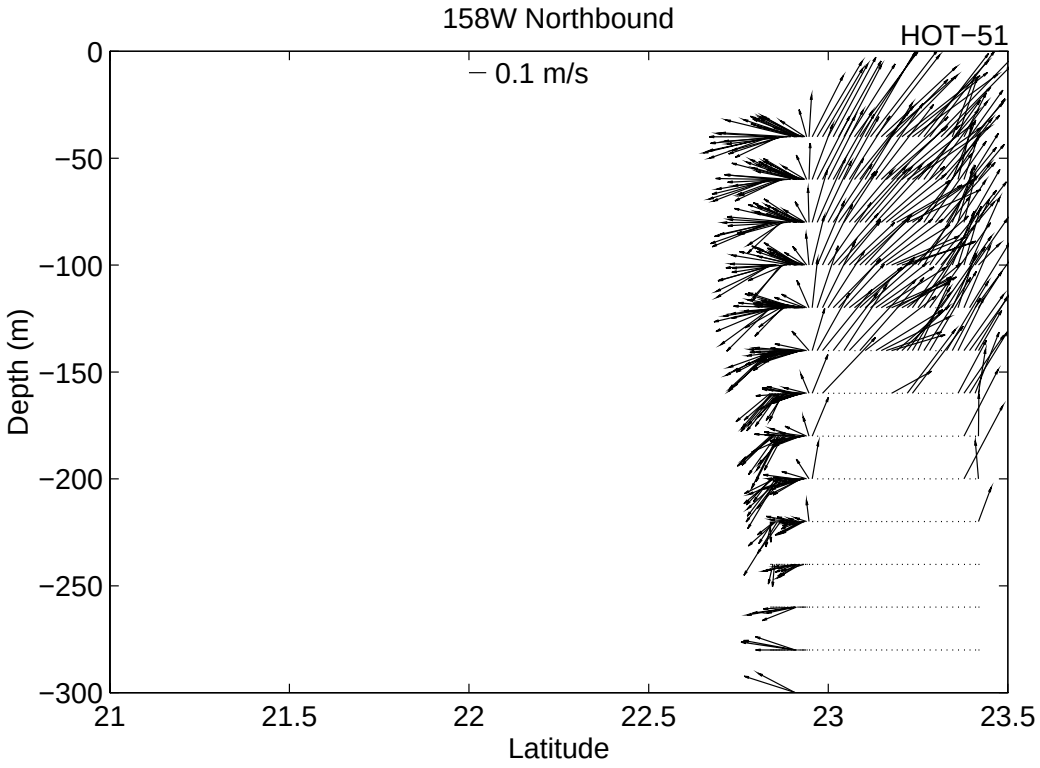
158W Northbound
HOT−51
0.1 m/s
0
−50
−100
−150
−200
−250
−300
Depth (m)
21
21.5
22
22.5
23
23.5
Latitude

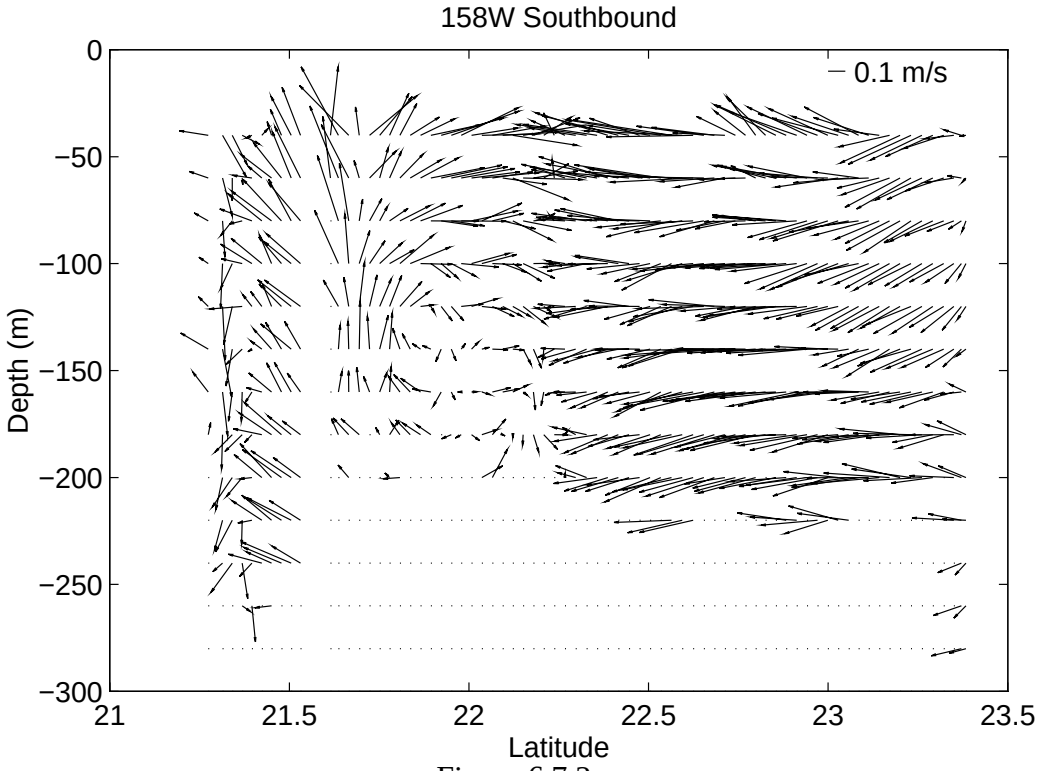
158W Southbound
0.1 m/s
0
−50
−100
−150
−200
−250
−300
Depth (m)
21
21.5
22
22.5
23
23.5
Latitude

Figure 6.7.2a

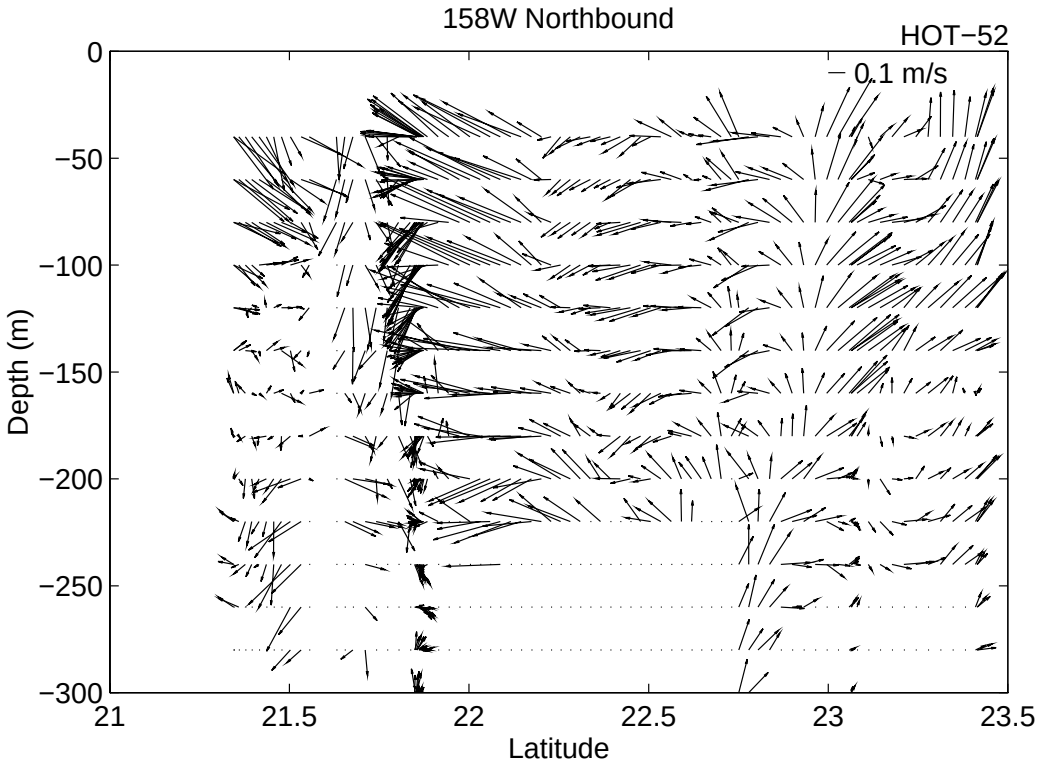
158W Northbound
HOT−52
0.1 m/s
0
−50
−100
−150
−200
−250
−300
Depth (m)
21
21.5
22
22.5
23
23.5
Latitude

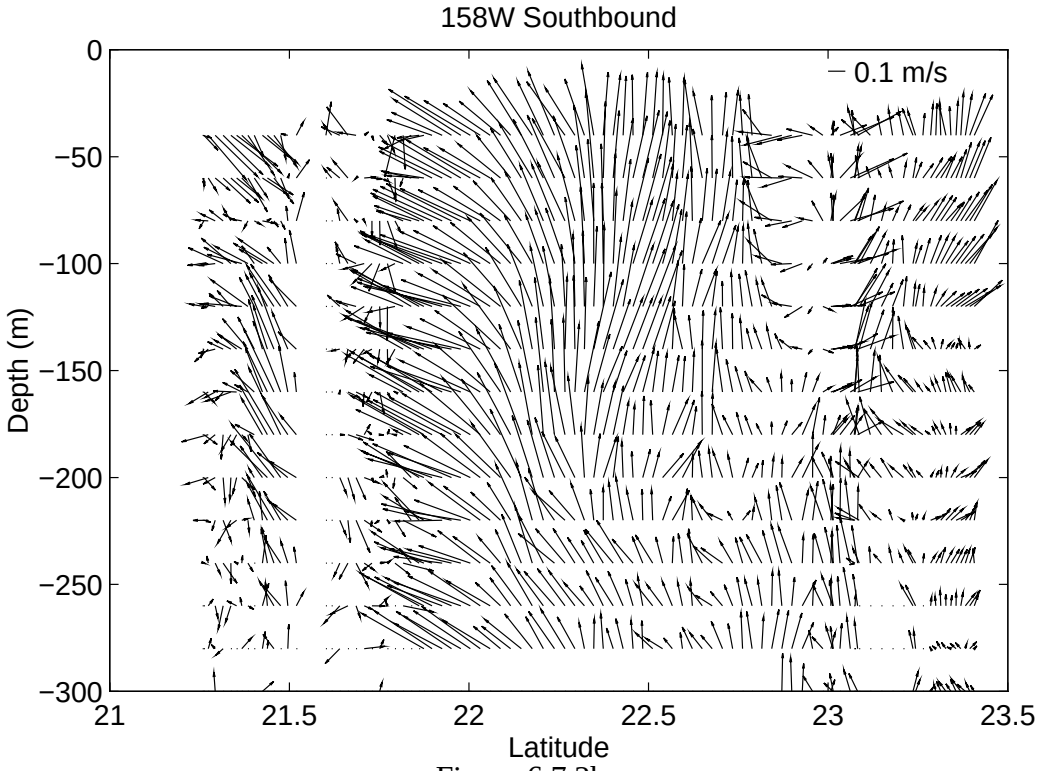
158W Southbound
0.1 m/s
0
−50
−100
−150
−200
−250
−300
Depth (m)
21
21.5
22
22.5
23
23.5
Latitude

Figure 6.7.2b

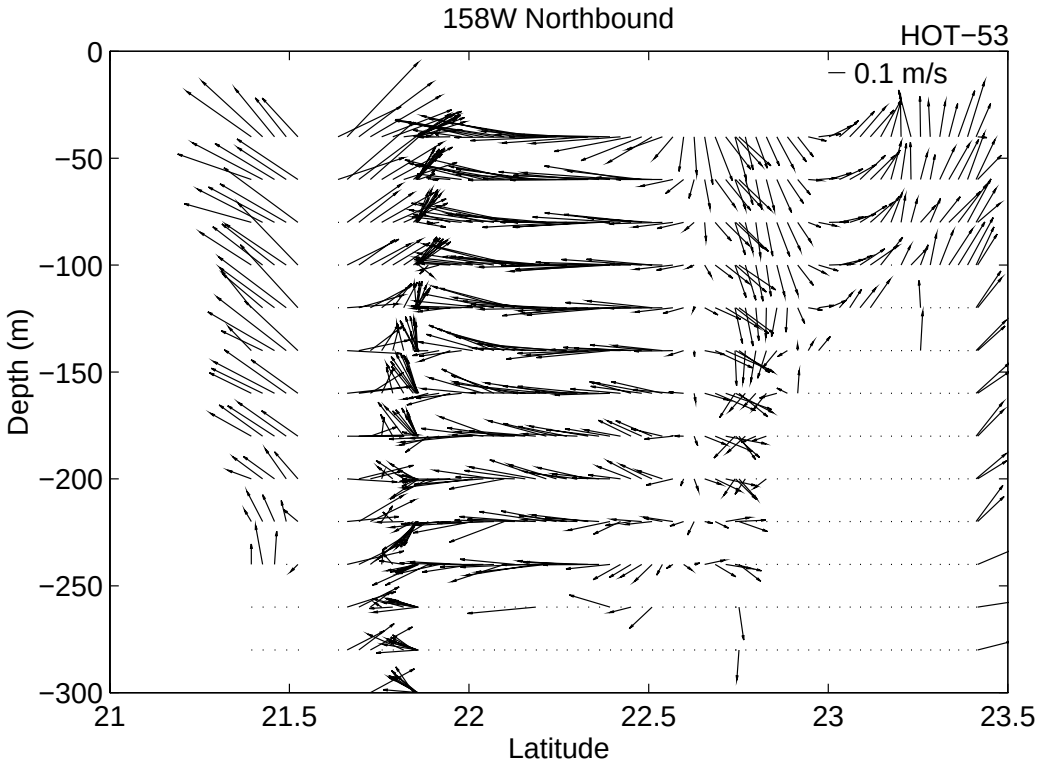
158W Northbound
HOT−53
0.1 m/s
0
−50
−100
−150
−200
−250
−300
Depth (m)
21
21.5
22
22.5
23
23.5
Latitude

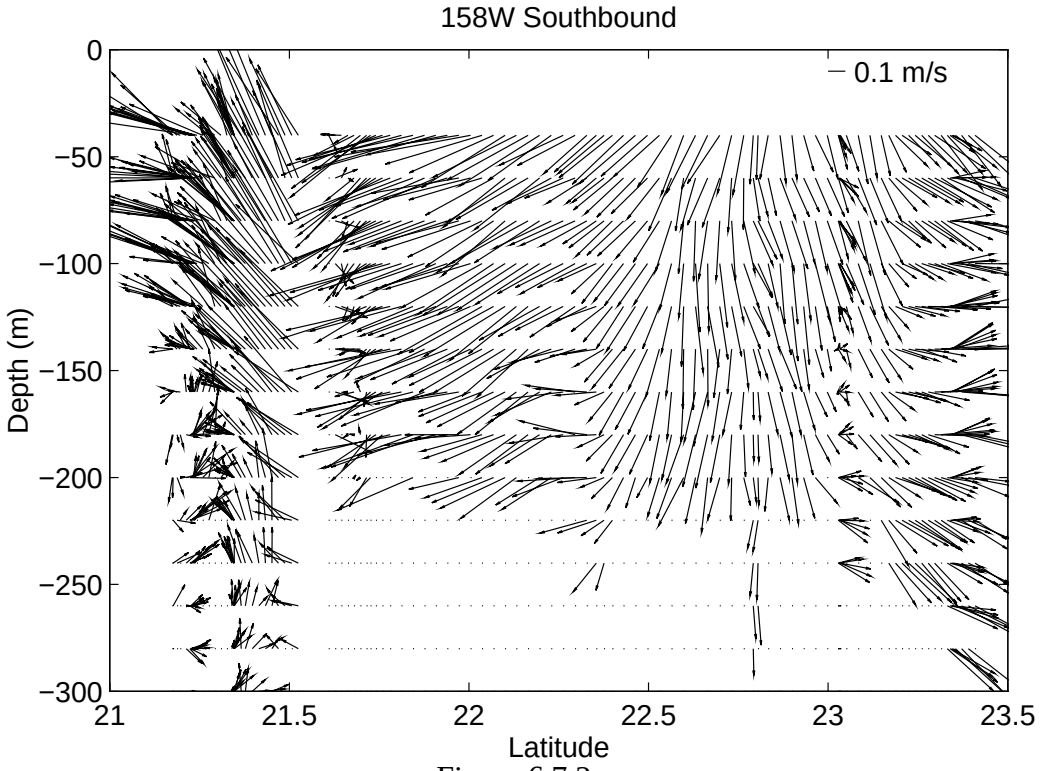
158W Southbound
0.1 m/s
0
−50
−100
−150
−200
−250
−300
Depth (m)
21
21.5
22
22.5
23
23.5
Latitude

Figure 6.7.2c

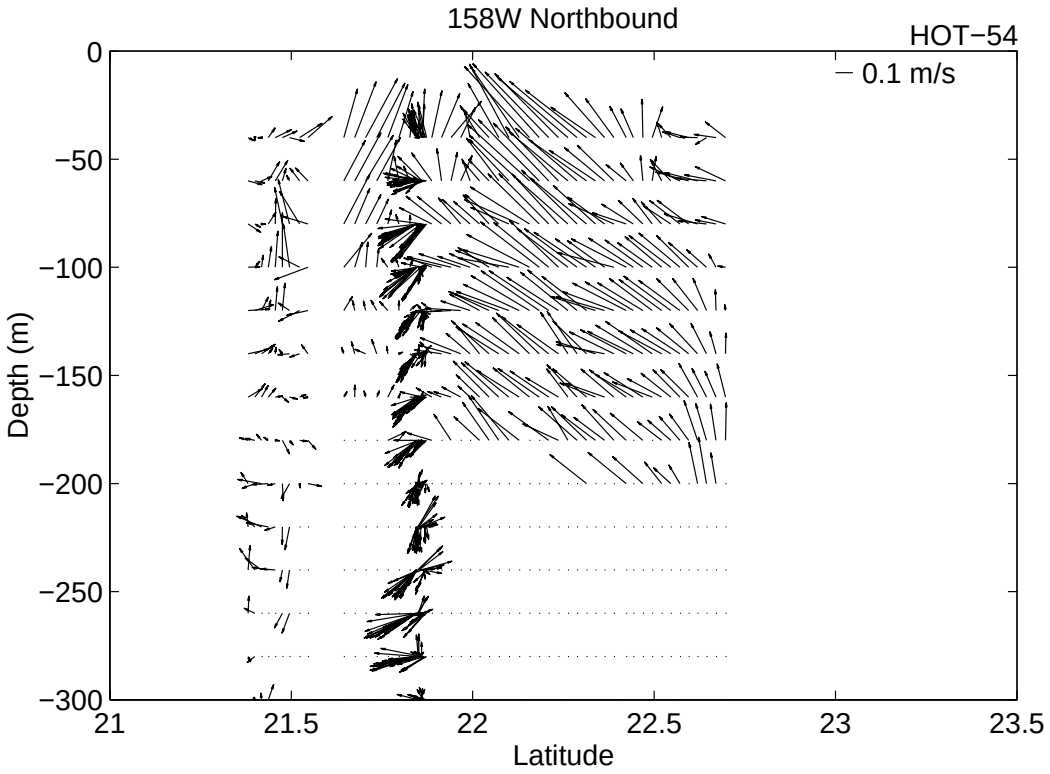
158W Northbound
HOT−54
0.1 m/s
0
−50
−100
−150
−200
−250
−300
Depth (m)
21
21.5
22
22.5
23
23.5
Latitude

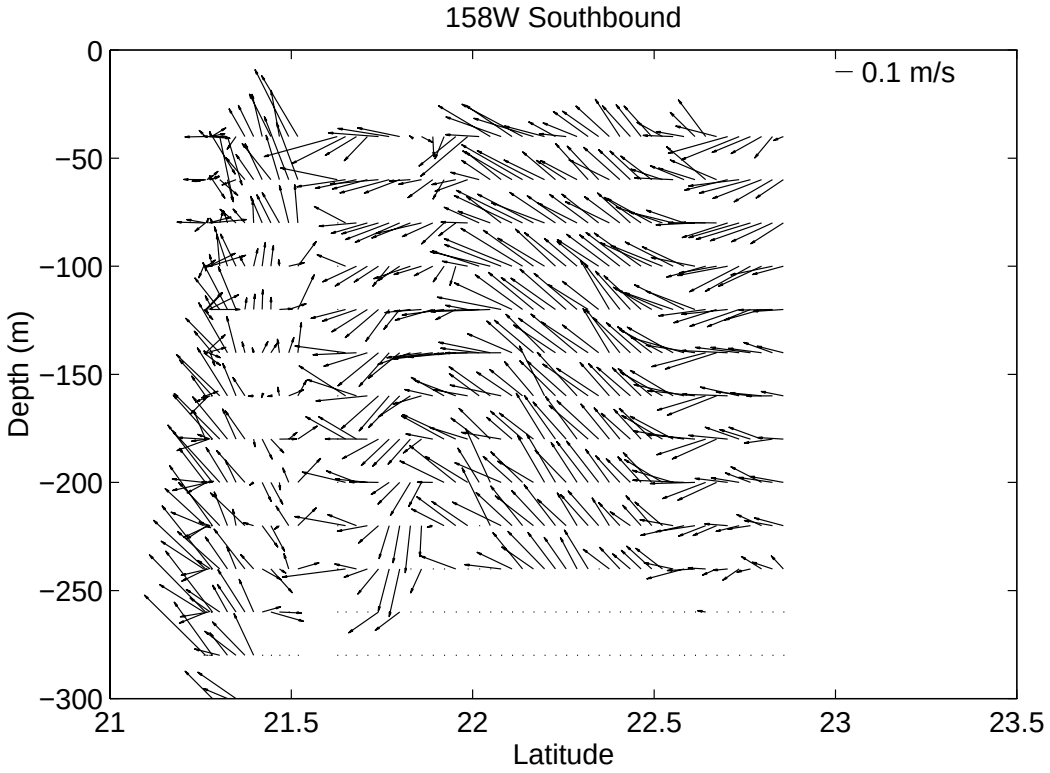
158W Southbound
0.1 m/s
0
−50
−100
−150
−200
−250
−300
Depth (m)
21
21.5
22
22.5
23
23.5
Latitude

Figure 6.7.2d

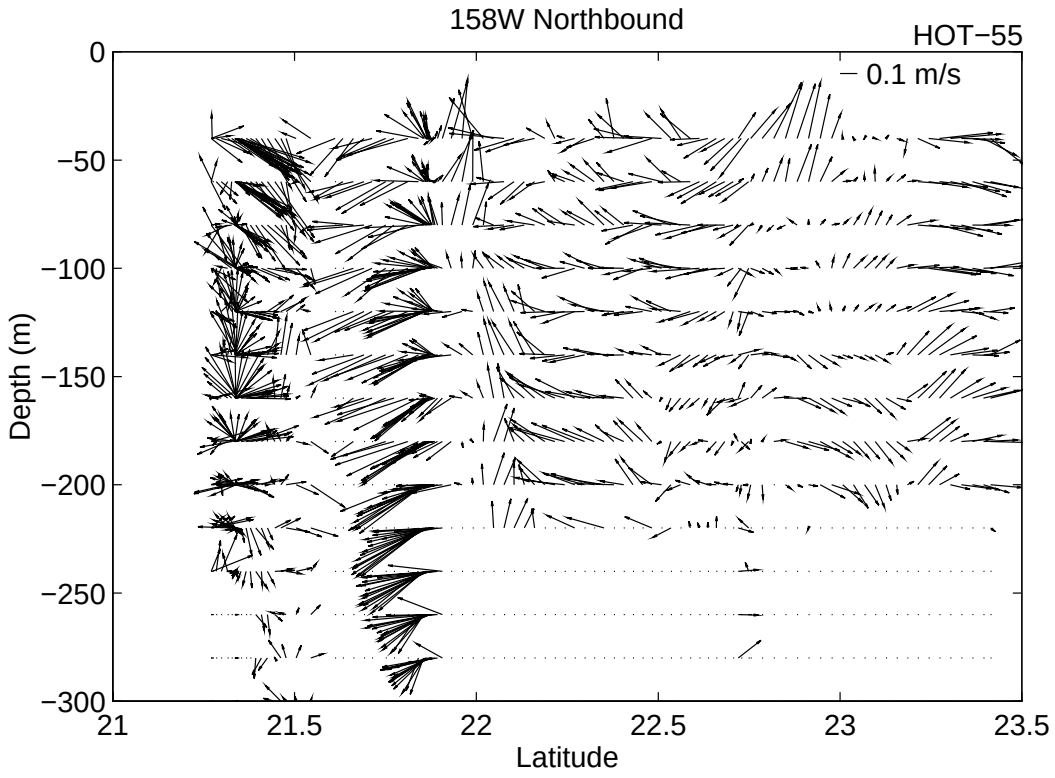
158W Northbound
HOT−55
0.1 m/s
0
−50
−100
−150
−200
−250
−300
Depth (m)
21
21.5
22
22.5
23
23.5
Latitude

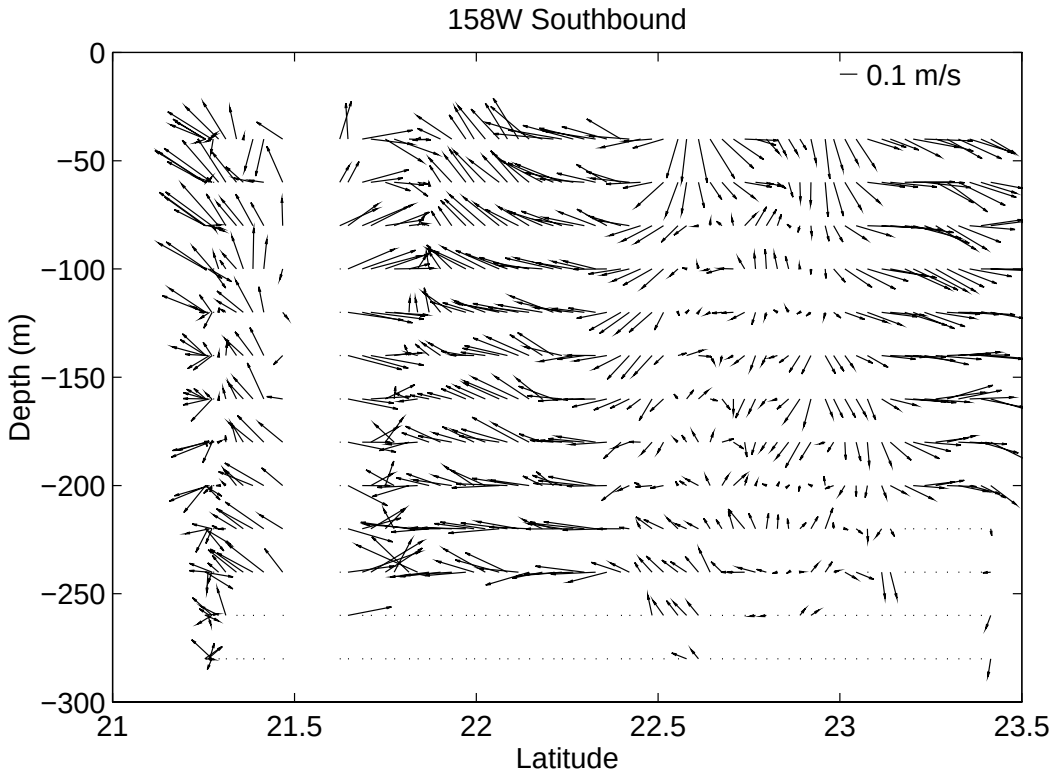
158W Southbound
0.1 m/s
0
−50
−100
−150
−200
−250
−300
Depth (m)
21
21.5
22
22.5
23
23.5
Latitude

Figure 6.7.2e

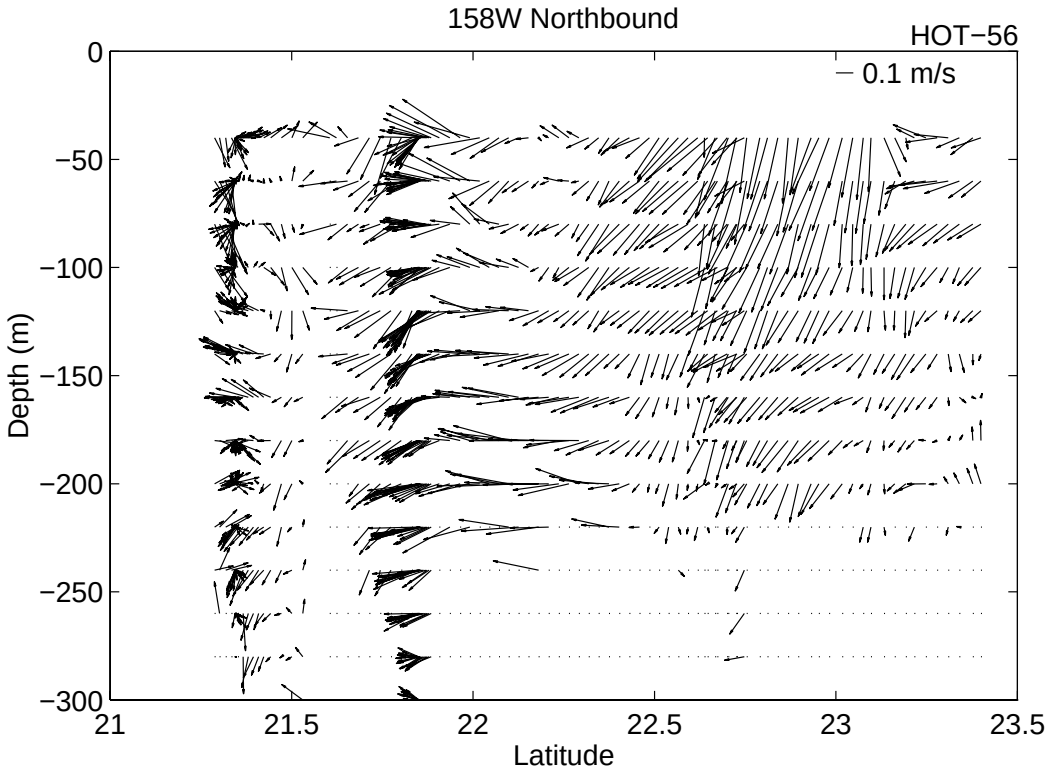
158W Northbound
HOT−56
0.1 m/s
0
−50
−100
−150
−200
−250
−300
Depth (m)
21
21.5
22
22.5
23
23.5
Latitude

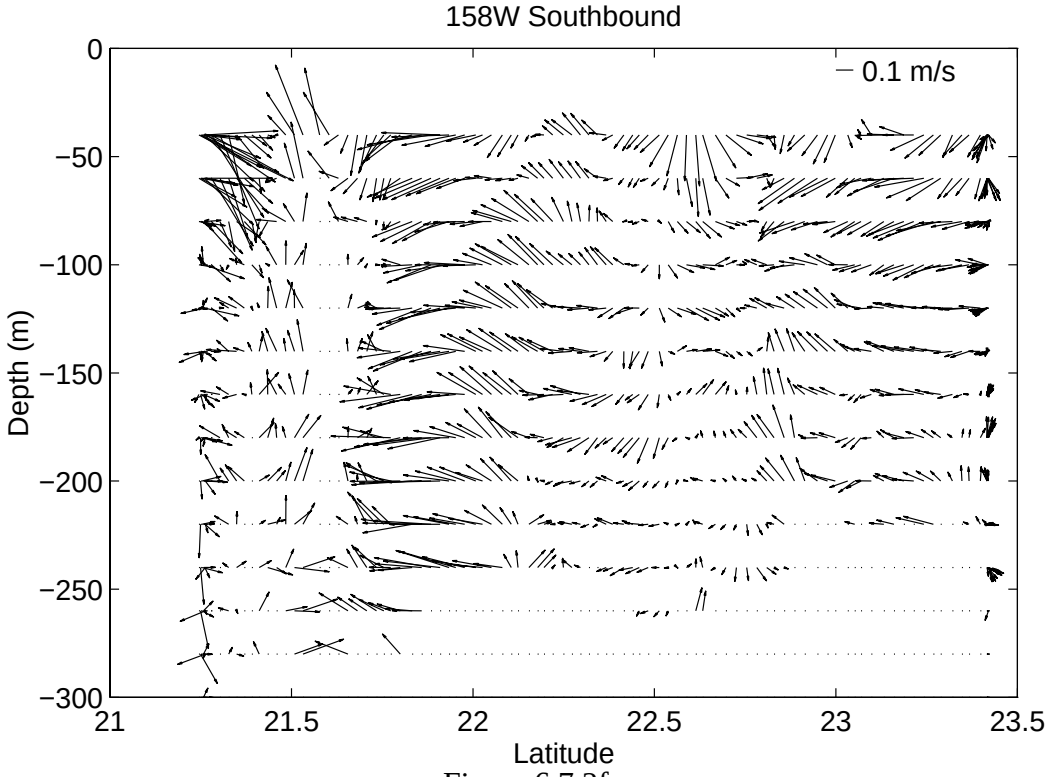
158W Southbound
0.1 m/s
0
−50
−100
−150
−200
−250
−300
Depth (m)
21
21.5
22
22.5
23
23.5
Latitude

Figure 6.7.2f

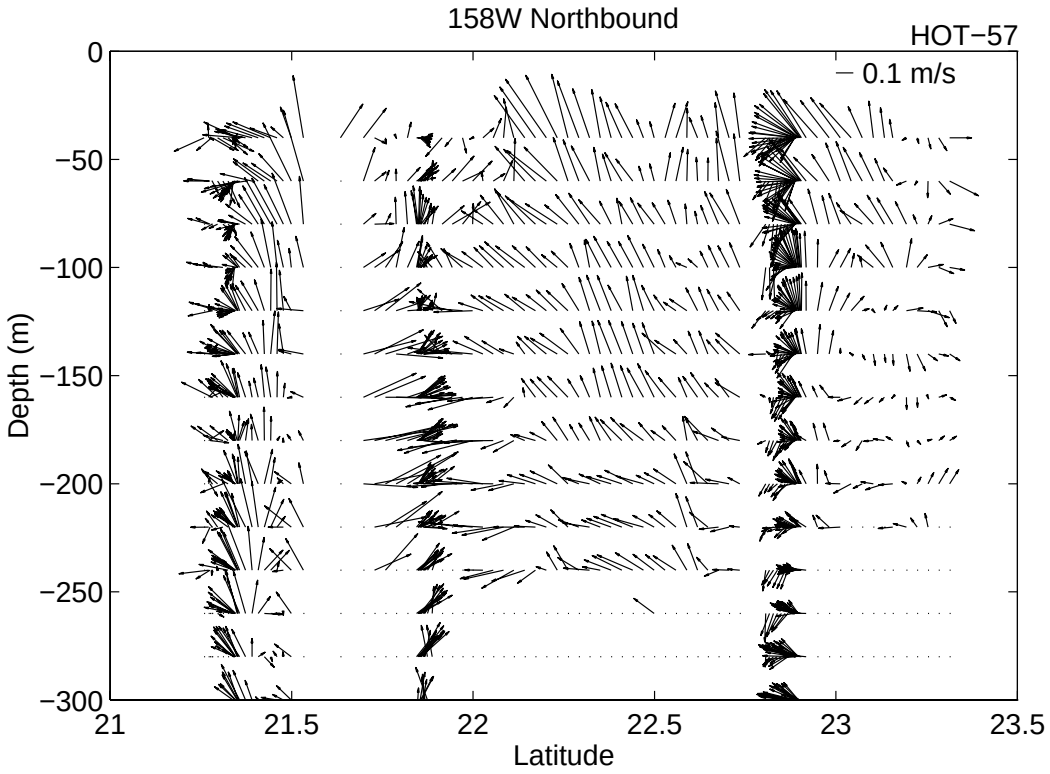
158W Northbound
HOT−57
0.1 m/s
0
−50
−100
−150
−200
−250
−300
Depth (m)
21
21.5
22
22.5
23
23.5
Latitude

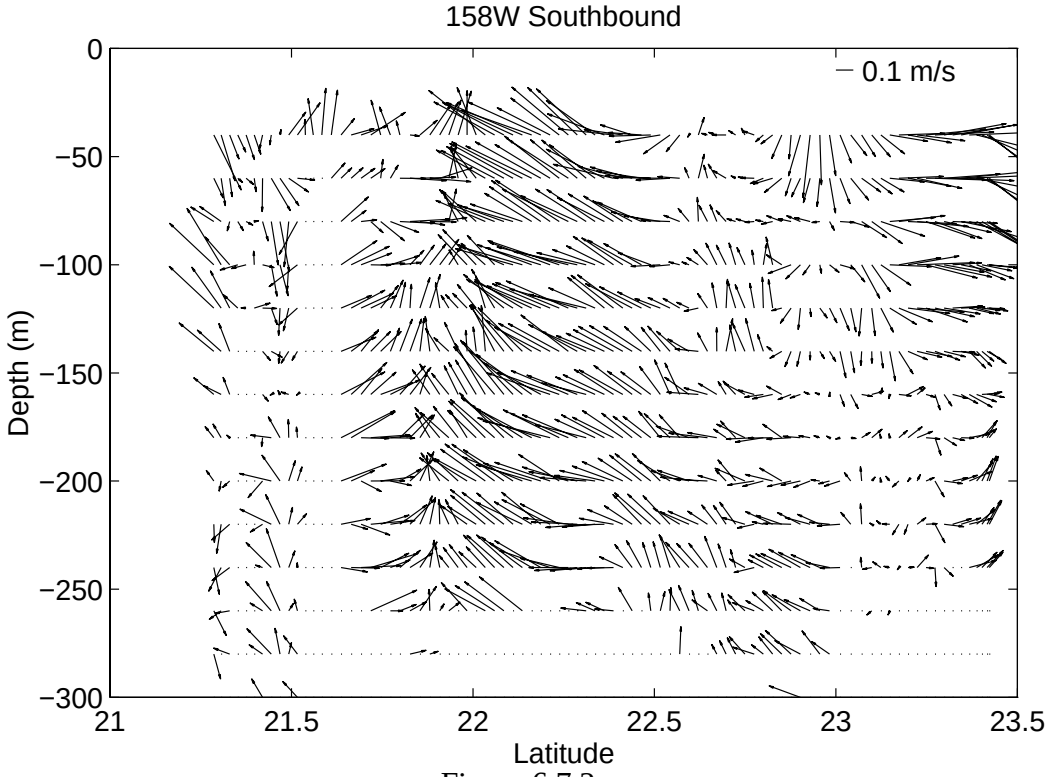
158W Southbound
0.1 m/s
0
−50
−100
−150
−200
−250
−300
Depth (m)
21
21.5
22
22.5
23
23.5
Latitude

Figure 6.7.2g

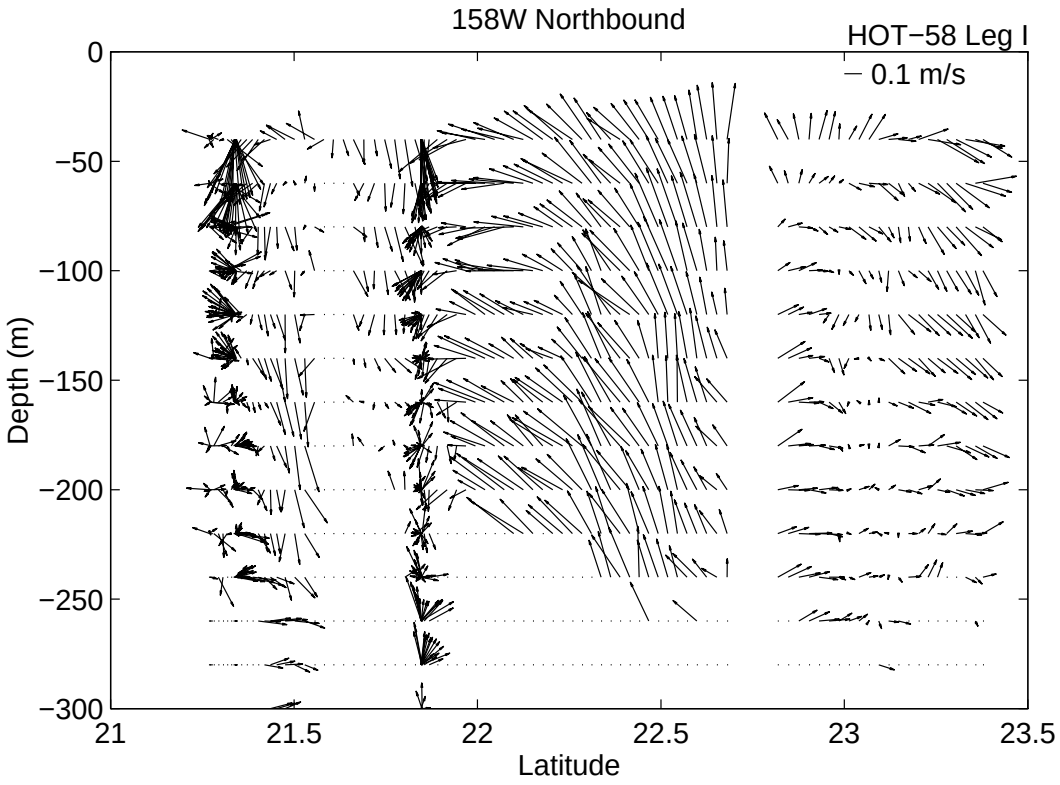
158W Northbound
HOT−58 Leg I
0.1 m/s
0
−50
−100
−150
−200
−250
−300
Depth (m)
21
21.5
22
22.5
23
23.5
Latitude

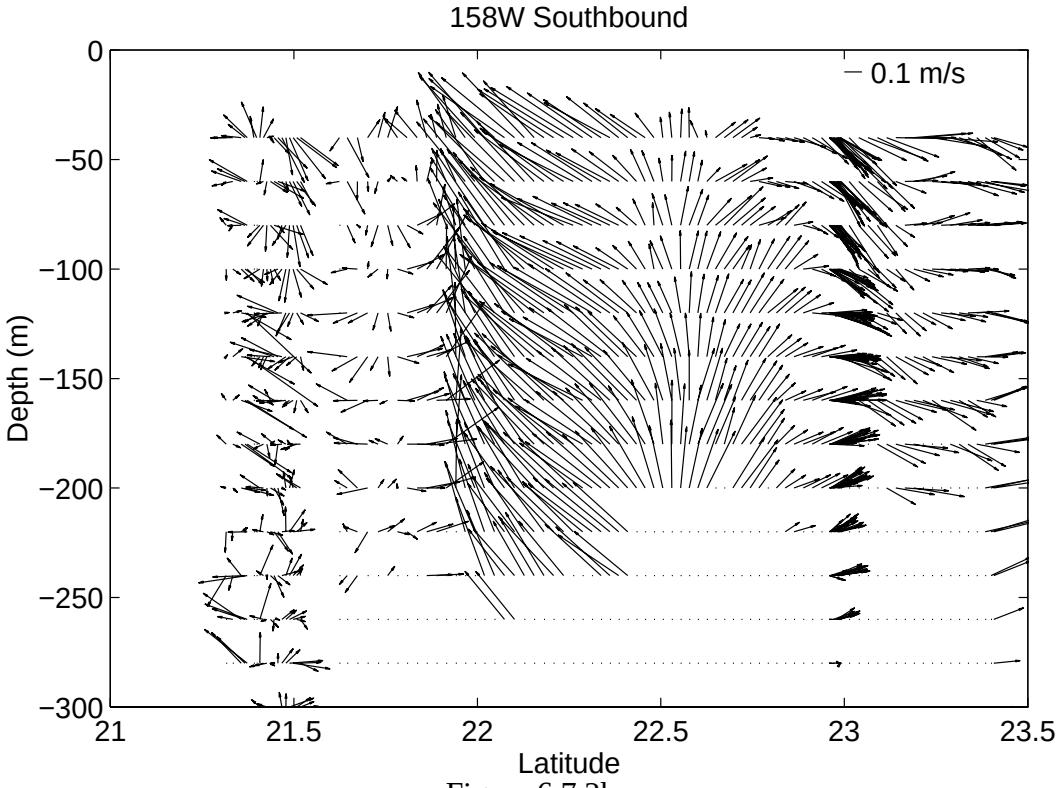
158W Southbound
0.1 m/s
0
−50
−100
−150
−200
−250
−300
Depth (m)
21
21.5
22
22.5
23
23.5
Latitude

Figure 6.7.2h

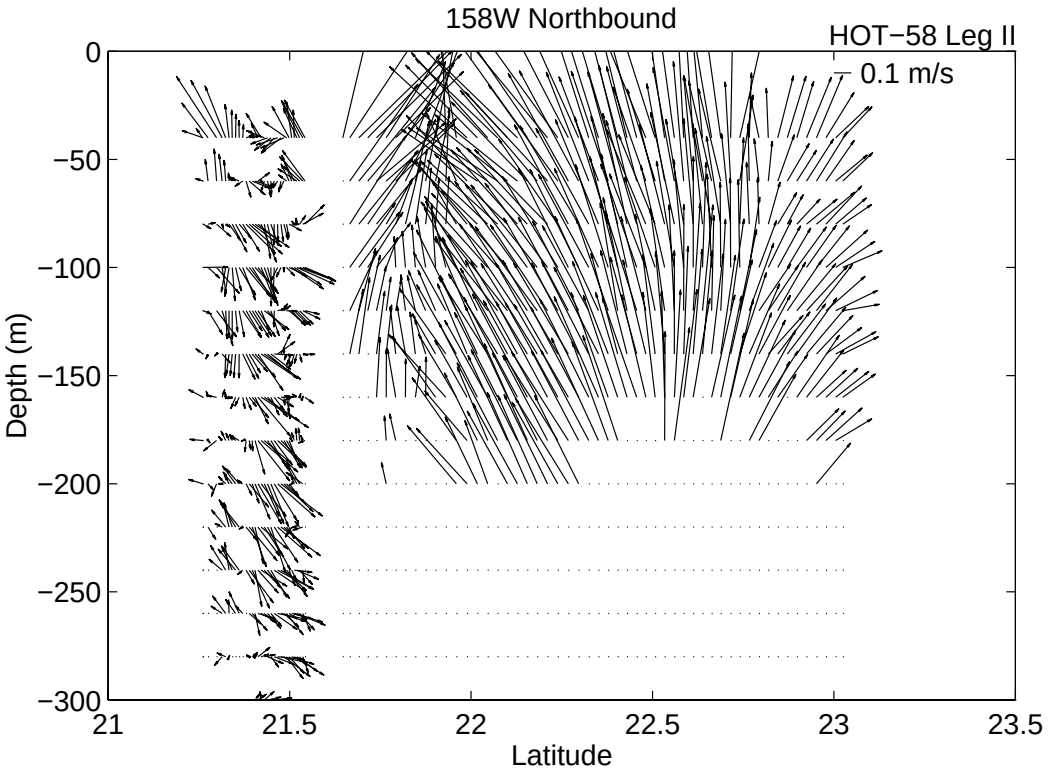
158W Northbound
HOT−58 Leg II
0.1 m/s
0
−50
−100
−150
−200
−250
−300
Depth (m)
21
21.5
22
22.5
23
23.5
Latitude

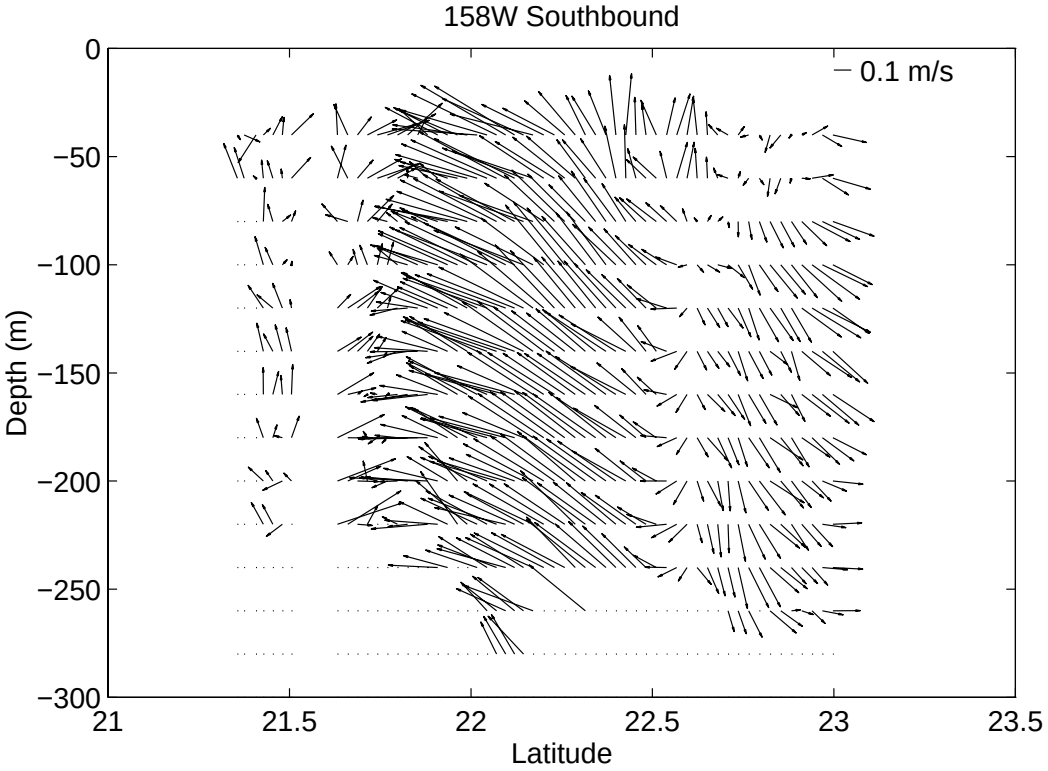
158W Southbound
0.1 m/s
0
−50
−100
−150
−200
−250
−300
Depth (m)
21
21.5
22
22.5
23
23.5
Latitude

Figure 6.7.2i

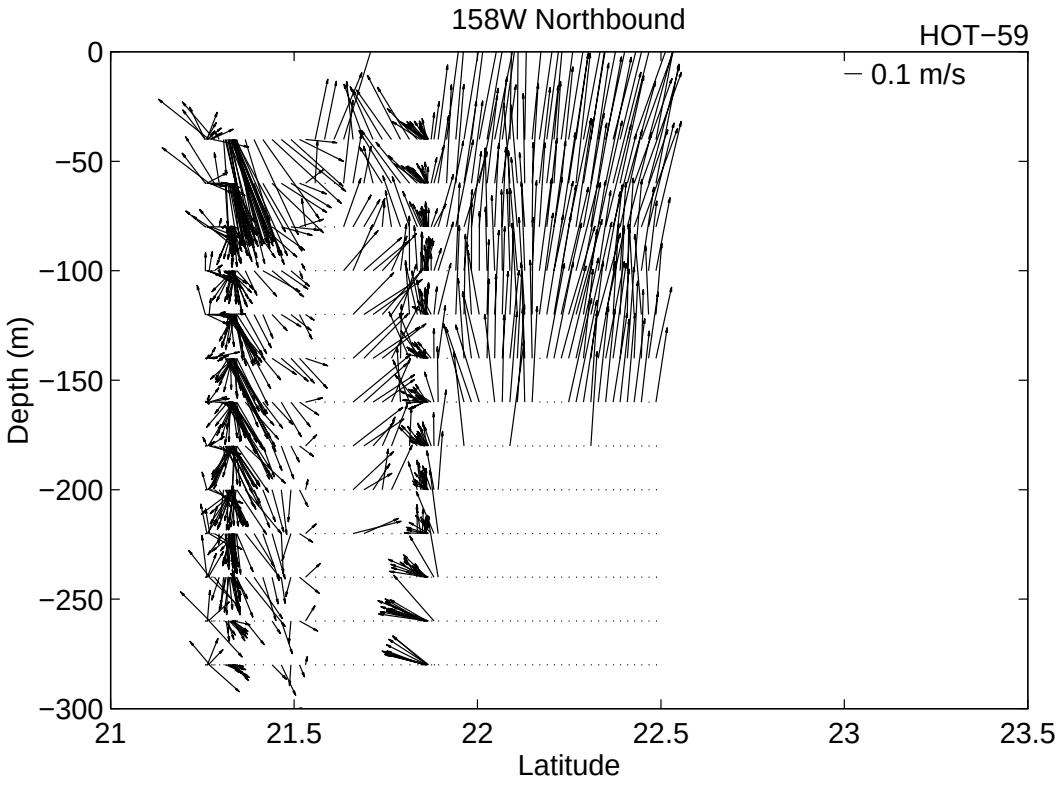
158W Northbound
HOT−59
0.1 m/s
0
−50
−100
−150
−200
−250
−300
Depth (m)
21
21.5
22
22.5
23
23.5
Latitude

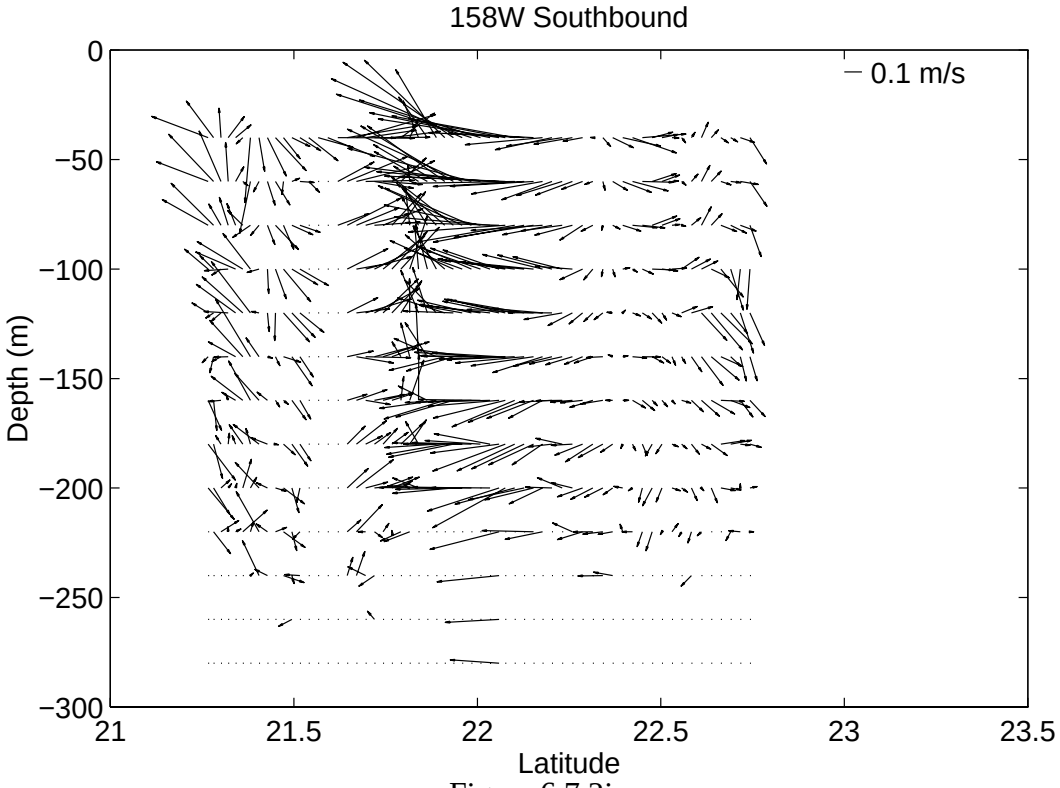
158W Southbound
0.1 m/s
0
−50
−100
−150
−200
−250
−300
Depth (m)
21
21.5
22
22.5
23
23.5
Latitude

Figure 6.7.2j

6.8. Meteorology

Figure 6.8.1. Upper panel: Atmospheric pressure measured while at Station ALOHA during 1994. Open circles represent individual measurements. Lower panel: Sea surface temperature measured from bucket sample while at Station ALOHA during 1994.

Figure 6.8.2. Upper panel: Dry bulb temperature measured while on station during 1994. Lower panel: Wet bulb air temperature measure while as Station ALOHA during 1994.

Figure 6.8.3. Upper panel: SST-dry air temperature measured at Station ALOHA during 1994. Lower panel: Dry-wet air temperature measured at Station ALOHA during 1994.

Figure 6.8.4. Upper panel: True winds measured at Station ALOHA during HOT-51. Lower panel: True winds collected by NDBC Buoy 51001 during HOT-51. The orientation of the arrows indicate the wind direction; up is northward, to the right is eastward.

Figure 6.8.5: As in Figure 6.8.4, except for HOT-52.

Figure 6.8.6: As in Figure 6.8.4, except for HOT-53.

Figure 6.8.7: As in Figure 6.8.4, except for HOT-54.

Figure 6.8.8: As in Figure 6.8.4, except for HOT-55.

Figure 6.8.9: As in Figure 6.8.4, except for HOT-56.

Figure 6.8.10: As in Figure 6.8.4, except for HOT-57.

Figure 6.8.11: As in Figure 6.8.4, except for HOT-58.

Figure 6.8.12: As in Figure 6.8.4, except for HOT-59.

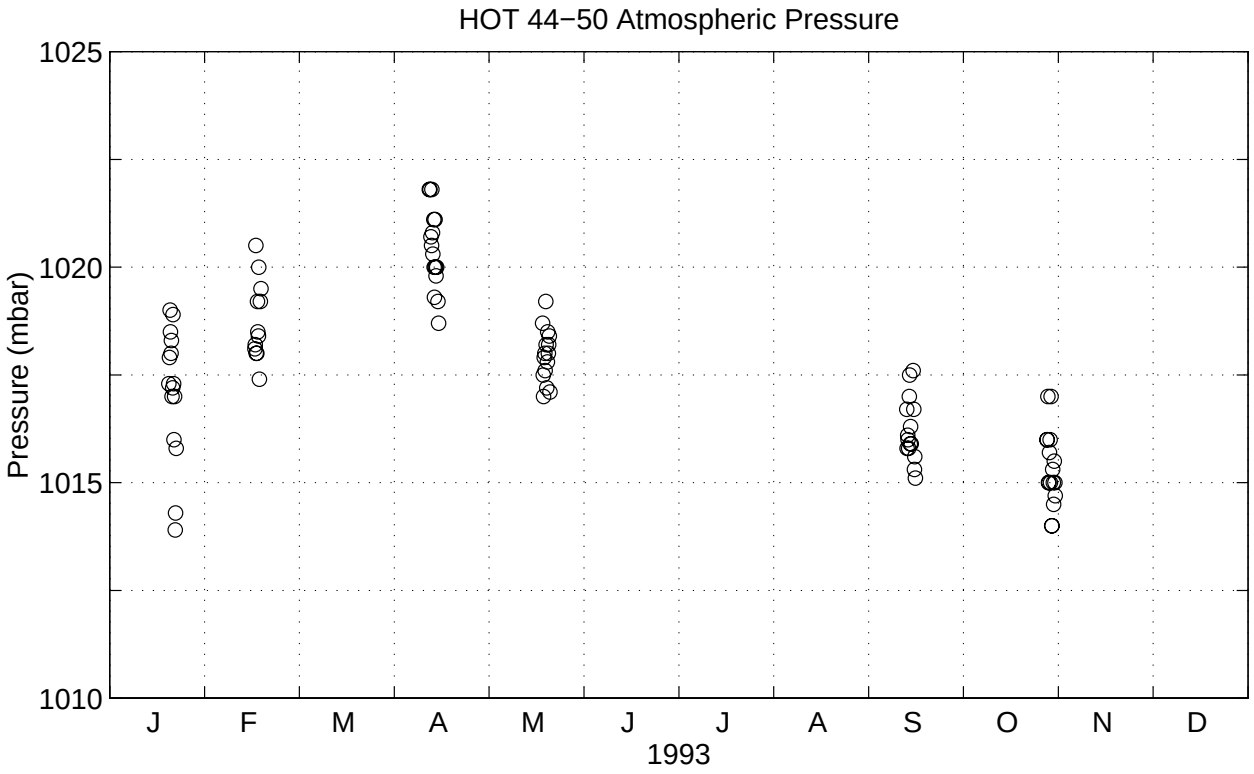
HOT 44−50 Atmospheric Pressure
Pressure (mbar)
1025
1020
1015
1010
J
F
M
A
M
J
J
A
S
O
N
D
1993

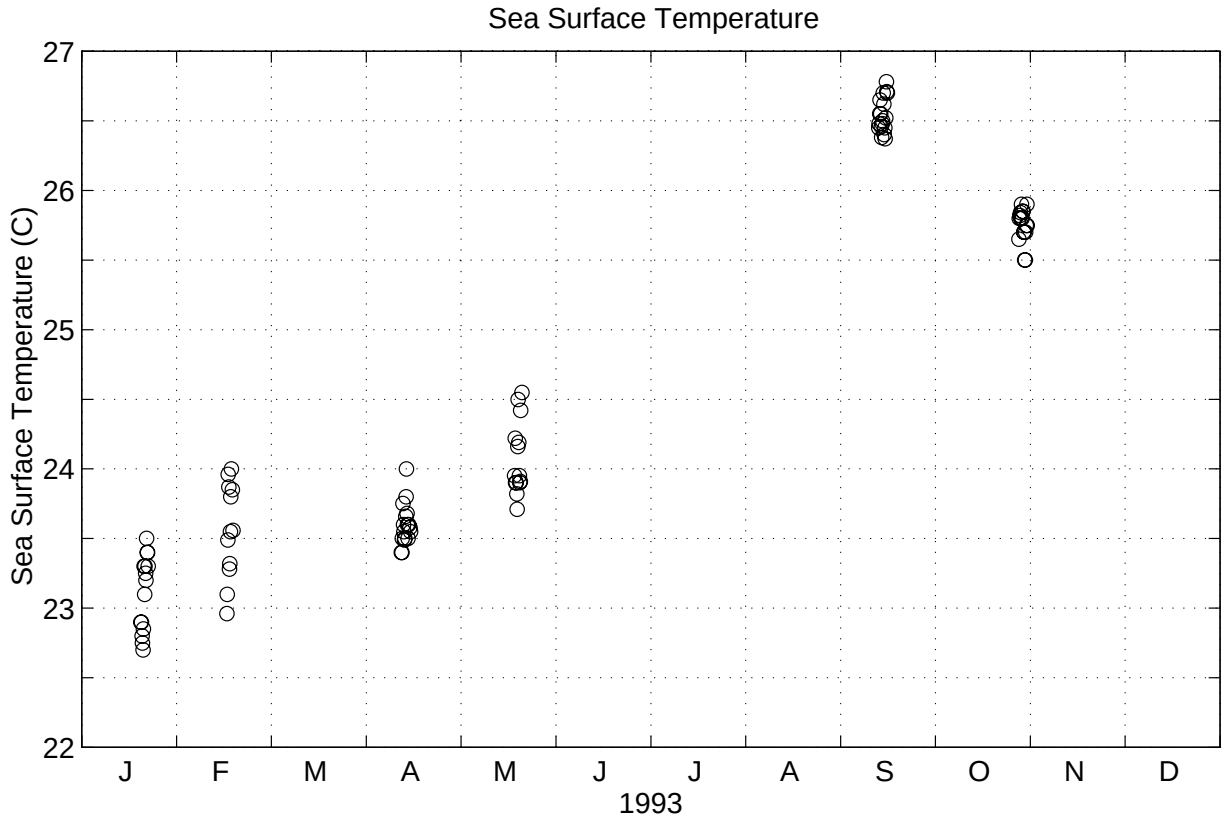
Sea Surface Temperature
Sea Surface Temperature (C)
27
26
25
24
23
22
J
F
M
A
M
J
J
A
S
O
N
D
1993

Figure 6.8.1

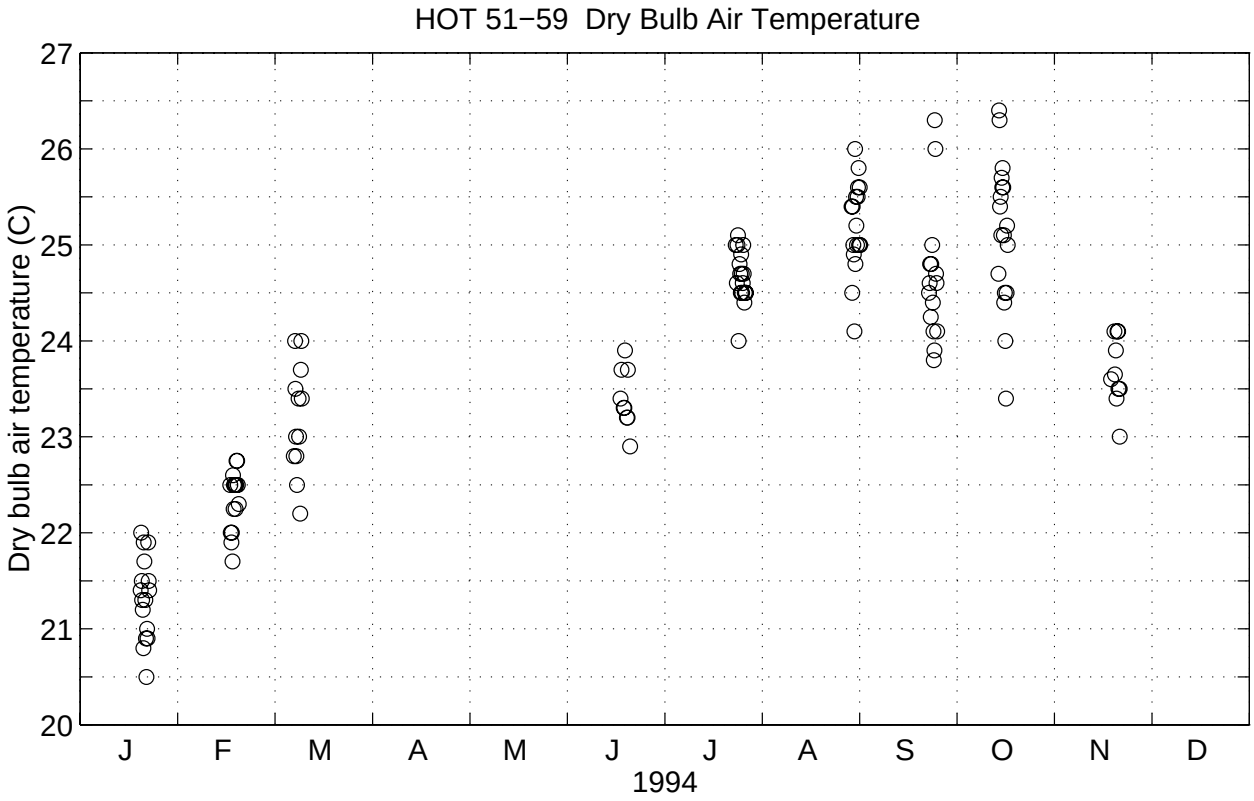
HOT 51−59 Dry Bulb Air Temperature
Dry bulb air temperature (C)
27
26
25
24
23
22
21
20
J
F
M
A
M
J
J
A
S
O
N
D
1994

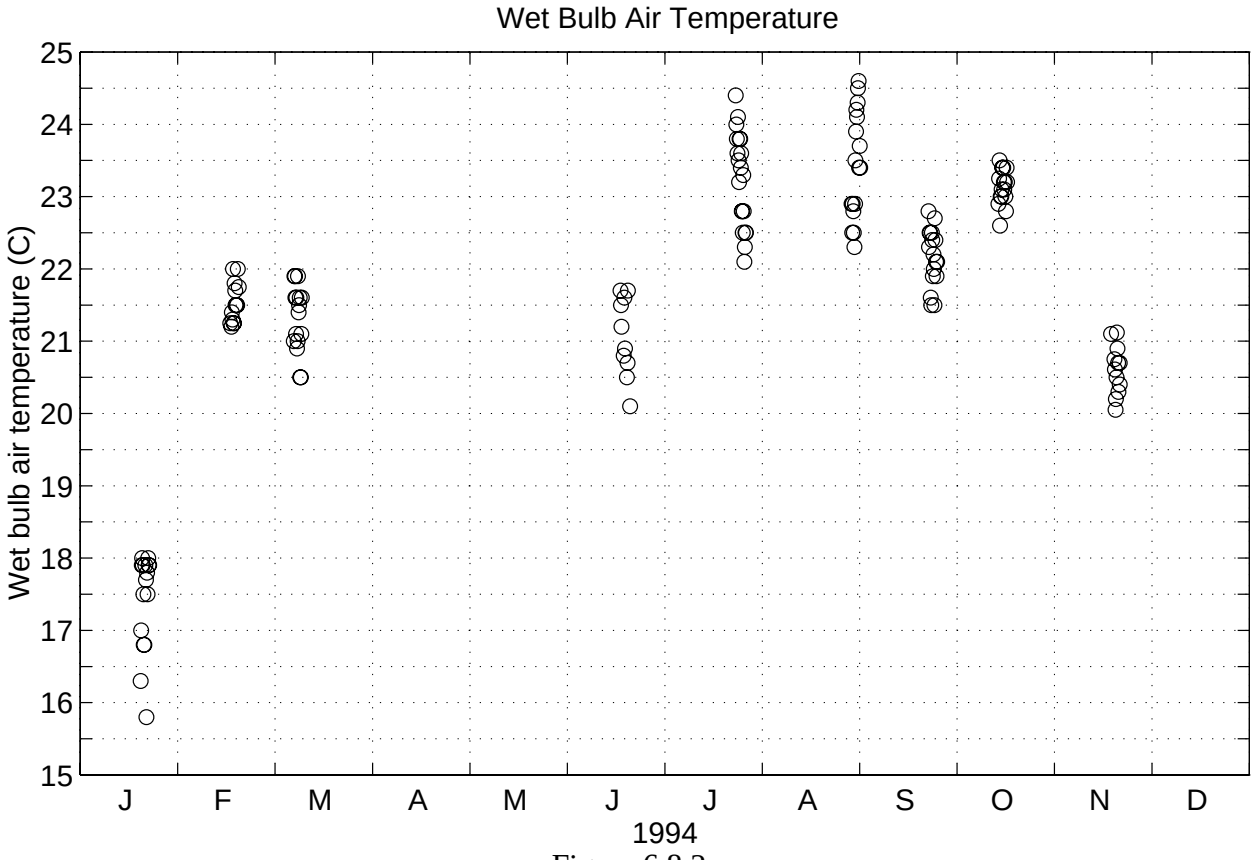
Wet Bulb Air Temperature
Wet bulb air temperature (C)
25
24
23
22
21
20
19
18
17
16
15
J
F
M
A
M
J
J
A
S
O
N
D
1994

Figure 6.8.2

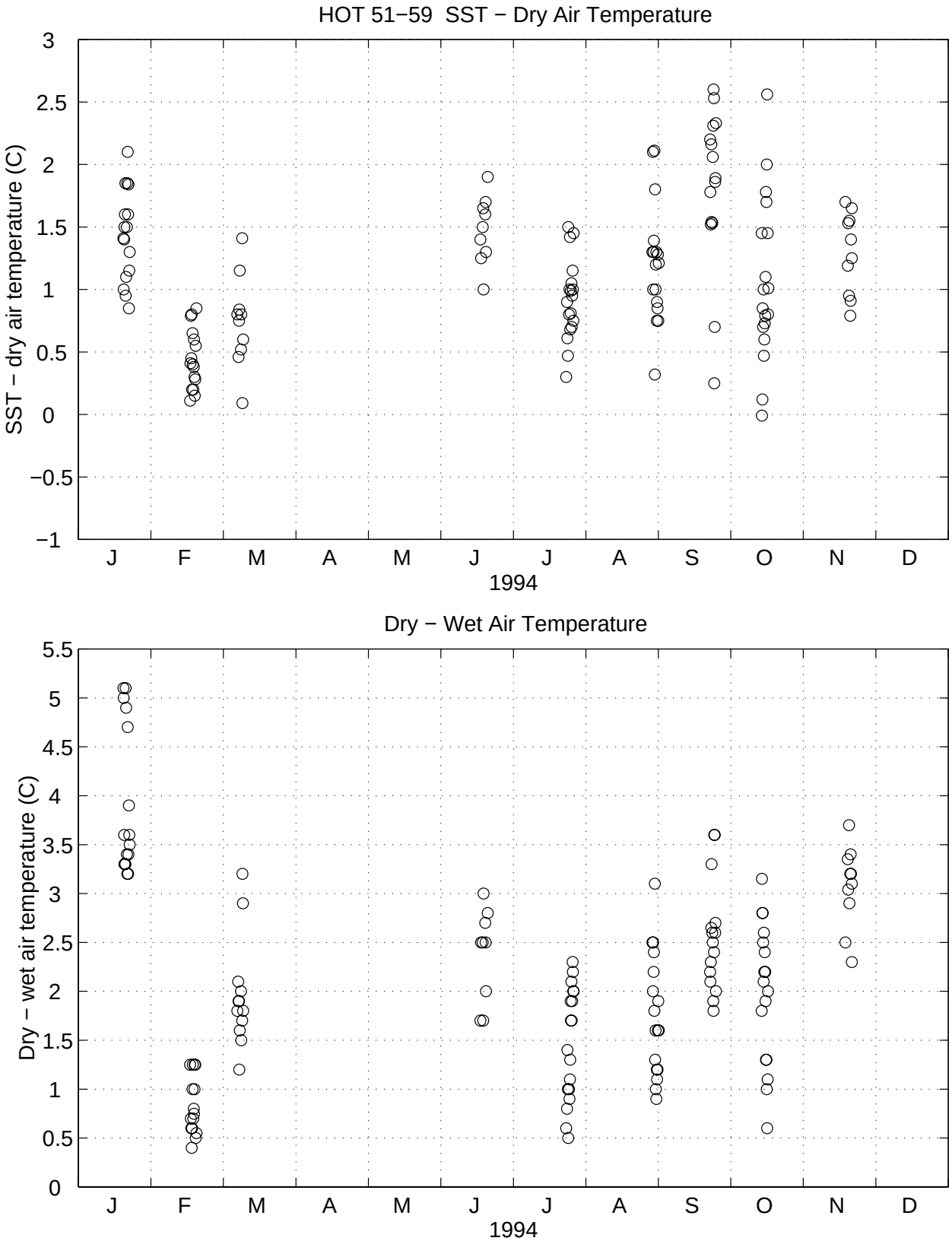
HOT 51−59 SST − Dry Air Temperature
SST − dry air temperature (C)
3
2.5
2
1.5
1
0.5
0
−0.5
−1
J F M A M J J A S O N D
1994
Dry − Wet Air Temperature
Dry − wet air temperature (C)
5.5
5
4.5
4
3.5
3
2.5
2
1.5
1
0.5
0
J F M A M J J A S O N D
1994
Figure 6.8.3

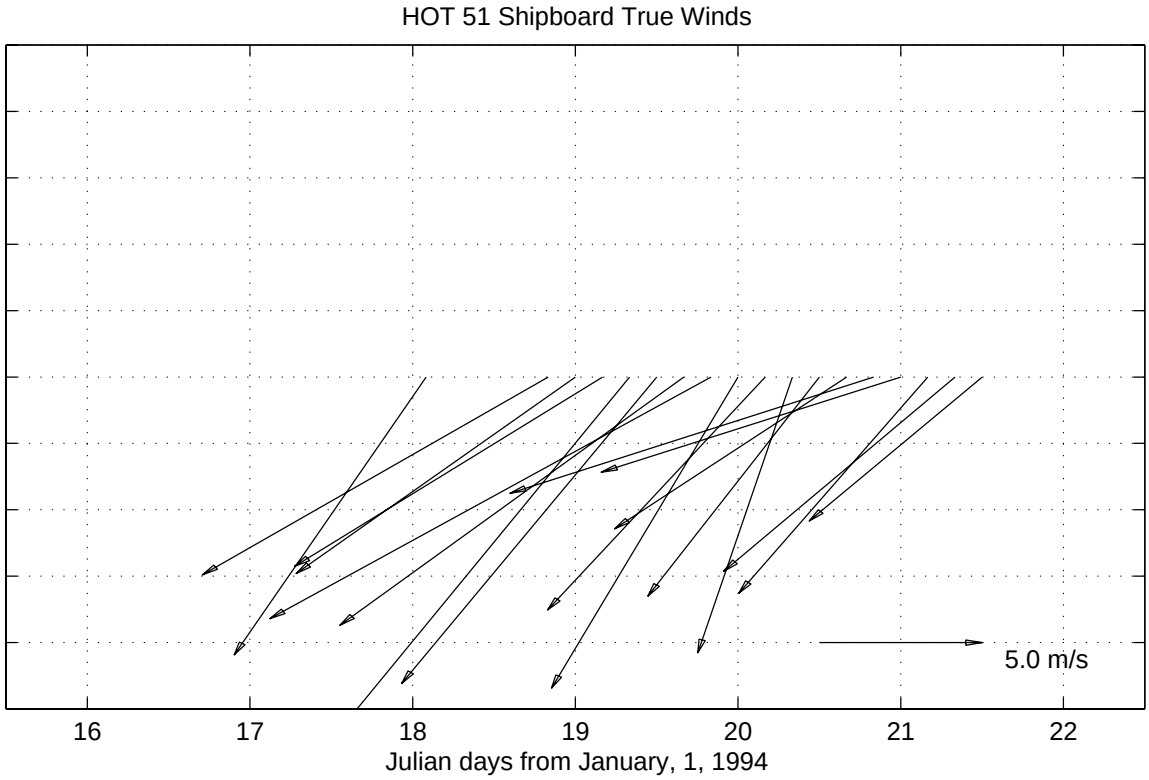
HOT 51 Shipboard True Winds
5.0 m/s
16
17
18
19
20
21
22
Julian days from January, 1, 1994

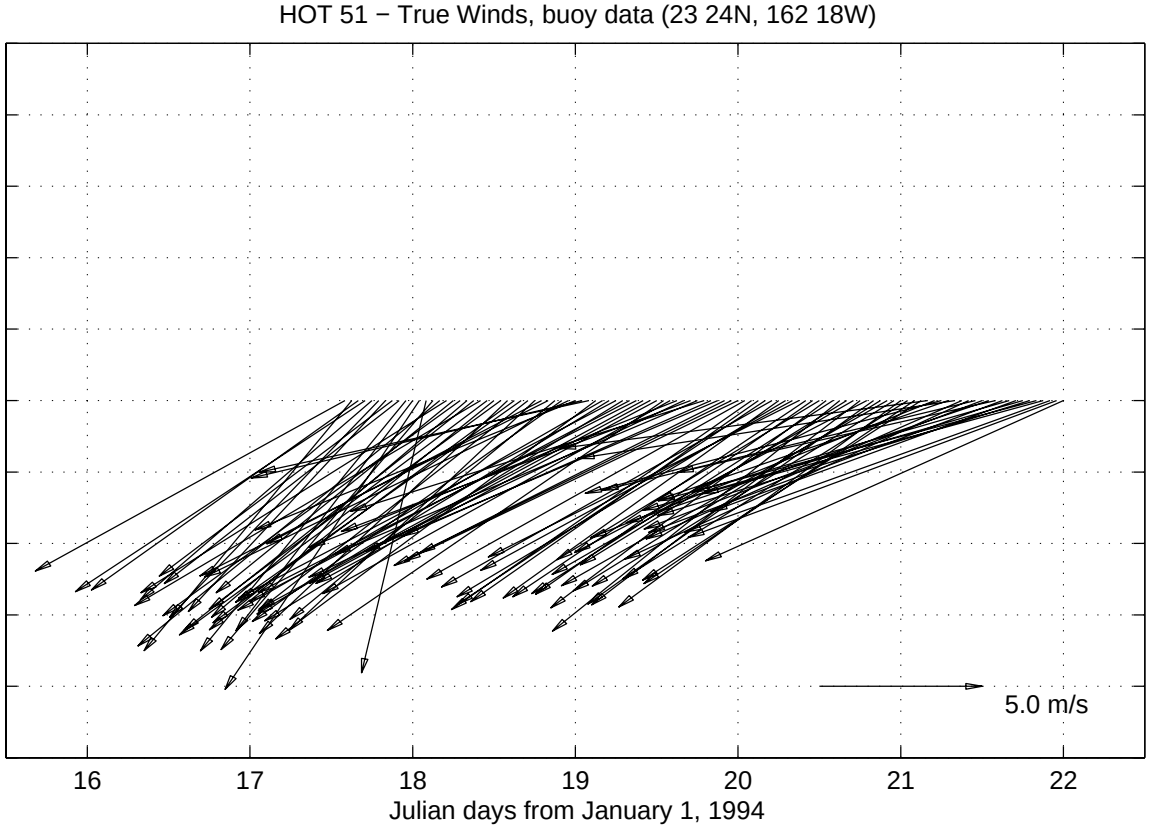
HOT 51 − True Winds, buoy data (23 24N, 162 18W)
5.0 m/s
16
17
18
19
20
21
22
Julian days from January 1, 1994

Figure 6.8.4

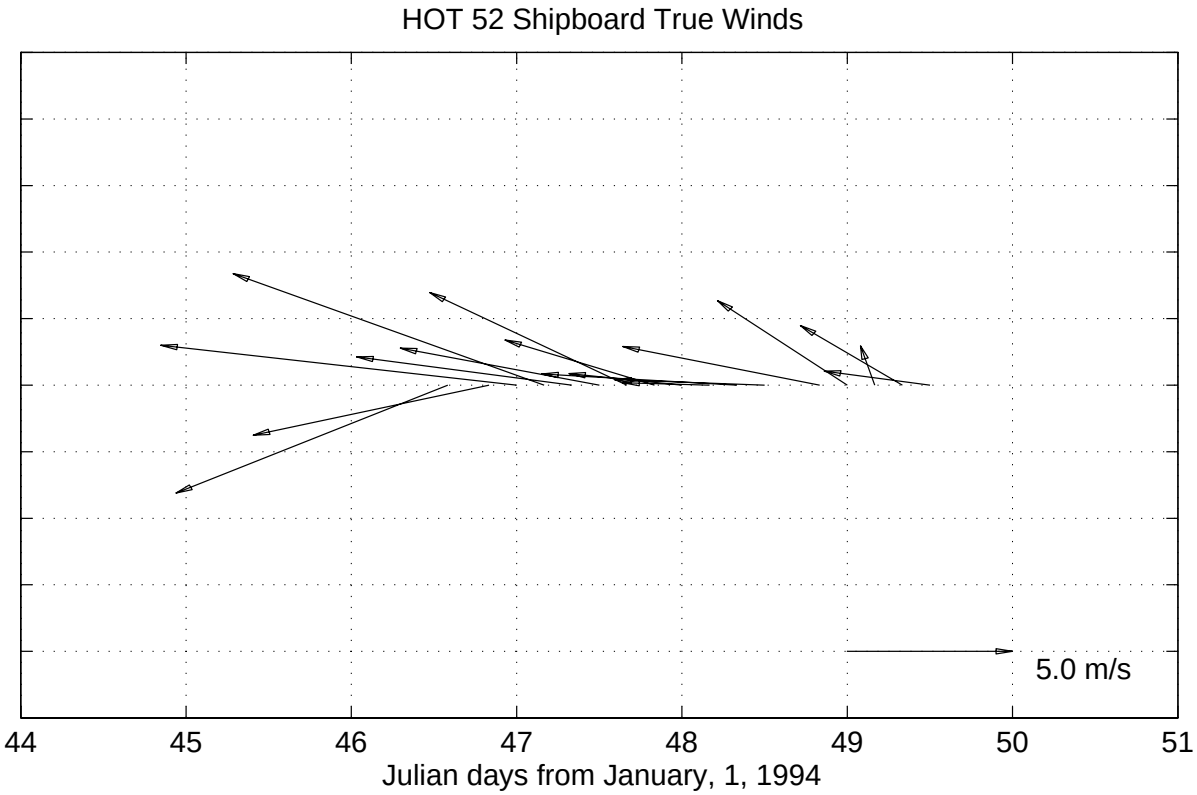
HOT 52 Shipboard True Winds
5.0 m/s
44
45
46
47
48
49
50
51
Julian days from January, 1, 1994

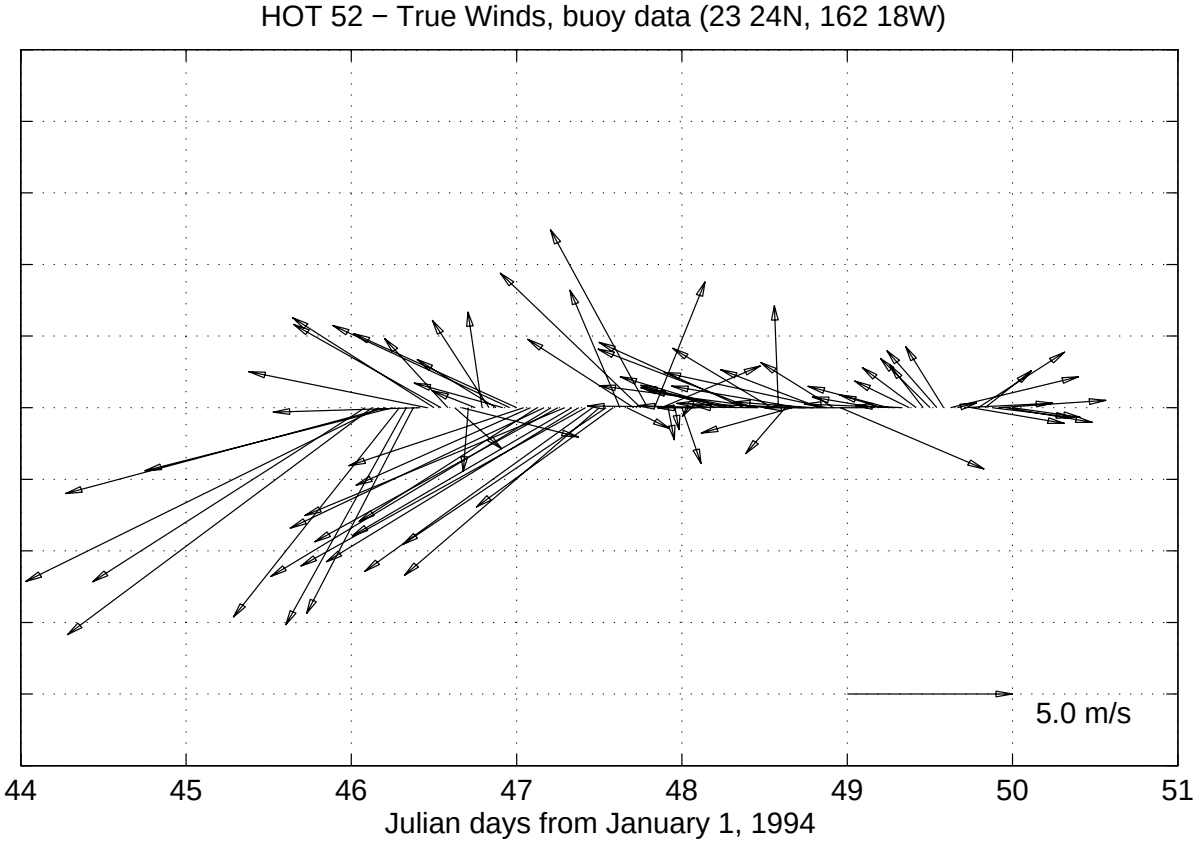
HOT 52 − True Winds, buoy data (23 24N, 162 18W)
5.0 m/s
44
45
46
47
48
49
50
51
Julian days from January 1, 1994

Figure 6.8.5

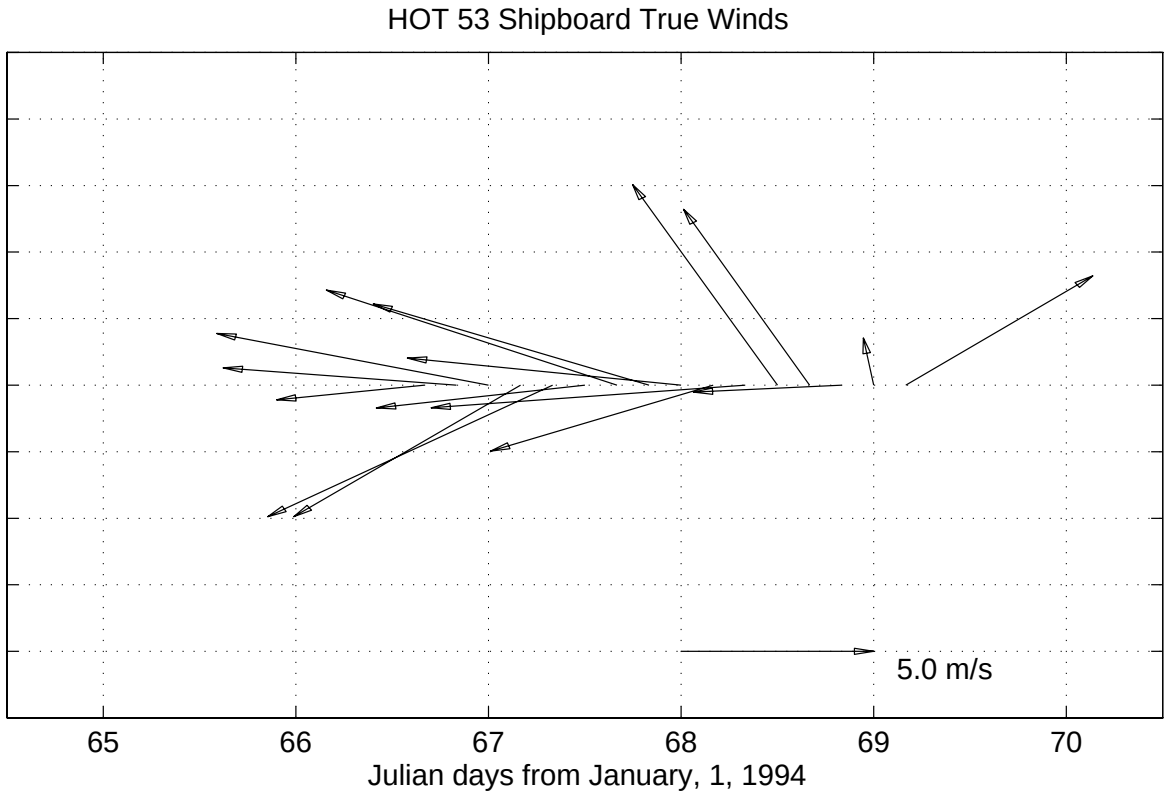
HOT 53 Shipboard True Winds
5.0 m/s
65
66
67
68
69
70
Julian days from January, 1, 1994

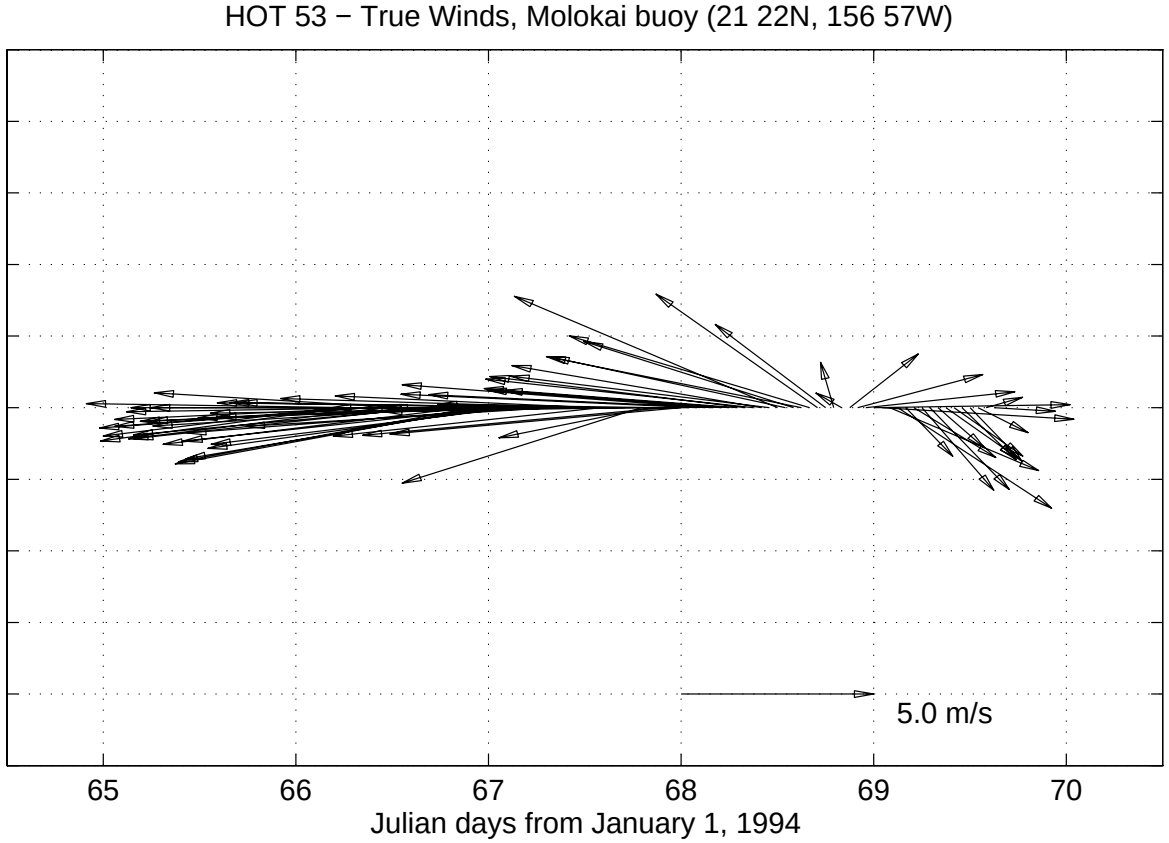
HOT 53 − True Winds, Molokai buoy (21 22N, 156 57W)
5.0 m/s
65
66
67
68
69
70
Julian days from January 1, 1994

Figure 6.8.6

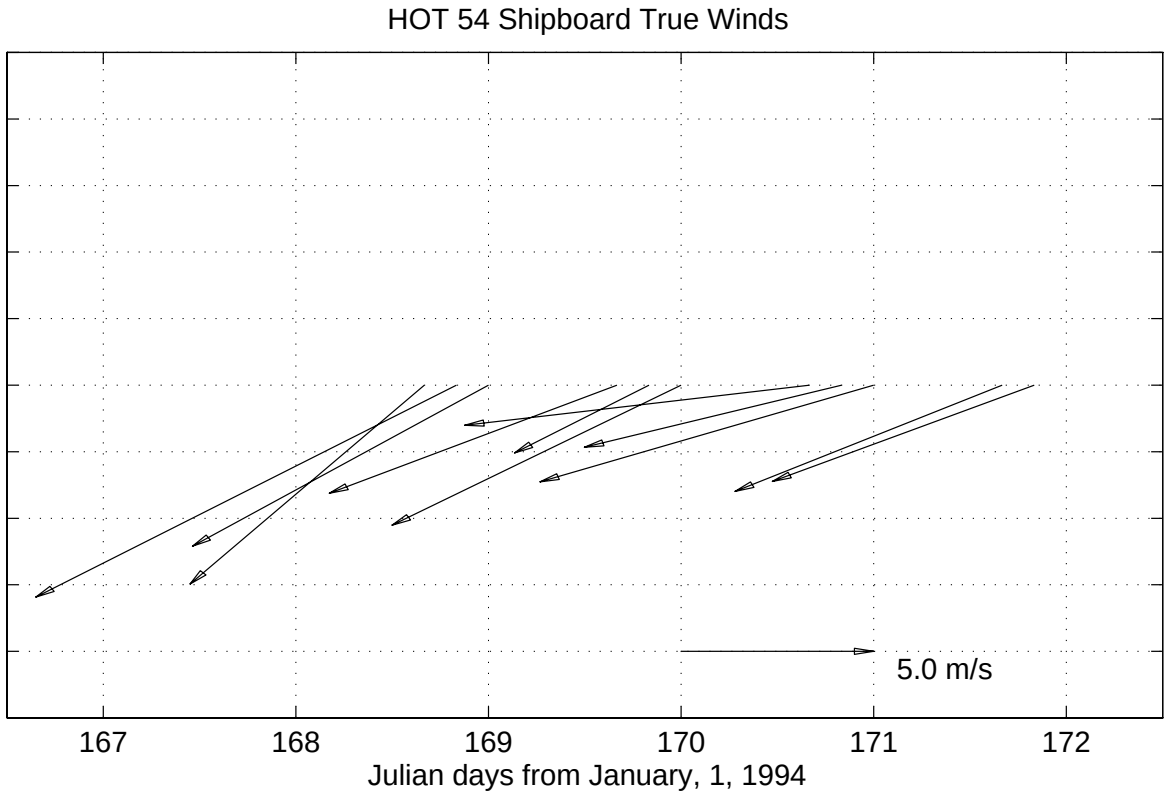
HOT 54 Shipboard True Winds
5.0 m/s
167
168
169
170
171
172
Julian days from January, 1, 1994

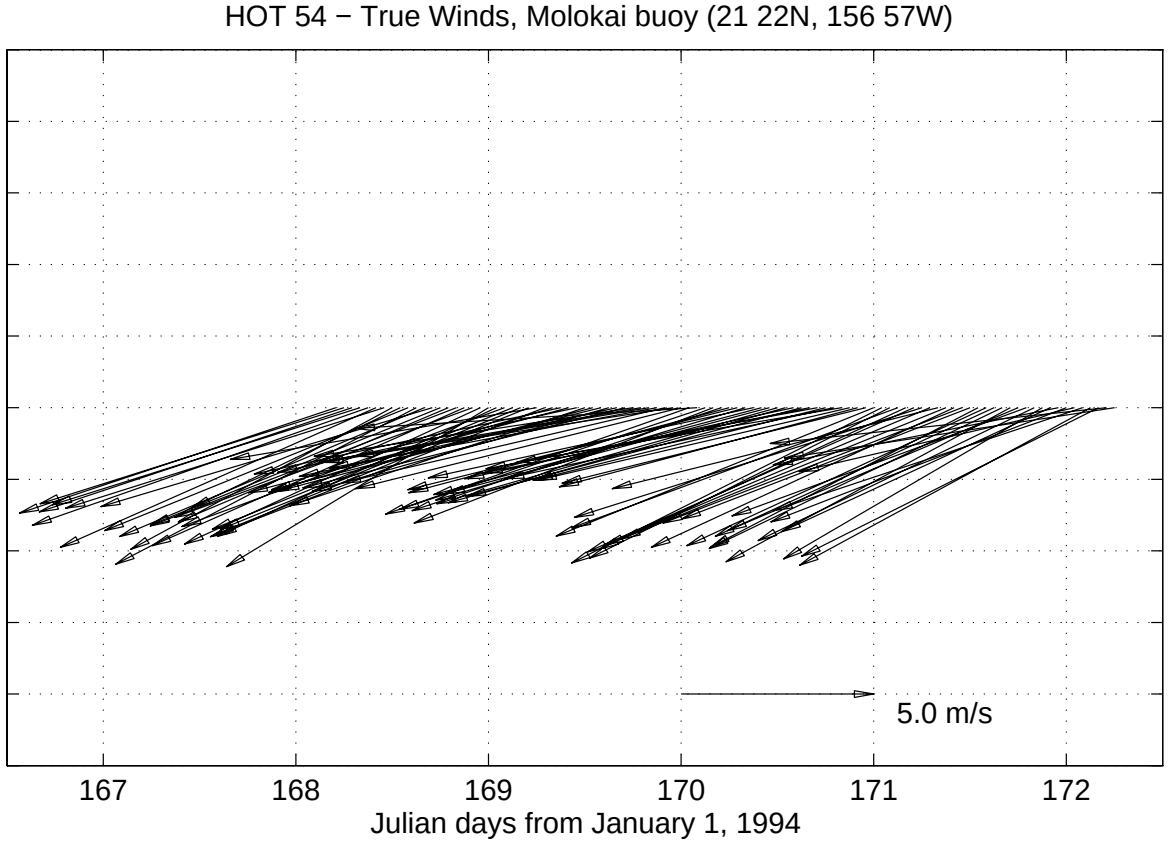
HOT 54 − True Winds, Molokai buoy (21 22N, 156 57W)
5.0 m/s
167
168
169
170
171
172
Julian days from January 1, 1994

Figure 6.8.7

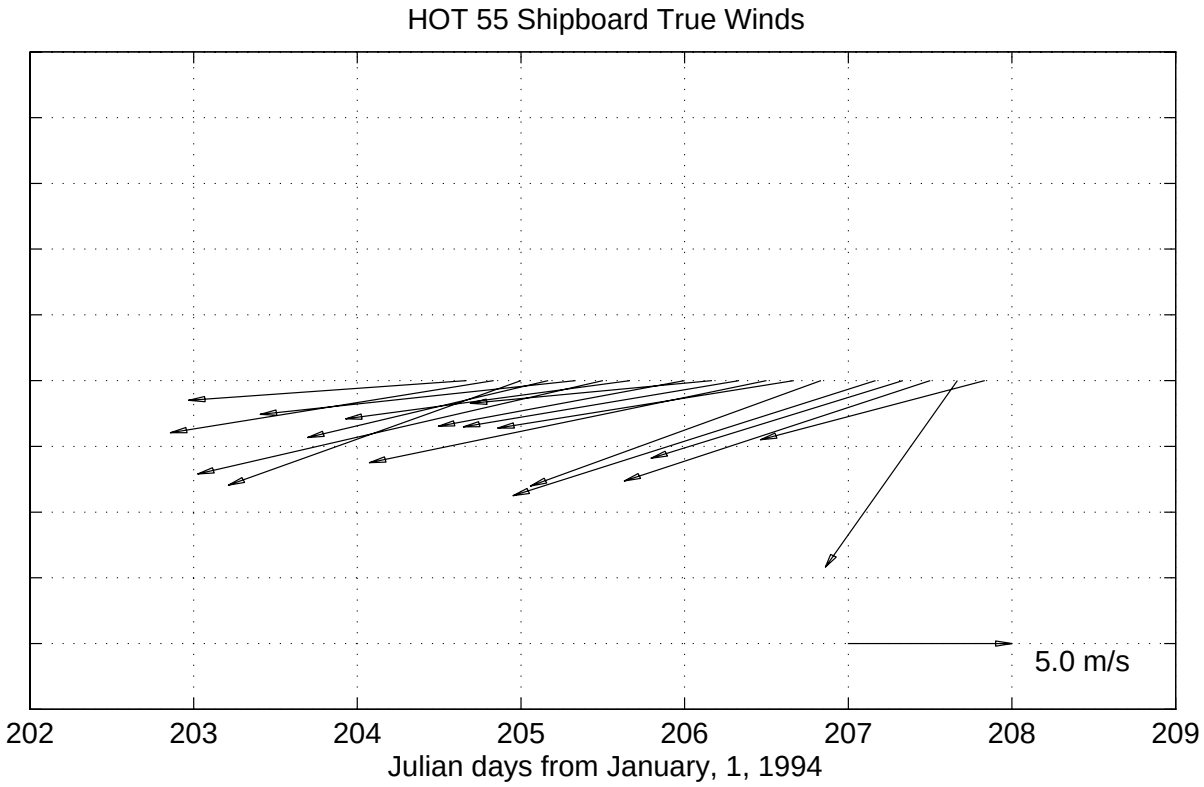
HOT 55 Shipboard True Winds
5.0 m/s
202
203
204
205
206
207
208
209
Julian days from January, 1, 1994

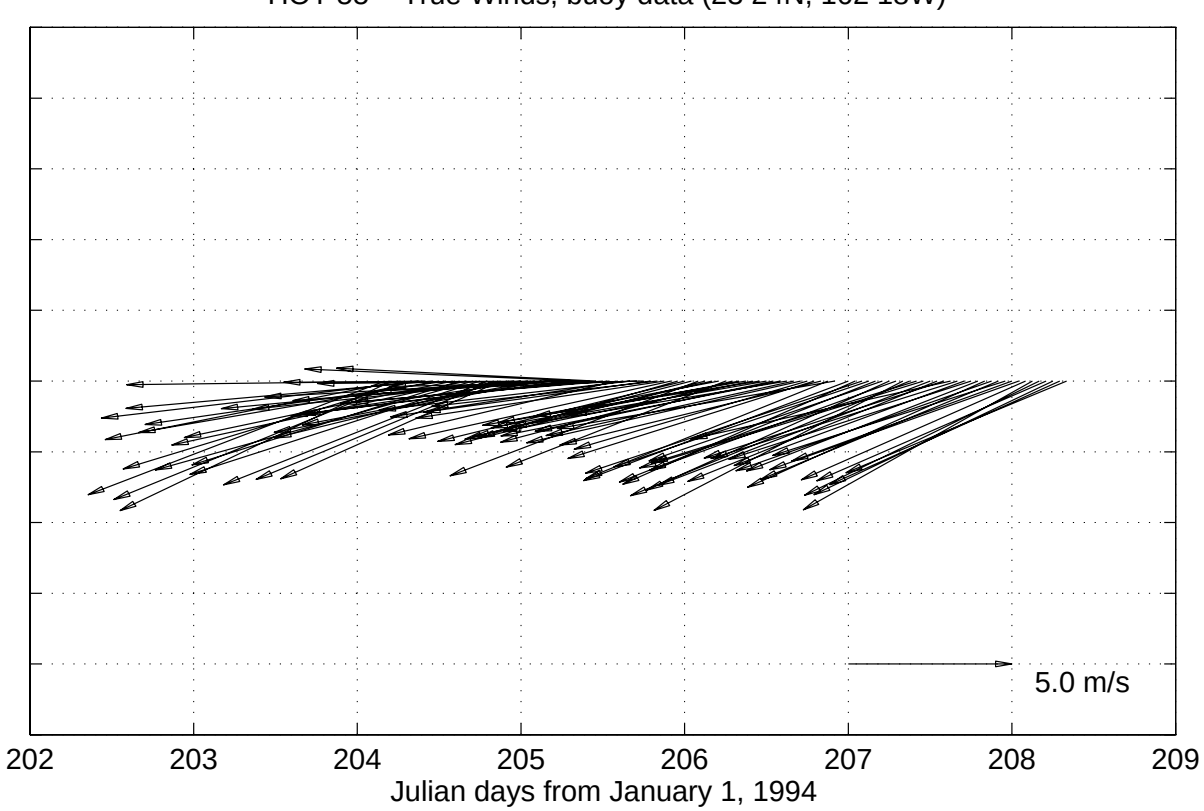
HOT 55 − True Winds, buoy data (23 24N, 162 18W)
5.0 m/s
202
203
204
205
206
207
208
209
Julian days from January 1, 1994

Figure 6.8.8

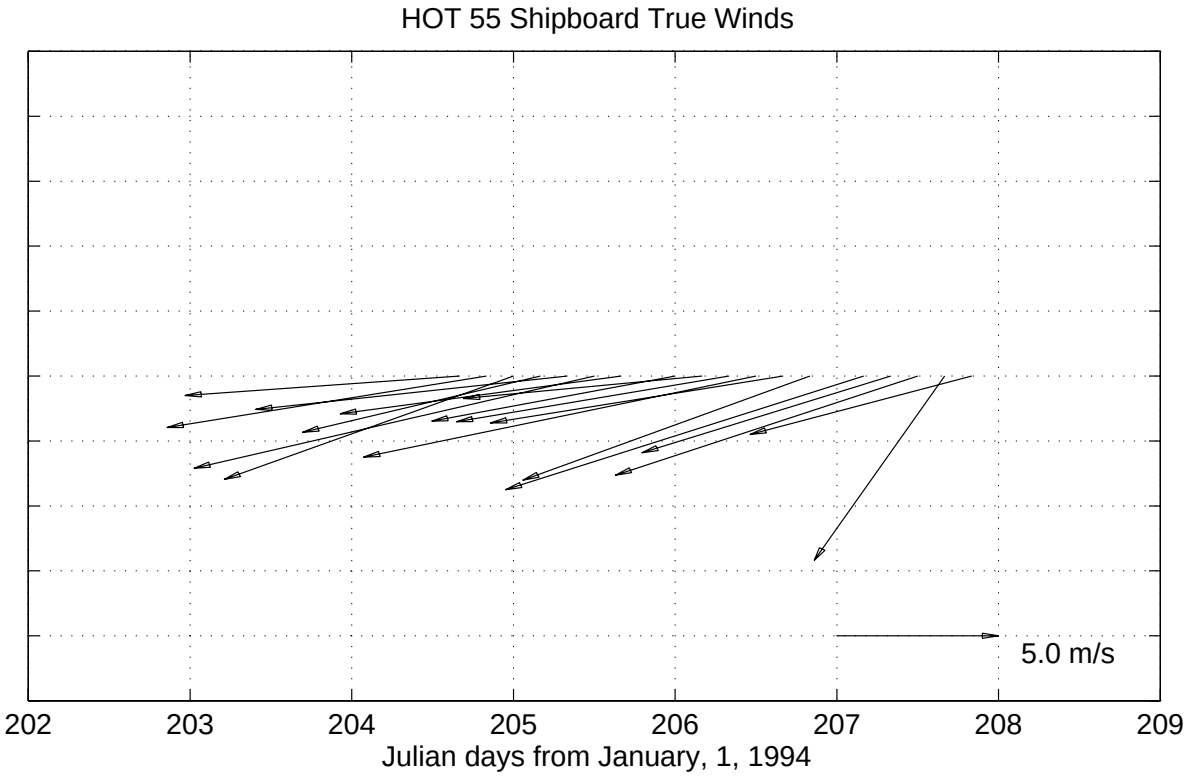
HOT 55 Shipboard True Winds
5.0 m/s
202
203
204
205
206
207
208
209
Julian days from January, 1, 1994

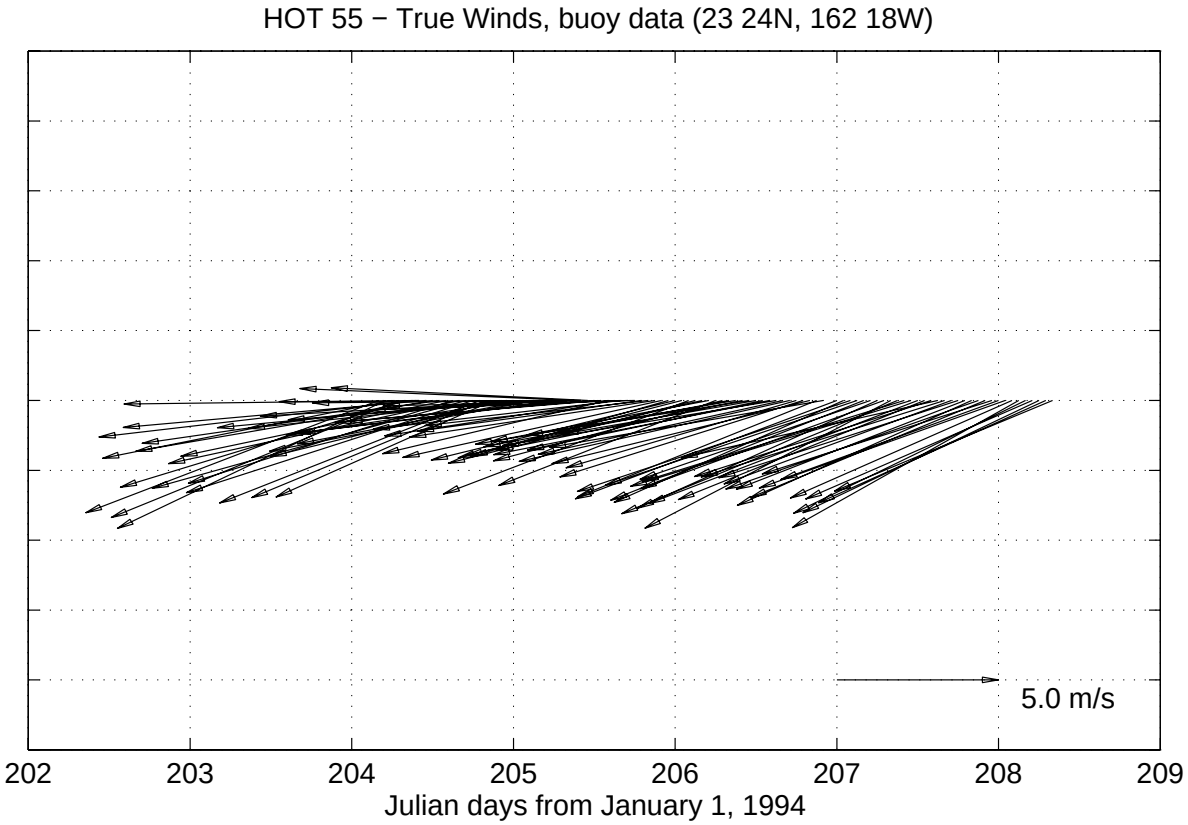
HOT 55 − True Winds, buoy data (23 24N, 162 18W)
5.0 m/s
202
203
204
205
206
207
208
209
Julian days from January 1, 1994

Figure 6.8.9

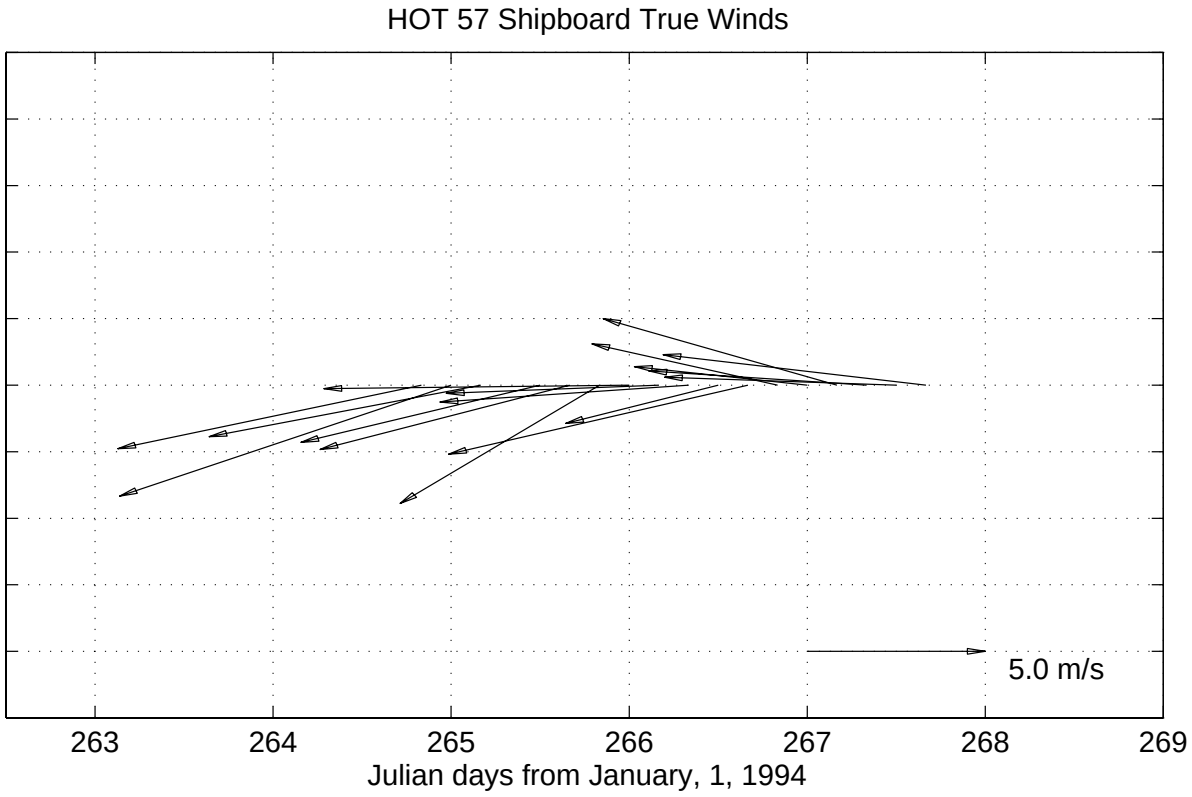
HOT 57 Shipboard True Winds
5.0 m/s
263
264
265
266
267
268
269
Julian days from January, 1, 1994

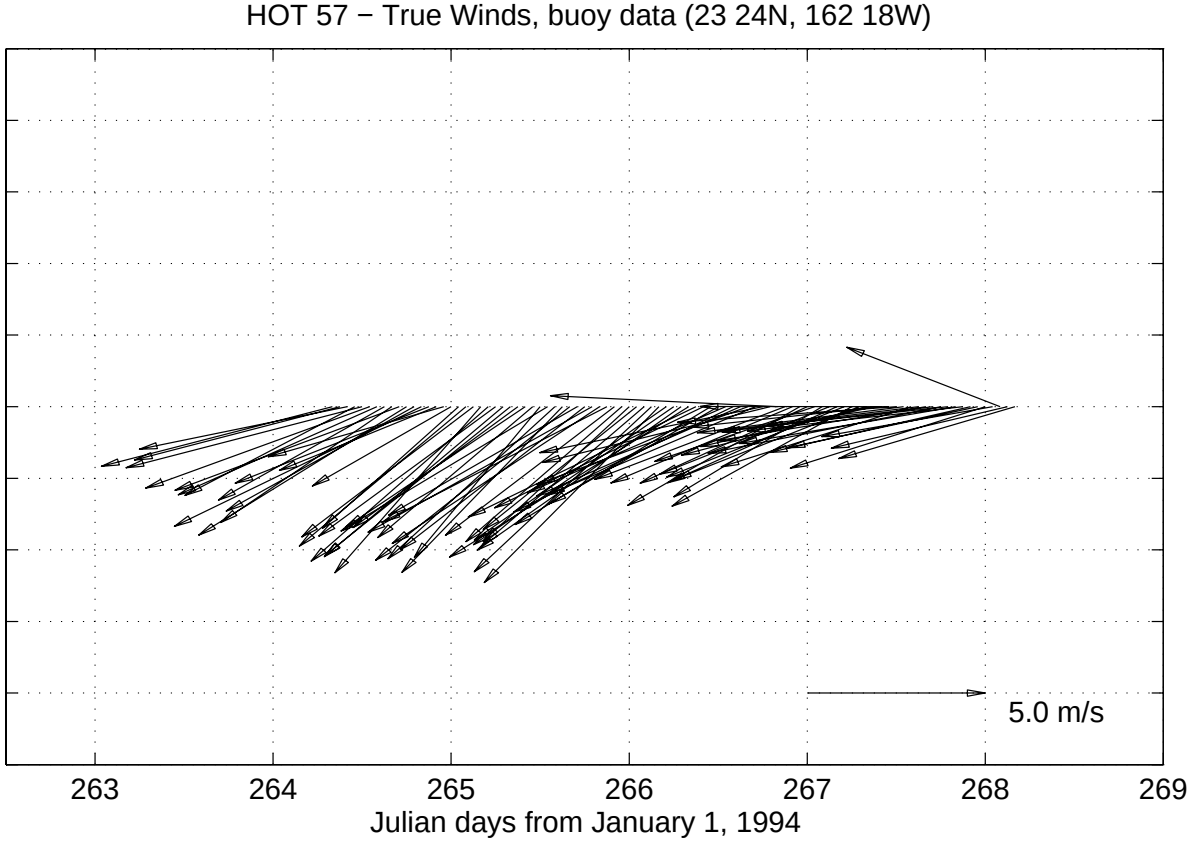
HOT 57 − True Winds, buoy data (23 24N, 162 18W)
5.0 m/s
263
264
265
266
267
268
269
Julian days from January 1, 1994

Figure 6.8.10

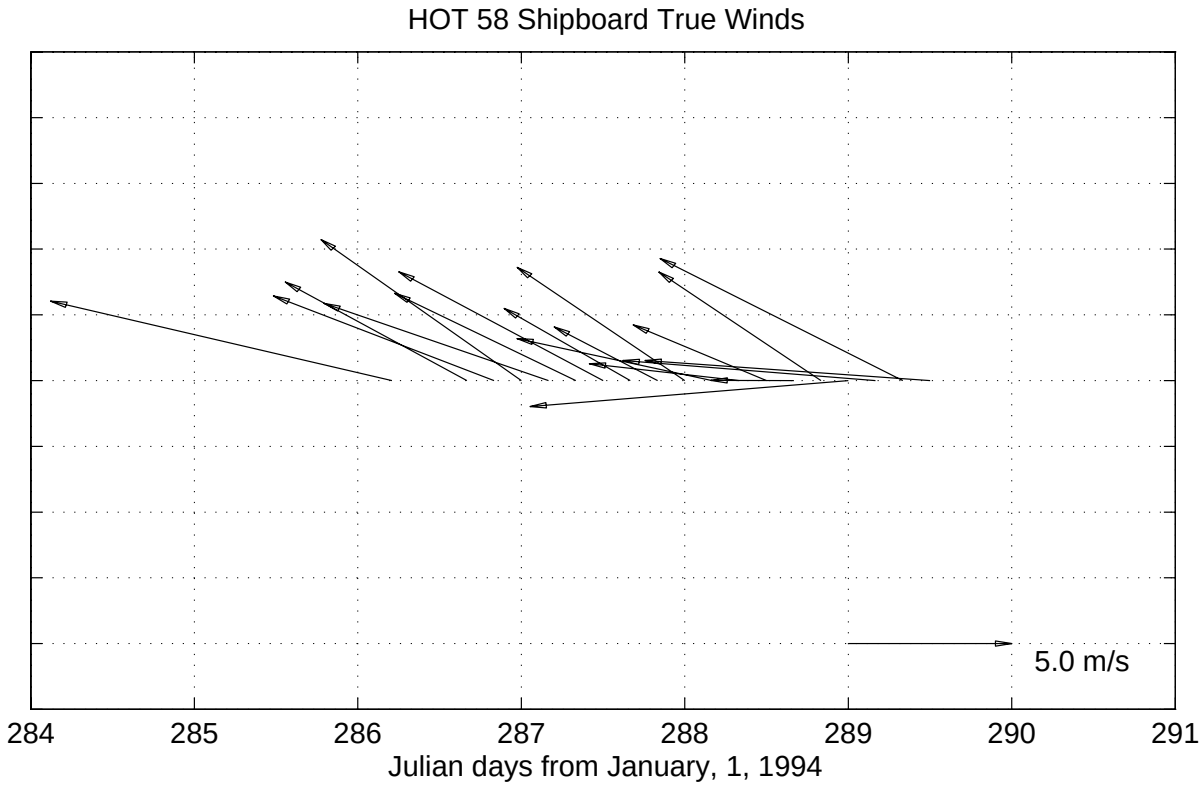
HOT 58 Shipboard True Winds
5.0 m/s
284
285
286
287
288
289
290
291
Julian days from January, 1, 1994

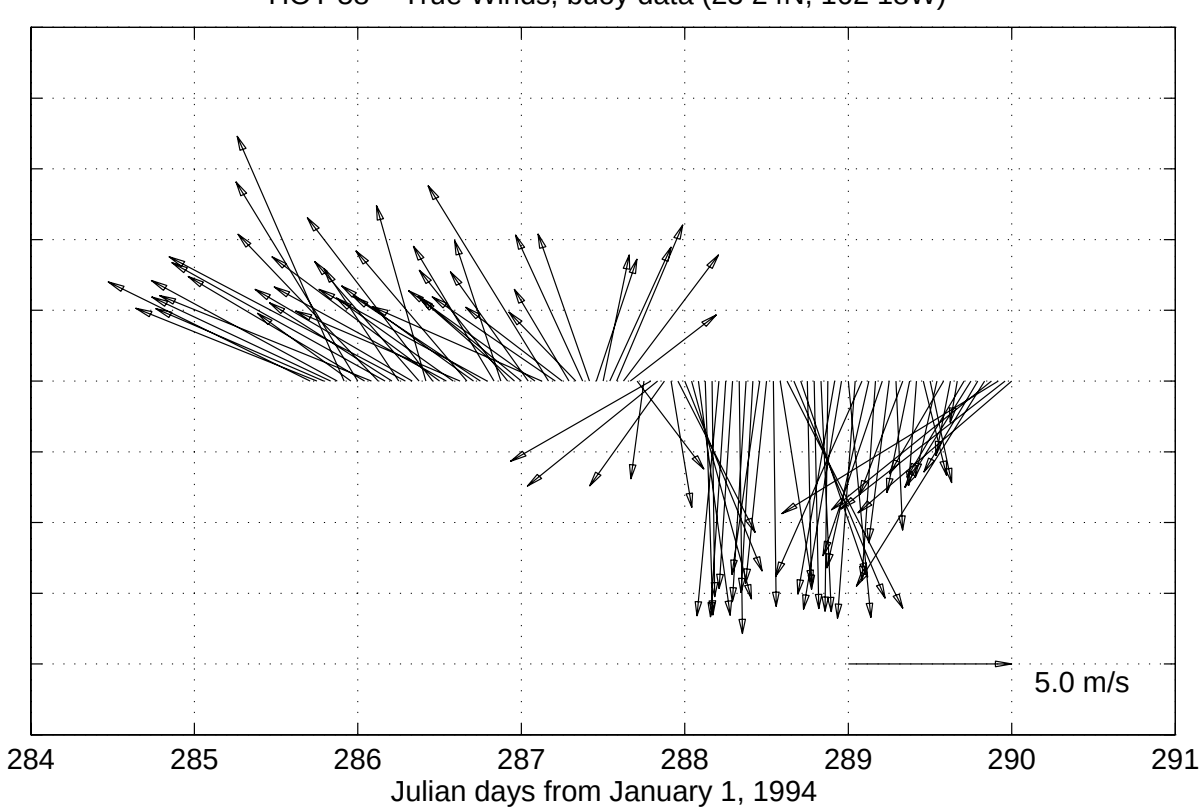
HOT 58 − True Winds, buoy data (23 24N, 162 18W)
5.0 m/s
284
285
286
287
288
289
290
291
Julian days from January 1, 1994

Figure 6.8.11

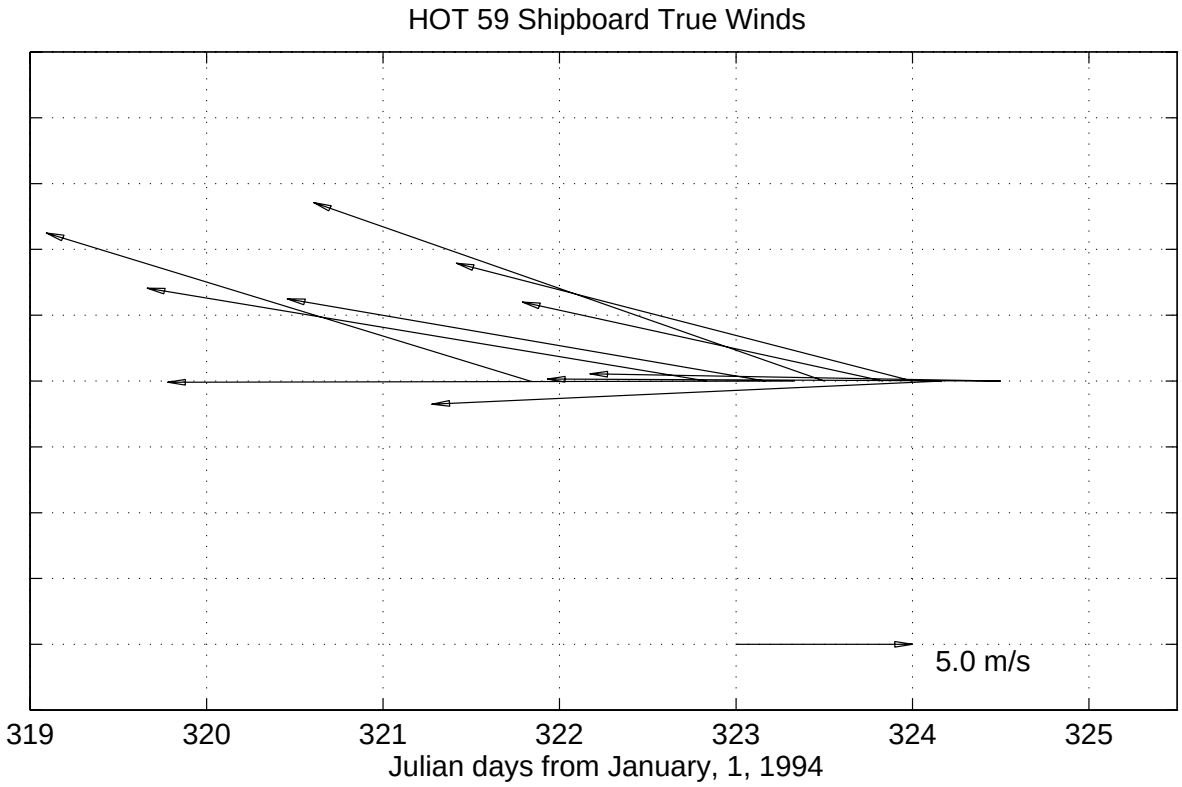
HOT 59 Shipboard True Winds
5.0 m/s
319
320
321
322
323
324
325
Julian days from January, 1, 1994

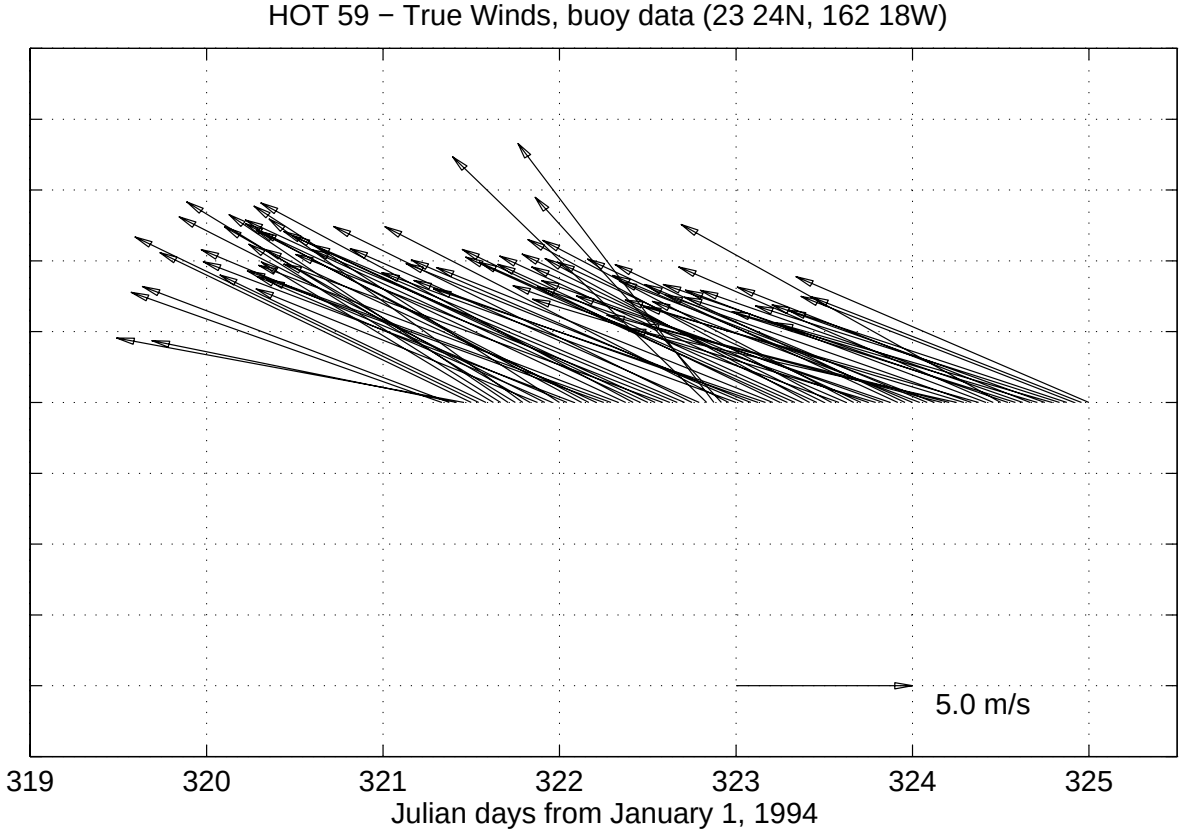
HOT 59 − True Winds, buoy data (23 24N, 162 18W)
5.0 m/s
319
320
321
322
323
324
325
Julian days from January 1, 1994

Figure 6.8.12

7. HOT PROGRAM PRESENTATIONS AND PUBLICATIONS

I. Invited Presentations and Published Abstracts

I.1. 1988 Karl, D. NSF-sponsored symposium on Dissertations in Chemical Oceanography, "Research opportunities in Hawaiian waters", Honolulu, Hawaii, November 1988.

I.2. 1988 Karl, D. NSF/GOFS-sponsored workshop on sediment traps, "Determination of total C, N, P flux" and "Screens: A potential solution to the problem of swimmers", Gulf Coast Research Laboratory, Mississippi, November 1988.

I.3. 1989 Winn, C. D., S. Chiswell, D. M. Karl and R. Lukas. Long time-series research in the Central Pacific Ocean. The Oceanography Society 1st Annual Meeting, Monterey, California.

I.4. 1990 Karl, D., R. Letelier, D. Bird, D. Hebel, C. Sabine and C. Winn. An *Oscillatoria* bloom in the oligotrophic North Pacific Ocean near the GOFS station ALOHA. *EOS, Transactions of the American Geophysical Union* 71, 177-178.

I.5. 1990 Winn, C. D., D. Hebel, R. Letelier, D. Bird and D. Karl. Variability in biogeochemical fluxes in the oligotrophic central Pacific: Results of the Hawaii Ocean Time- Series Program. *EOS, Transactions of the American Geophysical Union* 71, 190.

I.6. 1990 Chiswell, S. M. and R. Lukas. The Hawaii Ocean Time-series (HOT). *EOS, Transactions of the American Geophysical Union* 71, 1397.

I.7. 1990 Karl, D. "JGOFS time-series programs," San Francisco, California, December 1990.

I.8. 1991 Winn, C., C. Sabine, D. Hebel, F. Mackenzie and D. M. Karl. Inorganic carbon system dynamics in the central Pacific Ocean: Results of the Hawaii Ocean Time-series program. *EOS, Transactions of the American Geophysical Union* 72, 70.

I.9. 1991 Lukas, R. Water mass variability observed in the Hawaii Ocean Time Series. *EOS, Transactions of the American Geophysical Union* 72, 70.

I.10. 1991 Letelier, R., D. Karl, R. Bidigare, J. Christian, J. Dore, D. Hebel and C. Winn. Temporal variability of phytoplankton pigments at the U.S.-JGOFS station ALOHA (22°45'N, 158°W). *EOS, Transactions of the American Geophysical Union* 72, 74.

I.11. 1991 Karl, D. "The Hawaii Ocean Time-series program: Carbon production and particle flux", The Oceanography Society 2nd Annual Meeting, St. Petersburg, Florida, March 1991.

I.12. 1991 Karl, D. NATO symposium on Biology and Ecology of Diazotrophic Marine Organisms, "*Trichodesmium* blooms and new nitrogen in the North Pacific gyre", Bamberg, Germany, May 1991.

I.13. 1992 Anbar, A. D. Rhenium in seawater: Confirmation of generally conservative behavior. *EOS, Transactions of the American Geophysical Union* 73, 278.

I.14. 1992 Schudlich, R. and S. R. Emerson. Modelling dissolved gases in the subtropical upper ocean: JGOFS/WOCE Hawaiian Ocean Time-series. *EOS, Transactions of the American Geophysical Union* 73, 287.

I.15. 1992 Tupas, L. M., B. N. Popp and D. M. Karl. Dissolved organic carbon in oligotrophic waters: experiments on sample preservation, storage and analysis. *EOS, Transactions of the American Geophysical Union* 73, 287.

I.16. 1992 Karl, D., C. Winn, D. Hebel, R. Letelier, J. Dore and J. Christian. The U.S.-JGOFS Hawaii Ocean Time-Series (HOT) program. American Society for Limnology and Oceanography Aquatic Sciences Meeting, Santa Fe, NM, February 1992.

I.17. 1992 Campbell, L., R. R. Bidigare, R. Letelier, M. Ondrusek, S. Hall, B. Tsai and C. Winn. Phytoplankton population structure at the Hawaii Ocean Time-series station. American Society for Limnology and Oceanography Aquatic Sciences Meeting, Santa Fe, NM, February 1992.

I.18. 1992 Karl, D. NSF-sponsored GLOBEC scientific steering committee meeting, "Hawaii Ocean Time-series (HOT) program: A GLOBEC 'Blue Water' initiative", Honolulu, Hawaii, March 1992.

I.19. 1992 Karl, D. IGBP International Symposium on Global Change, "Oceanic ecosystem variability: Initial results from the JGOFS Hawaii Ocean Time-series (HOT) experiment", Tokyo, Japan, March 1992.

I.20. 1992 Karl, D. Conoco HOT Topics Seminar Series, "The U.S.-JGOFS Hawaii Ocean Time- Series (HOT) Program: Biogeochemical Vignettes from the Oligotrophic North Pacific Ocean" and "Temporal Variability in Bioelement Flux at Station ALOHA (22°45'N, 158°W)", Woods Hole, Massachusetts, May 1992

I.21. 1992 Bidigare, R. R., L. Campbell, M. Ondrusek, R. Letelier and D. Vaulot. Characterization of picophytoplankton at Station ALOHA (22°45'N, 158°W) using HPLC, flow cytometry and immunofluorescence techniques. PACON 1992 Meeting, June 1992.

I.22. 1992 Winn, C. D., D. Hebel, R. Letelier, J. Christian, J. Dore, R. Lukas and D. M. Karl. Long time-series measurements in the central North Pacific: Results of the Hawaii Ocean Time-series program. PACON conference, Kona, Hawaii, June 1992.

I.23. 1993 Atkinson, M. J. A potentiometric solid state sensor for oceanic CTDs, Abstract of The Oceanography Society Annual Meeting, Seattle, Washington, April 1993.

I.24. 1993 Campbell, L., H. A. Nolla and D. Vaulot. Microbial biomass in the subtropical central North Pacific Ocean (Station ALOHA): The importance of Prochlorococcus, Abstract of The Oceanography Society Annual Meeting, Seattle, Washington, April 1993.

I.25. 1993 Emerson, S., P. Quay, C. Stump, D. Wilbur and R. Schudlich. Oxygen cycles and productivity in the oligotrophic subtropical Pacific Ocean. Abstract of of the Oceanography SocietyAnnual Meeting, Seattle, Washington, April 1993.

I.26. 1993 Sharp, J. H., R. Benner, L. Bennett, C. A. Carlson, S. E. Fitzwater, E. T. Peltzer, and L. Tupas. Dissolved organic carbon: Intercalibration of analyses with equatorial Pacific samples. Abstract of The Oceanography Society Annual Meeting, Seattle, Washington, April 1993.

I.27. 1993 Winn, C. D., C. J. Carrillo, F. T. Mackenzie and D. M. Karl. Variability in the inorganic carbon system parameters in the North Pacific subtropical gyre. Abstract of The Oceanography Society Annual Meeting, Seattle, Washington, April 1993.

I.28. 1993 Yanagi, K. and D. M. Karl. Note on the fractional determination of TDP in seawater by an UV-irradiation method combined with the MAGIC procedure. Abstract of the Oceanography Society of Japan annual meeting, Tokyo, Japan, April 1993.

I.29. 1993 Campbell, L., H. Liu, R. R. Bidigare and D. Vaulot. Immunochemical characterization of *Prochlorococcus*. Abstract of the American Society of Limnology and Oceanography 1993 Annual Meeting, Edmonton, Alberta, Canada, May 1993.

I.30. 1993 Christian, J. R. and D. M. Karl. Bacterial exoenzymes in marine waters: Implications for global biogeochemical cycles. Abstract of the American Society of Limnology and Oceanography 1993 Annual Meeting, Edmonton, Alberta, Canada, May 1993.

I.31. 1993 Moyer, C. L., L. Campbell, D. M. Karl and J. Wilcox. Restriction fragment length polymorphism (RFLP) and DNA sequence analysis of PCR-generated clones to assess diversity of picoeukaryotic algae in the subtropical central North Pacific Ocean (Station ALOHA). Abstract of the American Society of Limnology and Oceanography 1993 Annual Meeting, Edmonton, Alberta, Canada, May 1993.

I.32. 1993 Sharp, J. H., R. Benner, L. Bennett, C. A. Carlson, S. E. Fitzwater and L. Tupas. The equatorial Pacific intercalibration analyses of dissolved organic carbon in seawater. Abstract of the American Society of Limnology and Oceanography 1993 Annual Meeting, Edmonton, Alberta, Canada, May 1993.

I.33. 1994 Yuan, J., C. I. Measures and J. A. Resing. Rapid determination of iron in seawater: In-line preconcentration flow injection analysis with spectrophotometric detection. *EOS, Transactions of the American Geophysical Union* 75, 25.

I.34. 1994 Smith, C. R., S. Garner, D. Hoover and R. Pope. Macrobenthos, mechanisms of bioturbation and carbon flux proxies at the abyssal seafloor along the JGOFS Equatorial Pacific Transect. *EOS, Transactions of the American Geophysical Union* 75, 70.

I.35. 1994 Farrenkopf, A. M., G. W. Luther, III and C. H. Van Der Weijden. Vertical distribution of dissolved iodine species in the northwest Indian Ocean. *EOS, Transactions of the American Geophysical Union* 75, 78.

I.36. 1994 Campbell, L., C. D. Winn, R. Letelier, D. Hebel and D. M. Karl. Temporal variability in phytoplankton fluorescence at Station ALOHA. *EOS, Transactions of the American Geophysical Union* 75, 100.

I.37. 1994 Winn, C., F. T. Mackenzie, C. Carrillo, T. Westby and D. M. Karl. Air-sea carbon dioxide exchange at Station ALOHA. *EOS, Transactions of the American Geophysical Union* 75, 112.

I.38. 1994 Lukas, R., F. Bingham and A. Mantyla. An anomalous cold event in the bottom water observed north of Oahu. *EOS, Transactions of the American Geophysical Union* 75, 205.

I.39. 1994 Tupas, L. M., B. N. Popp and D. M. Karl. Dissolved organic carbon in oligotrophic waters; experiments on sample preservation, storage and analysis. *EOS, Transactions of the American Geophysical Union* 75, 287.

I.40. 1994 Bingham, F.M. Drifter observations of the North Hawaiian Ridge Current. *EOS, Transactions of the American Geophysical Union* 75, 307.

I.41. 1994 HOT Program P.I.s, staff and students. The Hawaii Ocean Time-series (HOT) program: The first five years, p. 59. Abstract of The Oceanography Society Pacific Basin Meeting, Honolulu, Hawaii, July 1994.

I.42. 1994 HOT Program P.I.s, staff and students. HOT: a time-series study of carbon cycling in the oligotrophic North Pacific, p. 24. Abstract of The Oceanography Society Pacific Basin Meeting, Honolulu, Hawaii, July 1994.

I.43. 1994 Bidigare, R. R., L. Campbell, M. E. Ondrusek, R. Letelier, D. Vaulot and D. M. Karl. Phytoplankton community structure at station ALOHA (22°45'N, 158°W) during fall 1991, p. 58. Abstract of The Oceanography Society Pacific Basin Meeting, Honolulu, Hawaii, July 1994.

I.44. 1994 Bingham, F. M. and B. Qiu. Interannual varibility of surface and mixed layer properties observed in the Hawaii Ocean Time-series, p. 89. Abstract of The Oceanography Society Pacific Basin Meeting, Honolulu, Hawaii, July 1994.

I.45. 1994 Bingham, F. M. and R. Lukas. Seasonal cycles of temperature, salinity and dissolved oxygen observed in the Hawaii Ocean Time-series, p. 90. Abstract of The Oceanography Society Pacific Basin Meeting, Honolulu, Hawaii, July 1994.

I.46. 1994 Christian, J. Vertical fluxes of carbon and nitrogen at Station ALOHA, p. 61. Abstract of The Oceanography Society Pacific Basin Meeting, Honolulu, Hawaii, July 1994.

I.47. 1994 Dore, J. E. and D. M. Karl. Nitrite distributions and dynamics at Station ALOHA, p. 60. Abstract of The Oceanography Society Pacific Basin Meeting, Honolulu, Hawaii, July 1994.

I.48. 1994 Firing, E. Currents observed north of Oahu during the first five years of HOT, p. 90. Abstract of The Oceanography Society Pacific Basin Meeting, Honolulu, Hawaii, July 1994.

I.49. 1994 Fujieki, L. A., D. V. Hebel, L. M. Tupas and D. M. Karl. Hawaii Ocean Time-series Data Organization and Graphical System (HOT-DOGS), p. 61. Abstract of The Oceanography Society Pacific Basin Meeting, Honolulu, Hawaii, July 1994.

I.50. 1994 Hebel, D. V., F. P. Chavez, K. R. Buck, R. R. Bidigare, D. M. Karl, M. Latasa, M. E. Ondrusek, L. Campbell and J. Newton. Do GF/F filters underestimate particulate chlorophyll *a* and primary production in the oligotrophic ocean?, p. 62. Abstract of The Oceanography Society Pacific Basin Meeting, Honolulu, Hawaii, July 1994.

I.51. 1994 Houlihan, T., J. E. Dore, L. Tupas, D. V. Hebel, G. Tien and D. M. Karl. Freezing as a method of preservation for seawater dissolved nutrient and organic carbon samples, p. 62. Abstract of The Oceanography Society Pacific Basin Meeting, Honolulu, Hawaii, July 1994.

I.52. 1994 Kennan, S. C. and R. Lukas. Saline intrusions in the intermediate waters north of Oahu, p. 91. Abstract of The Oceanography Society Pacific Basin Meeting, Honolulu, Hawaii, July 1994.

I.53. 1994 Letelier, R. M., J. Dore, C. D. Winn and D. M. Karl. Temporal variations in photosynthetic carbon assimilation efficiencies at Station ALOHA (22°45'N; 158°00'W), p. 60. Abstract of The Oceanography Society Pacific Basin Meeting, Honolulu, Hawaii, July 1994.

I.54. 1994 Liu, H. and L. Campbell. Growth and grazing rates of *Prochlorococcus* and *Synechococcus* at Station ALOHA measured by the selective inhibitor technique, p. 59.

Abstract of The Oceanography Society Pacific Basin Meeting, Honolulu, Hawaii, July 1994.

I.55. 1994 Lukas, R. Interannual variability of Pacific deep and bottom waters observed in the Hawaii Ocean Time-series, p. 91. Abstract of The Oceanography Society Pacific Basin Meeting, Honolulu, Hawaii, July 1994.

I.56. 1994 Lukas, R., F. Bingham and E. Firing. Seasonal-to-interannual variability observed in the Hawaii Ocean Time-series, p. 28. Abstract of The Oceanography Society Pacific Basin Meeting, Honolulu, Hawaii, July 1994.

I.57. 1994 Tupas, L. M., B. N. Popp, D. V. Hebel, G. Tien and D. M. Karl. Dissolved organic carbon measurements at Station ALOHA measured by high temperature catalytic oxidation: Characteristics and variation in the water column, p. 63. Abstract of The Oceanography Society Pacific Basin Meeting, Honolulu, Hawaii, July 1994.

I.58. 1994 Winn, C. D., F. T. Mackenzie, C. Carrillo and D. M. Karl. Air-sea carbon dioxide exchange at Station ALOHA, p. 58. Abstract of The Oceanography Society Pacific Basin Meeting, Honolulu, Hawaii, July 1994.

I.59. 1994 Liu, H. and L. Campbell. Measurement of growth and mortality rate of *Prochloroccus* and *Synechococcus* at Station ALOHA using a new selective inhibitor technique. Fifth International Phycological Congress, Qingdao, China, July 1994.

I.60. 1994 Winn, C., F. T. Mackenzie, C. Carrillo, T. Westby and D. M. Karl. Air-sea carbon dioxide exchange at Station ALOHA, p. 112. Abstract of the American Society of Limnology and Oceanography 1994 Ocean Sciences Meeting, San Diego, California.

I.61. 1994 Measures, C. I., J. Yuan and J. A. Resing. The rapid determination of iron in seawater at sub-nanomolar concentrations using in-line preconcentration and spectrophotometric detection. Sixth Winter Conference on Flow Injection Analysis, San Diego, CA.

I.62. 1994 Measures, C.I., J. Yuan and J. A. Resing. Determination of iron in seawater using in-line preconcentration and spectrophotometric detection. Workshop on Iron Speciation and its Biological Activity, Bermuda Biological Station for Research, Bermuda.

I.63. 1995 Campos, M. L. A. M., T. D. Jickells, A. M. Farrenkopf and G. W. Luther, III. A comparison of dissolved iodine cycling at the Bermuda Atlantic Time Series station and Hawaii Ocean Time-series station. *EOS, Transactions of the American Geophysical Union* 76, S175.

I.64. 1995 Yuan, J. Collecting iron samples from well mounted on CTD rosette. *EOS, Transactions of the American Geophysical Union* 76, S175.

I.65. 1995 Michaels, A. F., D. Karl and A. H. Knap. Insights on ocean variability from the JGOFS time-series stations. Invited plenary lecture, The Oceanography Society Biennial Meeting, April 1995.

I.66. 1995 Emerson, S., P. Quay, L. Tupas and D. Karl. Chemical tracers of productivity and respiration in the upper ocean at U.S. JGOFS station ALOHA, 10th Anniversary JGOFS Science Conference, Villefranche, France, May 1995.

I.67. 1995 Michaels, A. F., D. Karl and A. H. Knap. Insights on ocean variability from the JGOFS time-series stations. Invited lecture, 10th Anniversary JGOFS Science Conference, Villefranche, France, May 1995.

I.68. 1995 Karl, D. M. Oceanic carbon cycle and global environmental change: A microbiological perspective. Invited plenary talk, 7th International Symposium on Microbial Ecology, Santos, Brazil, August 1995.

I.69. 1995 Winn, C., D. Sadler and D. M. Karl. Carbon dioxide dynamics at the Hawaii JGOFS/WOCE time-series station. International Association for the Physical Sciences of the Oceans, Honolulu, Hawaii, August 1995.

II. Invited/Contributed Book Chapters and Refereed Publications

II.1. 1990 Firing, E. and R. L. Gordon. Deep ocean acoustic Doppler current profiling. In: G. F. Appell and T. B. Curtin (eds.), *Proceedings of the Fourth IEEE Working Conference on Current Measurements*, pp. 192-201. IEEE, New York.

II.2. 1990 Giovannoni, S. J., E. F. DeLong, T. M. Schmidt and N. R. Pace. Tangential flow filtration and preliminary phylogenetic analysis of marine picoplankton. *Applied and Environmental Microbiology*, 56, 2572-2575.

II.3. 1991 Chiswell, S. M. Dynamic response of CTD pressure sensors to temperature. *Journal of Atmospheric and Oceanic Technology* 8, 659-668.

II.4 1991 Karl, D. M., J. E. Dore, D. V. Hebel and C. Winn. Procedures for particulate carbon, nitrogen, phosphorus and total mass analyses used in the US-JGOFS Hawaii Ocean Time- Series Program. In: D. Spencer and D. Hurd (eds.), *Marine Particles: Analysis and Characterization*, pp. 71-77. American Geophysical Union, Geophysical Monograph 63.

II.5. 1991 Karl, D. M., W. G. Harrison, J. Dore et al. Chapter 3. Major bioelements workshop report. In: D. C. Hurd and D. W. Spencer (eds.), *Marine Particles: Analysis and Characterization*, pp. 33-42. American Geophysical Union, Geophysical Monograph 63.

II.6. 1991 Karl, D. M. and C. D. Winn. A sea of change: Monitoring the oceans' carbon cycle. *Environmental Science & Technology* 25, 1976-1981.

II.7. 1991 Sabine, C. L. and F. T. Mackenzie. Oceanic sinks for anthropogenic CO_2. *International Journal of Energy, Environment, Economics* 1, 119-127.

II.8. 1991 Schmidt, T. M., E. F. DeLong and N. R. Pace. Analysis of a marine picoplankton community by 16S rRNA gene cloning and sequencing. *Journal of Bacteriology* 173, 4371- 4378.

II.9. 1992 Benner, R., J. D. Pakulski, M. McCarthy, J. I. Hedges and P. G. Hatcher. Bulk chemical characteristics of dissolved organic matter in the ocean. *Science* 255, 1561-1564.

II.10. 1992 Chen, R. F. and J. L. Bada. The fluorescence of dissolved organic matter in seawater. *Marine Chemistry* 37, 191-221.

II.11. 1992 Karl, D. M. The oceanic carbon cycle: Primary production and carbon flux in the oligotrophic North Pacific Ocean. In: Y. Oshima (ed.), *Proceedings of the IGBP Symposium on Global Change*, pp. 203-219. Japan National Committee for the IGBP, Waseda University, Tokyo, Japan.

II.12. 1992 Karl, D. M., R. Letelier, D. V. Hebel, D. F. Bird and C. D. Winn. *Trichodesmium* blooms and new nitrogen in the North Pacific gyre. In: E. J. Carpenter et al. (eds.), *Marine Pelagic Cyanobacteria: Trichodesmium and Other Diazotrophs*, pp. 219-237. Kluwer Academic Publishers, Netherlands.

II.13. 1992 Karl, D. M. and G. Tien. MAGIC: A sensitive and precise method for measuring dissolved phosphorus in aquatic environments. *Limnology and Oceanography* 37, 105-116.

II.14. 1992 Quay, P.D., B. Tilbrook and C. S. Wong. Oceanic uptake of fossil fuel CO_2: Carbon- 13 evidence. *Science* 256, 74-78.

II.15. 1993 Anbar, A. D., R. A. Creaser, D. A. Papanastassiou and G. J. Wasserburg. Rhenium in seawater: Confirmation of generally conservative behavior. *Geochimica et Cosmochimica Acta* 56, 4099-4103.

II.16. 1993 Campbell, L. and D. Vaulot. Photosynthetic picoplankton community structure in the subtropical North Pacific Ocean near Hawaii (station ALOHA). *Deep-Sea Research* 40, 2043- 2060.

II.17. 1993 Coble, P. G., C. A. Schultz and K. Mopper. Fluorescence contouring analysis of DOC intercalibration experiment samples: a comparison of techniques. *Marine Chemistry* 41, 173-178.

II.18. 1993 Emerson, S., P. Quay, C. Stump, D. Wilbur and R. Schudlich. Determining primary production from the mesoscale oxygen field. *ICES Marine Science Symposium* 197, 196-206.

II.19. 1993 Hedges, J. I., B. A. Bergamaschi and R. Benner. Comparative analyses of DOC and DON in natural waters. *Marine Chemistry* 41, 121-134.

II.20. 1993 Karl, D. M. Total microbial biomass estimation derived from the measurement of particulate adenosine-5'-triphosphate. In: P. F. Kemp, B. F. Sherr, E. B. Sherr and J. J. Cole (eds.), *Current Methods in Aquatic Microbial Ecology*, pp. 359-368. Lewis Publishers, Boca Raton.

II.21. 1993 Karl, D. M., G. Tien, J. Dore and C. D. Winn. Total dissolved nitrogen and phosphorus concentrations at US-JGOFS Station ALOHA: Redfield reconciliation. *Marine Chemistry* 41, 203-208.

II.22. 1993 Keeling, C. D. Lecture 2: Surface ocean CO_2. *NATO ASI Series* I(15), 413-429.

II.23. 1993 Letelier, R. M., R. R. Bidigare, D. V. Hebel, C. D. Winn and D. M. Karl. Temporal variability study of the phytoplankton community structure at the US-JGOFS Time-series Station ALOHA (22°45'N, 158°00'W) based on pigment analyses. *Limnology and Oceanography* 38, 1420-1437.

II.24. 1993 Mopper, K. and C. A. Schultz. Fluorescence as a possible tool for studying the nature and water column distribution of DOC components. *Marine Chemistry* 41, 229-238.

II.25. 1993 Selph, K. E., D. M. Karl and M. R. Landry. Quantification of chemiluminescent DNA probes using liquid scintillation counting. *Analytical Biochemistry* 210, 394-401.

II.26. 1993 Sharp, J. H., E. T. Peltzer, M. J. Alperin, G. Cauwet, J. W. Farrington, B. Fry, D. M. Karl, J. H. Martin, A. Spitzy, S. Tugrul and C. A. Carlson. Procedures subgroup report. *Marine Chemistry* 41, 37-49.

II.27. 1993 Winn, C. D., R. Lukas, D. Hebel, C. Carrillo, R. Letelier and D. M. Karl. The Hawaii Ocean Time-series program: Resolving variability in the North Pacific. In: N. Saxena (ed.), *Recent Advances in Marine Science and Technology*, pp. 139-150. Proceedings of the Pacific Ocean Congress (PACON).

II.28. 1994 Baines, S. B., M. L. Pace and D. M. Karl. Why does the relationship between sinking flux and planktonic primary production differ between lakes and ocean? *Limnology and Oceanography* 39, 213-226.

II.29. 1994 Bjorkman, K. and D. M. Karl. Bioavailability of inorganic and organic phosphorus compounds to natural assemblages of microorganisms in Hawaiian coastal waters. *Marine Ecology Progress Series*, 111, 265-273.

II.30. 1994 Campbell, L., H. A. Nolla and D. Vaulot. The importance of photosynthetic prokaryote biomass in the subtropical central North Pacific Ocean (Station ALOHA). *Limnology and Oceanography*, 39, 954-961.

II.31. 1994 Campbell, L., L. P.Shapiro and E. M. Haugen. Immunochemical characterization of the eukaryotic ultraplankton in the Atlantic and Pacific Oceans. *Journal of Plankton Research* 16, 35-51.

II.32. 1994 Christian, J. R. and D. M. Karl. Microbial community structure at the U.S.-Joint Global Ocean Flux Study Station ALOHA: Inverse methods for estimating biochemical indicator ratios. *Journal of Geophysical Research* 99, 14,269-14,276.

II.33. 1994 Karl, D. M. Accurate estimation of microbial loop processes and rates. *Microbial Ecology*, 28, 147-150.

II.34. 1994 Karl, D. M. and B. D. Tilbrook. Production and transport of methane in oceanic particulate organic matter. *Nature* 368, 732-734.

II.35. 1994 Tupas, L. M., B. N. Popp and D. M. Karl. Dissolved organic carbon in oligotrophic waters: experiments on sample preservation, storage and analysis. *Marine Chemistry* 45, 207- 216.

II.36. 1994 Winn, C. D., F. T. Mackenzie, C. J. Carrillo, C. L. Sabine and D. M. Karl. Air-sea carbon dioxide exchange in the North Pacific subtropical gyre: Implications for the global carbon budget. *Global Biogeochemical Cycles* 8, 157-163.

II.37. 1995 Andersen, R., R. Bidigare, M. Keller and M. Latasa. A comparison of HPLC pigment signatures and electron microscopic observations for oligotrophic waters of the North Atlantic and Pacific Oceans. *Deep-Sea Research*, in press.

II.38. 1995 Atkinson, M. J., F. Thomas and N. Larson. Effects of pressure on oxygen sensors: a new pressure term for calibration equations. *Journal of Atmospheric and Oceanic Technology*, in press.

II.39. 1995 Atkinson, M. A., F. I. M. Thomas, N. Larson, E. Terrill, K. Morita and C. Liu. A micro-hole potentiostatic oxygen sensor for oceanic CTDs. *Deep-Sea Research*, in press.

II.40. 1995 Atkinson, M. A., F. Thomas, R. Lukas and C. Winn. New calibration equations for amperometric membrane oxygen sensors. *Deep-Sea Research*, in press.

II.41. 1995 Bingham, F. and R. Lukas Seasonal cycles of temperature, salinity and dissolved oxygen observed in the Hawaii Ocean Time-series. *Deep-Sea Research*, in press.

II.42. 1995 Campos, M. L., A. Farrenkopf, T. Jickells and G. Luther. A comparison of dissolved iodine cycling at the Bermuda Atlantic Time-series Study station and Hawaii Ocean Time-series station. *Deep-Sea Research*, in press.

II.43. 1995 Chavez, F. P., K. R. Buck, R. R. Bidigare, D. M. Karl, D. Hebel, M. Latasa, M. E. Ondrusek, L. Campbell and J. Newton. On the chlorophyll *a* retention properties of glass- fiber GF/F filters. *Limnology and Oceanography*, 40, 428-433.

II.44. 1995 Chiswell, S. Intraseasonal oscillations at Station ALOHA, north of Oahu, Hawaii. *Deep-Sea Research,* in press.

II.45. 1995 Chiswell, S. Using an array of inverted echo sounders to measure dynamic height and geostrophic current in the North Pacific subtropical gyre. *Journal of Atmospheric and Oceanic Technology,* in press.

II.46. 1995 Christian, J. R. and D. M. Karl. Bacterial exocellular enzymes in marine waters: activity ratios and temperature kinetics in three oceanographic provinces. *Limnology and Oceanography*, in press.

II.47. 1995 Christian, J. R. and D. M. Karl. Measuring bacterial ectoenzyme activities in marine waters using mercuric chloride as a preservative and a control. *Marine Ecology Progress Series*, 123, 217-224.

II.48. 1995 Dore, J. E. and D. M. Karl. Nitrite distributions and dynamics at Station ALOHA. *Deep-Sea Research*, in press.

II.49. 1995 Emerson, S., P. D. Quay, C. Stump, D. Wilber and R. Schudlich. Chemical tracers of biological productivity and respiration in the subtropical Pacific Ocean. *Journal of Geophysical Research,* in press.

II.50. 1995 Firing, E. Currents observed north of Oahu during the first 5 years of HOT. *Deep-Sea Research*, in press.

II.51. 1995 Jones, D. R., D. M. Karl and E. A. Laws. DNA:ATP ratios in marine microalgae and bacteria: Implications for growth rate estimates based on rates of DNA synthesis. *Journal of Phycology*, 31, 215-223.

II.52. 1995 Karl, D. M. Oceanic carbon cycle and global environmental change: A microbiological perspective. In: M. T. Martins (ed.), *Global Aspects of Microbial Ecology,* in press.

II.53. 1995 Karl, D. M., J. R. Christian, J. E. Dore, D. V. Hebel, R. M Letelier, L. M. Tupas and C. D. Winn. Seasonal and interannual variability in primary production and particle flux at Station ALOHA. *Deep-Sea Research*, in press.

II.54. 1995 Karl, D. M., R. Letelier, D. Hebel, L. Tupas, J. Dore, J. Christian and C. Winn. Ecosystem changes in the North Pacific subtropical gyre attributed to the 1991-92 El Niño. *Nature,* 373, 230-234.

II.55. 1995 Karl, D. M. and R. Lukas. The Hawaii Ocean Time-series (HOT) program: Background, rationale and field implementation. *Deep-Sea Research*, in press.

II.56. 1995 Kennan, S. C. and R. Lukas. Saline intrusions in the intermediate waters north of Oahu, Hawaii. *Deep-Sea Research,* in press.

II.57. 1995 Lawson, L., Y. Spitz and E. Hofmann. Time series sampling and data assimilation in a simple marine ecosystem model. *Deep-Sea Research*, in press.

II.58. 1995 Letelier, R. M., J. E. Dore, C. D. Winn and D. M. Karl. Temporal variations in photosynthetic carbon assimilation efficiencies at Station ALOHA. *Deep-Sea Research*, in press.

II.59. 1995 Letelier, R. M. and D. M. Karl. The role of *Trichodesmium* spp. in the productivity of the subtropical North Pacific Ocean. *Marine Ecology Progress Series*, in press.

II.60. 1995 Lukas, R. and F. Santiago-Mandujano. Interannual variability of Pacific deep and bottom waters observed in the Hawaii Ocean Time-series. *Deep-Sea Research*, in press.

II.61. 1995 Mitchum, G. On using satellite altimetric heights to provide a spatial context for the Hawaii Ocean Time-series measurements. *Deep-Sea Research*, in press.

II.62. 1995 Sabine, C. L. and F. T. Mackenzie. Bank-derived carbonate sediment transport and dissolution in the Hawaiian Archipelago. *Aquatic Geochemistry*, 1, 189-230.

II.63. 1995 Sabine, C. L., F. T. Mackenzie, C. Winn and D. M. Karl. Geochemistry of particulate and dissolved inorganic carbon at the Hawaii Ocean Time-series station, ALOHA. *Journal of Biogeochemical Cycles*, in press.

II.64. 1995 Schudlich, R. and S. Emerson. Gas saturation in the surface ocean: The roles of heat flux, gas exchange and bubbles. *Deep-Sea Research*, in press.

II.65. 1995 Sharp, J. H., R. Benner, L. Bennett, C. A. Carlson, S. E. Fitzwater, E. T. Peltzer and L. M. Tupas. Analyses of dissolved organic carbon in seawater: the JGOFS EqPac methods comparison. *Marine Chemistry,* 48, 91-108.

II.66. 1995 Thomas, F. I. M. and M. J. Atkinson. Calibration procedure of a micro-hole potentiostatic oxygen sensor for profiling CTD's. *Journal of Atmospheric and Oceanic Technology*, in press.

II.67. 1995 Thomas, F. I. M., S. A. McCarthy, J. Bower, S. Krothapalli, M. J. Atkinson and P. Flament. Response characteristics of two oxygen sensors for oceanic CTDs. *Journal of Atmospheric and Oceanic Technology*, in press.

II.68. 1995 Winn, C. D., L. Campbell, R. Letelier, D. Hebel, L. Fujieki and D. M. Karl. Seasonal variability in chlorophyll concentrations in the North Pacific subtropical gyre. *Global Biogeochemical Cycles*, in press.

III. Submitted Papers

III.1. 1995 Dore, J. E., T. Houlihan, D. V. Hebel, G. Tien, L. M. Tupas and D. M. Karl. Freezing as a method of seawater preservation for the analysis of dissolved inorganic nutrients in seawater. Submitted to *Marine Chemistry*.

III.2. 1995 Dore, J. E. and D. M. Karl. Nitrification in the euphotic zone as a source for nitrite, nitrate and nitrous oxide at Station ALOHA. Submitted to *Limnology and Oceanography.*

III.3. 1995 Jones, D. R., D. M. Karl and E. A. Laws. Growth rates and production of heterotrophic bacteria and phytoplankton in the North Pacific subtropical gyre. Submitted to *Deep-Sea Research*.

III.4. 1995 Karl, D. M. In defense of Station ALOHA. Submitted to *Nature.*

III.5. 1995 Karl, D. M. and G. Tien. Temporal variability in dissolved phosphorus concentrations at Station ALOHA (22°45'N, 158°W). Submitted to *Marine Chemistry.*

III.6. 1995 Winn, C. D., T. Westby and D. M. Karl. Air-sea carbon flux in the North Pacific subtropical gyre: The role of Ekman transport. Submitted to *Deep-Sea Research*.

IV. Theses and Dissertations

IV.1. 1992 Sabine, C. L. Geochemistry of particulate and dissolved inorganic carbon in the central North Pacific. Ph.D. Dissertation, May 1992

IV.2. 1993 Kennan, S. Variability of the intermediate water north of Oahu. M.S. Thesis, December 1993.

IV.3. 1994 Letelier, R. M. Studies on the ecology of *Trichodesmium* spp. (*Cyanophyceae*) in the central North Pacific gyre. Ph.D. Dissertation, April 1994.

IV.4. 1994 Liu, H. B. Growth and mortality rates of *Prochlorococcus* and *Synechococcus* measured by a selective inhibitor technique. M.S. Thesis, May 1994.

IV.5. 1995 Dore, J. E. Microbial nitrification in the marine euphotic zone: Rates and relationships with nitrite distributions, recycled production and nitrous oxide generation. Ph.D. Dissertation, May 1995.

V. Data Reports and Manuals

V.1. 1990 Karl, D. M., C. D. Winn, D. V. W. Hebel and R. Letelier. Hawaii Ocean Time-series Program Field and Laboratory Protocols, September 1990. School of Ocean and Earth Science and Technology, Univ. of Hawaii, Honolulu, HI, 72 pp.

V.2. 1990 Collins, D. J., W. J. Rhea and A. van Tran. Bio-optical profile data report: HOT-3. National Aeronautics and Space Administration JPL Publ. #90-36.

V.3. 1990 Chiswell, S., E. Firing, D. Karl, R. Lukas and C. Winn. Hawaii Ocean Time-series Program Data Report 1, 1988-1989. SOEST Tech. Rept. #1, School of Ocean and Earth Science and Technology, Univ. of Hawaii, Honolulu, HI, 269 pp.

V.4. 1992 Winn, C., S. Chiswell, E. Firing, D. Karl and R. Lukas. Hawaii Ocean Time-series Program Data Report 2, 1990. SOEST Tech. Rept. 92-1, School of Ocean and Earth Science and Technology, Univ. of Hawaii, Honolulu, HI, 175 pp.

V.5. 1993 Winn, C., R. Lukas, D. Karl and E. Firing. Hawaii Ocean Time-series Program Data Report 3, 1991. SOEST Tech. Report 93-3, School of Ocean and Earth Science and Technology, Univ. of Hawaii, Honolulu, HI, 228 pp.

V.6. 1993 Tupas, L., F. Santiago-Mandujano, D. Hebel, R. Lukas, D. Karl and E. Firing. Hawaii Ocean Time-series Program Data Report 4, 1992. SOEST Tech. Report 93-14, School of Ocean and Earth Science and Technology, Univ. of Hawaii, Honolulu, HI, 248 pp.

V.7. 1994 Tupas, L., F. Santiago-Mandujano, D. Hebel, E. Firing, F. Bingham, R. Lukas and D. Karl. Hawaii Ocean Time-series Program Data Report 5, 1993. SOEST Tech. Report 94-5, School of Ocean and Earth Science and Technology, Univ. of Hawaii, Honolulu, HI, 156 pp.

V.8. 1994 Voss, C. I. and W. W. Wood Synthesis of geochemical, isotopic and groundwater modelling analysis to explain regional flow in a coastal aquifer of Southern Oahu, Hawaii. In: *Mathematical Models and Their Applications to Isotope Studies in Groundwater Hydrology*, pp. 147-178, International Atomic Energy Agency, Vienna, Austria.

V.9. 1995 Tupas, L., F. Santiago-Mandujano, D. Hebel, E. Firing, R. Lukas and D. Karl. Hawaii Ocean Time-series Program Data Report 6, 1994. SOEST Tech. Report 95-6, School of Ocean and Earth Science and Technology, Univ. of Hawaii, Honolulu, HI, in press.

VI. Newsletters

VI.1. 1989 Karl, D. M. Hawaiian Ocean Time-series program: It's HOT. *GOFS Newsletter* 1(2), 1-3.

VI.2. 1990 Karl, D. M. HOT Stuff: An update on the Hawaiian Ocean Time-series program. *U.S. JGOFS Newsletter* 2(1), 6,9.

VI.3. 1990 Karl, David M. HOT Stuff: Rescue at sea. *U.S. JGOFS Newsletter* 2(2), 8.

VI.4. 1991 Karl, D. M. HOT Stuff: Retrospect and prospect. *U.S. JGOFS Newsletter* 2(3), 10.

VI.5. 1991 Karl, D. M. HOT Stuff: Hectic spring schedule keeps HOT team hustling. *U.S. JGOFS Newsletter* 2(4), 9-10.

VI.6. 1991 Lukas, R. and S. Chiswell. Submesoscale water mass variations in the salinity minimum of the North Pacific. *WOCE Notes*, 3(1), 6-8.

VI.7. 1992 Karl, D. M. Hawaii Time-series program: Progress and prospects. *U.S. JGOFS Newsletter* 3(4), 1,15.

VI.8. 1992 Michaels, A. F. Time-series programs compare results, methods and plans for future. *U.S. JGOFS Newsletter* 4(1), 7,9.

VI.9. 1992 Winn, C. W. HOT program builds time-series set of carbon measurements for central Pacific. *U.S. JGOFS Newsletter* 4(2), 7.

VI.10. 1992 Dickey, T. D. Oversight committee reviews time-series programs, issues recommendations. *U.S. JGOFS Newsletter* 4(2), 14-15.

VI.11. 1992 Firing, E. and P. Hacker. ADCP results from WHP P16/P17. *WOCE Notes*, 4(3), 6- 12.

VI.12. 1992 Chiswell, S. Inverted echo sounders at the WOCE deep-water station. *WOCE Notes*, 4(4), 1,3-6.

VI.13. 1993 Karl, D. M. HOT Stuff: The five-year perspective. *U.S. JGOFS Newsletter* 5(1), 6,15.

VI.14. 1994 Karl, D. M. HOT Stuff: Surprises emerging from five years' worth of data. *U.S. JGOFS Newsletter* 5(4), 9-10.

VI.15. 1994 Tupas, L. M. Euphotic zone nitrate variability in the central North Pacific gyre at the Hawaii Ocean Time-series Station ALOHA. *International WOCE Newsletter* 17, 21-23.

VI.16. 1994 Lukas, R. HOT results show interannual variability of Pacific Deep and Bottom waters. *WOCE Notes* 6(2), 1, 3, 14-15.

VII. Other

VII.1. Presentations from the "HOT Program: Progress and Prospectus" symposium, 3-4 June 1992, East-West Center, Honolulu, HI

Campbell, L. Bacterial numbers by flow cytometry: A new approach
Chiswell, S. Results from the inverted echo sounder network
Christian, J. Biomass closure in the epipelagic zone
Christian, J. Exoenzymatic hydrolysis of high molecular weight organic matter
Dore, J. Annual and short-term variability in the distribution of nitrite at the US-JGOFS time-series station ALOHA
Dore, J. and D. Hebel. Low-level nitrate and nitrite above the nutricline at Station ALOHA
Firing, E. Ocean currents near ALOHA
Hebel, D., R. Letelier and J. Dore. Evaluation of the depth dependence and temporal variability of primary production at Station ALOHA
Hebel, D., R. Letelier and J. Dore. Past and present dissolved oxygen trends, methodology, and quality control during the Hawaii Ocean Time series
Hebel, D. and U. Magaard. Structure and temporal variability in biomass estimates at Station ALOHA
Houlihan, T. and D. Hebel. Organic and inorganic nutrients: Water column structure and usefulness in time-series analysis
Karl, D. Carbon utilization in the mesopelagic zone: AOU-DOC relationships
Karl, D. HOT/JGOFS program objectives: A brief overview
Karl, D. P-control of N_2 fixation: An ecosystem model
Karl, D. Primary production and particle flux
Karl, D. et al. Review and re-assessment of core measurements: Suggestions for refinement and improvement
Karl, D. and G. Tien. Low-level SRP above the nutricline at Station ALOHA
Karl, D., L. Tupas, G. Tien and B. Popp. "High-temperature" DOC: Pools and implications
Karl, D., K. Yanagi and K. Bjorkman. Composition and turnover of oceanic DOP
Letelier, R. Temporal variability of algal accessory pigments at Station ALOHA: What does it tell about the phytoplankton community structure at the DCML?

Letelier, R. and D. Hebel. Evaluation of fluorometric and HPLC chlorophyll *a* measurements at Station ALOHA

Letelier, R. and F. Santiago-Mandujano. Wind, sea surface temperature and significant wave height records from NDBC buoy #51001 compared to ship observations at Station ALOHA

Lukas, R. Water mass variability observed in the Hawaii Ocean Time-series

Sadler, D., C. Winn and C. Carrillo. Time-series measurements of pH: A new approach for HOT

Schudlich, R. Upper ocean gas modelling at Station ALOHA

Winn, C. DIC variability

Winn, C. and C. Carrillo. DIC and alkalinity profiles and elemental ratios

VII.2. Presentations from the "HOT Golden Anniversary Science Symposium," 16 November 1993, East-West Center, Honolulu, HI

Bingham, F. M. The oceanographic context of HOT

Campbell, L., H. Nolla, H. Liu and D. Vaulot. Phytoplankton population dynamics at the Hawaii Ocean Time series Station ALOHA

Campbell, L., H. Nolla and D. Vaulot. The importance of *Prochlorococcus* to community structure in the central North Pacific Ocean

Christian, J. Vertical fluxes of carbon and nitrogen at Station ALOHA

Dore, J. Nitrate diffusive flux cannot support new production during quiescent periods at Station ALOHA

Dore, J. Nitrification in lower euphotic zone at Station ALOHA: Patterns and significance

Firing, E. The north Hawaiian ridge current and other flows near ALOHA

Hebel, D. Temporal distribution, abundance and variability of suspended particualte matter (particulate carbon, nitrogen and phosphorus) at Station ALOHA -- Observations of a seasonal cycle

Karl, D., D. Hebel, L. Tupas, J. Dore and C. Winn. Station ALOHA particle fluxes and estimates of export production

Karl, D. M., R. Letelier, L. Tupas, J. Dore, D. Hebel and C. Winn. N_2 fixation as a contributor to new production at Station ALOHA

Karl, D. M., G. Tien and K. Yanagi. Phosphorus dynamics at Station ALOHA

Kennan, S. C. Possibilities for stirring along the Hawaiian ridge

Krothapalli, S., Y. H. Li and F. T. Mackenzie. What controls the temporal variability of carbon flux at Station ALOHA?

Letelier, R. M. Inorganic carbon assimilation at Station ALOHA: Possible evidence of a change in carbon fluxes

Letelier, R. M. Spatial and temporal distribution of *Trichodesmium* sp. at Station ALOHA: How important are they?

Liu, H. and L. Campbell. Measurement of growth and mortality rates of *Prochlorococcus* and *Synechococcus* at Station ALOHA using a new selective inhibitor technique

Lukas, R. and F. Bingham. Annual and interannual variations of hydrographic properties observed in the Hawaii Ocean Time-series (HOT)

Lukas, R., F. M. Bingham and A. Mantyla An anomalous cold event in the bottom water observed at Station ALOHA

Moyer, C. L., L. Campbell, D. M. Karl and J. Wilcox. Restriction fragment length polymorphism (RFLP) and DNA sequence analysis of PCR-generated clones to assess diversity of picoeukaryotic algae in the subtropical central North Pacific Ocean (Station ALOHA)

Polovina, J. J. and D. R. Kobayashi. HOT and Hawaii's fisheries landings: Complementary or independent time-series?

Sadler, D. Time series measurement of pH at Station ALOHA

Smith, C. R., D. J. DeMaster, R. H. Pope, S. P. Garner, D. J. Hoover and S. E. Doan. Seabed radionuclides, bioturbation and benthic community structure at the Hawaii Ocean Time-series Station ALOHA

Tupas, L. M., B. N. Popp and D. M. Karl. Dissolved organic carbon in oligotrophic waters: Experiments on sample preservation, storage and analysis

Winn, C. D. Air-sea carbon dioxide exchange at Station ALOHA

Yuan, J.and C. I. Measures. Sampling and analysis of dissolved iron

8. Data Availability and Distribution

Data collected by HOT program scientist are made available to the oceanographic community as soon after processing as possible. In order to provide easy access to our data, we have provided summaries of our CTD and water column chemistry data on the enclosed IBM PC 3.5" high-density floppy diskette. CTD data at NODC standard pressures for temperature, potential temperature, salinity, oxygen and potential density are provided in ASCII files; water column chemistry data are provided in Lotus 1-2-3™ files. The pressure and temperature reported for each water column sample are derived from CTD temperature and pressure readings at the time of bottle trip. Densities are calculated from calibrated CTD temperature, pressure and salinity values. These densities are used, where appropriate, to express chemical concentrations on a per kilogram basis. With the exception of the results of replicate analysis, all water column chemical data collected during 1994 are given in these data sets.

The data included in the Lotus 1-2-3™ files have been quality controlled and the flags associated with each value indicate our estimate of the quality of each value. The text file readme.txt gives a description of data formats and quality flags.

A more complete data set, containing data collected since year 1 of the HOT program, as well as 2 dbar averaged CTD data, are available from two sources. The first is through NODC in the normal manner. The second source is via the world-wide Internet system. The measurements reside in a data base on a workstation at the University of Hawaii, and may be accessed using anonymous ftp or the world-wide-web (www) on Internet. The www address is ***http://hahana.soest.hawaii.edu/hot/hot.html***. Access via ftp is described in more detail below.

In order to maximize ease of access, the data are in ASCII files. File names are chosen so that they may be copied to DOS machines without ambiguity. (DOS users should be aware that Unix is case-sensitive, and Unix extensions may be longer than 3 characters.)

The data are in a subdirectory called /pub/hot. More information about the data base is given in several files called Readme.* at this level. The file Readme.first gives general information on the data base; we encourage users to read it first.

The following is an example of how to use ftp to obtain HOT data. The user's command are denoted by underlined text. The workstation's Internet address is ***mana.soest.hawaii.edu***, or 128.171.154.9 (either address should work). All information except optical data resdie on this address. Optical data are stored at ***hahana.soest.hawaii.edu***., or 128. 171. 154. 13.

1. At the Prompt >, type ftp 128.171.154.9. or ftp mana.soest.hawaii.edu.

2. When asked for your login name, type anonymous.

3. When asked for a password, type your email address.

4. To change to the HOT database, type cd /pub/hot.
To view files type ls. A directory of files and subdirectories will appear.

4a. To obtain a list of publications, type cd publication-list then get hotpub.lis

4b. To obtain the JGOFS protocol manual, type cd protocols then get 1142.asc.

4c. To obtain water column data, type cd water, then get <filename> where the filename is hot#.gof (JGOFS data) or hot#.sea (WOCE data) and # is the HOT cruise of interest.

5. To obtain further information about the database type get Readme.first. This will transfer an ASCII file to your system. Use any text editor to view it.

6. To exit type bye.

7. Data on optical parameters are located on another server. To obtain light data, at the prompt type ftp 128.171.154.13 or ftp hahana.soest.hawaii.edu then follow steps 2 to 4.